Normal Vascular and Glomerular Anatomy

Arthur H. Cohen
Richard J. Glassock

The topic of normal vascular and glomerular anatomy is introduced here to serve as a reference point for later illustrations of disease-specific alterations in morphology.

CHAPTER

1

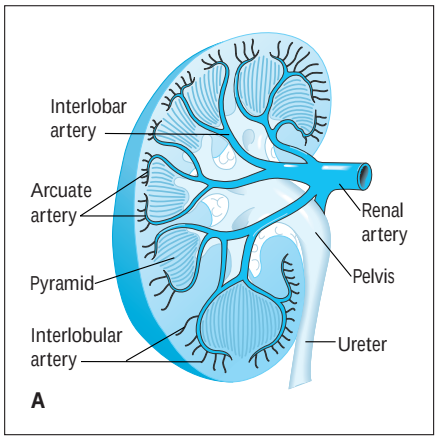

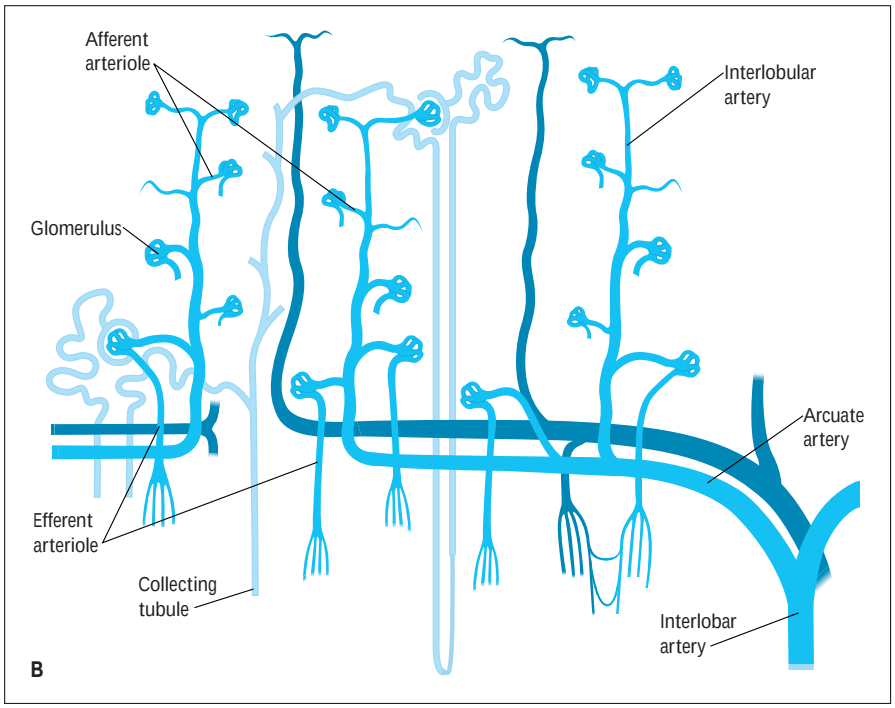

FIGURE 1-1

A, The major renal circulation. The renal artery divides into the interlobar arteries (usually 4 or 5 divisions) that then branch into arcuate arteries encompassing the corticomedullary junction of each renal pyramid. The interlobular arteries (multiple) originate from the arcuate arteries. **B**, The renal microcirculation. The afferent arterioles branch from the interlobular arteries and form the glomerular capillaries (hemi-arterioles). Efferent arterioles then reform and collect to form the post-glomerular circulation (peritubular capillaries, venules and renal veins [not shown]). The efferent arterioles at the corticomedullary junction dip deep into the medulla to form the vasa recta, which embrace the collecting tubules and form hairpin loops. (*Courtesy of* Arthur Cohen, MD.)

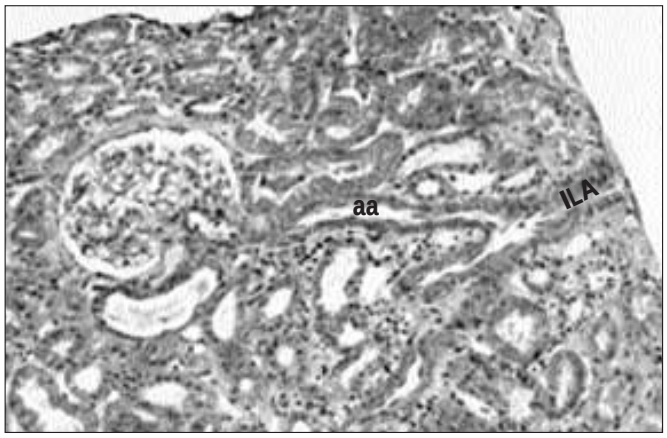

FIGURE 1-2 (*see* Color Plate)
Microscopic view of the normal vascular and glomerular anatomy. The largest intrarenal arteries (interlobar) enter the kidneys between adjacent lobes and extend toward the cortex on the side of a pyramid. These arteries branch dichotomously at the corticomedullary junction, forming arcuate arteries that course between the cortex and medulla. The arcuate arteries branch into a series of interlobular arteries that course at roughly right angles through the cortex toward the capsule. Blood reaches glomeruli through afferent arterioles, most of which are branches of interlobular arteries, although some arise from arcuate arteries. ILA—interlobular artery; aa—afferent arteriole.

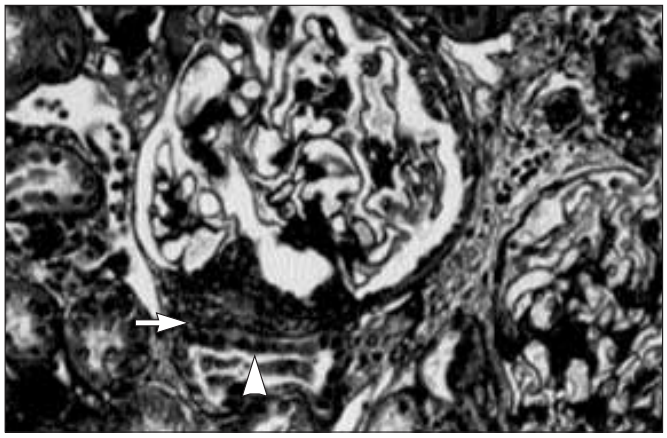

FIGURE 1-3
Microscopic view of the juxtaglomerular apparatus. The juxtaglomerular apparatus (*arrow*) located immediately adjacent to the glomerular hilus, is a complex structure with vascular and tubular components. The vascular component includes the afferent and efferent arterioles, and the region between them is known as the lacis. The tubular component consists of the macula densa (*arrowhead*). The juxtaglomerular apparatus is an integral component of the renin-angiotensin system.

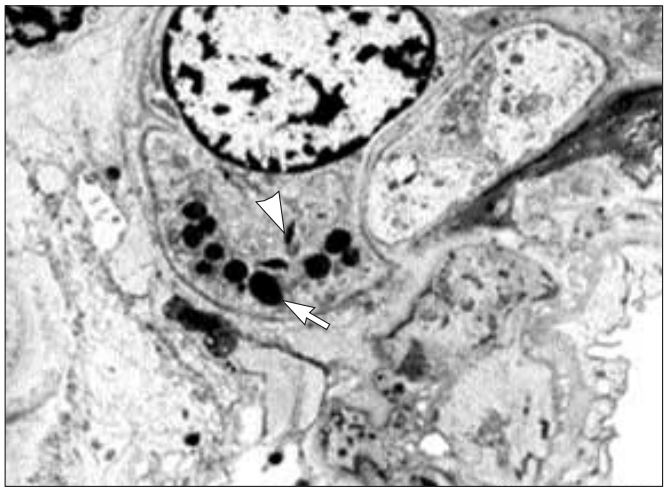

FIGURE 1-4
Electron micrograph of the arterioles. Modified smooth muscle cells of the arterioles of the juxtaglomerular apparatus produce and secrete renin. Renin is packaged in characteristic amorphous mature granules (*arrow*) derived from smaller rhomboid-shaped immature protogranules (*arrowhead*).

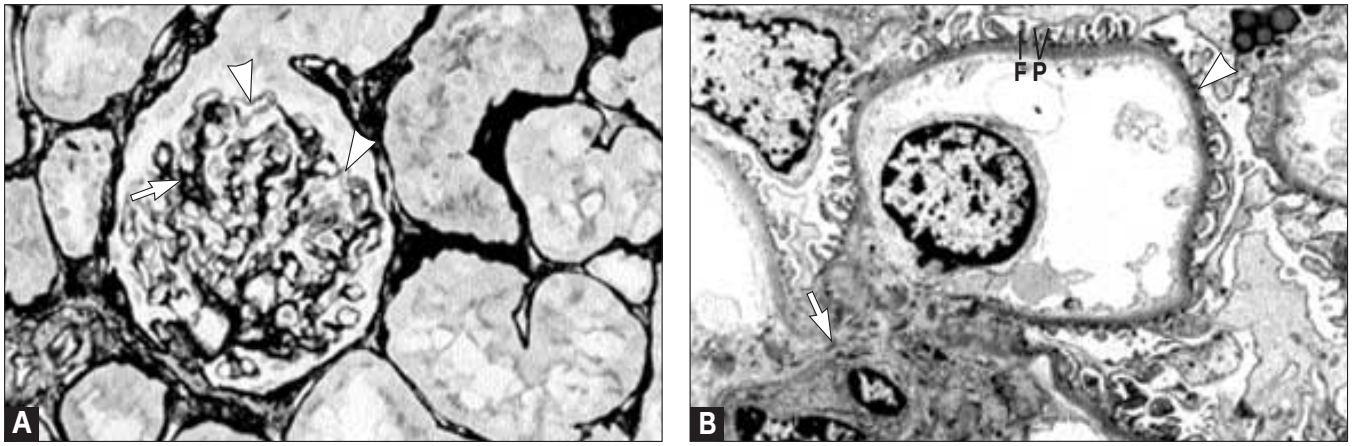

FIGURE 1-5 (*see* Color Plate)

Microscopic view of the glomeruli. Glomeruli are spherical "bags" of capillaries emanating from afferent arterioles and confined within the urinary space, which is continuous with the proximal tubule. The capillaries are partially attached to the mesangium, a continuation of the arteriolar wall consisting of mesangial cells (**A**, *arrow*) and the matrix (**B**, *arrow*). The free wall of glomerular capillaries, across which filtration takes place, consists of a basement membrane (*arrowheads*) covered by visceral epithelial cells with individual foot processes (FP) and lined by endothelial cells.

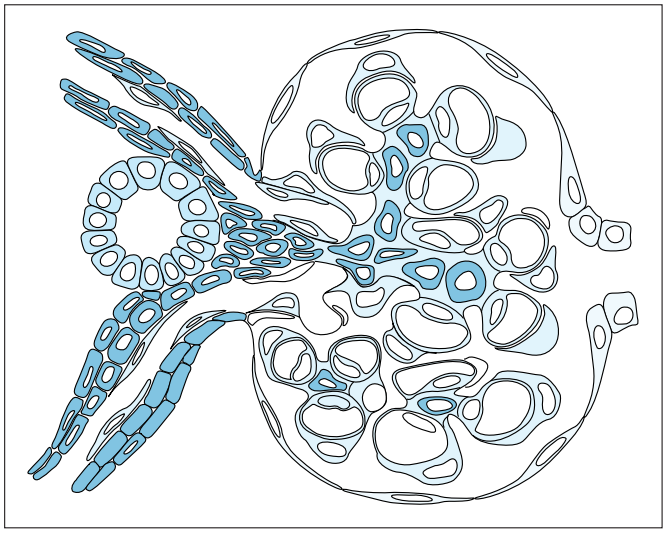

FIGURE 1-6

Schematic illustration of a glomerulus and adjacent hilar structure. Note the relationship of mesangial cells to the juxtaglomerular apparatus and distal tubule (macula densa). Red—mesangial cells; blue—mesangial matrix; black—basement membrane; green—visceral and parietal epithelial cells; yellow—endothelial cells. (*From* Churg and coworkers [1]; with permission.)

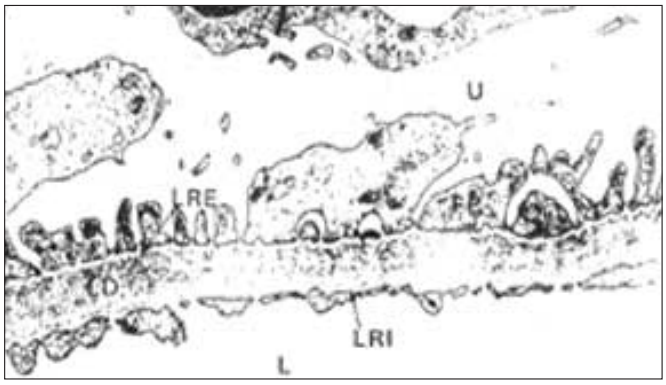

FIGURE 1-7

Electron photomicrograph illustrating a portion of the ultrastructure of the glomerular capillary wall. The normal width of the lamina rara externa (LRE) plus the lamina densa (LD) plus the lamina rara interna (LRI) equals about 250 to 300 nm. The spaces between the foot processes (FP), having diameters of 20 to 60 nm, are called *filtration slit pores*. It is believed they are the path by which filtered fluid reaches the urinary space (U). The endothelial cells on the luminal aspect of the basement membrane (BM) are fenestrated, having diameters from 70 to 100 nm (*see* Fig. 1-9). The BM (LRE plus LD plus LRI) is composed of Type IV collagen and negativity charged proteoglycans (heparan sulfate). L—lumen. (*From* Churg and coworkers [1]; with permission.)

FIGURE 1-8
Scanning electron microscopy of the glomerulus. The surface anatomy of the interdigitating foot processes of normal visceral epithelial cells (podocytes) is demonstrated. These cells and their processes cover the capillary, and ultrafiltration occurs between the fine branches of the cells. (*From* Churg and coworkers [1]; with permission.)

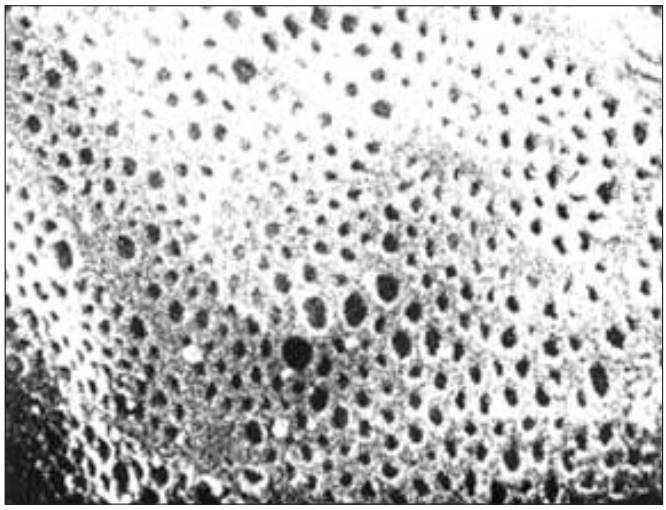

FIGURE 1-9
Scanning electron microscopy of the glomerulus. The surface anatomy of endothelial cells of a normal glomerulus is demonstrated. Note the fenestrated appearance. (*From* Churg and coworkers [1]; with permission.)

Reference

1. Churg J, Bernstein J, Glassock RJ: *Renal Disease. Classification and Atlas of Glomerular Diseases*, edn 2. New York: Igaku-Shoin; 1995.

The Primary Glomerulopathies

Arthur H. Cohen
Richard J. Glassock

The primary glomerulopathies are those disorders that affect glomerular structure, function, or both in the absence of a multisystem disorder. The clinical manifestations are predominately the consequence of the glomerular lesion (such as proteinuria, hematuria, and reduced glomerular filtration rate). The combination of clinical manifestations leads to a variety of clinical syndromes. These syndromes include acute glomerulomphritis; rapidly progressive glomerulonephritis; chronic renal failure; the nephrotic syndrome or "asymptomatic" hematuria, proteinuria, or both.

CHAPTER

2

CLINICAL SYNDROMES OF GLOMERULAR DISEASE

Acute glomerulonephritis
Rapidly progressive glomerulonephritis
Chronic glomerulonephritis
Nephrotic syndrome
"Asymptomatic" hematuria, proteinuria, or both

FIGURE 2-1
Each of these syndromes arises as a consequence of disturbances of glomerular structure and function. Acute glomerulonephritis consists of the abrupt onset of hematuria, proteinuria, edema, and hypertension. Rapidly progressive glomerulonephritis is characterized by features of nephritis and progressive renal insufficiency. Chronic glomerulonephritis features proteinuria and hematuria with indolent progressive renal failure. Nephrotic syndrome consists of massive proteinuria (>3.5 g/d in adults), hypoalbuminemia with edema, lipiduria, and hyperlipidemia. "Asymptomatic" hematuria, proteinuria, or both is not associated initially with renal failure or edema. Each of these syndromes may be complicated by hypertension.

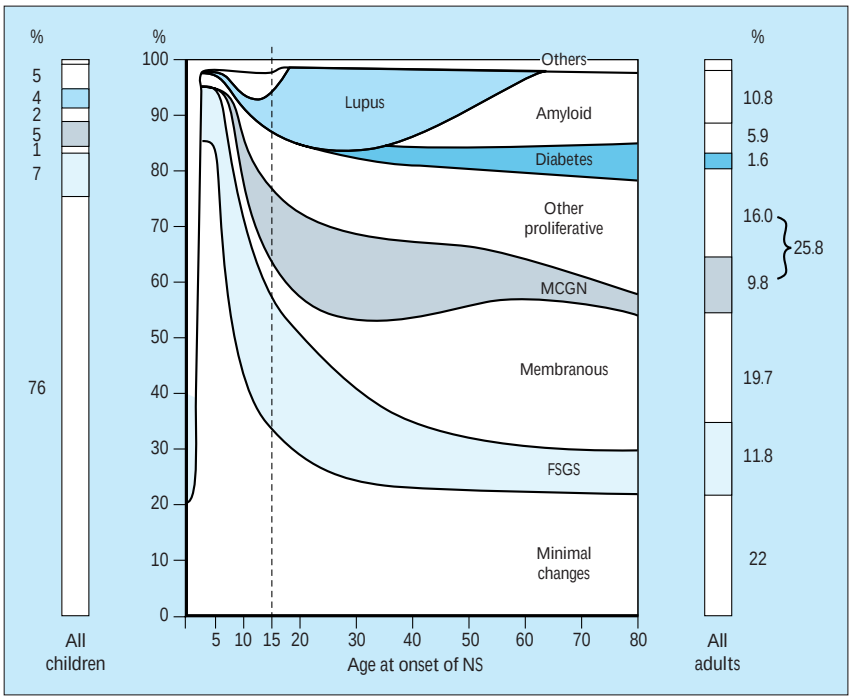

FIGURE 2-2
Age-associated prevalence of various glomerular lesions in nephrotic syndrome. This schematic illustrates the age-associated prevalence of various diseases and glomerular lesions among children and adults undergoing renal biopsy for evaluation of nephrotic syndrome (Guy's Hospital and the International Study of Kidney Disease in Children) [1]. Both the systemic and primary causes of nephrotic syndrome are included. (Diabetes mellitus with nephropathy is underrepresented because renal biopsy is seldom needed for diagnosis.) The bar on the left summarizes the prevalence of various lesions in children aged 0 to 16 years; the bar on the right summarizes the prevalence of various lesions in adults aged 16 to 80 years. Note the high prevalence of minimal change disease in children and the increasing prevalence of membranous glomerulonephritis in the age group of 16 to 60 years. FSGS—focal segmental glomerulosclerosis; MCGN—mesangiocapillary glomerulonephritis. (*From* Cameron [1]; with permission.)

PRIMARY GLOMERULAR LESIONS

Minimal change disease
Focal segmental glomerulosclerosis with hyalinosis
Membranous glomerulonephritis
Membranoproliferative glomerulonephritis
Mesangial proliferative glomerulonephritis
Crescentic glomerulonephritis
Immunoglobulin A nephropathy
Fibrillary and immunotactoid glomerulonephritis
Collagenofibrotic glomerulopathy
Lipoprotein glomerulopathy

FIGURE 2-3
The primary glomerular lesions.

Minimal Change Disease

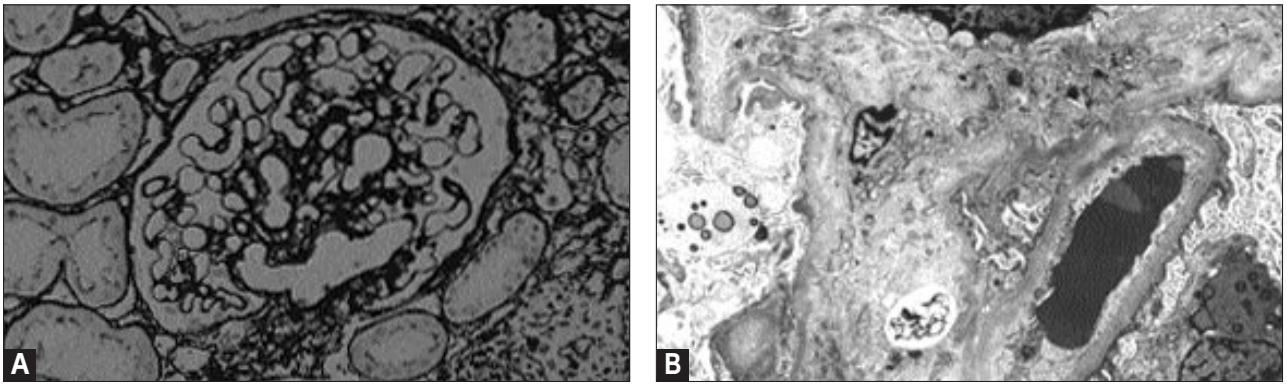

FIGURE 2-4

Light and electron microscopy in minimal change disease (lipoid nephrosis). **A**, This glomerulopathy, one of many associated with nephrotic syndrome, has a normal appearance on light microscopy. No evidence of antibody (immune) deposits is seen on immunofluorescence. **B**, Effacement (loss) of foot processes of visceral epithelial cells is observed on electron microscopy. This last feature is the major morphologic lesion indicative of massive proteinuria.

Minimal change disease is considered to be the result of glomerular capillary wall damage by lymphokines produced by abnormal T cells. This glomerulopathy is the most common cause of nephrotic syndrome in children (>70%) and also accounts for approximately 20% of adult patients with nephrotic syndrome. This glomerulopathy typically is a corticosteroid-responsive lesion, and usually has a benign outcome with respect to renal failure.

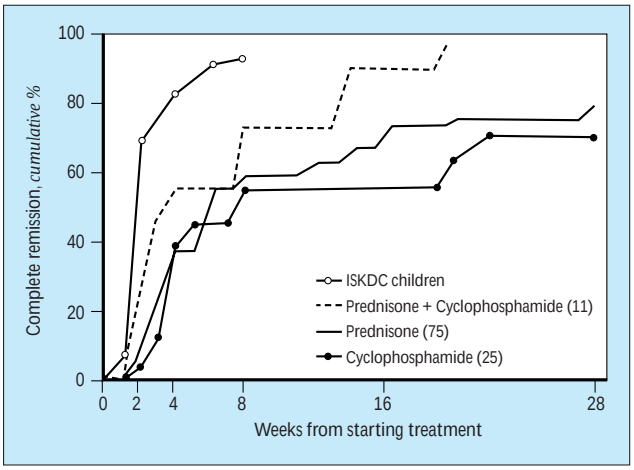

FIGURE 2-5

Therapeutic response in minimal change disease. This graph illustrates the cumulative complete response rate (absence of abnormal proteinuria) in patients of varying ages in relation to type and duration of therapy [1]. Note that most children with minimal change disease respond to treatment within 8 weeks. Adults require prolonged therapy to reach equivalent response rates. Number of patients are indicated in parentheses. (*From* Cameron [2]; with permission.)

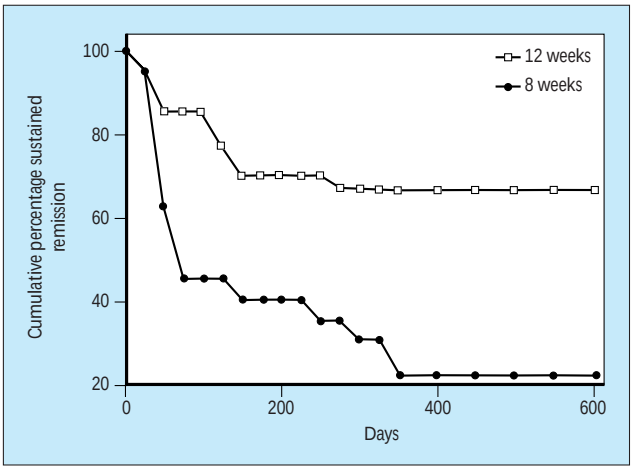

FIGURE 2-6

Cyclophosphamide in minimal change disease. One of several controlled trials of cyclophosphamide therapy in pediatric patients that pursued a relapsing steroid-dependent course is illustrated. Note the relative freedom from relapse when children were given a 12-week course of oral cyclophosphamide. An 8-week course of chlorambucil (0.15–0.2 mg/kg/d) may be equally effective. (*From* Arbeitsgemeinschaft für pediatrische nephrologie [3]; with permission.)

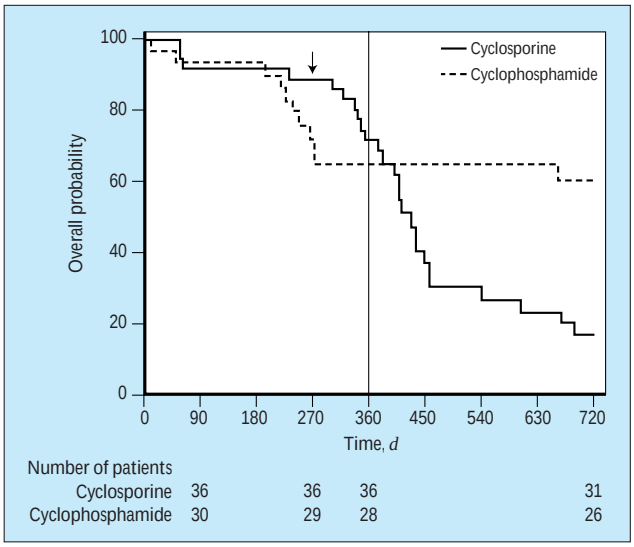

FIGURE 2-7

Cyclosporine in minimal change disease. One of several controlled trials of cyclosporine therapy in this disease is illustrated. Note the relapses that occur after discontinuing cyclosporine therapy (*arrow*). Cyclophosphamide was given for 2 months, and cyclosporine for 9 months. Probability—actuarial probability of remaining relapse-free. (*From* Ponticelli and coworkers [4]; with permission.)

Focal Segmental Glomerulosclerosis

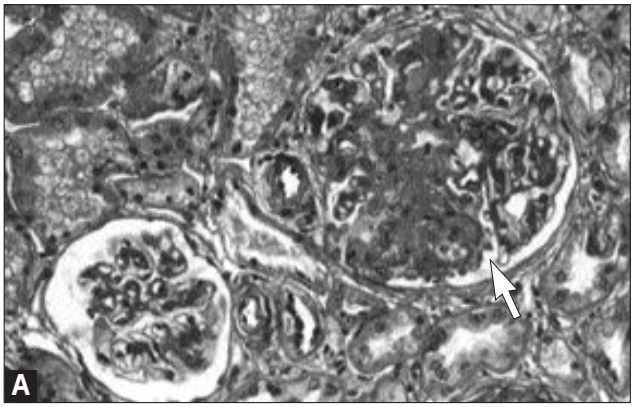

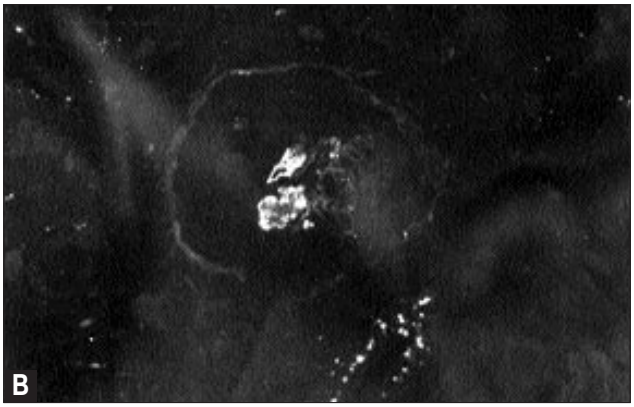

FIGURE 2-8

Light and immunofluorescent microscopy in focal segmental glomerulosclerosis (FSGS). Patients with FSGS exhibit massive proteinuria (usually nonselective), hypertension, hematuria, and renal functional impairment. Patients with nephrotic syndrome often are not responsive to corticosteroid therapy. Progression to chronic renal failure occurs over many years, although in some patients renal failure may occur in only a few years. **A**, This glomerulopathy is defined primarily by its appearance on light microscopy. Only a portion of the glomerular population, initially in the deep cortex, is affected. The abnormal glomeruli exhibit segmental obliteration of capillaries by increased extracellular matrix–basement membrane material, collapsed capillary walls, or large insudative lesions. These lesions are called hyalinosis (arrow) and are composed of immunoglobulin M and complement C3 (**B**, IgM immunofluorescence). The other glomeruli usually are enlarged but may be of normal size. In some patients, mesangial hypercellularity may be a feature. Focal tubular atrophy with interstitial fibrosis invariably is present.

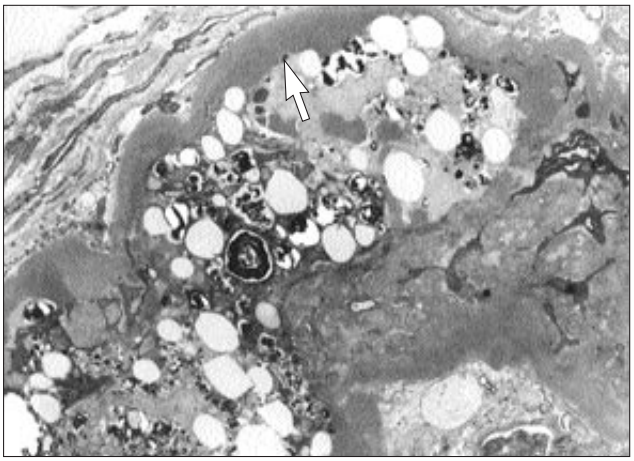

FIGURE 2-9

Electron microscopy of focal segmental glomerulosclerosis. The electron microscopic findings in the involved glomeruli mirror the light microscopic features, with capillary obliteration by dense hyaline "deposits" (*arrow*) and lipids. The other glomeruli exhibit primarily foot process effacement, occasionally in a patchy distribution.

CLASSIFICATION OF FOCAL SEGMENTAL GLOMERULOSCLEROSIS WITH HYALINOSIS

Primary (Idiopathic)
- Classic
- Tip lesion
- Collapsing

Secondary
- Human immunodeficiency virus–associated
- Heroin abuse
- Vesicoureteric reflux nephropathy
- Oligonephronia (congenital absence or hypoplasia of one kidney)
- Obesity
- Analgesic nephropathy
- Hypertensive nephrosclerosis
- Sickle cell disease
- Transplantation rejection (chronic)
- Vasculitis (scarring)
- Immunoglobulin A nephropathy (scarring)

FIGURE 2-10

Note that a variety of disease processes can lead to the lesion of focal segmental glomerulosclerosis. Some of these are the result of infections, whereas others are due to loss of nephron population. Focal sclerosis may also complicate other primary glomerular diseases (*eg*, Immunoglobulin A nephropathy).

CLASSIFICATION OF MEMBRANOUS GLOMERULONEPHRITIS

Primary (Idiopathic)

Secondary
- Neoplasia (carcinoma, lymphoma)
- Autoimmune disease (systemic lupus erythematosus thyroiditis)
- Infectious diseases (hepatitis B, hepatitis C, schistosomiasis)
- Drugs (gold, mercury, nonsteroidal anti-inflammatory drugs, probenecid, captopril)
- Other causes (kidney transplantation, sickle cell disease, sarcoidosis)

FIGURE 2-11

Most adult patients (75%) have primary or idiopathic disease. Most children have some underlying disease, especially viral infection. It is not uncommon for adults over the age of 60 years to have an underlying carcinoma (especially lung, colon, stomach, or breast).

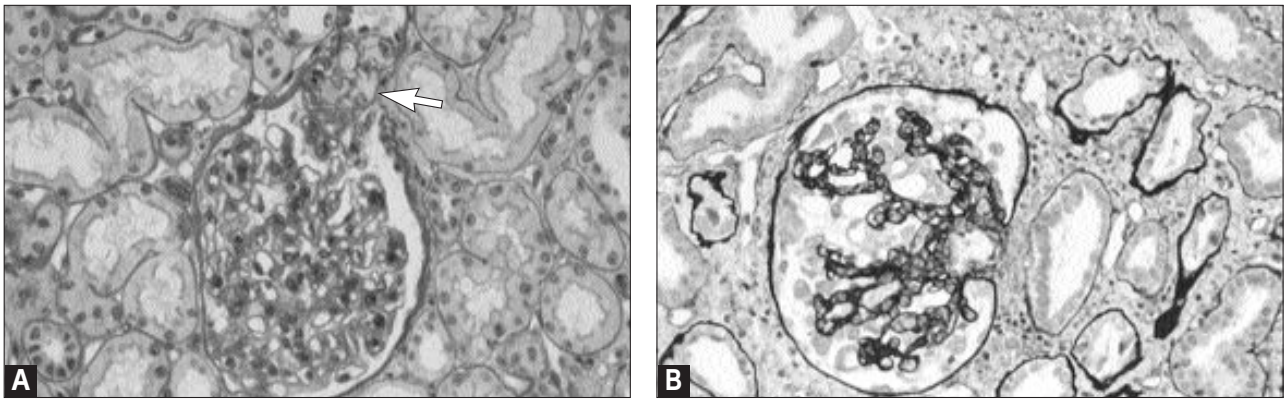

FIGURE 2-12

Histologic variations of focal segmental glomerulosclerosis (FSGS). Two important variants of FSGS exist. In contrast to the histologic appearance of the involved glomeruli, with the sclerotic segment in any location in the glomerulus, the glomerular tip lesion (**A**) is characterized by segmental sclerosis at an early stage of evolution, at the tubular pole (tip) of all affected glomeruli (*arrow*). Capillaries contain monocytes with abundant cytoplasmic lipids (foam cells), and the overlying visceral epithelial cells are enlarged and adherent to cells of the most proximal portion of the proximal tubule. Some investigators have described a more favorable response to steroids and a more benign clinical course.

The other variant, known as *collapsing glomerulopathy*, most likely represents a virulent form of FSGS. In this form of FSGS, most visceral epithelial cells are enlarged and coarsely vacuolated and most capillary walls are wrinkled or collapsed (**B**). These features indicate a severe lesion, with a corresponding rapidly progressing clinical course of the disease. Integral and concomitant acute abnormalities of tubular epithelia and interstitial edema occur.

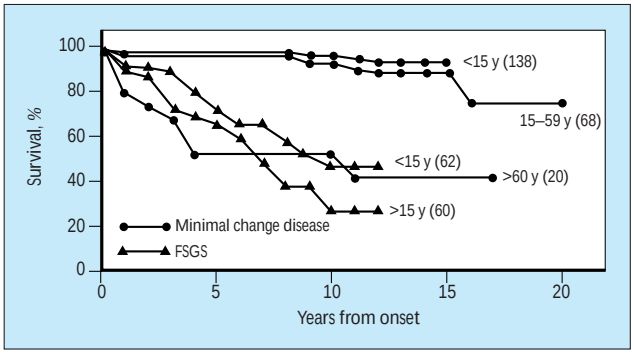

FIGURE 2-13

Evolution of focal segmental glomerulosclerosis (FSGS). This graph compares the renal functional survival rate of patients with FSGS to that seen in patients with minimal change disease (in adults and children). Note the poor prognosis, with about a 50% rate of renal survival at 10 years. (*From* Cameron [2]; with permission.)

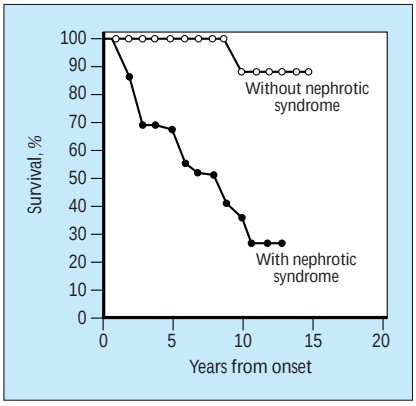

FIGURE 2-14

The outcome of focal segmental glomerulosclerosis according to the degree of proteinuria at presentation is shown. Note the favorable prognosis in the absence of nephrotic syndrome. Spontaneous or therapeutically induced remissions have a similar beneficial effect on long-term outcome. (*From* Ponticelli, *et al.* [5]; with permission.)

Membranous Glomerulonephritis

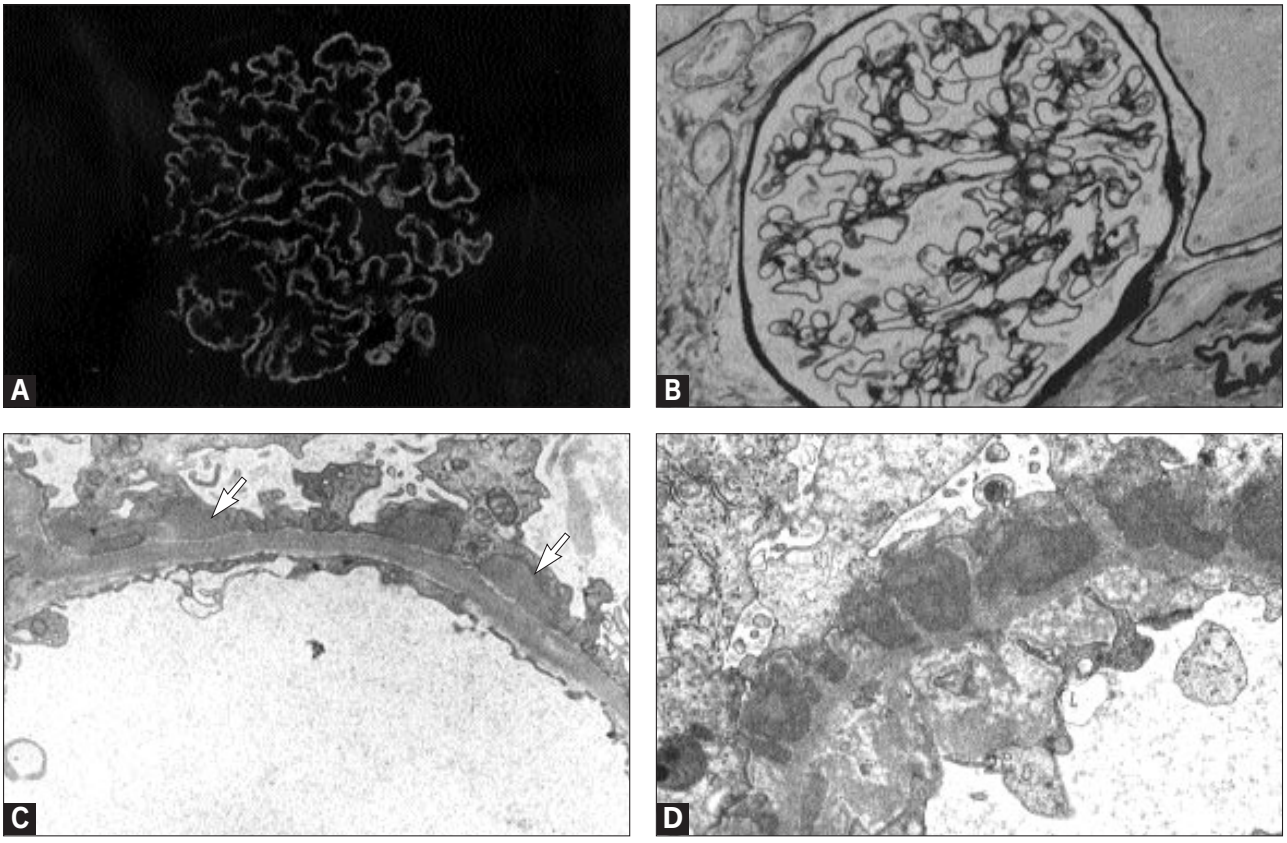

FIGURE 2-15 (*see* Color Plate)
Light, immunofluorescent, and electron microscopy in membranous glomerulonephritis. Membranous glomerulonephritis is an immune complex–mediated glomerulonephritis, with the immune deposits localized to subepithelial aspects of almost all glomerular capillary walls. Membranous glomerulonephritis is the most common cause of nephrotic syndrome in adults in developed countries. In most instances (75%), the disease is idiopathic and the antigen(s) of the immune complexes are unknown. In the remainder, membranous glomerulonephritis is associated with well-defined diseases that often have an immunologic basis (*eg*, systemic lupus erythematosus and hepatitis B or C virus infection); some solid malignancies (especially carcinomas); or drug therapy, such as gold, penicillamine, captopril, and some nonsteroidal anti-inflammatory reagents. Treatment is controversial.

The changes by light and electron microscopy mirror one another quite well and represent morphologic progression that is likely dependent on duration of the disease. **A**, At all stages immunofluorescence discloses the presence of uniform granular capillary wall deposits of immunoglobulin G and complement C3. **B**, In the early stage the deposits are small and without other capillary wall changes; hence, on light microscopy, glomeruli often are normal in appearance. **C**, On electron microscopy, small electron-dense deposits (*arrows*) are observed in the subepithelial aspects of capillary walls. **D**, In the intermediate stage the deposits are partially encircled by basement membrane material. **E**, When viewed with periodic acid-methenamine stained sections, this abnormality appears as spikes of basement membrane perpendicular to the basement membrane, with adjacent nonstaining deposits. Similar features are evident on electron microscopy, with dense deposits and intervening basement membrane (**D**). Late in the disease the deposits are completely surrounded by basement membranes and are undergoing resorption.

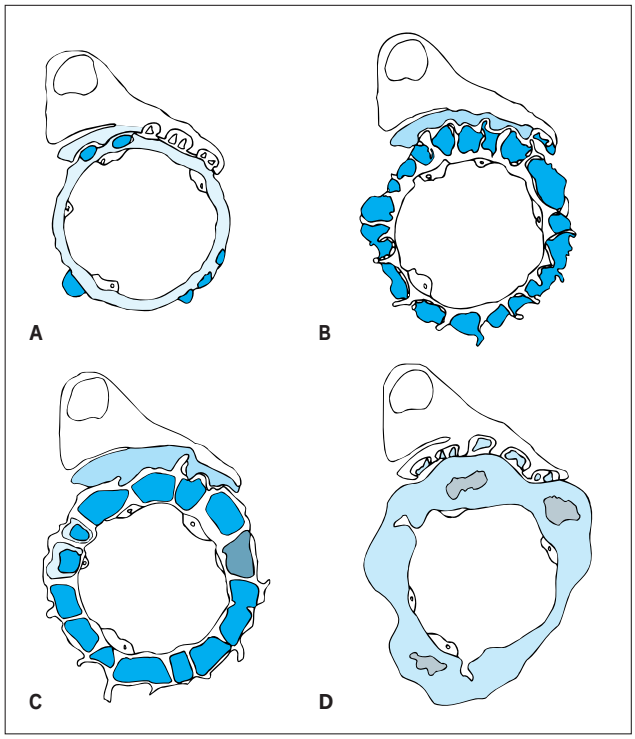

FIGURE 2-16
Evolution of deposits in membranous glomerulonephritis. This schematic illustrates the sequence of immune deposits in red; basement membrane (BM) alterations in blue; and visceral epithelial cell changes in yellow. Small subepithelial deposits in membranous glomerulonephritis (predominately immunoglobulin G) initially form (**A**) then coalesce. BM expansion results first in spikes (**B**) and later in domes (**C**) that are associated with foot process effacement, as shown in gray. In later stages the deposits begin to resorb (dotted and crosshatched areas) and are accompanied by thickening of the capillary wall (**D**). (*From* Churg, *et al.* [6]; with permission.)

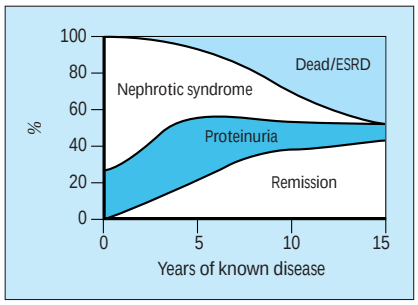

FIGURE 2-17
Natural history of membranous glomerulonephritis. This schematic illustrates the clinical evolution of idiopathic membranous glomerulonephritis over time. Almost half of all patients undergo spontaneous or therapy-related remissions of proteinuria. Another group of patients (25–40%), however, eventually develop chronic renal failure, usually in association with persistent proteinuria in the nephrotic range. (*From* Cameron [2]; with permission.)

Membranoproliferative Glomerulonephritis

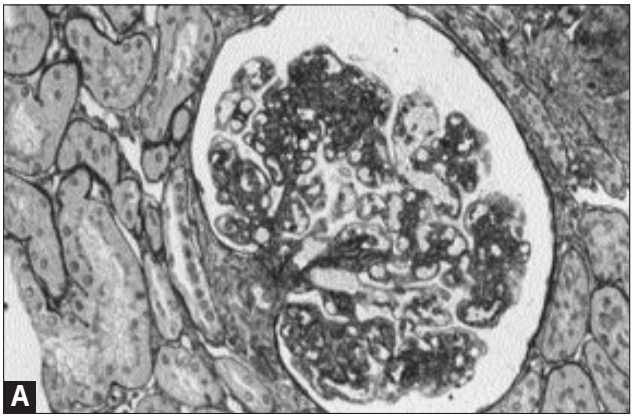

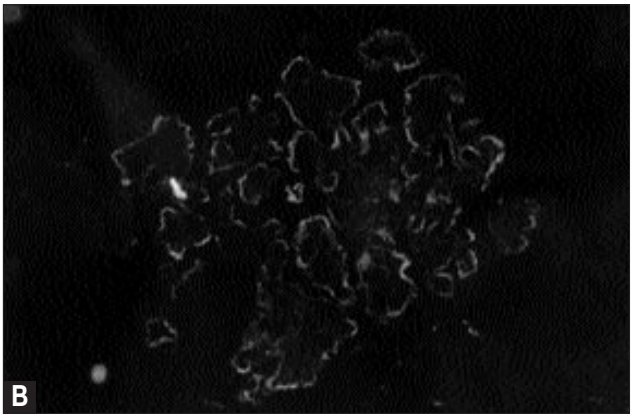

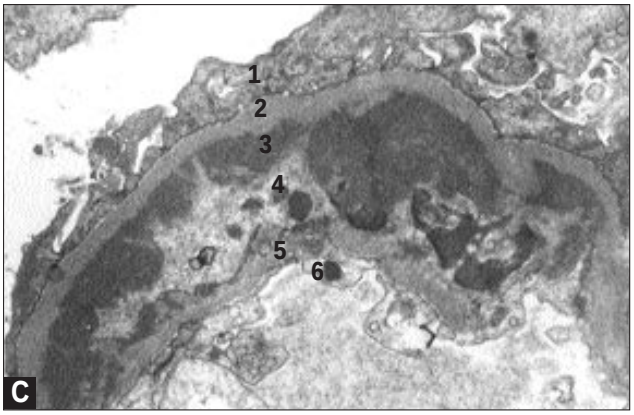

FIGURE 2-18 (*see* Color Plate)
Light, immunofluorescence, and electron microscopy in membranoproliferative glomerulonephritis type I. In these types of immune complex–mediated glomerulonephritis, patients often exhibit nephrotic syndrome accompanied by hematuria and depressed levels of serum complement C3. The morphology is varied, with at least three pathologic subtypes, only two of which are at all common. The first, known as *membranoproliferative (mesangiocapillary) glomerulonephritis type I*, is a primary glomerulopathy most common in children and adolescents. The same pattern of injury may be observed during the course of many diseases with chronic antigenemic states; these include systemic lupus erythematosus and hepatitis C virus and other infections. In membranoproliferative glomerulonephritis type I, the glomeruli are enlarged and have increased mesangial cellularity and variably increased matrix, resulting in lobular architecture. The capillary walls often are thickened with double contours, an abnormality resulting from peripheral migration and interposition of mesangium (**A**). Immunofluorescence discloses granular to confluent granular deposits of C3 (**B**), immunoglobulin G, and immunoglobulin M in the peripheral capillary walls and mesangial regions. The characteristic finding on electron microscopy is in the capillary walls. **C**, Between the basement membrane and endothelial cells are, in order inwardly: (1) epithelial cell, (2) basement membrane, (3) electron-dense deposits, (4) mesangial cell cytoplasm, (5) mesangial matrix, and (6) endothelial cell. Electron-dense deposits also are in the central mesangial regions. Subepithelial deposits may be present, albeit typically in small numbers. The electron-dense deposits may contain an organized (fibrillar) substructure, especially in association with hepatitis C virus infection and cryoglobulemia.

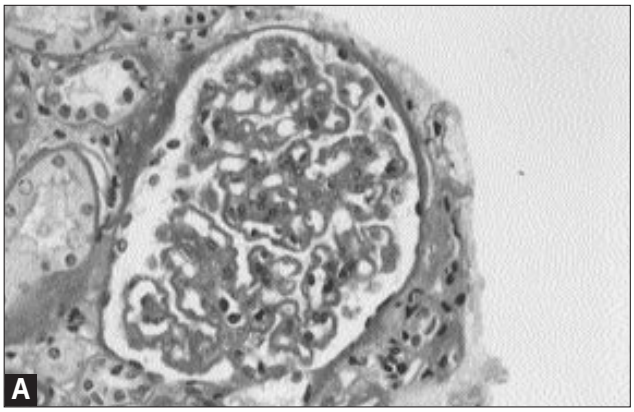

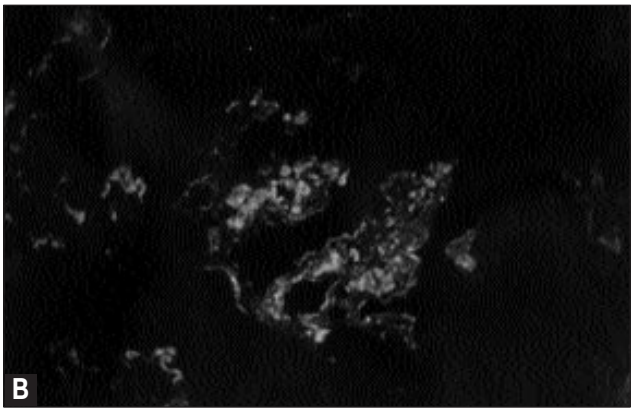

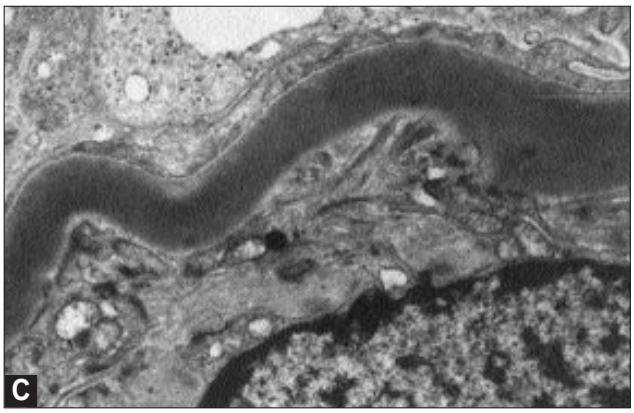

FIGURE 2-19 (*see* Color Plate)
Light, immunofluorescence, and electron microscopy in membranoproliferative glomerulonephritis type II. In this disease, also known as *dense deposit disease*, the glomeruli may be lobular or may manifest only mild widening of mesangium. **A**, The capillary walls are thickened, and the basement membranes are stained intensely positive periodic acid–Schiff reaction, with a refractile appearance. **B**, On immunofluorescence, complement C3 is seen in all glomerular capillary basement membranes in a coarse linear pattern. With the use of thin sections, it can be appreciated that the linear deposits actually consist of two thin parallel lines. Round granular deposits are in the mesangium. Coarse linear deposits also are in Bowman's capsule and the tubular basement membranes. **C**, Ultrastructurally, the glomerular capillary basement membranes are thickened and darkly stained; there may be segmental or extensive involvement of the basement membrane. Similar findings are seen in Bowman's capsule and tubular basement membranes; however, in the latter, the dense staining is usually on the interstitial aspect of that structure. Patients with dense deposit disease frequently show isolated C3 depression and may have concomitant lipodystrophy. These patients also have autoantibodies to the C3 convertase enzyme C3Nef.

SERUM COMPLEMENT CONCENTRATIONS IN GLOMERULAR LESIONS

Lesion	Serum Concentration			
	C3	C4	C'H50	Other
Minimal change disease	Normal	Normal	Normal	–
Focal sclerosis	Normal	Normal	Normal	–
Membranous glomerulonephritis (idiopathic)	Normal	Normal	Normal	–
Immunoglobulin A nephropathy	Normal	Normal	Normal	–
Membranoproliferative glomerulonephritis:				
Type I	Moderate decrease	Mild decrease	Mild decrease	–
Type II	Severe decrease	Normal	Mild decrease	C3 nephritic factor+
Acute poststreptococcal glomerulonephritis	Moderate decrease	Normal	Mild decrease	Antistreptolysin 0 titer increased
Lupus nephritis:				
(World Health Organization Class IV)	Moderate to severe decrease	Moderate to severe decrease	Mild decrease	anti–double-stranded DNA antibody+
(World Health Organization Class V)	Normal or mild decrease	Normal or mild decrease	Normal or mild decrease	anti–double-stranded DNA antibody+
Cryoglobulinemia (hepatitis C)	Normal or mild decrease	Severe decrease	Moderate decrease	Cryoglobulins; hepatitis C ab
Amyloid	Normal	Normal	Normal	–
Vasculitis	Normal or increased	Normal or increased	Normal	Antineutrophil cytoplasmic antibody+

C'H50—serum hemolytic complement activity.

FIGURE 2-20

The serum complement component concentration (C3 and C4) and serum hemolytic complement activity (C'H50) in various primary and secondary glomerular lesions are depicted. Note the limited number of disorders associated with a low C3 or C4 level.

CLASSIFICATION OF MEMBRANOPROLIFERATIVE GLOMERULONEPHRITIS TYPE I

Primary (Idiopathic)
Secondary
- Hepatitis C (with or without cryoglobulinemia)
- Hepatitis B
- Systemic lupus erythematosus
- Light or heavy chain nephropathy
- Sickle cell disease
- Sjögren's syndrome
- Sarcoidosis
- Shunt nephritis
- Antitrypsin deficiency
- Quartan malaria
- Chronic thrombotic microangiopathy
- Buckley's syndrome

FIGURE 2-21

Note that although there is the wide variety of underlying causes for the lesion of membranoproliferative glomerulonephritis hepatitis C, with or without cryoglobulinemia, accounts for most cases.

Mesangial Proliferative Glomerulonephritis

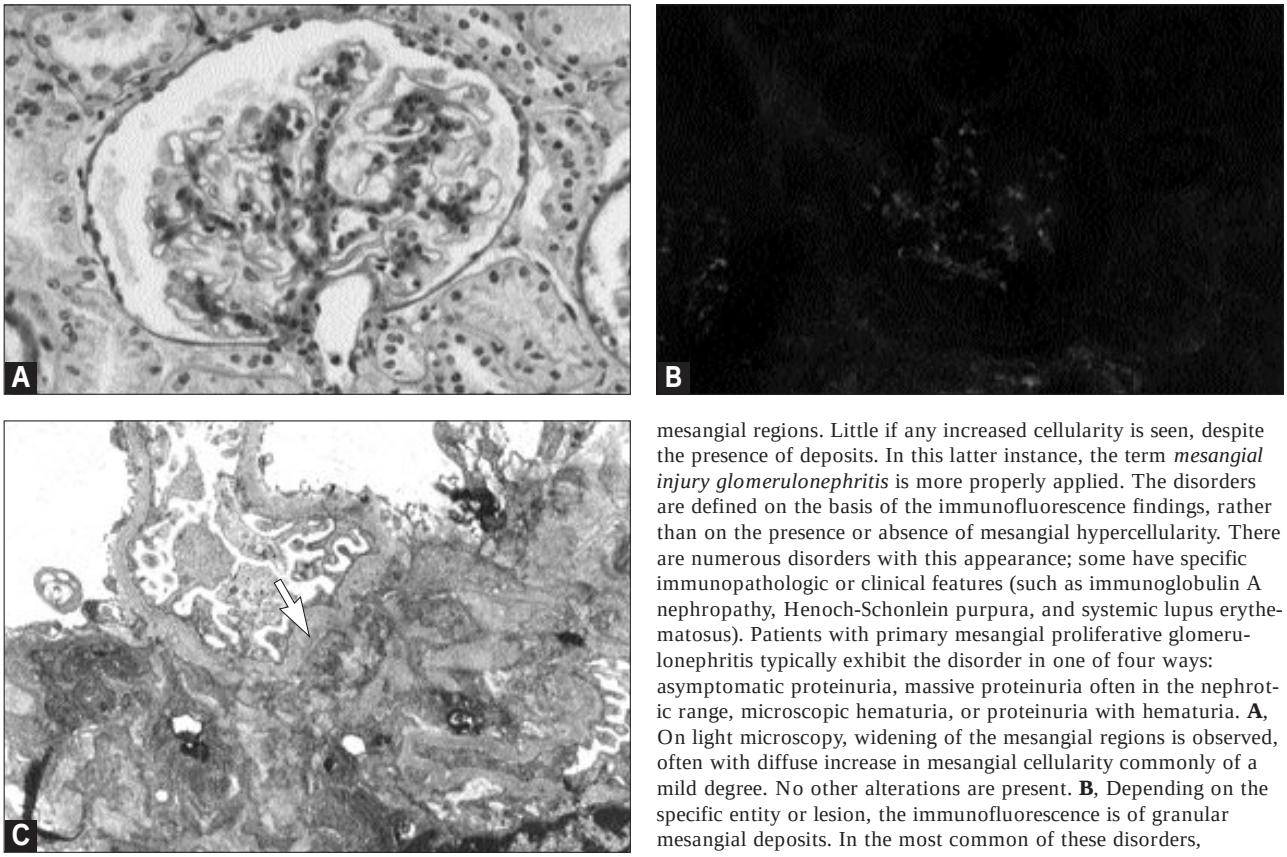

FIGURE 2-22 (*see* Color Plate)
Light, immunofluorescence, and electron microscopy in mesangial proliferative glomerulonephritis. This heterogeneous group of disorders is characterized by increased mesangial cellularity in most of the glomeruli associated with granular immune deposits in the mesangial regions. Little if any increased cellularity is seen, despite the presence of deposits. In this latter instance, the term *mesangial injury glomerulonephritis* is more properly applied. The disorders are defined on the basis of the immunofluorescence findings, rather than on the presence or absence of mesangial hypercellularity. There are numerous disorders with this appearance; some have specific immunopathologic or clinical features (such as immunoglobulin A nephropathy, Henoch-Schonlein purpura, and systemic lupus erythematosus). Patients with primary mesangial proliferative glomerulonephritis typically exhibit the disorder in one of four ways: asymptomatic proteinuria, massive proteinuria often in the nephrotic range, microscopic hematuria, or proteinuria with hematuria. **A**, On light microscopy, widening of the mesangial regions is observed, often with diffuse increase in mesangial cellularity commonly of a mild degree. No other alterations are present. **B**, Depending on the specific entity or lesion, the immunofluorescence is of granular mesangial deposits. In the most common of these disorders, immunoglobulin M is the dominant or sole deposit. Other disorders are characterized primarily or exclusively by complement C3, immunoglobulin G, or C1q deposits. **C**, On electron microscopy the major finding is of small electron-dense deposits in the mesangial regions (*arrow*). Foot process effacement is variable, depending on the clinical syndrome (*eg*, whether massive proteinuria is present).

Crescentic Glomerulonephritis

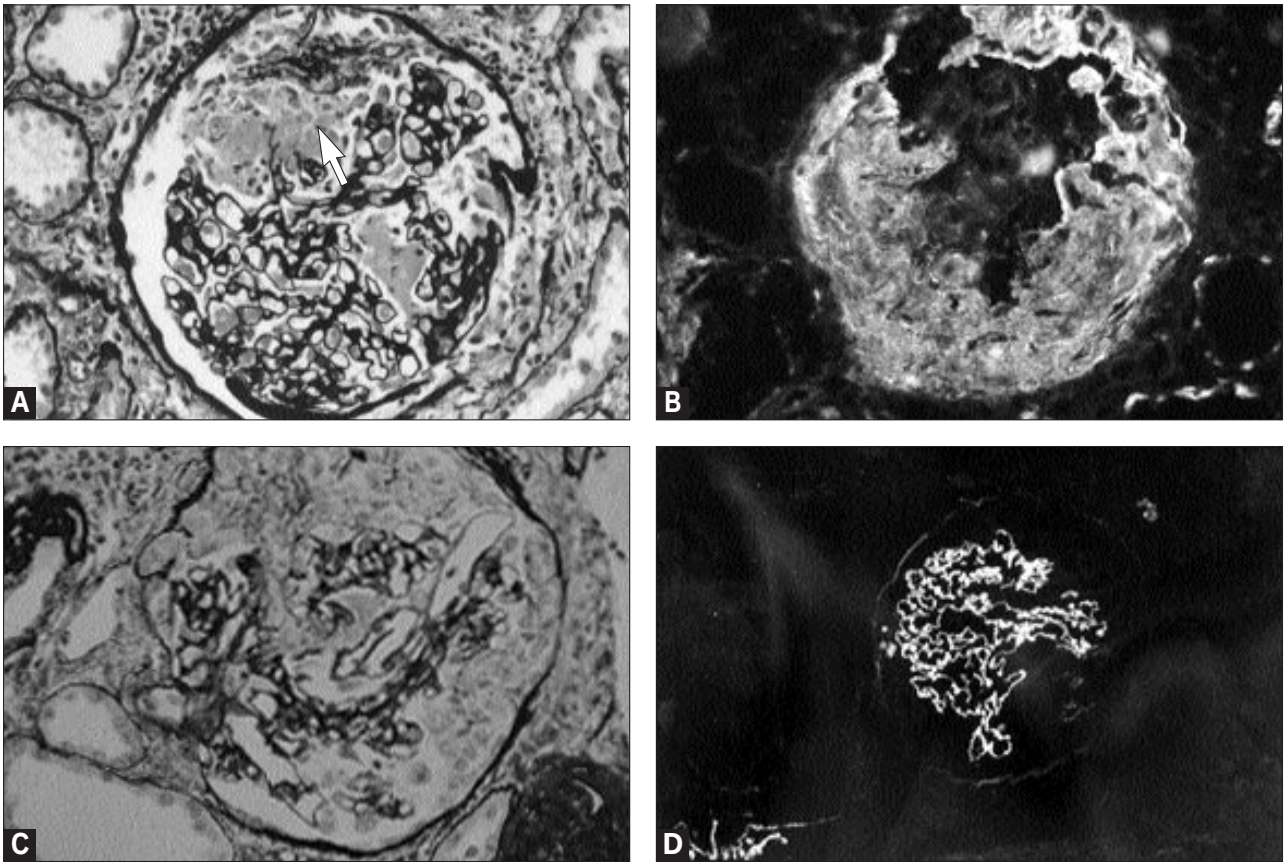

FIGURE 2-23 (*see* Color Plate)

Crescentic glomerulonephritis. A crescent is the accumulation of cells and extracellular material in the urinary space of a glomerulus. The cells are parietal and visceral epithelia as well as monocytes and other blood cells. The extracellular material is fibrin, collagen, and basement membrane material. In the early stages of the disease, the crescents consist of cells and fibrin. In the later stages the crescents undergo organization, with disappearance of fibrin and replacement by collagen. Crescents represent morphologic consequences of severe capillary wall damage. **A**, In most instances, small or large areas of destruction of capillary walls (cells and basement membranes) are observed (*arrow*), thereby allowing fibrin, other high molecular weight substances, and blood cells to pass readily from capillary lumina into the urinary space. **B**, Immunofluorescence frequently discloses fibrin in the urinary space. **C**, The proliferating cells in Bowman's space ultimately give rise to the typical crescent shape. Whereas crescents may complicate many forms of glomerulonephritis, they are most commonly associated with either antiglomerular basement membrane (AGBM) antibodies or antineutrophil cytoplasmic antibodies (ANCAs). The clinical manifestations are typically of rapidly progressive glomerulonephritis with moderate proteinuria, hematuria, oliguria, and uremia. The immunomorphologic features depend on the basic disease process. On light microscopy in both AGBM antibody–induced disease and ANCA–associated crescentic glomerulonephritis, the glomeruli without crescents often have a normal appearance. It is the remaining glomeruli that are involved with crescents. **D**, Anti-GBM disease is characterized by linear deposits of immunoglobulin G and often complement C3 in all capillary basement membranes, and in approximately two thirds of affected patients in tubular basement membranes. The ANCA-associated lesion typically has little or no immune deposits on immunofluorescence; hence the term *pauci-immune crescentic glomerulonephritis* is used. By electron microscopy, as on light microscopy, defects in capillary wall continuity are easily identified. Both AGBM- and ANCA-associated crescentic glomerulonephritis can be complicated by pulmonary hemorrhage (*see* Fig. 2-25).

CLASSIFICATION OF CRESCENTIC GLOMERULONEPHRITIS

Type	Serologic Pattern	Primary	Secondary
I	Anti-GBM+ ANCA-	Anti-GBM antibody–mediated crescentic glomerular nephritis	Goodpasture's disease
II	Anti-GBM- ANCA-	Idiopathic crescentic glomerular nephritis (with or without immune complex deposits)	Systemic lupus erythematosus, immunoglobulin A, MPGN cryoimmunoglobulin (with immune complex deposits
III	Anti-GBM- ANCA+	Pauci-immune crescentic glomerular nephritis (microscopic polyangiitis)	Drug-induced crescentic glomerulonephritis
IV	Anti-GBM+ANCA+	Anti-GBM antibody–mediated crescentic glomerular nephritis with ANCA	Goodpasture's syndrome with ANCA

ANCA—antineutrophil cytoplasmic antibody; anti-GBM—glomerular basement membrane antibody; MPGN— membranoproliferative glomerulonephritis.

FIGURE 2-24

Note that the serologic findings allow for a differentiation of the various forms of primary and secondary (*eg*, multisystem disease) forms of crescentic glomerulonephritis.

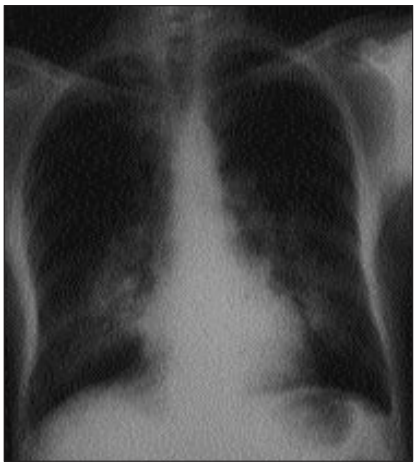

FIGURE 2-25

Chest radiograph of alveolar hemorrhage. This patient has antiglomerular basement membrane–mediated glomerulonephritis complicated by pulmonary hemorrhage (Goodpasture's disease). Note the butterfly appearance of the alveolar infiltrates characteristic of intrapulmonary (alveolar) hemorrhage. Such lesions can also occur in patients with antineutrophil cytoplasmic autoantibody–associated vasculitis and glomerulonephritis, lupus nephritis (SLE), cryoglobulinemia, and rarely in Henoch-Schonlein purpura (HSP).

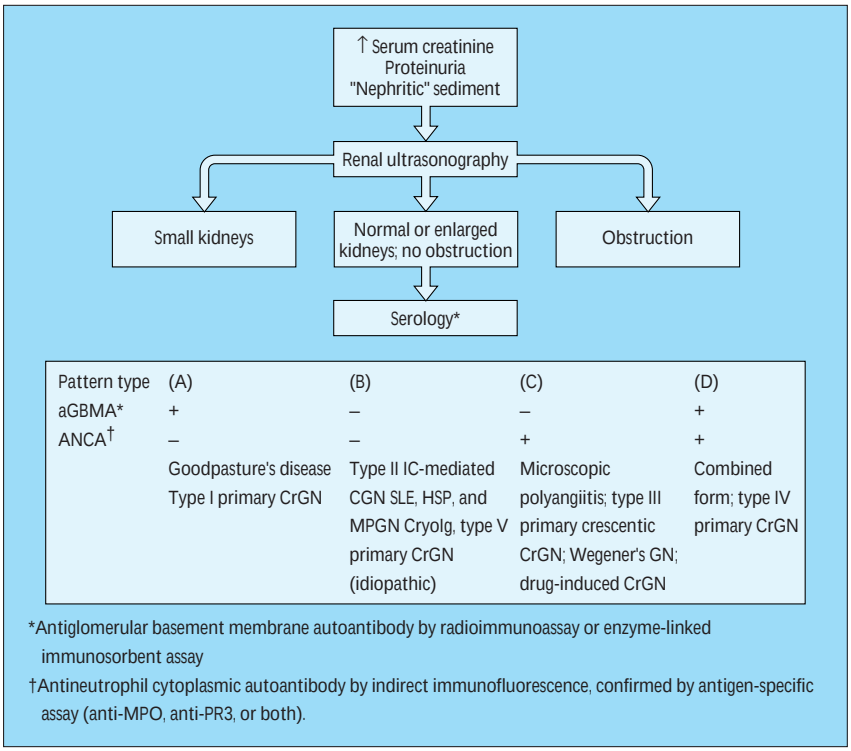

Pattern type	(A)	(B)	(C)	(D)
aGBMA*	+	–	–	+
ANCA†	–	–	+	+
	Goodpasture's disease Type I primary CrGN	Type II IC-mediated CGN SLE, HSP, and MPGN Cryolg, type V primary CrGN (idiopathic)	Microscopic polyangiitis; type III primary crescentic CrGN; Wegener's GN; drug-induced CrGN	Combined form; type IV primary CrGN

*Antiglomerular basement membrane autoantibody by radioimmunoassay or enzyme-linked immunosorbent assay

†Antineutrophil cytoplasmic autoantibody by indirect immunofluorescence, confirmed by antigen-specific assay (anti-MPO, anti-PR3, or both).

FIGURE 2-26

Evaluation of rapidly progressive glomerulonephritis. This algorithm schematically illustrates a diagnostic approach to the various causes of rapidly progressive glomerulonephritis (Figure 2-24), Serologic studies, especially measurement of circulating antiglomerular basement membrane antibodies, antineutrophil cytoplasmic antibodies, antinuclear antibodies, and serum complement component concentrations, are used for diagnosis. Serologic patterns (*A* through *D*)permit categorization of probable disease entities.

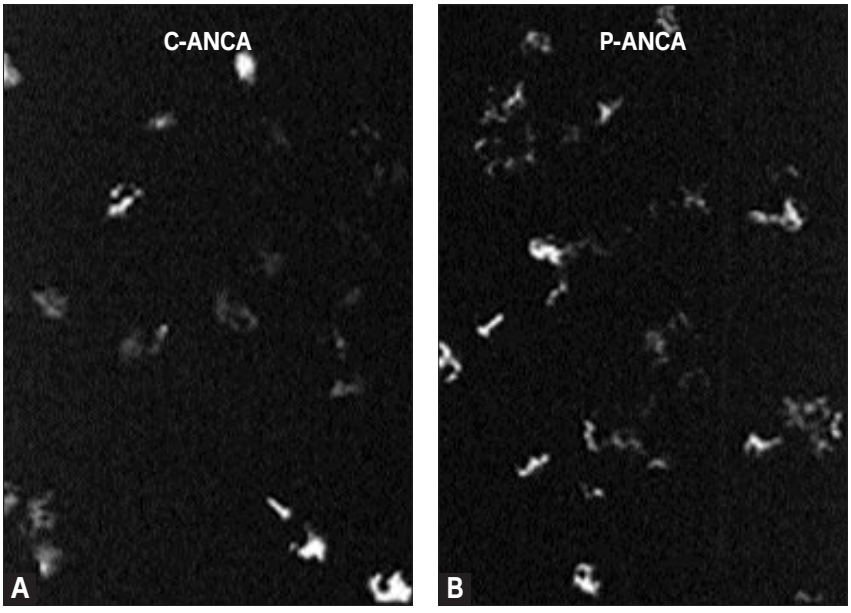

FIGURE 2-27 (*see* Color Plate)

Antineutrophil cytoplasmic autoantibodies (ANCA). Frequently, ANCA are found in crescentic glomerulonephritis, particularly type III (Figure 2-24). Two varieties are seen (on alcohol-fixed slides). **A**, C-ANCA are due to antibodies reacting with cytoplasmic granule antigens (mainly proteinase-3). **B**, P-ANCA are due to antibodies reacting with other antigens (mainly myeloperoxidase).

Immunoglobulin A Nephropathy

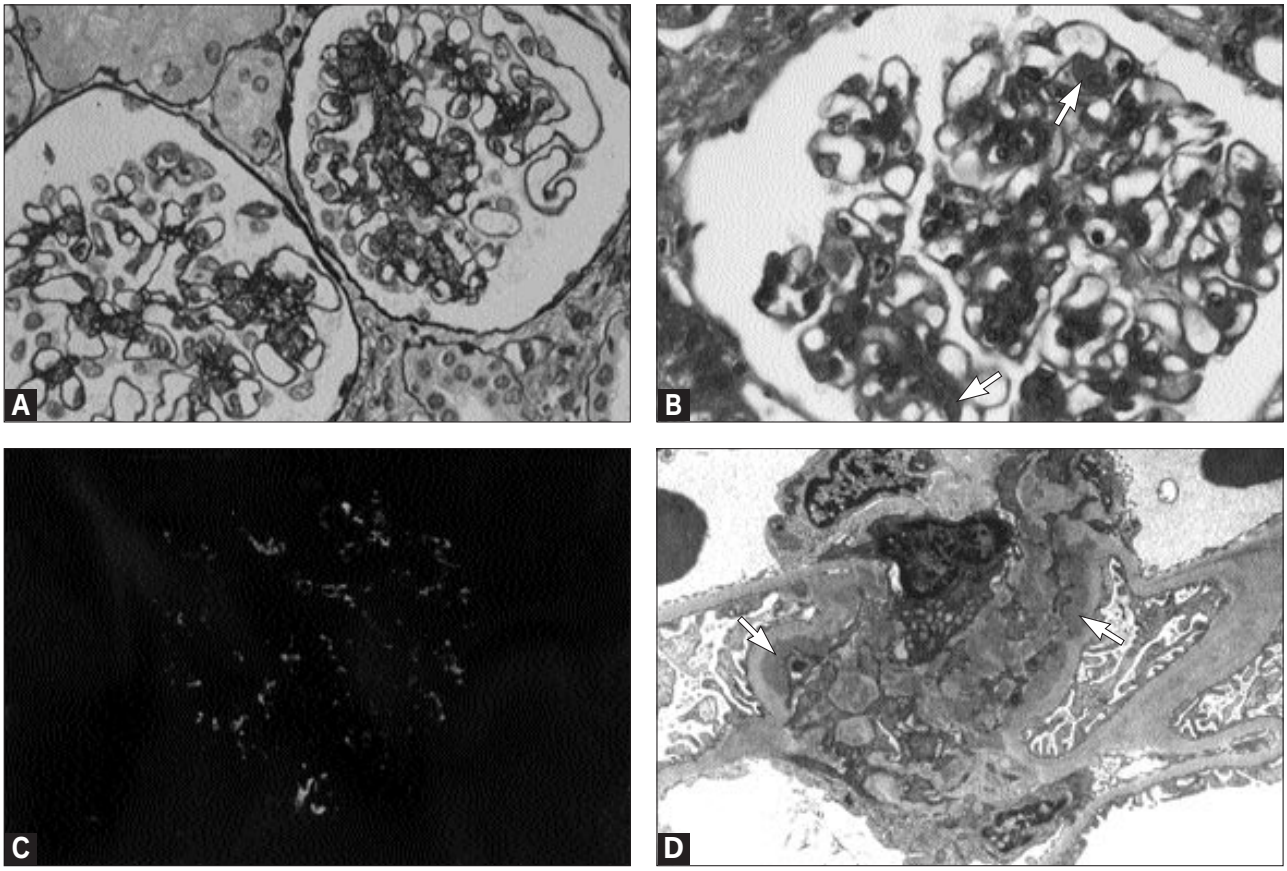

FIGURE 2-28 (*see* Color Plate)

Light, immunofluorescence, and electron microscopy in immunoglobulin A (IgA) nephropathy. IgA nephropathy is a chronic glomerular disease in which IgA is the dominant or sole component of deposits that localize in the mesangial regions of all glomeruli. In severe or acute cases, these deposits also are observed in the capillary walls. This disorder may have a variety of clinical presentations. Typically, the presenting features are recurrent macroscopic hematuria, often coincident with or immediately after an upper respiratory infection, along with persistent microscopic hematuria and low-grade proteinuria between episodes of gross hematuria. Approximately 20% to 25% of patients develop end-stage renal disease over the 20 years after onset. **A**, On light microscopy, widening and often an increase in cellularity in the mesangial regions are observed, a process that affects the lobules of some glomeruli to a greater degree than others. This feature gives rise to the term *focal proliferative glomerulonephritis*. In advanced cases, segmental sclerosis often is present and associated with massive proteinuria. During acute episodes, crescents may be present. **B**, Large round paramesangial fuchsinophilic deposits often are identified with Masson's trichrome or other similar stains (*arrows*). **C**, Immunofluorescence defines the disease; granular mesangial deposits of IgA are seen with associated complement C3, and IgG or IgM, or both. IgG and IgM often are seen in lesser degrees of intensity than is IgA. **D**, On electron microscopy the abnormalities typically are those of large rounded electron-dense deposits (*arrows*) in paramesangial zones of most if not all lobules. Capillary wall deposits (subepithelial, subendothelial, or both) may be present, especially in association with acute episodes. In addition, capillary basement membranes may show segmental thinning and rarefaction.

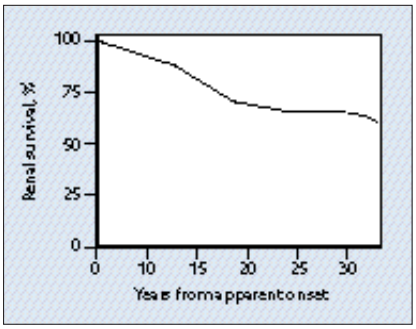

FIGURE 2-29

Natural history of immunoglobulin A (IgA) nephropathy. The evolution of IgA nephropathy over time with respect to the occurrence of end-stage renal failure (ESRF) is illustrated. The percentage of renal survival (freedom from ESRF) is plotted versus the time in years from the apparent onset of the disease. Note that on average about 1.5% of patients enter ESRF each year over the first 20 years of this nephropathy. Factors indicating an unfavorable outcome include elevated serum creatinine, tubulointerstitial lesions or glomerulosclerosis, and moderate proteinuria (>1.0 g/d). (*Modified from* Cameron [2].)

Fibrillary and Immunotactoid Glomerulonephritis

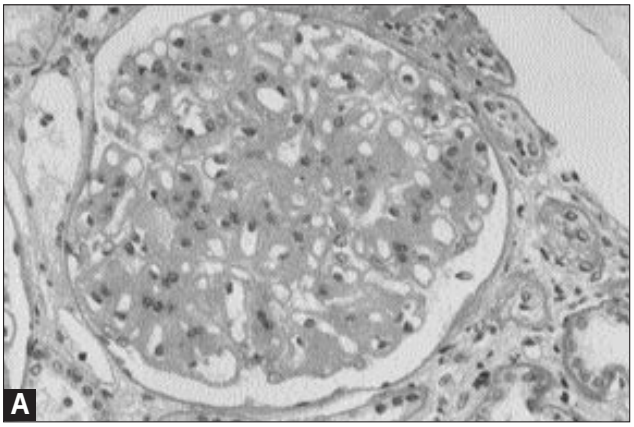

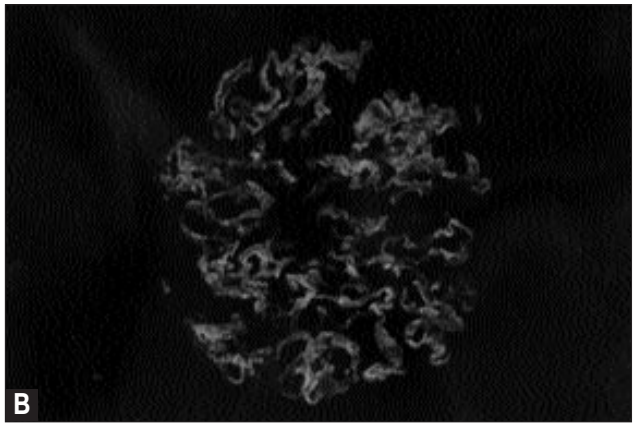

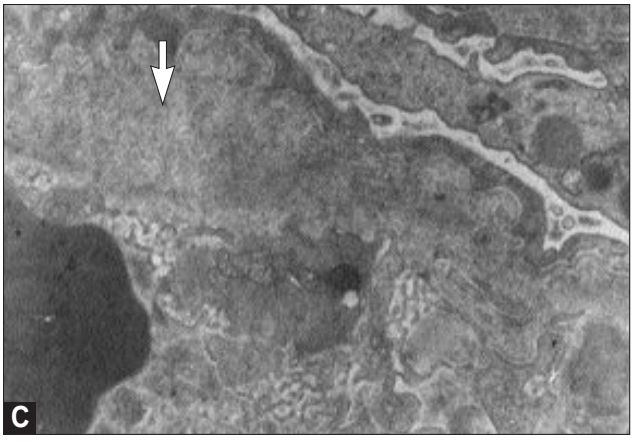

FIGURE 2-30 (*see* Color Plate)

Light, immunofluorescent, and electron microscopy in nonamyloid fibrillary glomerulonephritis. Fibrillary glomerulonephritis is an entity in which abnormal extracellular fibrils, typically ranging from 10- to 20-nm thick, permeate the glomerular mesangial matrix and capillary basement membranes. The fibrils are defined only on electron microscopy and have an appearance, at first glance, similar to amyloid. Congo red stain, however, is negative. Patients with fibrillary glomerulonephritis usually exhibit proteinuria often in the nephrotic range, with variable hematuria, hypertension, and renal insufficiency. **A**, On light microscopy the glomeruli display widened mesangial regions, with variable increase in cellularity and thickened capillary walls and often with irregularly thickened basement membranes, double contours, or both. **B**, On immunofluorescence, there is coarse linear or confluent granular staining of capillary walls for immunoglobulin G and complement C3 and similar staining in the mesangial regions. Occasionally, monoclonal immunoglobulin G κ deposits are identified; in most instances, however, both light chains are equally represented. The nature of the deposits is unknown. **C**, On electron microscopy the fibrils are roughly 20-nm thick, of indefinite length, and haphazardly arranged. The fibrils permeate the mesangial matrix and basement membranes (*arrow*). The fibrils have been infrequently described in organs other than the kidneys.

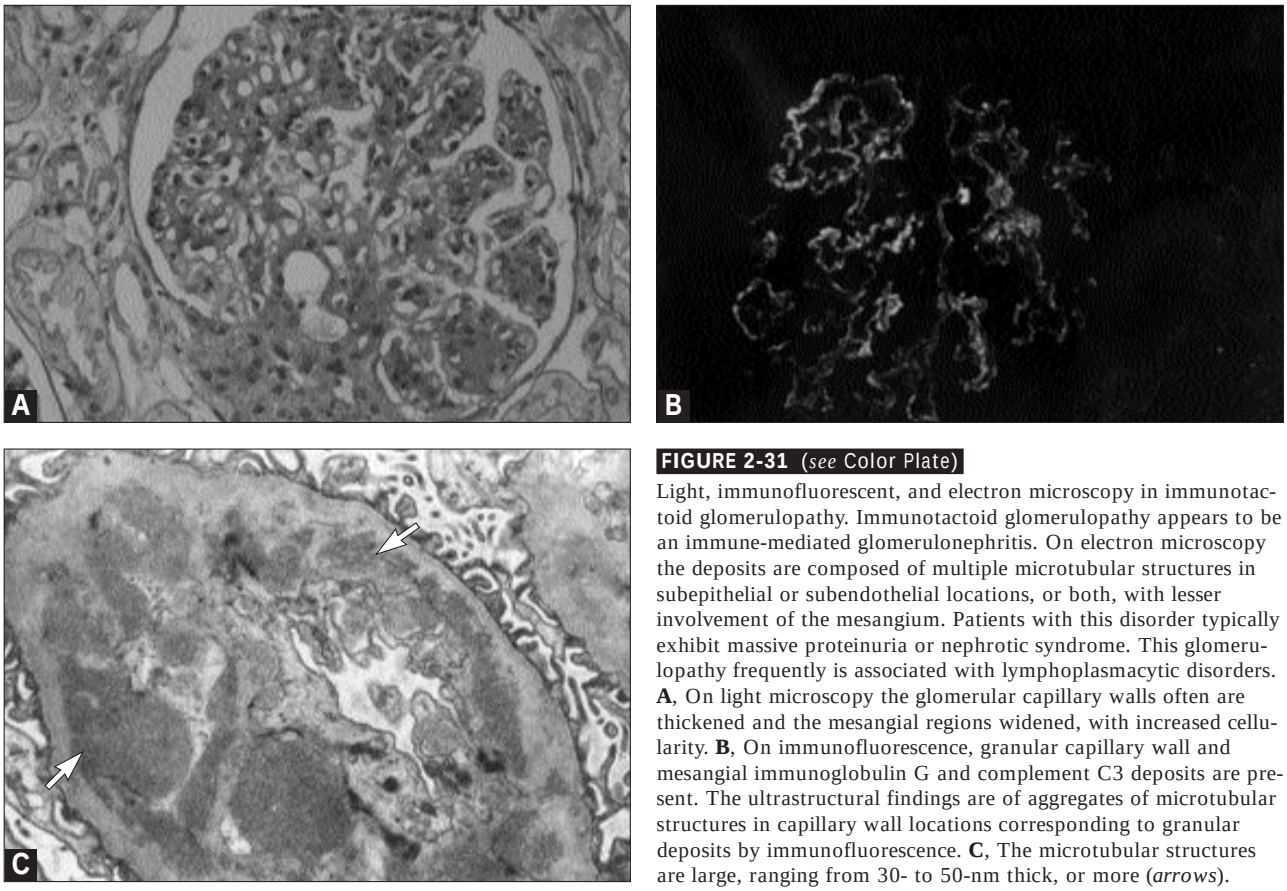

FIGURE 2-31 (*see* Color Plate)

Light, immunofluorescent, and electron microscopy in immunotactoid glomerulopathy. Immunotactoid glomerulopathy appears to be an immune-mediated glomerulonephritis. On electron microscopy the deposits are composed of multiple microtubular structures in subepithelial or subendothelial locations, or both, with lesser involvement of the mesangium. Patients with this disorder typically exhibit massive proteinuria or nephrotic syndrome. This glomerulopathy frequently is associated with lymphoplasmacytic disorders. **A**, On light microscopy the glomerular capillary walls often are thickened and the mesangial regions widened, with increased cellularity. **B**, On immunofluorescence, granular capillary wall and mesangial immunoglobulin G and complement C3 deposits are present. The ultrastructural findings are of aggregates of microtubular structures in capillary wall locations corresponding to granular deposits by immunofluorescence. **C**, The microtubular structures are large, ranging from 30- to 50-nm thick, or more (*arrows*).

Collagenofibrotic Glomerulopathy

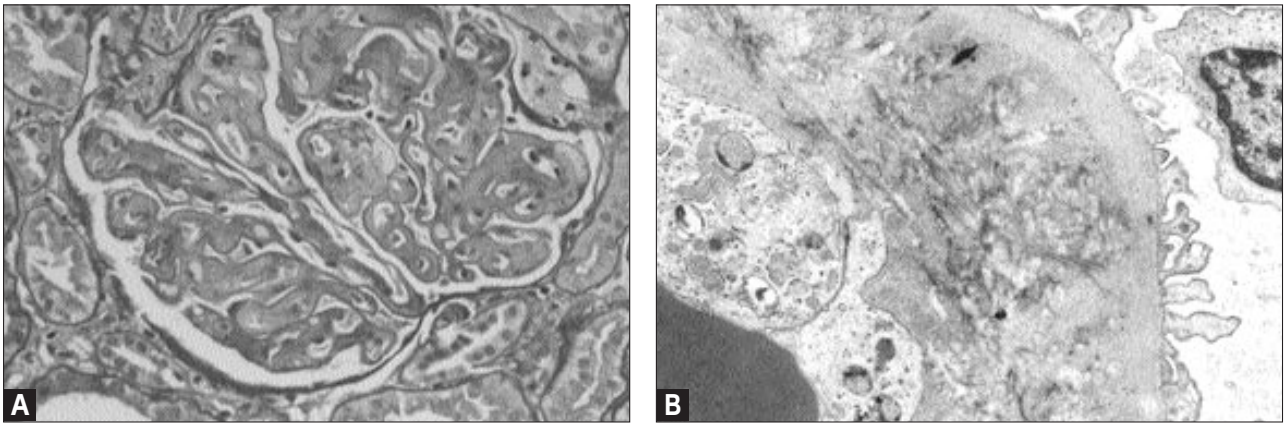

FIGURE 2-32 (see Color Plate)
Collagenofibrotic glomerulopathy (collagen III glomerulopathy). The collagens normally found in glomerular basement membranes and the mesangial matrix are of types IV (which is dominant) and V. In collagenofibrotic glomerulopathy, accumulation of type III collagen occurs largely in capillary walls in a subendothelial location. It is likely that this disease is hereditary; however, because it is very rare, precise information regarding transmission is not known. Collagenofibrotic glomerulopathy originally was thought to be a variant of nail-patella syndrome. Current evidence suggests little relationship exists between the two disorders. Patients with collagen III glomerulopathy often exhibit proteinuria and mild progressive renal insufficiency. For reasons that are not clear, hemolytic-uremic syndrome has evolved in a small number of pediatric patients. **A**, On light microscopy the capillary walls are thickened and mesangial regions widened by pale staining material. These features are in sharp contrast to the normal staining of the capillary basement membranes, as evidenced by the positive period acid–Schiff reaction. With this stain, collagen type III is not stained and therefore is much paler. Amyloid stains (Congo red) are negative. **B**, On electron microscopy, banded collagen fibrils are evident in the subendothelial aspect of the capillary wall.

References

1. Cameron JS, Glassock RJ: The natural history and outcome of the nephrotic syndrome. In *The Nephrotic Syndrome*. Edited by Cameron JS and Glassock RJ. New York: Marcel Dekker, 1987.
2. Cameron JS: The long-term outcome of glomerular diseases. In *Diseases of the Kidney* Vol II, edn 6. Edited by Schrier RW, Gottschalk CW. Boston: Little Brown; 1996.
3. Arbeitsgemeinschaft für pediatrische nephrologie. Cyclophosphamide treatment of steroid-dependent nephrotic syndrome: comparison of an eight-week with a 12-week course. *Arch Dis Child* 1987, 62:1102–1106.
4. Ponticelli C: Cyclosporine versus cyclophosphamide for patients with steroid-dependent and frequently relapsing idiopathic nephrotic syndrome. A multi-center randomized trial. *Nephrol Dial Transplant* 1993, 8:1326–1332.
5. Ponticelli C, Glassock RJ: *Treatment of Segmental Glomerulonephritis*. Oxford: Oxford Medical Publishers, 1996:110.
6. Churg J, Bernstein J, Glassock RJ: *Renal Disease. Classification and Atlas of Glomerular Disease*, edn 2. New York: Igaku-Shoin; 1995.

Heredofamilial and Congenital Glomerular Disorders

Arthur H. Cohen
Richard J. Glassock

The principal characteristics of some of the more common heredofamilial and congenital glomerular disorders are described and illustrated. Diabetes mellitus, the most common heredofamilial glomerular disease, is illustrated in Volume IV, Chapter 1. These disorders are inherited in a variety of patterns (X-linked, autosomal dominant, or autosomal recessive). Many of these disorders appear to be caused by defective synthesis or assembly of critical glycoprotein (collagen) components of the glomerular basement membrane.

CHAPTER

3

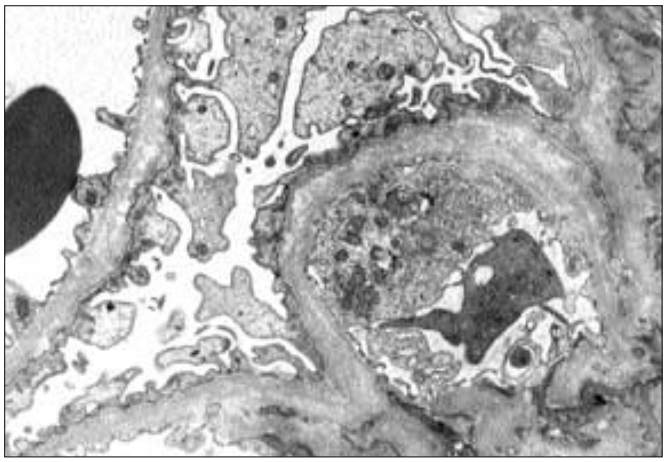

FIGURE 3-1

Alport's syndrome. Alport's syndrome (hereditary nephritis) is a hereditary disorder in which glomerular and other basement membrane collagen is abnormal. This disorder is characterized clinically by hematuria with progressive renal insufficiency and proteinuria. Many patients have neurosensory hearing loss and abnormalities of the eyes. The disease is inherited as an X-linked trait; in some families, however, autosomal recessive and perhaps autosomal dominant forms exist. Clinically, the disease is more severe in males than in females. End-stage renal disease develops in persons 20 to 40 years of age. In some families, ocular manifestations, thrombocytopenia with giant platelets, esophageal leiomyomata, or all of these also occur. In the X-linked form of Alport's syndrome, mutations occur in genes encoding the α-5 chain of type IV collagen (COL4A5). In the autosomal recessive form of this syndrome, mutations of either α-3 or α-4 chain genes have been described. On light microscopy, in the early stages of the disease the glomeruli appear normal. With progression of the disease, however, an increase in the mesangial matrix and segmental sclerosis develop. Interstitial foam cells are common but are not used to make a diagnosis. Results of immunofluorescence typically are negative, except in glomeruli with segmental sclerosis in which segmental immunoglobulin M and complement (C3) are in the sclerotic lesions. Ultrastructural findings are diagnostic and consist of profound abnormalities of glomerular basement membranes. These abnormalities range from extremely thin and attenuated to considerably thickened membranes. The thickened glomerular basement membranes have multiple layers of alternating medium and pale staining strata of basement membrane material, often with incorporated dense granules. The subepithelial contour of the basement membrane typically is scalloped.

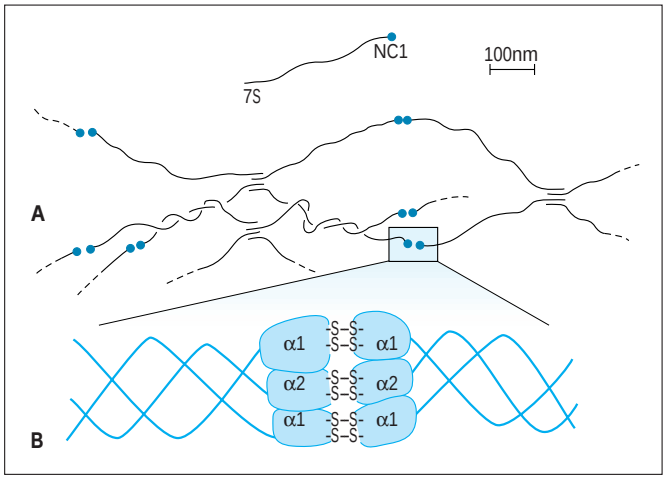

FIGURE 3-2

Schematic of basement membrane collagen type IV. The postulated arrangement of type IV collagen chains in a normal glomerular basement membrane is illustrated. The joining of noncollagen (NC-1) and 75 domains creates a lattice (chicken wire) arrangement (**A**). In the glomerular basement membrane, α1 and α2 chains predominate in the triple helix (**B**), but α3, 4, 5, and 6 chains are also found (not shown). Disruption of synthesis of any of these chains may lead to anatomic and pathologic alternations, such as those seen in Alport's syndrome. Arrows indicate fibrils. (*From* Abrahamson and coworkers [1]; with permission.)

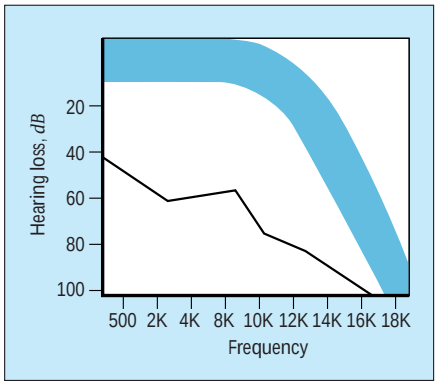

FIGURE 3-3

Neurosensory hearing defect in Alport's syndrome. In patients with adult onset Alport's syndrome, classic X-linked sensorineural hearing defects occur. These defects often begin with an auditory loss of high-frequency tone, as shown in this audiogram. The shaded area represents normal ranges. (*Modified from* Gregory and Atkin [2]; with permission.)

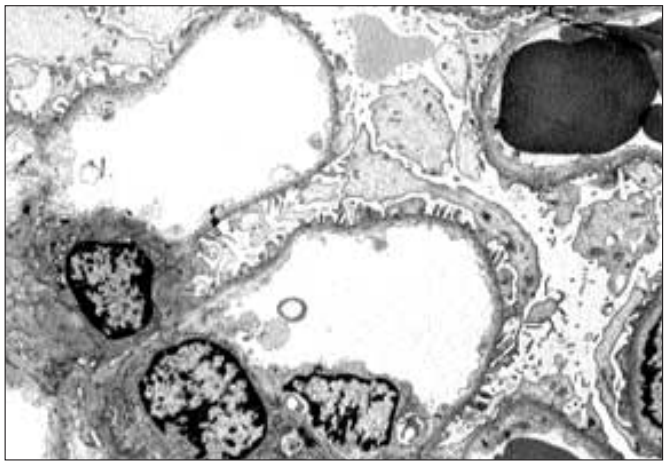

FIGURE 3-4

Thin basement membrane nephropathy. Glomeruli with abnormally thin basement membranes may be a manifestation of benign familial hematuria. Glomeruli with thin basement membranes many also occur in persons who do not have a family history of renal disease but who have hematuria, low-grade proteinuria, or both. Although the ultrastructural abnormalities have some similarities in common with the capillary basement membranes of Alport's syndrome, these two glomerulopathies are not directly related. Clinically, persistent microscopic hematuria or occasional episodic gross hematuria are important features. Nonrenal abnormalities are absent. On light microscopy, the glomeruli are normal; no deposits are seen on immunofluorescence. Here, the electron microscopic abnormalities are diagnostic; all or virtually all glomerular basement membranes are markedly thin (<200 nm in adults) without other features such as splitting, layering, or abnormal subepithelial contours.

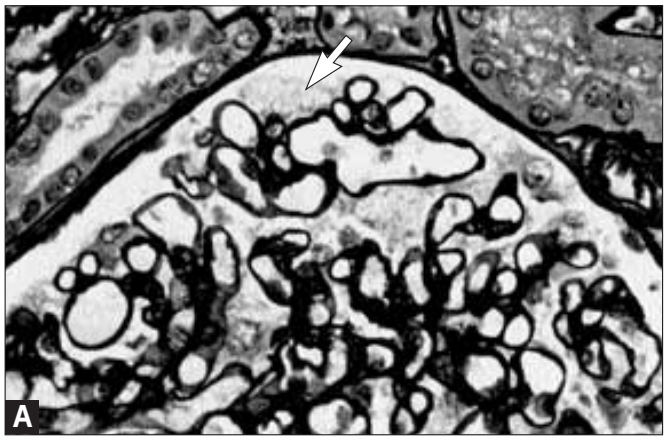

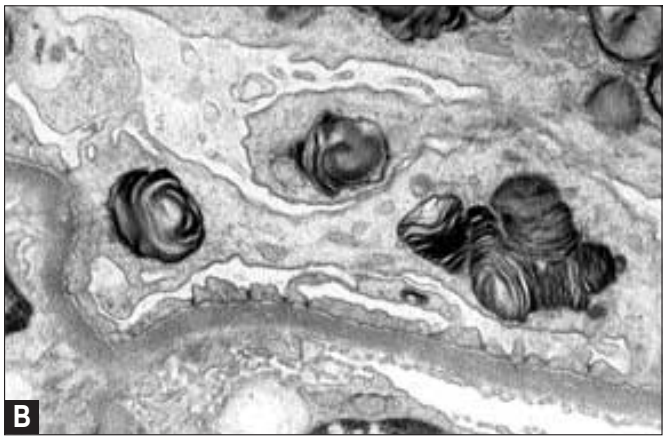

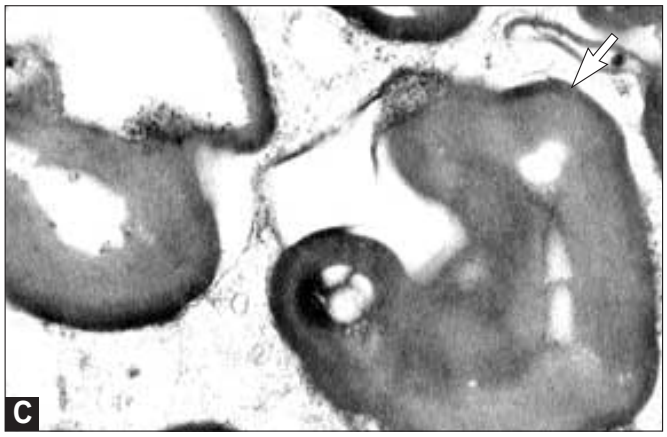

FIGURE 3-5 (*see* Color Plate)

Fabry's disease. Fabry's disease, also known as *angiokeratoma corporis diffusum* or Anderson-Fabry's disease, is the result of deficiency of the enzyme α-galactosidase with accumulation of sphingolipids in many cells. In the kidney, accumulation of sphingolipids especially affects glomerular visceral epithelial cells. Deposition of sphingolipids in the vascular tree may lead to premature coronary artery occlusion (angina or myocardial infarction) or cerebrovascular insufficiency (stroke). Involvement of nerves leads to painful acroparesthesias and decreased perspiration (anhidrosis). The most common renal manifestation is that of proteinuria with progressive renal insufficiency. On light microscopy, the morphologic abnormalities of the glomeruli primarily consist of enlargement of visceral epithelial cells and accumulation of multiple uniform small vacuoles in the cytoplasm (*arrow* in Panel **A**). Ultrastructurally, the inclusions are those of whorled concentric layers appearing as "zebra bodies" or myeloid bodies representing sphingolipids (**B**). These structures also may be observed in mesangial and endothelial cells and in arterial and arteriolar smooth muscle cells and tubular epithelia. At considerably higher magnification, the inclusions are observed to consist of multiple concentric alternating clear and dark layers, with a periodicity ranging from 3.9 to 9.8 nm. This fine structural appearance (best appreciated at the *arrow*) is characteristic of stored glycolipids (**C**).

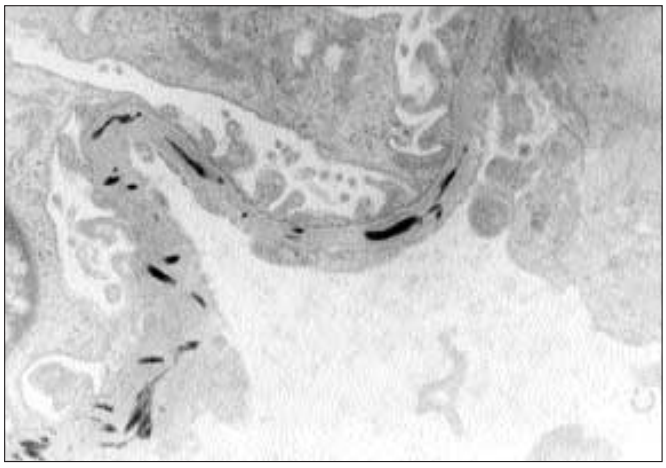

FIGURE 3-6

Electron microscopy of nail-patella syndrome. This disorder having skeletal and renal manifestations affects the glomeruli, with accumulation of banded collagen fibrils within the substance of the capillary basement membrane. This accumulation appears as empty lacunae when the usual stains with electron microscopy (lead citrate and uranyl acetate) are used. However, as here, the fibrils easily can be identified with the use of phosphotungstic acid stain in conjunction with or instead of typical stains. Note that this disorder differs structurally from collagen type III glomerulopathy in which the collagen fibrils are subendothelial and not intramembranous in location. Patients with nail-patella syndrome may develop proteinuria, sometimes in the nephrotic range, with variable progression to end-stage renal failure. No distinguishing abnormalities are seen on light microscopy.

FIGURE 3-7

Radiography of nail-patella syndrome. The skeletal manifestations of nail-patella syndrome are characteristic and consist of absent patella and absent and dystrophic nails. These photographs illustrate absent patella (**A**) and the characteristic nail changes (**B**) that occur in patients with the disorder. (*From* Gregory and Atkin [2]; with permission.)

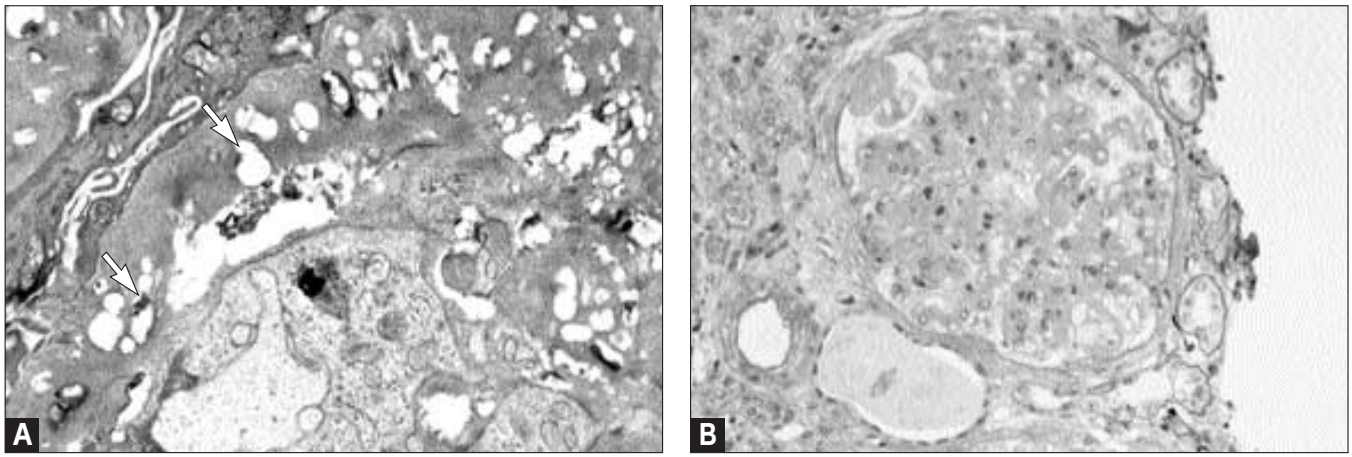

FIGURE 3-8 (*see* Color Plate)

Lecithin-cholesterol acyl transferase deficiency. Lipid accumulation occurs in this hereditary metabolic disorder, especially in extracellular sites throughout glomerular basement membranes and the mesangial matrix. **A**, On electron microscopy the lipid appears as multiple small lacunae, often with small round dense granular or membranous structures (*arrows*). Lipid-containing monocytes may be in the capillary lumina. **B**, The mesangial regions are widened on light microscopy, usually with expansion of the matrix that stains less intensely than normal. Basement membranes are irregularly thickened. Some capillary lumina may contain foam cells. Although quite rare, this autosomal recessive disease has been described in most parts of the world; however, it occurs most commonly in Norway. Patients exhibit proteinuria, often with microscopic hematuria usually noted in childhood. Renal insufficiency may develop in the fourth or fifth decade of life and may progress rapidly. Nonrenal manifestations include corneal opacification, hemolytic anemia, early atherosclerosis, and sea-blue histocytes in the bone marrow and spleen.

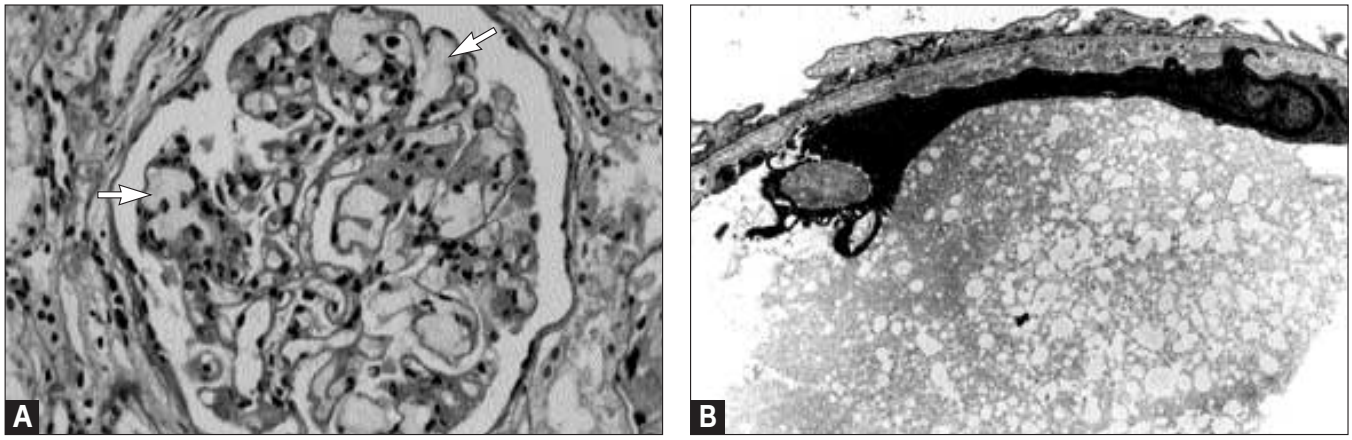

FIGURE 3-9 (*see* Color Plate)

Lipoprotein glomerulopathy. Patients with this rare disease, which often is sporadic (although some cases occur in the same family), exhibit massive proteinuria. Lipid profiles are characterized by increased plasma levels of cholesterol, triglycerides, and very low density lipoproteins. Most patients have heterozygosity for apolipoprotein E2/3 or E2/4. **A**, The glomeruli are the sites of massive intracapillary accumulation of lipoproteins, which appear as slightly tan masses (*thrombi*) dilating capillaries (*arrows*). Segmental mesangial hypercellularity or mesangiolysis may be present. With immunostaining for β-lipoprotein, apolipoproteins E and B are identified in the luminal masses. **B**, Electron microscopic findings indicate the thrombi consist of finely granular material with numerous vacuoles (lipoprotein). Lipoprotein glomerulopathy may progress to renal insufficiency over a long period of time. Recurrence of the lesions in a transplanted organ has been reported infrequently. Lipid-lowering agents are mostly ineffective.

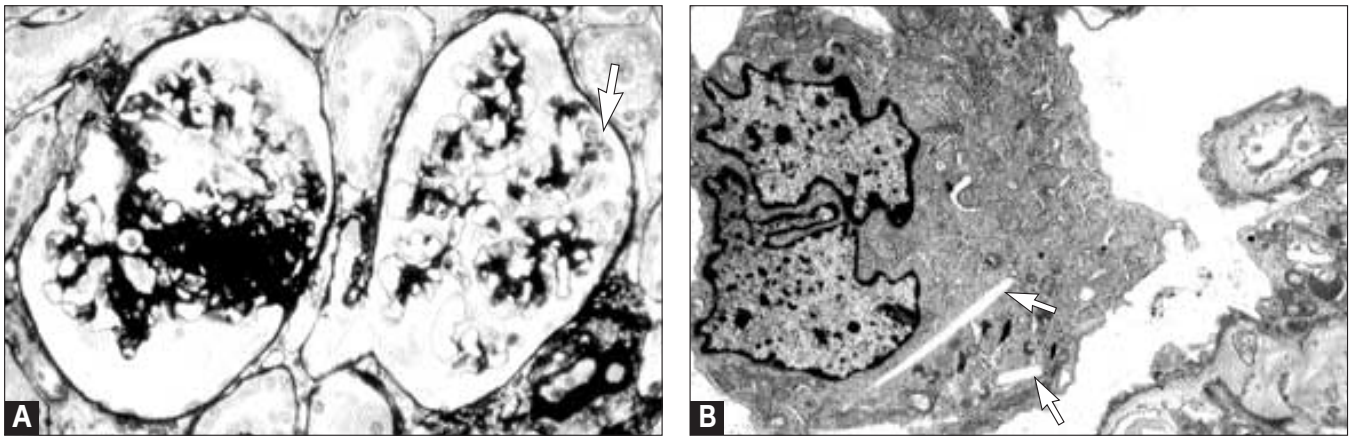

FIGURE 3-10 (*see* Color Plate)

Nephropathic cystinosis. In older children and young adults, compared with young children, patients with cystinosis commonly exhibit glomerular involvement rather than tubulointerstitial disease. Proteinuria and renal insufficiency are the typical initial manifestations. **A**, As the most constant abnormality on light microscopy, glomeruli have occasionally enlarged and multinucleated visceral epithelial cells (*arrow*). As the disease progresses, segmental sclerosis becomes evident as in the photomicrograph. **B**, Crystalline inclusions are identified on electron microscopy. The crystals of cysteine are usually dissolved in processing, leaving an empty space as shown here by the arrows.

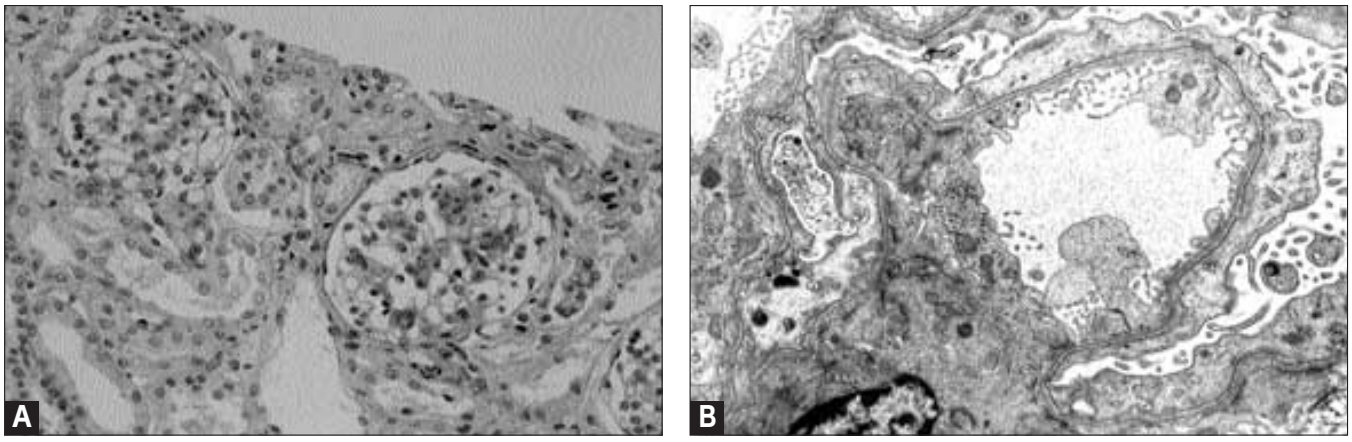

FIGURE 3-11 (*see* Color Plate)

Finnish type of congenital nephrotic syndrome. Several disorders are responsible for nephrotic syndrome within the first few months to first year of life. The most common and important of these is known as congenital nephrotic syndrome of Finnish type because the initial descriptions emphasized the more common occurrence in Finnish families. This nephrotic syndrome is an inherited disorder in which infants exhibit massive proteinuria shortly after birth; typically, the placenta is enlarged. This disorder can be diagnosed *in utero*; increased α-fetoprotein levels in amniotic fluid is a common feature. **A**, The microscopic appearance of the kidneys is varied. Some glomeruli are small and infantile without other alterations, whereas others are enlarged, more mature, and have diffuse mesangial hypercellularity. Because of the massive proteinuria, some tubules are microcystically dilated, a finding responsible for the older term for this disorder, *microcystic disease*. Because this syndrome is primarily a glomerulopathy, the tubular abnormalities are a secondary process and should not be used to designate the name of the disease. **B**, On electron microscopy, complete effacement of the foot processes of visceral epithelial cells is observed.

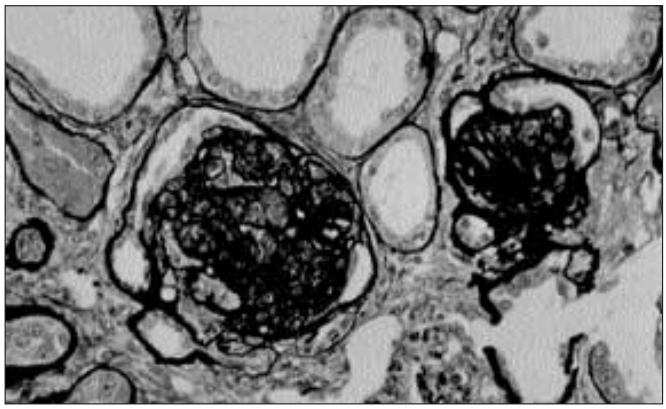

FIGURE 3-12

Diffuse mesangial sclerosis. This disorder is exhibited within the first few months of life with massive proteinuria, often with hematuria and progressive renal insufficiency. Currently, no evidence exists that this disorder is an inherited process with genetic linkage. The glomeruli characteristically are small compact masses of extracellular matrix with numerous or all capillary lumina being obliterated. As here, the visceral epithelial cells typically are arranged as a corona or crown overlying the contracted capillary tufts. Earlier stages of glomerular involvement are characterized by variable increase in mesangial cellularity. Immunofluorescence is typically negative for immunoglobulin deposits because this disorder is not immune mediated. In some patients, diffuse mesangial sclerosis may be part of the triad of the Drash syndrome characterized by ambiguous genitalia, Wilms' tumor, and diffuse mesangial sclerosis. In some patients, only two of the three components may be present; however, some investigators consider all patients with diffuse mesangial sclerosis to be at risk for the development of Wilms' tumor even in the absence of genital abnormalities. Thus, close observation or bilateral nephrectomy as prophylaxis against the development of Wilms' tumor is employed occasionally.

References

1. Abrahamson D, Van der Heurel GB, Clapp WL, *et al*.: Nephritogenic antigens in the glomerular basement membrane. In *Immunologic Renal Diseases*. Edited by Nielson EG, Couser, WG. Philadelphia: Lippincott-Raven, 1997.
2. Gregory M, Atkin C: Alport's syndrome, Fabry disease and nail-patella syndrome. In *Diseases of the Kidney*, Vol. I. edn 6. Edited by Schrier RW, Gottschalk CW. Boston: Little Brown, 1995.

Infection-Associated Glomerulopathies

Arthur H. Cohen
Richard J. Glassock

Many glomerular diseases may be associated with acute and chronic infectious diseases of bacterial, viral, fungal, or parasitic origin. In many instances, the glomerular activators are transient and of little clinical consequence. In other instances, distinct clinical syndromes such as acute nephritis or nephrotic syndrome may be provoked. Some of the more important infection-related glomerular diseases are illustrated here. Others diseases, including human immunodeficiency virus and hepatitis, are also discussed in Volume IV.

CHAPTER

4

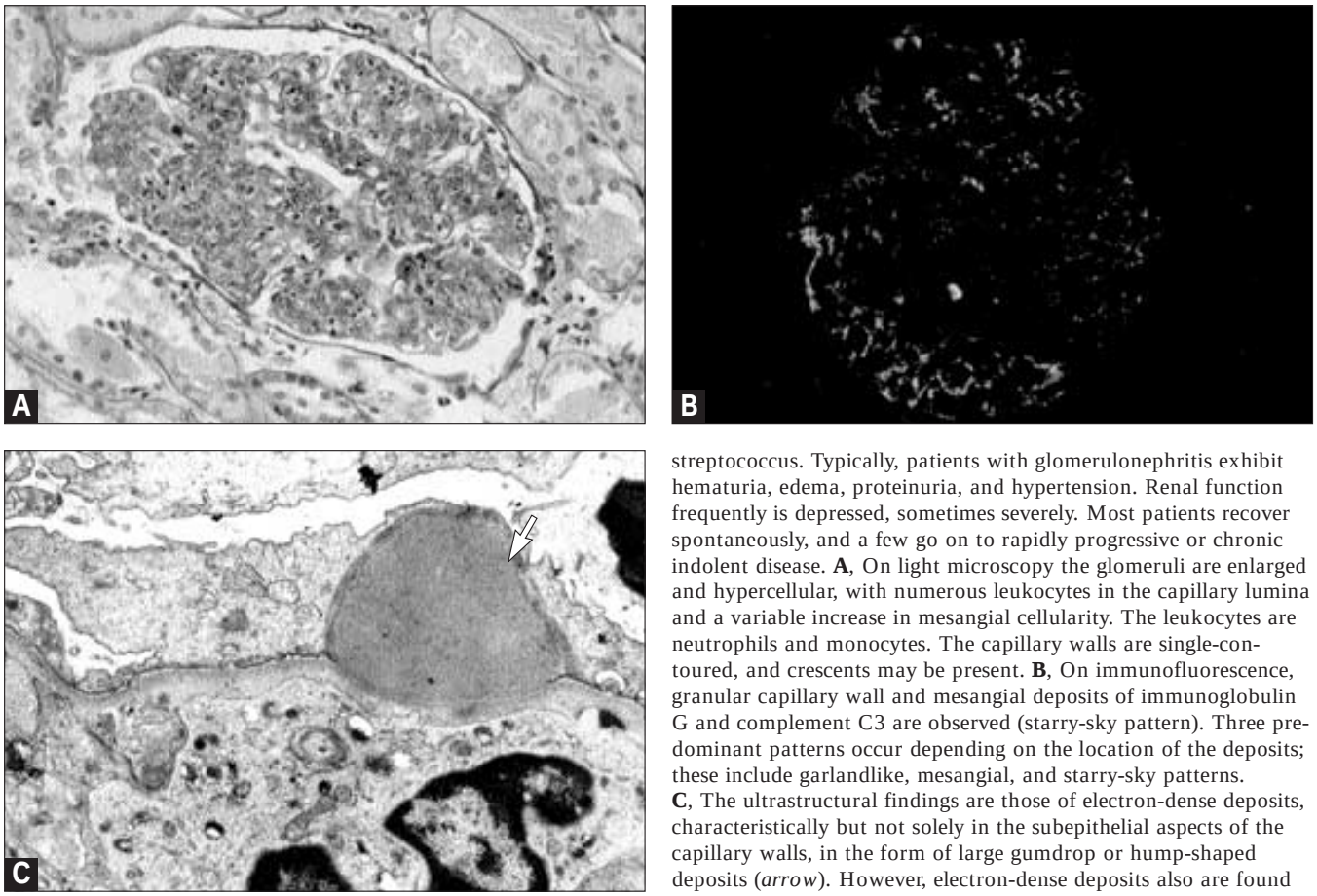

FIGURE 4-1 (*see* Color Plate)

Light, immunofluorescent, and electron microscopy of poststreptococcal (postinfectious) glomerulonephritis. Glomerulonephritis may follow in the wake of cutaneous or pharyngeal infection with a limited number of "nephritogenic" serotypes of group A β-hemolytic streptococcus. Typically, patients with glomerulonephritis exhibit hematuria, edema, proteinuria, and hypertension. Renal function frequently is depressed, sometimes severely. Most patients recover spontaneously, and a few go on to rapidly progressive or chronic indolent disease. **A**, On light microscopy the glomeruli are enlarged and hypercellular, with numerous leukocytes in the capillary lumina and a variable increase in mesangial cellularity. The leukocytes are neutrophils and monocytes. The capillary walls are single-contoured, and crescents may be present. **B**, On immunofluorescence, granular capillary wall and mesangial deposits of immunoglobulin G and complement C3 are observed (starry-sky pattern). Three predominant patterns occur depending on the location of the deposits; these include garlandlike, mesangial, and starry-sky patterns. **C**, The ultrastructural findings are those of electron-dense deposits, characteristically but not solely in the subepithelial aspects of the capillary walls, in the form of large gumdrop or hump-shaped deposits (*arrow*). However, electron-dense deposits also are found in the mesangial regions and occasionally subendothelial locations. Endothelial cells often are swollen, and leukocytes are not only found in the capillary lumina but occasionally in direct contact with basement membranes in capillary walls with deposits. Similar findings may be observed in glomerulonephritis after infectious diseases other than certain strains of *Streptococci*.

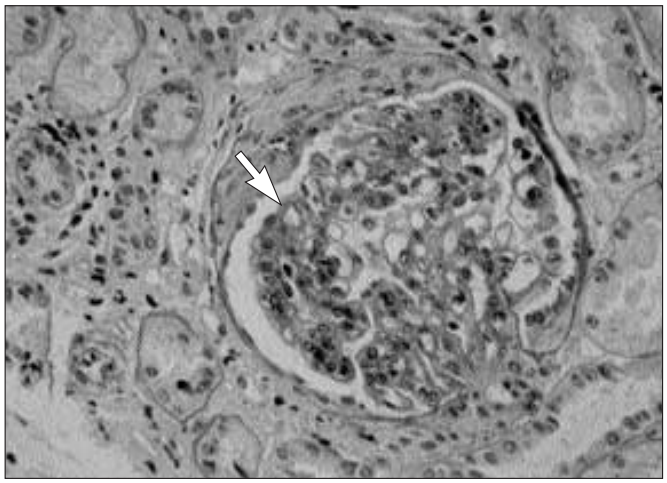

FIGURE 4-2

Infective endocarditis and shunt nephritis. The glomerulonephritis accompanying infective endocarditis or infected ventriculoatrial shunts or other indwelling devices is that of a postinfectious glomerulonephritis or membranoproliferative glomerulonephritis type I pattern, or both (*see* Fig. 2-18). In reality, the changes often are a combination of both. As shown here, this glomerulopathy is characterized by increased mesangial cellularity, with slight lobular architecture; occasionally thickened capillary walls, with double contours (*arrow*); and leukocytes in some capillary lumina. This glomerulus also has a small crescent.

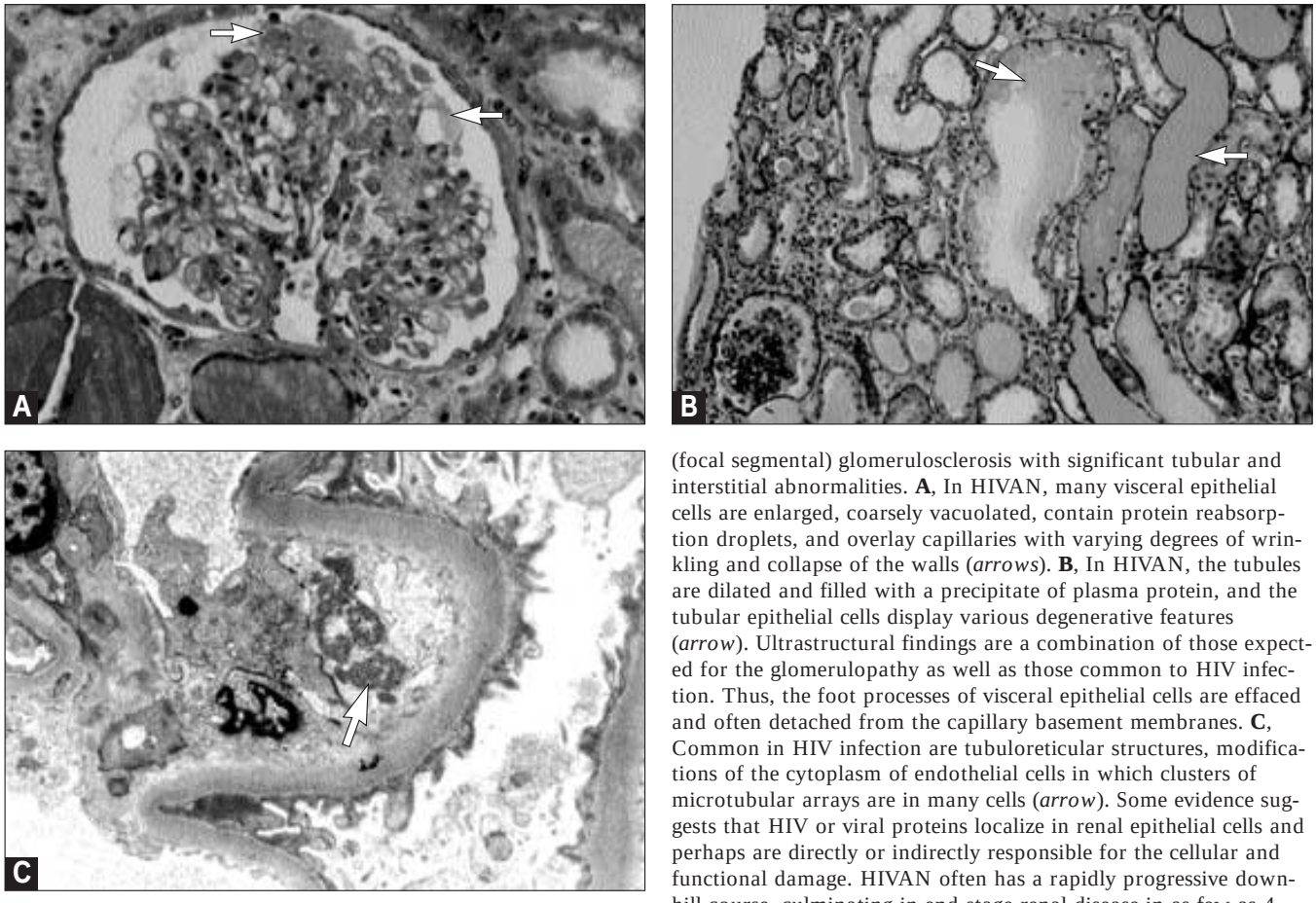

FIGURE 4-3 (*see* Color Plate)

Human immunodeficiency virus (HIV) infection. Many forms of renal disease have been described in patients infected with HIV. Various immune complex–mediated glomerulonephritides associated with complicating infections are known; however, several disorders appear to be directly or indirectly related to HIV itself. Perhaps the more common of these is known as HIV-associated nephropathy (HIVAN). This disease is a form of the collapsing (focal segmental) glomerulosclerosis with significant tubular and interstitial abnormalities. **A**, In HIVAN, many visceral epithelial cells are enlarged, coarsely vacuolated, contain protein reabsorption droplets, and overlay capillaries with varying degrees of wrinkling and collapse of the walls (*arrows*). **B**, In HIVAN, the tubules are dilated and filled with a precipitate of plasma protein, and the tubular epithelial cells display various degenerative features (*arrow*). Ultrastructural findings are a combination of those expected for the glomerulopathy as well as those common to HIV infection. Thus, the foot processes of visceral epithelial cells are effaced and often detached from the capillary basement membranes. **C**, Common in HIV infection are tubuloreticular structures, modifications of the cytoplasm of endothelial cells in which clusters of microtubular arrays are in many cells (*arrow*). Some evidence suggests that HIV or viral proteins localize in renal epithelial cells and perhaps are directly or indirectly responsible for the cellular and functional damage. HIVAN often has a rapidly progressive downhill course, culminating in end-stage renal disease in as few as 4 months. HIVAN has a striking racial predilection; over 90% of patients are black.

The other glomerulopathy that may be an integral feature of HIV infection is immunoglobulin A nephropathy. In this setting, HIV antigen may be part of the glomerular immune complexes and circulating immune complexes. The morphology and clinical course generally are the same as in immunoglobulin A nephropathy occurring in the non-HIV setting.

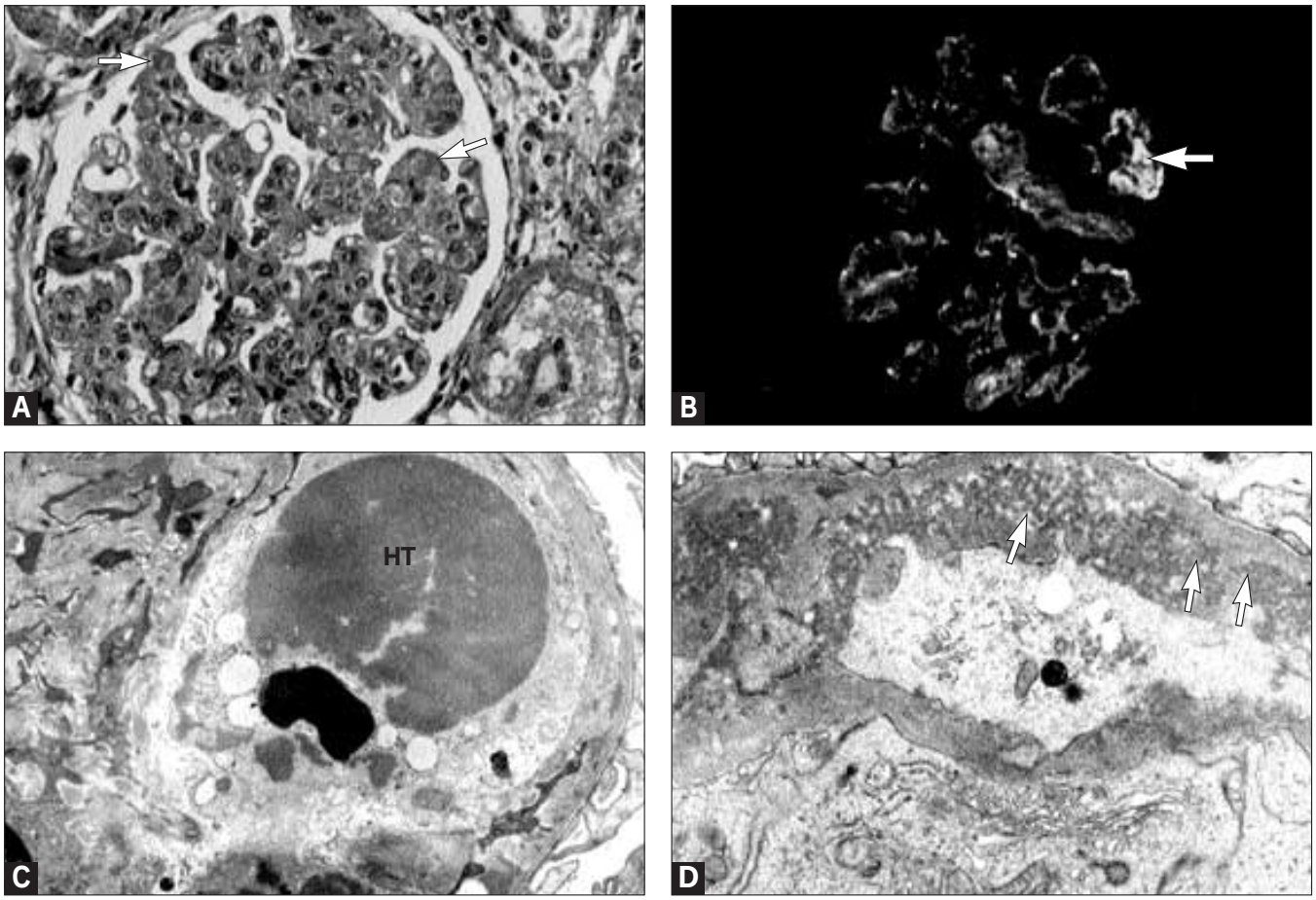

FIGURE 4-4 (*see* Color Plate)

Hepatitis C virus infection. The most common glomerulonephritis in patients infected with the hepatitis C virus is membranoproliferative glomerulonephritis with, in some instances, cryoglobulinemia and cryoglobulin precipitates in glomerular capillaries. Thus, the morphology is basically the same as in membranoproliferative glomerulonephritis type I (Fig. 2-18*A–C*). **A**, With cryoglobulins, precipitates of protein representing cryoglobulin in the capillary lumina and appearing as hyaline thrombi (HT)are observed (*arrows*), often with numerous monocytes in most capillaries. **B**, Immunofluorescence microscopy discloses peripheral granular to confluent granular capillary wall deposits of immunoglobulin M (IgM) and complement C3; the same immune proteins are in the luminal masses corresponding to hyaline thrombi (*arrow*). **C**, Electron microscopy indicates the luminal masses (HT). **D**, On electron microscopy the deposits also appear to be composed of curvilinear or annular structures (*arrows*). Hepatitis C viral antigen has been documented in the circulating cryoglobulins. Membranous glomerulonephritis with a mesangial component also has been infrequently described in patients infected with the hepatitis C virus.

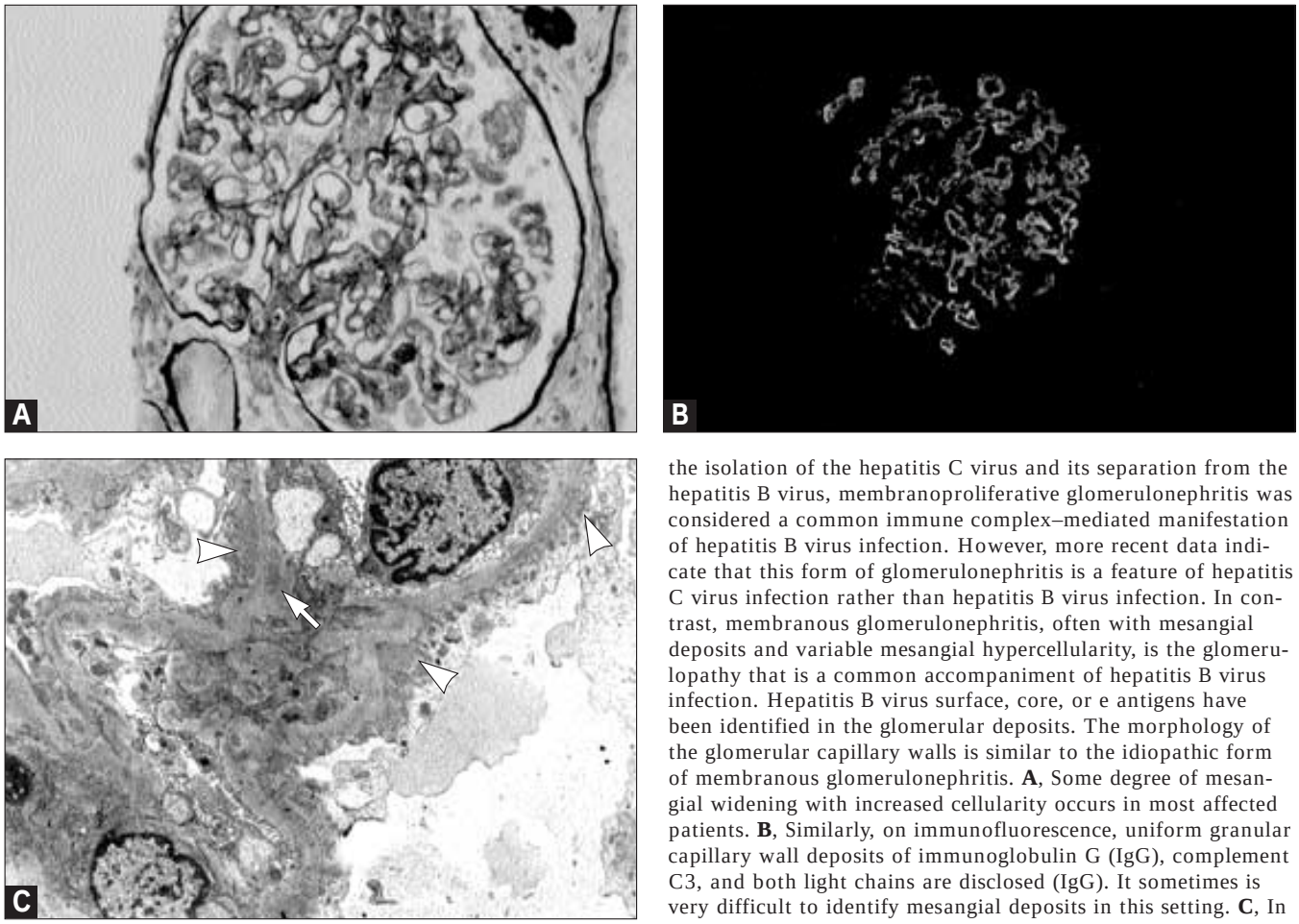

FIGURE 4-5 (*see* Color Plate)

Hepatitis B virus infection. Several glomerulopathies have been described in association with hepatitis B viral infection. Until the isolation of the hepatitis C virus and its separation from the hepatitis B virus, membranoproliferative glomerulonephritis was considered a common immune complex–mediated manifestation of hepatitis B virus infection. However, more recent data indicate that this form of glomerulonephritis is a feature of hepatitis C virus infection rather than hepatitis B virus infection. In contrast, membranous glomerulonephritis, often with mesangial deposits and variable mesangial hypercellularity, is the glomerulopathy that is a common accompaniment of hepatitis B virus infection. Hepatitis B virus surface, core, or e antigens have been identified in the glomerular deposits. The morphology of the glomerular capillary walls is similar to the idiopathic form of membranous glomerulonephritis. **A**, Some degree of mesangial widening with increased cellularity occurs in most affected patients. **B**, Similarly, on immunofluorescence, uniform granular capillary wall deposits of immunoglobulin G (IgG), complement C3, and both light chains are disclosed (IgG). It sometimes is very difficult to identify mesangial deposits in this setting. **C**, In addition to the expected capillary wall changes, electron microscopy discloses deposits in mesangial regions of many lobules (the *arrow* indicates mesangial deposits; the *arrowheads* indicate subepithelial deposits).

Vascular Disorders

Arthur H. Cohen
Richard J. Glassock

Vascular disorders of the kidney comprise a very heterogeneous array of lesions and abnormalities, depending on the site of the lesion and underlying pathogenesis. Here, three common disorders are the focus: thrombotic microangiopathies, benign and malignant nephrosclerosis, and vascular occlusive disease (atheroembolism). Vasculitis and renovascular hypertension are discussed in other chapters.

CHAPTER

5

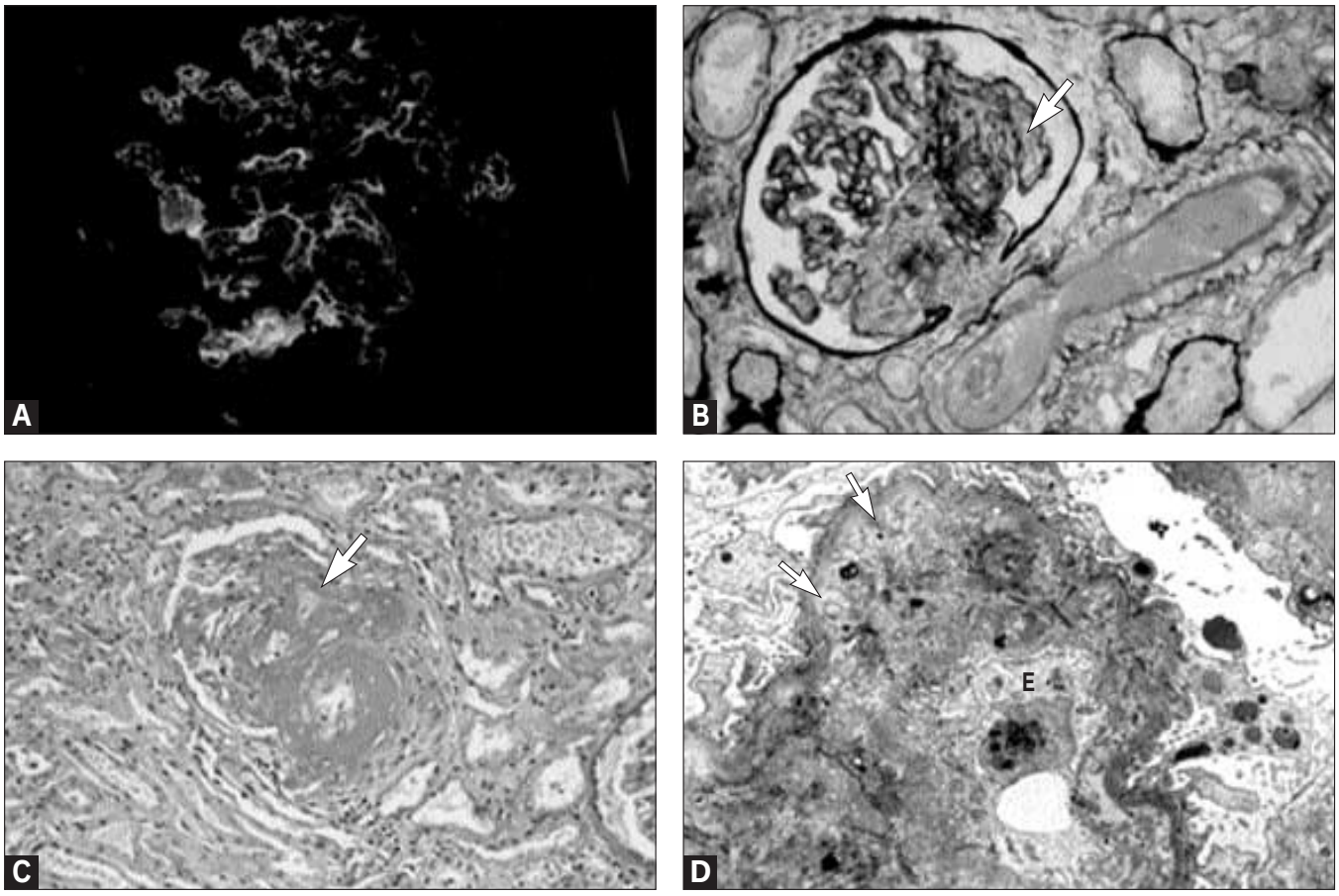

FIGURE 5-1

Light microscopy of thrombotic microangiopathies. This group of disorders includes hemolytic-uremic syndrome and thrombotic thrombocytopenic purpura, malignant hypertension, and renal disease in progressive systemic sclerosis (scleroderma renal crises). **A**, These lesions are characterized primarily by fibrin deposition in the walls of the glomeruli (fibrin). **B**, This fibrin deposition is associated with endothelial cell swelling (*arrow*) and thickened capillary walls, sometimes with a double contour. Variable capillary wall wrinkling and luminal narrowing occur. Mesangiolysis (dissolution of the mesangial matrix and cells) is not uncommon and may be associated with microaneurysm formation. With further endothelial cell damage, capillary thrombi ensue. **C**, Arteriolar thrombi also may be present. In arterioles, fibrin deposits in the walls and lumina are known as thrombonecrotic lesions, with extension of this process into the glomeruli on occasion (*arrow*). The arterial walls are thickened, with loose concentric intimal proliferation. **D**, On electron microscopy, the subendothelial zones of the glomerular capillary wall are widened (*arrows*). Flocculent material accumulates, corresponding to mural fibrin, with associated endothelial cell swelling. **E**, With widespread arterial thrombosis, cortical necrosis is a common complicating feature. The necrotic cortex consists of pale confluent multifocal zones throughout the cortex.

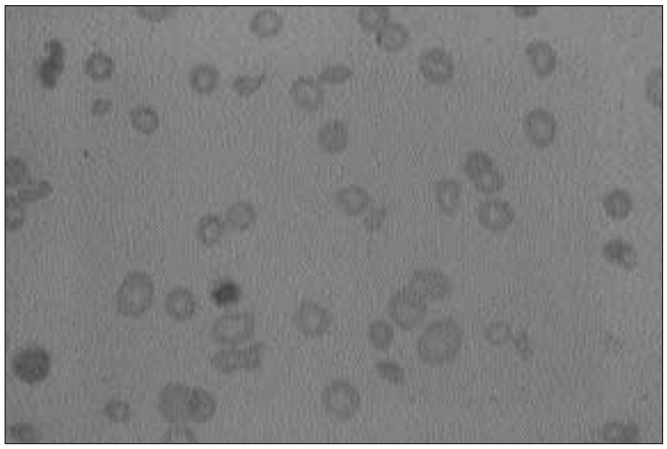

FIGURE 5-2 (*see* Color Plate)

Microangiopathic hemolytic anemia. Bizarrely shaped and fragmented erythrocytes are commonly seen in Wright's stained peripheral blood smears from patients with active lesions of thrombotic microangiopathy. These abnormally shaped erythrocytes presumably arise when the fibrin strands within small blood vessels shear the cell membrane, with imperfect resolution of the biconcave disk shape. The resultant intravascular hemolysis causes anemia, reticulocytosis, and reduced plasma haptoglobin level.

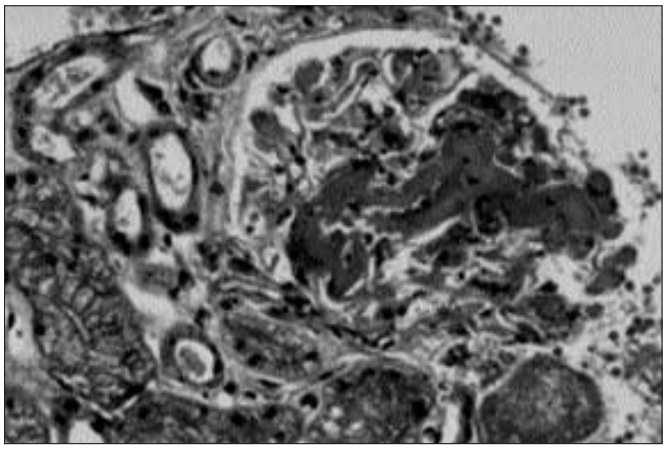

FIGURE 5-3 (*see* Color Plate)

Disseminated intravascular coagulation. In disseminated intravascular coagulation, fibrin thrombi are typically found in many glomerular capillary lumina. In contrast to the thrombotic microangiopathies, in disseminated intravascular coagulation, fibrin is not primarily in vessel walls but in the lumina. Consequently, the capillary wall thickening, endothelial cell swelling, and fibrin accumulation in subendothelial locations are not features of this lesion. In the glomerulus illustrated, the fibrin is in many capillary lumina and appears as bright fuchsin positive (red) masses.

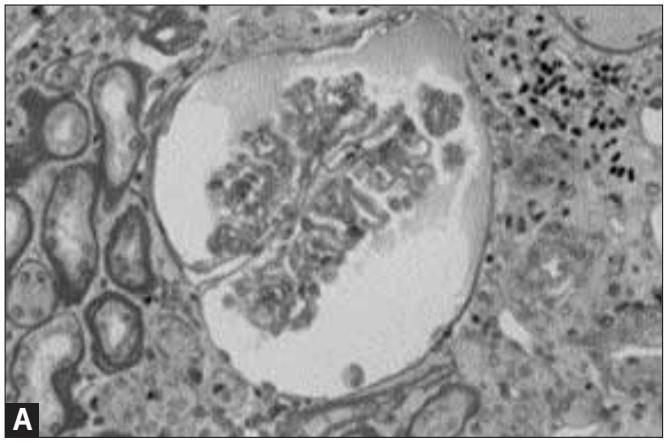

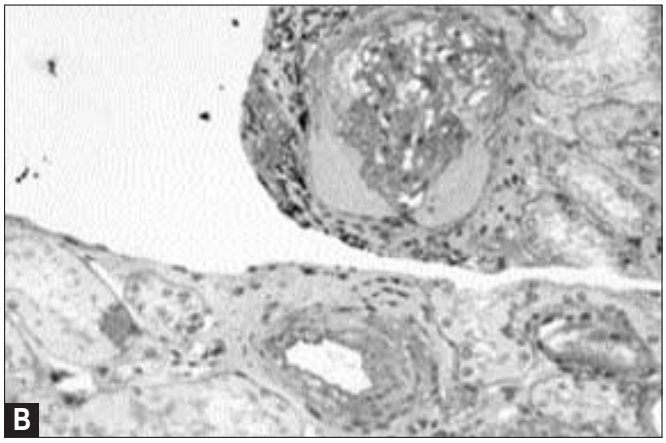

FIGURE 5-4

Benign and malignant nephrosclerosis. In benign nephrosclerosis the artery walls are thickened with intimal fibrosis and luminal narrowing. Arteriolar walls are thickened with insudative lesions, a process affecting afferent arterioles almost exclusively. Both of these processes, which can be quite patchy, result in chronic ischemia. **A**, In glomeruli, chronic ischemia is manifested by gradual capillary wall wrinkling, luminal narrowing, and shrinkage and solidification of the tufts. **B**, As these processes progress, collagen forms internal to Bowman's capsule, beginning at the vascular pole and growing as a collar around the wrinkled ischemic tufts. This collagen formation ultimately is associated with tubular atrophy and interstitial fibrosis.

In malignant nephrosclerosis the changes are virtually identical to those of thrombotic microangiopathies (Fig. 5-1 *C*). Malignant nephrosclerosis may be seen in essential hypertension, scleroderma, unilateral renovascular hypertension (with a contralateral or "unprotected" kidney), and as a complicating event in many chronic renal parenchymal diseases.

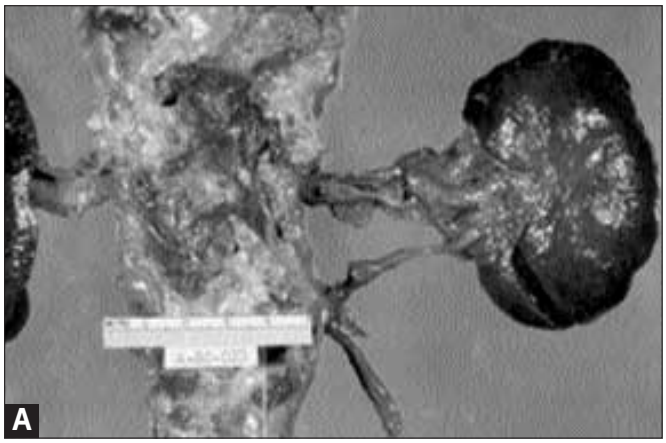

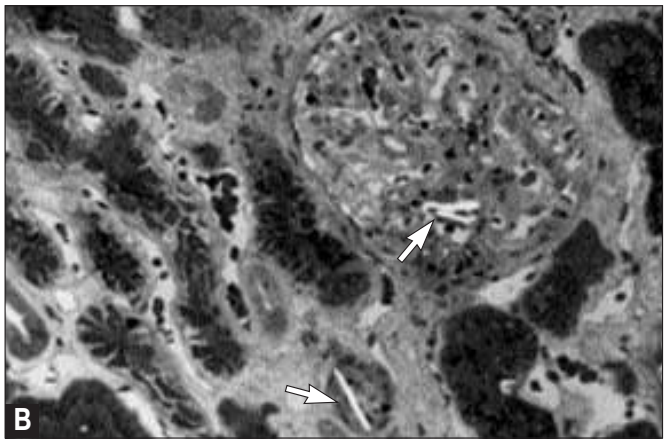

FIGURE 5-5

Vascular occlusive disease and thrombosis. Atheroemboli (cholesterol emboli) are most commonly associated with intravascular instrumentation of patients with severe arteriosclerosis. Most commonly, aortic plaques are complicated with ulceration and often adherent fibrin, **A**. Portions of plaques are dislodged and travel distally in the aorta. Because the kidneys receive a disproportionately large share of the cardiac output, they are a favored site of emboli. Typically, the emboli are in small arteries and arterioles, although glomerular involvement with a few cholesterol crystals in capillaries is not uncommon. Because of the size of the crystals, it is sometimes difficult if not impossible to identify them in glomerular capillaries in paraffin-embedded sections. In plastic-embedded sections prepared for electron microscopy, however, the crystals are quite easy to detect. On light microscopy, cholesterol is represented by empty crystalline spaces. In the early stages of the disease the crystals lie free in the vascular lumina. In time, the crystals are engulfed by multinucleated foreign body giant cells. **B**, In this light microscopic photograph, a few crystals are evident in the glomerular capillary lumina and in an arteriole (*arrows*). **C**, In the electron micrograph the elongated empty space represents dissolved cholesterol. Note that no cellular reaction is evident.

Renal Interstitium and Major Features of Chronic Tubulointerstitial Nephritis

Garabed Eknoyan
Luan D. Truong

As a rule, diseases of the kidney primarily affect the glomeruli, vasculature, or remainder of the renal parenchyma that consists of the tubules and interstitium. Although the interstitium and the tubules represent separate functional and structural compartments, they are intimately related. Injury initially involving either one of them inevitably results in damage to the other. Hence the term *tubulointerstitial diseases* is used. Because inflammatory cellular infiltrates of variable severity are a constant feature of this entity, the terms *tubulointerstitial diseases* and *tubulointerstitial nephritis* have come to be used interchangeably. The clinicopathologic syndrome that results from these lesions, commonly termed *tubulointerstitial nephropathy*, may pursue an acute or chronic course. The chronic course is discussed here. The abbreviation TIN is used to refer synonymously to chronic tubulointerstitial nephritis and tubulointerstitial nephropathy.

TIN may be classified as primary or secondary in origin. Primary TIN is defined as primary tubulointerstitial injury without significant involvement of the glomeruli or vasculature, at least in the early stages of the disease. Secondary TIN is defined as secondary tubulointerstitial injury, which is consequent to lesions initially involving either the glomeruli or renal vasculature. The presence of secondary TIN is especially important because the magnitude of impairment in renal function and the rate of its progression to renal failure correlate better with the extent of TIN than with that of glomerular or vascular damage.

Renal insufficiency is a common feature of chronic TIN, and its diagnosis must be considered in any patient who exhibits renal insufficiency. In most cases, however, chronic TIN is insidious in onset, renal insufficiency is slow to develop, and earliest manifestations of the disease are those of tubular dysfunction. As such, it is important to maintain a high

CHAPTER 6

index of suspicion of this entity whenever any evidence of tubular dysfunction is detected clinically. At this early stage, removal of a toxic cause of injury or correction of the underlying systemic or renal disease can result in preservation of residual renal function. Of special relevance in patients who exhibit renal insufficiency caused by primary TIN is the absence or modest degree of the two principal hallmarks of glomerular and vascular diseases of the kidney: salt retention, manifested by edema and hypertension; and proteinuria, which usually is modest and less than 1 to 2 g/d in TIN. These clinical considerations notwithstanding, a definite diagnosis of TIN can be established only by morphologic examination of kidney tissue.

Structure of the Interstitium

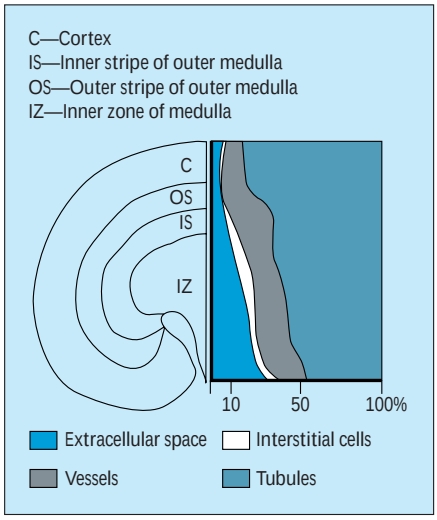

FIGURE 6-1

Diagram of the approximate relative volume composition of tissue compartments at different segments of the kidney in rats. The interstitium of the kidney consists of peritubular and periarterial spaces. The relative contribution of each of these two spaces to interstitial volume varies, reflecting in part the arbitrary boundaries used in assessing them, but increases in size from the cortex to the papilla. In the cortex there is little interstitium because the peritubular capillaries occupy most of the space between the tubules. The cortical interstitial cells are scattered and relatively inconspicuous. In fact, a loss of the normally very close approximation of the cortical tubules is the first evidence of TIN. In the medulla there is a noticeable increase in interstitial space. The interstitial cells, which are in greater evidence, have characteristic structural features and an organized arrangement. The ground substance of the renal interstitium contains different types of fibrils and basementlike material embedded in a glycosaminoglycan-rich substance. (*From* Bohman [1]; with permission.)

Cortex

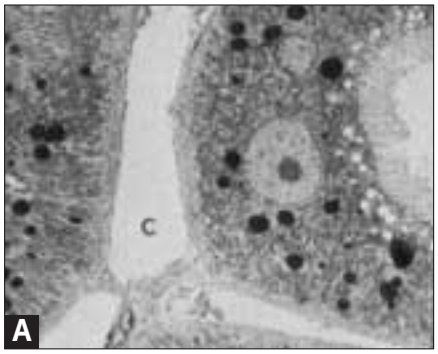

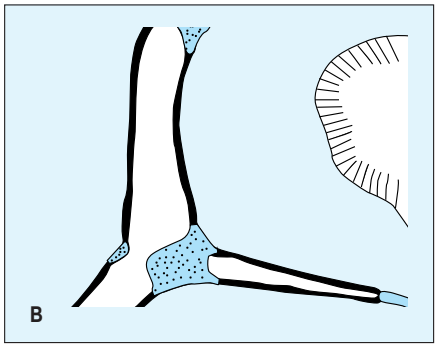

FIGURE 6-2

A, Electron micrograph of a rat kidney cortex, where *C* is the cortex. **B,** Schematic rendering, where the narrow interstitium is shown in black and the wide interstitium is shown by dots. The relative volume of the interstitium of the cortex is approximately 7%, consisting of about 3% interstitial cells and 4% extracellular space. The vasculature occupies another 6%; the remainder (*ie,* some 85% or more) is occupied by the tubules. The cortical interstitial space is unevenly distributed and has been divided into narrow and wide structural components. The tubules and peritubular capillaries either are closely apposed at several points, sometimes to the point of sharing a common basement membrane, or are separated by a very narrow space.

This space, the so-called *narrow interstitium*, has been estimated to occupy 0.6% of cortical volume in rats. The narrow interstitium occupies about one-half to two-thirds of the cortical peritubular capillary surface area. The remainder of the cortical interstitium consists of irregularly shaped clearly discernible larger areas, the so-called *wide interstitium*. The wide interstitium has been estimated to occupy 3.4% of cortical volume in rats. The capillary wall facing the narrow interstitium is significantly more fenestrated than is that facing the wide interstitium. Functional heterogeneity of these interstitial spaces has been proposed but remains to be clearly defined. (*From* Bohman [1]; with permission.)

Medulla

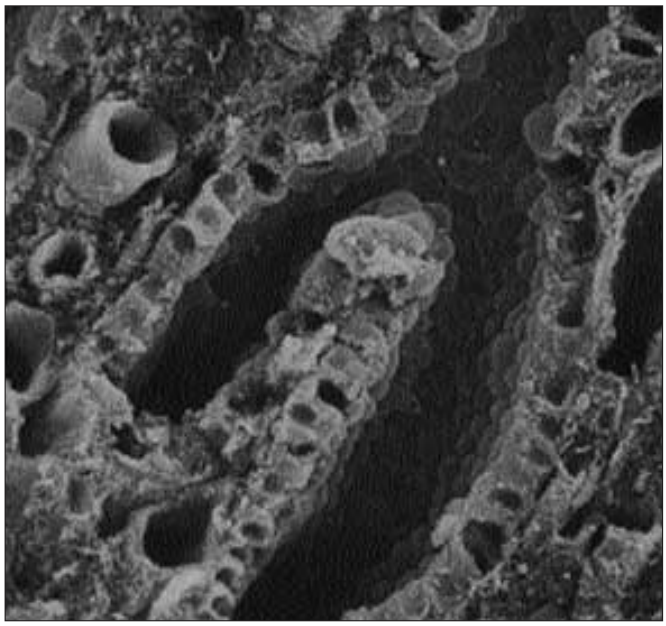

FIGURE 6-3

Scanning electron micrograph of the inner medulla, showing a prominent collecting duct, thin wall vessels, and abundant interstitium. A gradual increase in interstitial volume from the outer medullary stripe to the tip of the papilla occurs. In the outer stripe of the outer medulla, the relative volume of the interstitium is slightly less than is that of the cortex. This volume has been estimated to be approximately 5% in rats. It is in the inner stripe of the outer medulla that the interstitium begins to increase significantly in volume, in increments that gradually become larger toward the papillary tip.

The inner stripe of the outer medulla consists of the vascular bundles and the interbundle regions, which are occupied principally by tubules. Within the vascular bundles the interstitial spaces are meager, whereas in the interbundle region the interstitial spaces occupy some 10% to 20% of the volume. In the inner medulla the differentiation into vascular bundles and interbundle regions becomes gradually less obvious until the two regions merge. A gradual increase in the relative volume of the interstitial space from the base of the inner medulla to the tip of the papilla also occurs. In rats, the increment in interstitial space is from 10% to 15% at the base to about 30% at the tip. In rabbits, the increment is from 20% to 25% at the base to more than 40% at the tip.

Cell types

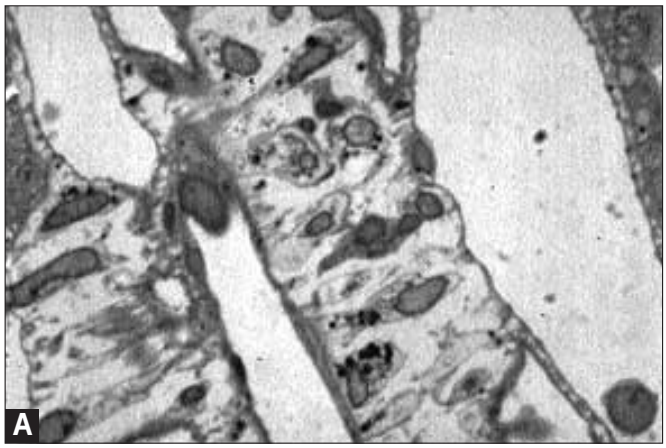

FIGURE 6-4

A, High-power view of the medulla showing the wide interstitium and interstitial cells, which are abundant, varied in shape, and arranged as are the rungs of a ladder. **B,** Renal interstitial cells. The interstitium contains two main cell types, whose numbers increase from the cortex to the papilla. Type I interstitial cells are fibroblastic cells that are active in the deposition and degradation of the interstitial matrix. Type I cells contribute to fibrosis in response to chronic irritation. Type II cells are macrophage-derived mononuclear cells with phagocytic and immunologic properties. Type II cells are important in antigen presentation. Their cytokines contribute to recruitment of infiltrating cells, progression of injury, and sustenance of fibrogenesis.

B. RENAL INTERSTITIAL CELLS

Cortex	Outer medulla	Inner medulla
Fibroblastic cells	Fibroblastic cells	Pericytes
Mononuclear cells	Mononuclear cells	Lipid-laden cells
		Mononuclear cells

In the cortex and outer zone of the outer medulla, type I cells are more common than are type II cells. In the inner zone of the medulla, some type I cells form pericytes whereas others evolve into specialized lipid-laden interstitial cells. These specialized cells increase in number toward the papillary tip and are a possible source of medullary prostaglandins and of production of matriceal glycosaminoglycans. A characteristic feature of these medullary cells is their connection to each other in a characteristic arrangement, similar to the rungs of a ladder. These cells have a distinct close and regular transverse apposition to their surrounding structures, specifically the limbs of the loop of Henle and capillaries, but not to the collecting duct cells.

Matrix

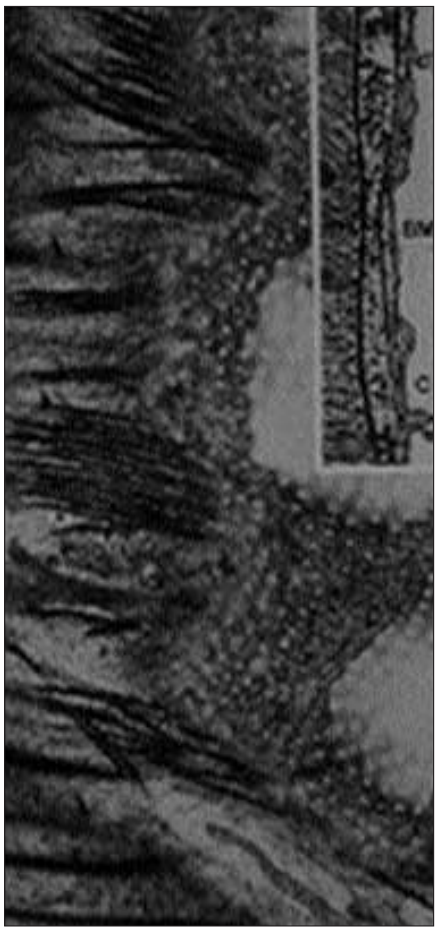

FIGURE 6-5

Peritubular interstitium in the cortex at the interface of a tubule (T) on the left and a capillary (C) on the right. The inset shows the same space in cross section, including the basement membrane (BM) of the two compartments. The extracellular loose matrix is a hydrated gelatinous substance consisting of glycoproteins and glycosaminoglycans (hyaluronic acid, heparan sulfate, dermatan sulfate, and chondroitin sulfate) that are embedded within a fibrillar reticulum. This reticulum consists of collagen fibers (types I, III, and VI) and unbanded microfilaments. Collagen types IV and V are the principal components of the basement membrane lining the tubules. Glycoprotein components (fibronectin and laminin) of the basement membrane connect it to the interstitial cell membranes and to the fibrillar structures of the interstitial matrix. The relative increase in the interstitial matrix of the medulla may be important for providing support to the delicate tubular and vascular structures in this region. (*From* Lemley and Kriz [2]; with permission.)

Pathologic Features of Chronic TIN

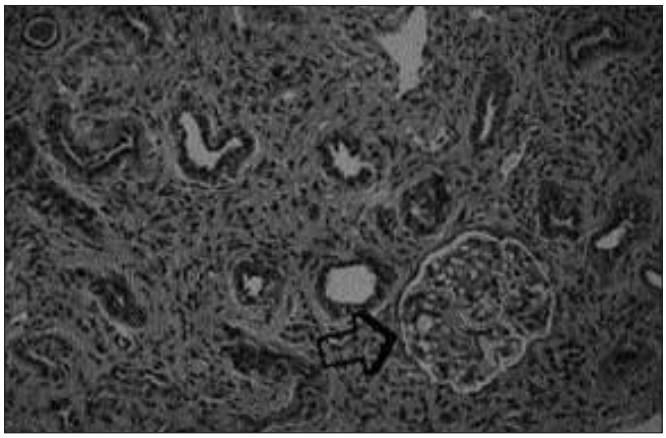

FIGURE 6-6

Primary chronic TIN. The arrow indicates a normal glomerulus. Apart from providing structural support, the interstitium serves as a conduit for solute transport and is the site of production of several cytokines and hormones (erythropoietin and prostaglandins). For the exchange processes to occur between the tubules and vascular compartment, the absorbed or secreted substances must traverse the interstitial space. The structure, composition, and permeability characteristics of the interstitial space must, of necessity, exert an effect on any such exchange. Although the normal structural and functional correlates of the interstitial space are poorly defined, changes in its composition and structure in chronic TIN are closely linked to changes in tubular function. In addition, replacement of the normal delicate interstitial structures by fibrosclerotic changes of chronic TIN would affect the vascular perfusion of the adjacent tubule, thereby contributing to tubular dysfunction and progressive ischemic injury.

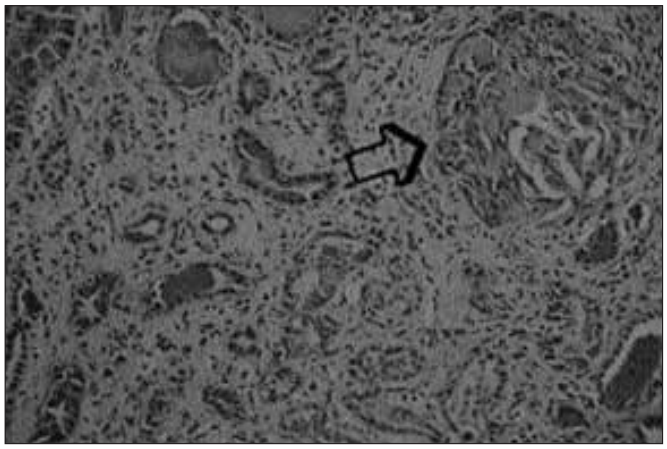

FIGURE 6-7

Secondary chronic TIN. The arrow indicates a glomerulus with a cellular crescent. The diagnosis of TIN can be established only by morphologic examination of kidney tissue. The extent of the lesions of TIN, whether focal or diffuse, correlates with the degree of impairment in renal function.

Tubular atrophy and dilation comprise a principal feature of TIN. The changes are patchy in distribution, with areas of atrophic chronically damaged tubules adjacent to dilated tubules displaying compensatory hypertrophy. In atrophic tubules the epithelial cells show simplification, decreased cell height, loss of brush border, and varying degrees of thickened basement membrane. In dilated tubules the epithelial cells are hypertrophic and the lumen may contain hyalinized casts, giving them the appearance of thyroid follicles. Hence the term *thyroidization* is used.

The interstitium is expanded by fibrous tissue, in which are interspersed proliferating fibroblasts and inflammatory cells comprised mostly of activated T lymphocytes and macrophages. Rarely, B lymphocytes, plasma cells, neutrophils, and even eosinophils may be present.

The glomeruli, which may appear crowded in some areas owing to tubulointerstitial loss, usually are normal in the early stages of the disease. Ultimately, the glomeruli become sclerosed and develop periglomerular fibrosis.

The large blood vessels are unremarkable in the early phases of the disease. Ultimately, these vessels develop intimal fibrosis, medial hypertrophy, and arteriolosclerosis. These vascular changes, which also are associated with hypertension, can be present even in the absence of elevated blood pressure in cases of chronic TIN.

CONDITIONS ASSOCIATED WITH PRIMARY CHRONIC TIN

Immunologic diseases	Urinary tract obstructions	Hematologic diseases	Miscellaneous	Hereditary diseases	Endemic diseases
Systemic lupus erythematosus	Vesicoureteral reflux	Sickle hemoglobinopathies	Vascular diseases	Medullary cystic disease	Balkan nephropathy
Sjögren syndrome	Mechanical	Multiple myeloma	Nephrosclerosis	Hereditary nephritis	Nephropathia epidemica
Transplanted kidney		Lymphoproliferative disorders	Atheroembolic disease	Medullary sponge kidney	
Cryoglobulinemia		Aplastic anemia	Radiation nephritis	Polycystic kidney disease	
Goodpasture's syndrome			Diabetes mellitus		
Immunoglobulin A nephropathy			Sickle hemoglobinopathies		
Amyloidosis			Vasculitis		
Pyelonephritis					

Infections	Drugs	Heavy metals	Metabolic disorders	Granulomatous disease	Idiopathic TIN
Systemic	Analgesics	Lead	Hyperuricemia-hyperuricosuria	Sarcoidosis	
Renal	Cyclosporine	Cadmium	Hypercalcemia-hypercalciuria	Tuberculosis	
Bacterial	Nitrosourea		Hyperoxaluria	Wegener's granulomatosis	
Viral	Cisplatin		Potassium depletion		
Fungal	Lithium		Cystinosis		
Mycobacterial	Miscellaneous				

FIGURE 6-8

Tubulointerstitial nephropathy occurs in a motley group of diseases of varied and diverse causes. These diseases are arbitrarily grouped together because of the unifying structural changes associated with TIN noted on morphologic examination of the kidneys.

Pathogenesis of Chronic TIN

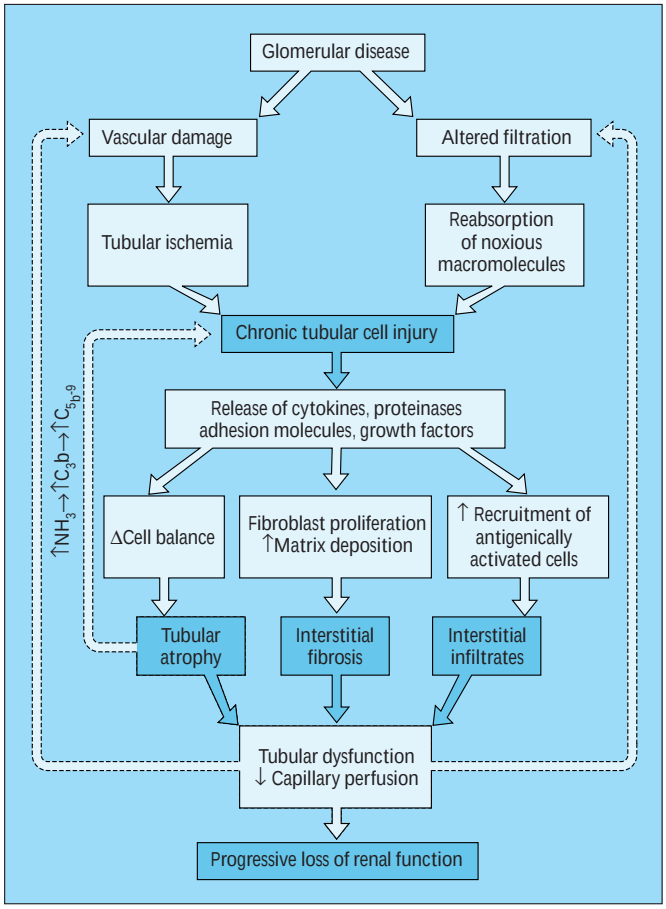

FIGURE 6-9

Schematic presentation of the potential pathways incriminated in the pathogenesis of chronic TIN caused by primary tubular injury (dark boxes) or secondary to glomerular disease (light boxes). The mechanism by which TIN is mediated remains to be elucidated. Chronic tubular epithelial cell injury appears to be pivotal in the process. The injury may be direct through cytotoxicity or indirect by the induction of an inflammatory or immunologic reaction. Studies in experimental models and humans provide compelling evidence for a role of immune mechanisms. The infiltrating lymphocytes have been shown to be activated immunologically. It is the inappropriate release of cytokines by the infiltrating cells and loss of regulatory balance of normal cellular regeneration that results in increased fibrous tissue deposition and tubular atrophy. Another potential mechanism of injury is that of increased tubular ammoniagenesis by the residual functioning but hypertrophic tubules. Increased tubular ammoniagenesis contributes to the immunologic injury by activating the alternate complement pathway.

Altered glomerular permeability with consequent proteinuria appears to be important in the development of TIN in primary glomerular diseases. By the same token, the proteinuria that develops late in the course of primary TIN may contribute to the tubular cell injury and aggravate the course of the disease.

In primary vascular diseases TIN has been attributed to ischemic injury. In fact, hypertension is probably the most common cause of TIN. The vascular lesions that develop late in the course of primary TIN, in turn, can contribute to the progression of TIN. (*From* Eknoyan [3]; with permission.)

ROLE OF TUBULAR EPITHELIAL CELLS

Chemoattractant cytokines	Pro-inflammatory cytokines	Cell surface markers	Matrix proteins
Monocyte chemo-attractant peptide-1	Interleukin-6 (IL-6), IL-8	Human leukocyte antigen class II	Collagen I, III, IV
Osteopontin	Platelet-derived growth factor-β	Intercellular adhesion molecule-1	Laminin, fibronectin
Chemoattractant lipids	Granulocyte -macrophage colony-stimulating factor	Vascular cell adhesion molecule-1	
Endothelin-1	Transforming growth factor-β1		
RANTES	Tumor necrosis factor-α		

From Palmer [4]; with permission.

FIGURE 6-10

The infiltrating interstitial cells contribute to the course TIN. However, increasing evidence exists for a primary role of the tubular epithelial cells in the recruitment of interstitial infiltrating cells and in perpetuation of the process. Injured epithelial cells secrete a variety of cytokines that have both chemoattractant and pro-inflammatory properties. These cells express a number of cell surface markers that enable them to interact with infiltrating cells. Injured epithelial cells also participate in the deposition of increased interstitial matrix and fibrous tissue. Listed are cytokines, cell surface markers, and matrix components secreted by the renal tubular cell that may play a role in the development of tubulointerstitial disease.

Role of Infiltrating Cells

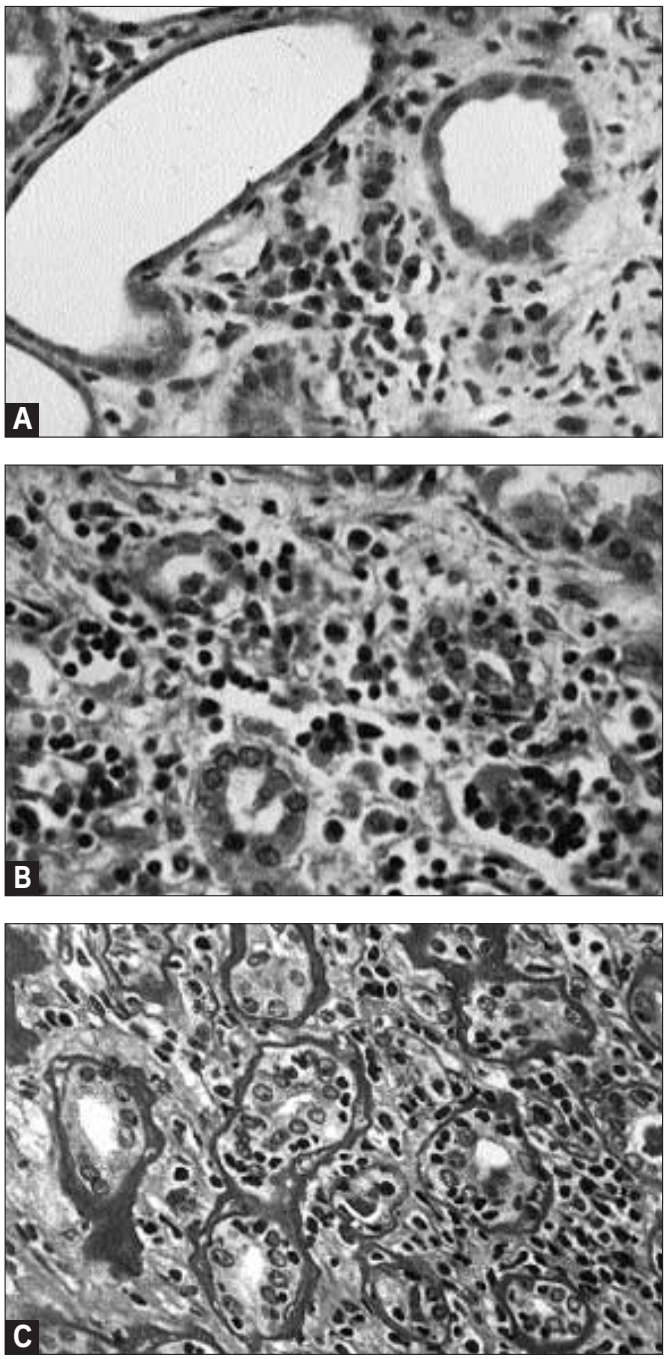

FIGURE 6-11

TIN showing early phase with focal (*A*) and more severe and diffuse (*B*) interstitial inflammatory cell infiltrates. Late phase showing thickened tubular basement membrane, distorted tubular shape, and cellular infiltration of the tubules, called *tubulitis* (*C*). The extent and severity of interstitial cellular infiltrates show a direct correlation with the severity of tubular atrophy and interstitial fibrosis. Experimental studies show the sequential accumulation of T cells and monocytes after the initial insult. Accumulation of these cells implicates their important role both in the early inflammatory stage of the disease and in the progression of subsequent injury.

Immunohistologic examination utilizing monoclonal antibodies, coupled with conventional and electron microscopy, indicates that most of the mononuclear inflammatory cells comprising renal interstitial infiltrates are T cells. These T cells are immunologically activated in the absence of any evidence of tubulointerstitial immune deposits, even in classic examples of immune complex–mediated diseases such as systemic lupus erythematosus. The profile of immunocompetent cells suggests a major role for cell-mediated immunity in the tubulointerstitial lesions. The infiltrating cells may be of the helper-inducer subset or the cyotoxic-suppressor subset, although generally there seems to be a selective prevalence for the former variety. Lymphocytes that are peritubular and are seen invading the tubular epithelial cells, so-called *tubulitis*, are generally of the cytotoxic (CD8+) variety.

The interstitial accumulation of monocytes and macrophages involves osteopontin (uropontin). Osteopontin is a secreted cell attachment glycoprotein whose messenger RNA expression becomes upregulated, and its levels are increased at the sites of tubular injury in proportion to the severity of tubular damage. The expression of other cell adhesion molecules (intercellular adhesion molecule-1, vascular cellular adhesion molecule-1, and E-selectin) also is increased at the sites of tubular injury. This increased expression may contribute to the recruitment of mononuclear cells and increase the susceptibility of renal cells to cell-mediated injury.

Fibroblastic (type I) interstitial cells, which normally produce and maintain the extracellular matrix, begin to proliferate in response to injury. They increase their well-developed rough endoplasmic reticulum and acquire smooth muscle phenotype (myofibroblast). Growth kinetic studies of these cells reveal a significant increase in their proliferating capacity and generation time, indicating hyperproliferative growth.

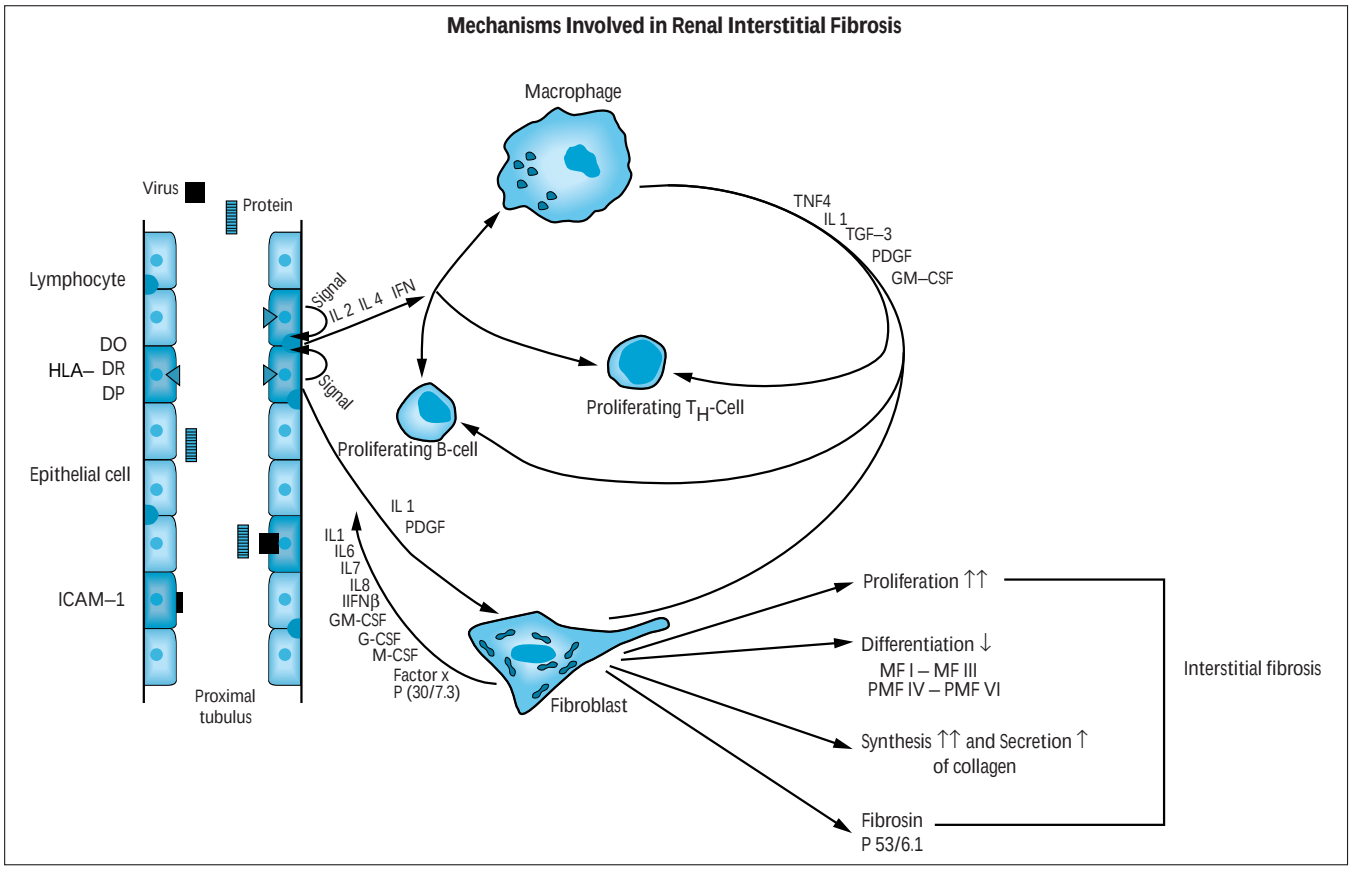

FIGURE 6-12

Expression of human leukocyte antigen class II and adhesion molecules released by injured tubular epithelial cells, as well as by infiltrating cells, modulate and magnify the process to repair the injury (Figure 6-10). When the process becomes unresponsive to controlling feedback mechanisms, fibroblasts proliferate and increase fibrotic matrix deposition. The precise mechanism of TIN remains to be identified. A number of pathogenetic pathways have been proposed to operate at different stages of the disease process. Each of these individual pathways usually is part of a recuperative process that works in concert in response to injury. However, it is the loss of their controlling feedback in chronic TIN that seems to account for the altered balance and results in persistent cellular infiltrates, progressive fibrosis, and tubular degeneration.

Patterns of Tubular Dysfunction

PATTERNS OF TUBULAR DYSFUNCTION IN CHRONIC TIN

Site of injury	Cause	Tubular dysfunction
Cortex		
Proximal tubule	Heavy metals Multiple myeloma Immunologic diseases Cystinosis	Decreased reabsorption of sodium, bicarbonate, glucose, uric acid, phosphate, amino acids
Distal tubule	Immunologic diseases Granulomatous diseases Hereditary diseases Hypercalcemia Urinary tract obstruction Sickle hemoglobinopathy Amyloidosis	Decreased secretion of hydrogen, potassium Decreased reabsorption of sodium
Medulla	Analgesic nephropathy Sickle hemoglobinopathy Uric acid disorders Hypercalcemia Infection Hereditary disorders Granulomatous diseases	Decreased ability to concentrate urine Decreased reabsorption of sodium
Papilla	Analgesic nephropathy Diabetes mellitus Infection Urinary tract obstruction Sickle hemoglobinopathy Transplanted kidney	Decreased ability to concentrate urine Decreased reabsorption of sodium

FIGURE 6-13

The principal manifestations of TIN are those of tubular dysfunction. Because of the focal nature of the lesions that occur and the segmental nature of normal tubular function, the pattern of tubular dysfunction that results varies, depending on the major site of injury. The extent of damage determines the severity of tubular dysfunction. The hallmarks of glomerular disease (such as salt retention, edema, hypertension, proteinuria, and hematuria) are characteristically absent in the early phases of chronic TIN. The type of insult determines the segmental location of injury. For example, agents secreted by the organic pathway in the pars recta (heavy metals) or reabsorbed in the proximal tubule (light chain proteins) cause predominantly proximal tubular lesions. Depositional disorders (amyloidosis and hyperglobulinemic states) cause predominantly distal tubular lesions. Insulting agents that are affected by the urine concentrating mechanism (analgesics and uric acid) or medullary tonicity (sickle hemoglobinopathy) cause medullary injury.

The tubulointerstitial lesions are localized either to the cortex or medulla. Cortical lesions mainly affect either the proximal or distal tubule. Medullary lesions affect the loop of Henle and the collecting duct. The change in the normal function of each of these affected segments then determines the manifestations of tubular dysfunction. Essentially, the proximal nephron segment reabsorbs the bulk of bicarbonate, glucose, amino acids, phosphate, and uric acid. Changes in proximal tubular function, therefore, result in bicarbonaturia (proximal renal acidosis), β_2-microglobinuria, glucosuria (renal glucosuria), aminoaciduria, phosphaturia, and uricosuria.

The distal nephron segment secretes hydrogen and potassium and regulates the final amount of sodium chloride excreted. Lesions primarily affecting this segment, therefore, result in the distal form of renal tubular acidosis, hyperkalemia, and salt wasting. Lesions that primarily involve the medulla and papilla disproportionately affect the loops of Henle, collecting ducts, and the other medullary structures essential to attaining and maintaining medullary hypertonicity. Disruption of these structures, therefore, results in different degrees of nephrogenic diabetes insipidus and clinically manifests as polyuria and nocturia.

Although this general framework is useful in localizing the site of injury, considerable overlap may be encountered clinically, with different degrees of proximal, distal, and medullary dysfunction present in the same individual. Additionally, the ultimate development of renal failure complicates the issue further because of the added effect of urea-induced osmotic diuresis on tubular function in the remaining nephrons. In this later stage of TIN, the absence of glomerular proteinuria and the more common occurrence of hypertension in glomerular diseases can be helpful in the differential diagnosis.

Correlates of Tubular Dysfunction with Severity of Chronic TIN

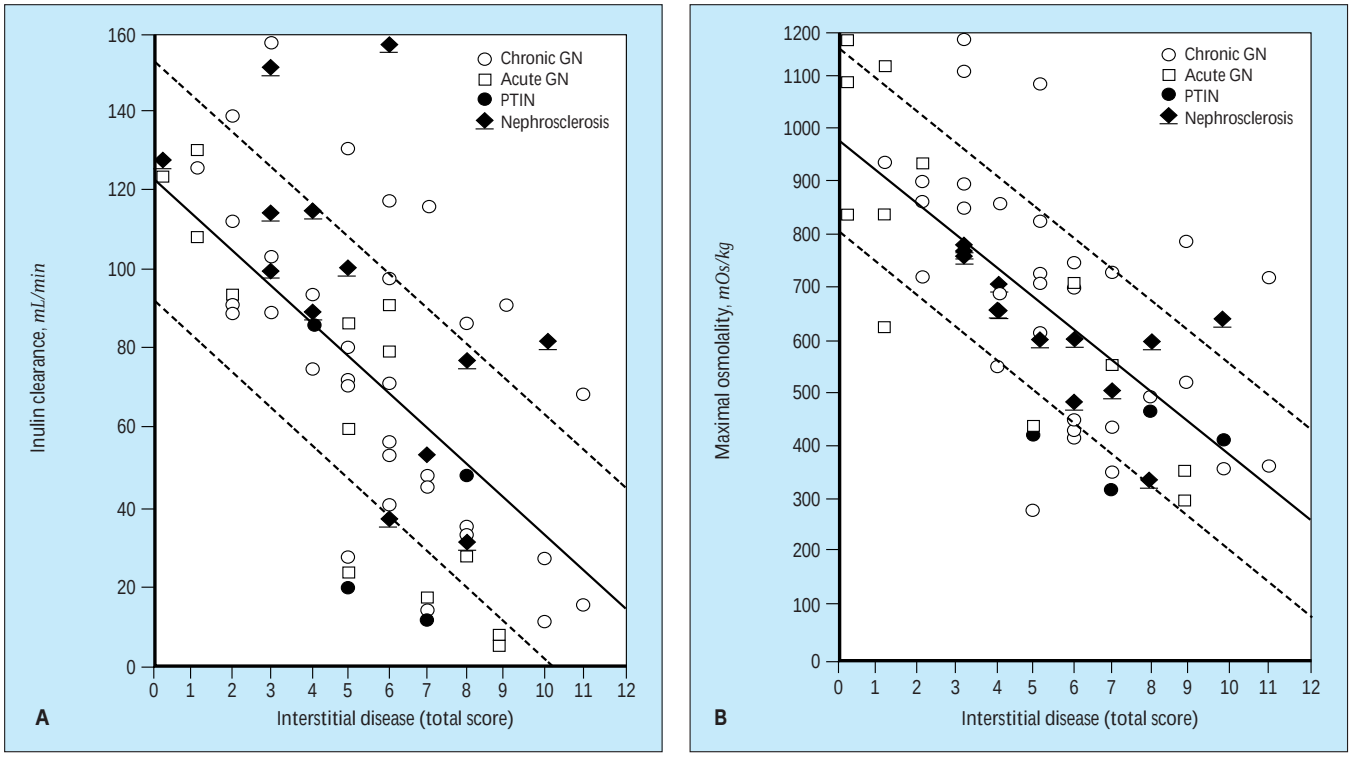

FIGURE 6-14

Relationship of inulin clearance (*A*), maximum urine concentration (*B*), and ammonium excretion in response to an acute acid load (*C*) to the severity of tubulointerstitial nephritis. A close correlation exists between the severity of chronic TIN and impaired renal tubular and glomerular function. Repeated evaluations of kidney biopsy for the extent of tubulointerstitial lesions have shown a close correlation with renal function test results in tests performed before biopsy. These tests include those for inulin clearance, maximal ability to concentrate the urine, and ability to acidify the urine. This correlation has been validated in a variety of renal diseases, including primary and secondary forms of chronic TIN. (*From* Shainuck and coworkers [5]; with permission.)

Correlates of Chronic TIN with Progressive Renal Failure

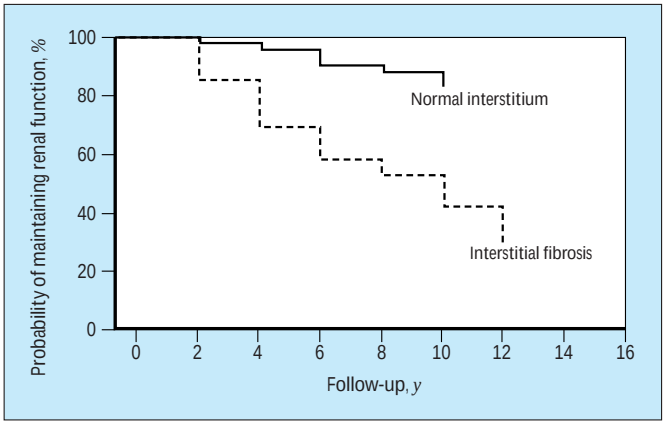

FIGURE 6-15

Effect on long-term prognosis of the presence of cortical chronic tubulointerstitial nephritis in patients with mesangioproliferative glomerulonephritis (n = 455), membranous nephropathy (n = 334), and membranoproliferative glomerulonephritis (n = 220). The extent of tubulointerstitial nephritis correlates not only with altered glomerular and tubular dysfunction at the time of kidney biopsy but also provides a prognostic index of the progression rate to end-stage renal disease. As shown, the presence of interstitial fibrosis on the initial biopsy exerts a significant detrimental effect on the progression rate of renal failure in a variety of glomerular diseases. (*From* Eknoyan [3]; with permission.)

Drugs

Analgesic Nephropathy

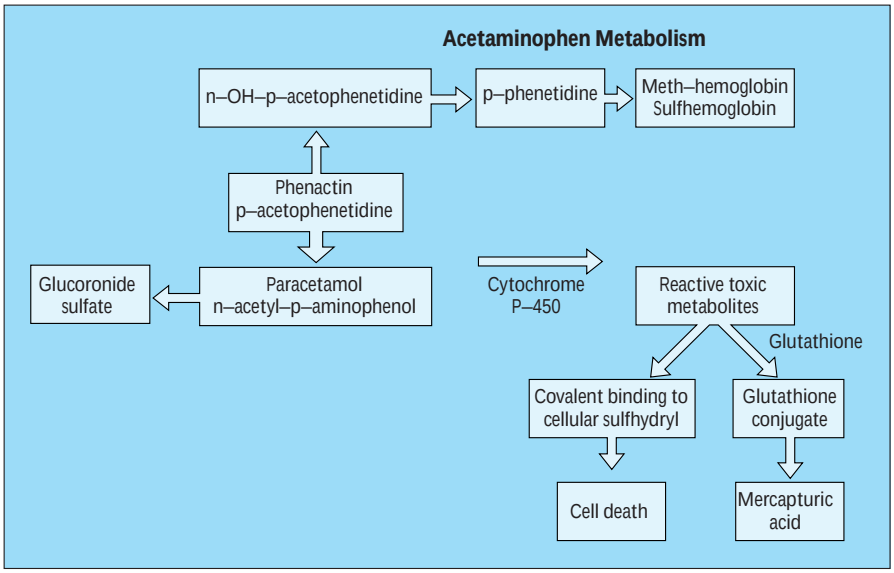

FIGURE 6-16

Metabolism of acetaminophen and its excretion by the kidney. Prolonged exposure to drugs can cause chronic TIN. Although a number of drugs (*eg*, lithium, cyclosporine, cisplatin, and nitrosoureas) have been implicated, the more commonly responsible agents are analgesics. As a rule, the lesions of analgesic nephropathy develop in persons who abuse analgesic combinations (phenacetin, or its main metabolite acetaminophen, plus aspirin, with or without caffeine). Experimental evidence indicates that phenacetin, or acetaminophen, plus aspirin taken alone are only moderately nephrotoxic and only at massive doses, but that the lesions can be more readily induced when these drugs are taken together. In all experimental studies the extent of renal injury has been dose-dependent and, when examined, water diuresis has provided protection from analgesic-induced renal injury. Relative to plasma levels, both acetaminophen (paracetamol) and its excretory conjugate attain significant (fourfold to fivefold) concentrations in the medulla and papilla, depending on the state of hydration of the animal studied. The toxic effect of these drugs apparently is related to their intrarenal oxidation to reactive intermediates that, in the absence of reducing substances such as glutathione, become cytotoxic by virtue of their capacity to induce oxidative injury. Salicylates also are significantly (sixfold to thirteenfold above plasma levels) concentrated in the medulla and papilla, where they attain a level sufficient to uncouple oxidative phosphorylation and compromise the ability of cells to generate reducing substances. Thus, both agents attain sufficient renal medullary concentration to individually exert a detrimental and injurious effect on cell function, which is magnified when they are present together. By reducing the medullary tonicity, and therefore the medullary concentration of drug attained, water diuresis protects from analgesic-induced cell injury. A direct role of analgesic-induced injury can be adduced from the improvement of renal function that can occur after cessation of analgesic abuse.

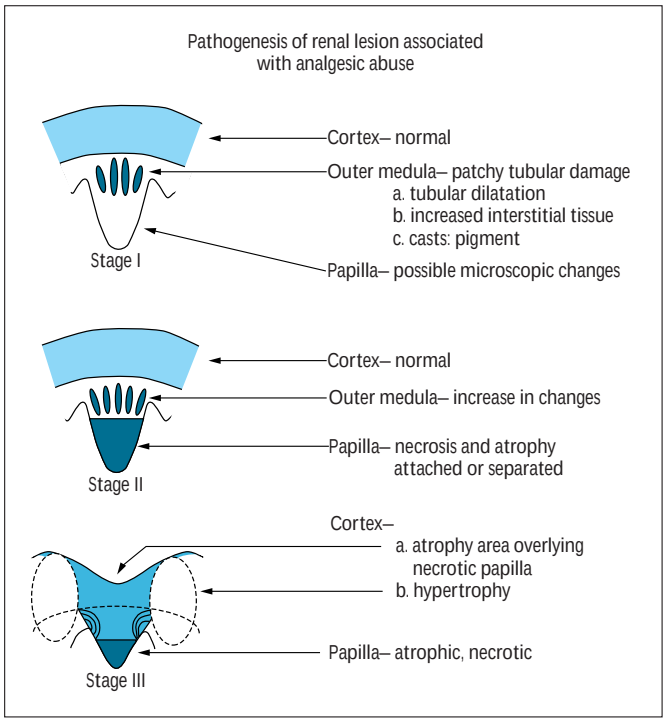

FIGURE 6-17

Course of the renal lesions in analgesic nephropathy. The intrarenal distribution of analgesics provides an explanation for the medullary location of the pathologic lesions of analgesic nephropathy. The initial lesions are patchy and consist of necrosis of the interstitial cells, thin limbs of the loops of Henle, and vasa recta of the papilla. The collecting ducts are spared. The quantities of tubular and vascular basement membrane and ground substance are increased. At this stage the kidneys are normal in size and no abnormalities have occurred in the renal cortex. With persistent drug exposure the changes extend to the outer medulla. Again, the lesions are initially patchy, involving the interstitial cells, loops of Henle, and vascular bundles. With continued analgesic abuse, the severity of the inner medullary lesions increases with sclerosis and obliteration of the capillaries, atrophy and degeneration of the loops of Henle and collecting ducts, and the beginning of calcification of the necrotic foci. Ultimately, the papillae become entirely necrotic, with sequestration and demarcation of the necrotic tissue. The necrotic papillae may then slough and are excreted into the urine or remain *in situ*, where they atrophy further and become calcified. Cortical scarring, characterized by interstitial fibrosis, tubular atrophy, and periglomerular fibrosis, develops over the necrotic medullary segments. The medullary rays traversing the cortex are usually spared and become hypertrophic, thereby imparting a characteristic cortical nodularity to the now shrunken kidneys. Visual observation of these configurational changes by computed tomography scan can be extremely useful in the diagnosis of analgesic nephropathy.

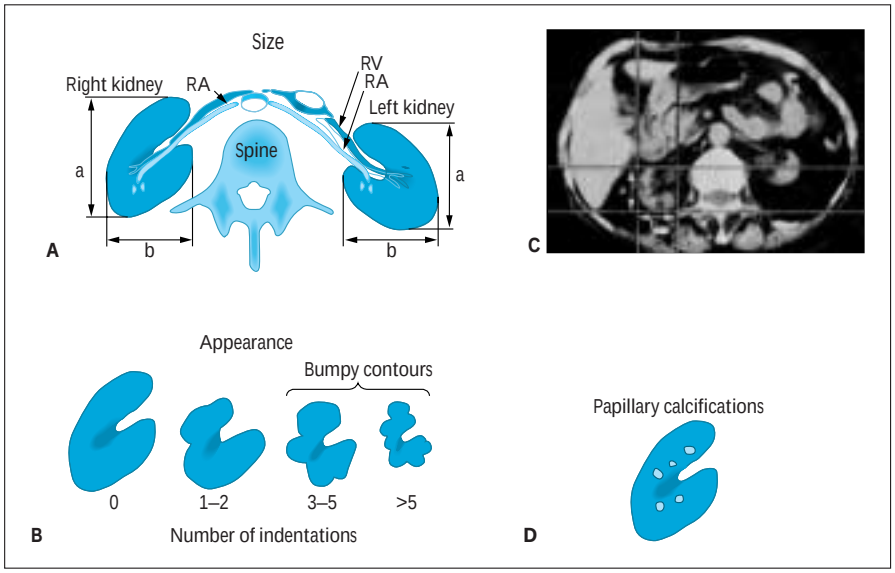

FIGURE 6-18

Computed tomography (CT) imaging criteria for diagnosing analgesic nephropathy. Renal size (*A*) is considered decreased if the sum of a and b (panels *A* and *B*) is less than 103 mm in men and 96 mm in women. Bumpy contours are considered to be present if at least three indentations are evident (panels *B* and *C*). The scan can reveal papillary calcifications (panels *B* and *D*). Visual observation of the configurational changes illustrated in Figure 6-18 can be extremely useful in diagnosing the scarred kidney in analgesic nephropathy. A series of careful studies using CT scans without contrast material have provided imaging criteria for the diagnosis of analgesic nephropathy. Validation of these criteria currently is underway by a study at the National Institutes of Health.

From studies comparing analgesic abusers to persons in control groups, it has been shown that a decrease in kidney size and bumpy contours of both kidneys provide a diagnostic sensitivity of 90% and a specificity of 95%. The additional finding of evidence of renal papillary necrosis provides a diagnostic sensitivity of 72% and specificity of 97%, giving a positive predictive value of 92%. RA—renal artery; RV— renal vein. (*From* DeBroe and Elseviers [6]; with permission.)

CLINICAL FEATURES

Female predominance, 60–85%

Age, >30 y

Personality disorders: introvert, dependent, anxiety, neurosis, family instability

Addictive habits: smoking, alcohol, laxatives, psychotropics, sedatives

Causes of analgesic dependency: headache, 40–60%; mood, 6–30%; musculoskeletal pain, 20–30%

FIGURE 6-19

Certain personality features and clinical findings characterize patients prone to analgesic abuse. These patients tend to deny analgesic use on direct questioning; however, their history can be revealing. In all cases, a relationship exists between renal function and the duration, intensity, and quantity of analgesic consumed. The magnitude of injury is related to the quantity of analgesic ingested chronically over years. In persons with significant renal impairment, the average dose ingested has been estimated at about 10 kg over a mean period of 13 years. The minimum amount of drug consumption that results in significant renal damage is unknown. It has been estimated that a cumulative dose of 3 kg of the index compound, or a daily ingestion of 1 g/d over 3 years or more, is a minimum that can result in detectable renal impairment.

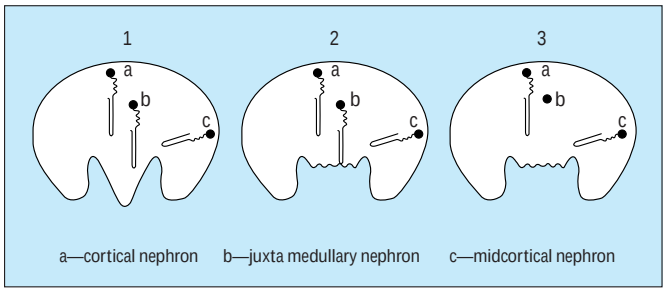

FIGURE 6-20

Diagram of cortical and juxtamedullary nephrons in the normal kidney (1). Papillary necrosis (2) and sloughing (3) result in loss of juxtamedullary nephrons. Cortical nephrons are spared, thereby preserving normal renal function in the early stages of the disease. The course of analgesic nephropathy is slowly progressive, and deterioration of renal function is insidious. One reason for these characteristics of the disease is that lesions beginning in the papillary tip affect only the juxtamedullary nephrons, sparing the cortical nephrons. It is only when the lesions are advanced enough to affect the whole medulla that the number of nephrons lost is sufficient to result in a reduction in filtration rate. However, renal injury can be detected by testing for sterile pyuria, reduced concentrating ability, and a distal acidifying defect. These features may be evident at levels of mild renal insufficiency and become more pronounced and prevalent as renal function deteriorates. Proximal tubular function is preserved in patients with mild renal insufficiency but can be abnormal in those with more advanced renal failure.

Cyclosporine

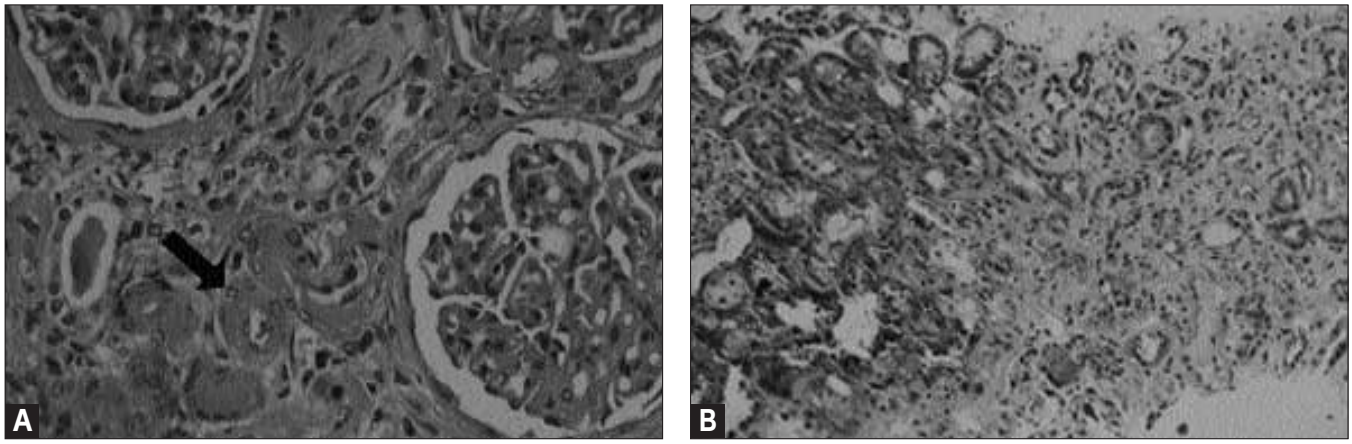

FIGURE 6-21

A, Chronic TIN caused by cyclosporine. The arrow indicates the characteristic hyaline-type arteriolopathy of cyclosporine nephrotoxicity. **B,** Patchy nature of chronic TIN caused by cyclosporine. Note the severe TIN on the right adjacent to an otherwise intact area on the left. Tubulointerstitial nephritis has emerged as the most serious side effect of cyclosporine. Cyclosporine-mediated vasoconstriction of the cortical microvasculature has been implicated in the development of an occlusive arteriolopathy and tubular epithelial cell injury. Whereas these early lesions tend to be reversible with cessation of therapy, an irreversible interstitial fibrosis and mononuclear cellular infiltrates develop with prolonged use of cyclosporine, especially at high doses. The irreversible nature of TIN associated with the use of cyclosporine and its attendant reduction in renal function have raised concerns regarding the long-term use of this otherwise efficient immunosuppressive agent.

Heavy Metals

Lead Nephropathy

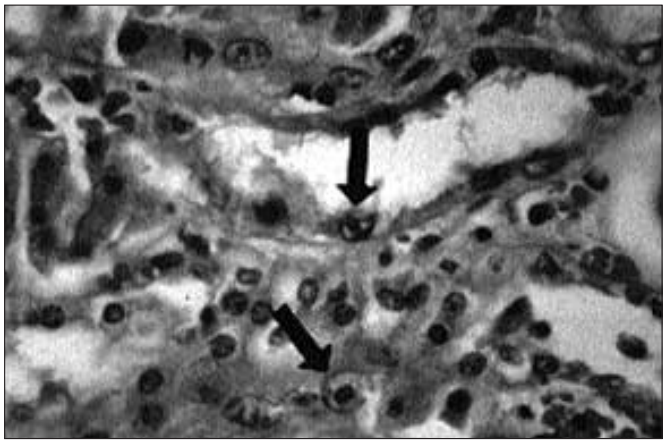

FIGURE 6-22

Lead nephropathy. Arrows indicate the characteristic intranuclear inclusions. Exposure to a variety of heavy metals results in development of chronic TIN. Of these metals, the more common and clinically important implicated agent is lead. Major sources of exposure to lead are lead-based paints; lead leaked into food during storage or processing, particularly in illegal alcoholic beverages (moonshine); and increasingly, through environmental exposure (gasoline and industrial fumes). This insidious accumulation of lead in the body has been implicated in the causation of hyperuricemia, hypertension, and progressive renal failure. Gout occurs in over half of cases. Blood levels of lead usually are normal. The diagnosis is established by demonstrating increased levels of urinary lead after infusion of 1 g of the chelating agent erthylenediamine tetraacetic acid (EDTA).

The renal lesions of lead nephropathy are those of chronic TIN. Cases examined early, before the onset of end-stage renal disease, show primarily focal lesions of TIN with relatively little interstitial cellular infiltrates. In more advanced cases the kidneys are fibrotic and shrunken. On microscopy, the kidneys show diffuse lesions of TIN. As expected from the clinical features, hypertensive vascular changes are prominent.

Other heavy metals associated with TIN are cadmium, silicon, copper, bismuth, and barium. Sufficient experimental evidence and some weak epidemiologic evidence suggest a possible role of organic solvents in the development of chronic TIN.

Ischemic Vascular Disease

Hypertensive Nephrosclerosis

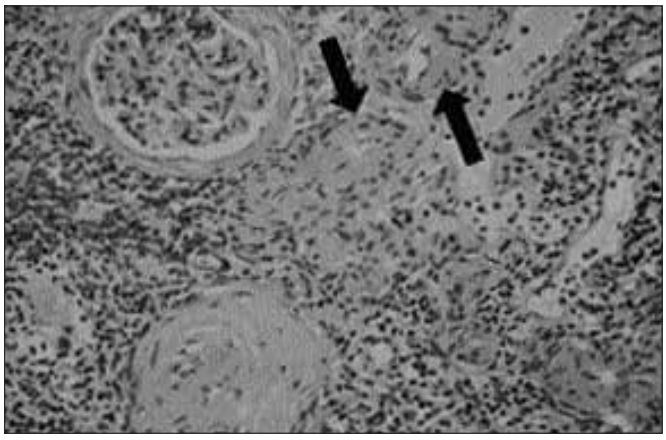

FIGURE 6-23

Chronic TIN associated with hypertension. The arrows indicate arterioles and small arteries with thickened walls. Tubular degeneration, interstitial fibrosis, and mononuclear inflammatory cell infiltration are part of the degenerative process that affects the kidneys in all vascular diseases involving the intrarenal vasculature with any degree of severity as to cause ischemic injury. Rarely, if the insult is sudden and massive (such as in fulminant vasculitis), the lesions are those of infarction and acute deterioration of renal function. More commonly, the vascular lesions develop gradually and go undetected until renal insufficiency supervenes. This chronic form of TIN accounts for the tubulointerstitial lesions of arteriolar nephrosclerosis in persons with hypertension. Ischemic vascular changes also contribute to the lesions of TIN in patients with diabetes, sickle cell hemoglobinopathy, cyclosporine nephrotoxicity, and radiation nephritis.

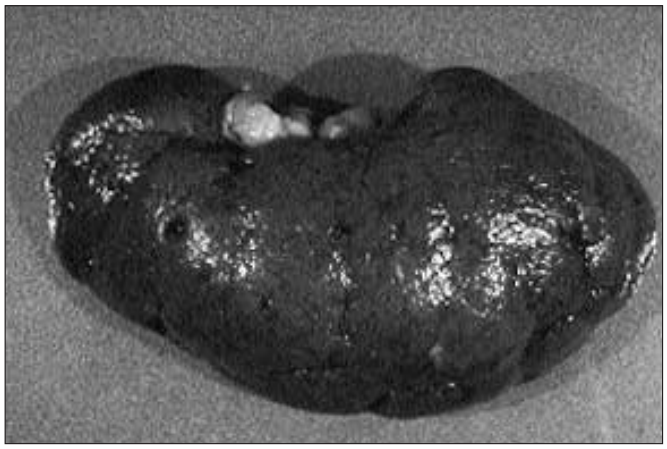

FIGURE 6-24
Gross appearance of the kidney as a result of arteriolonephrosclerosis, showing the granular and scarified cortex.

Obstruction

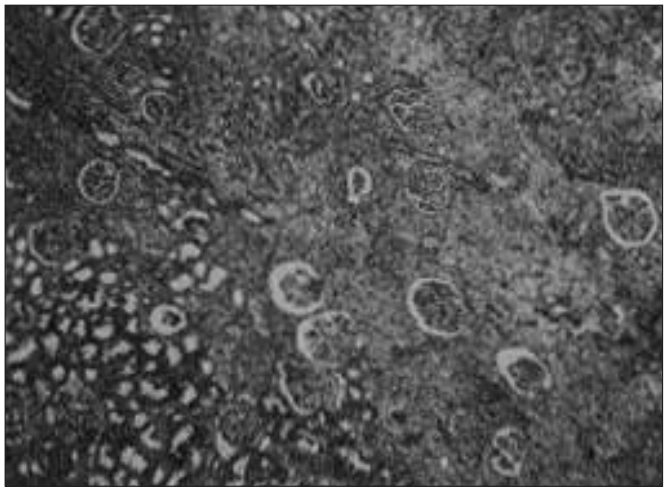

FIGURE 6-25 (*see* Color Plate)
Chronic TIN secondary to vesicoureteral reflux (VUR). Clearly demonstrated is an area that is fairly intact (lower left corner) adjacent to one that shows marked damage. Urinary tract obstruction, whether congenital or acquired, is a common cause of chronic TIN. Clinically, superimposed infection plays a secondary, adjunctive, and definitely aggravating role in the progressive changes of TIN. However, the entire process can occur in the absence of infection.

As clearly demonstrated in experimental models of obstruction, mononuclear inflammatory cell infiltration is one of the earliest responses of the kidney to ureteral obstruction. The infiltrating cells consist of macrophages and suppressor-cytotoxic lymphocytes. The release of various cytokines by the infiltrating cells of the hydronephrotic kidney appears to exert a significant modulating role in the transport processes and hemodynamic changes seen early in the course of obstruction. With persistent obstruction, changes of chronic TIN set in within weeks. Fibrosis gradually becomes prominent.

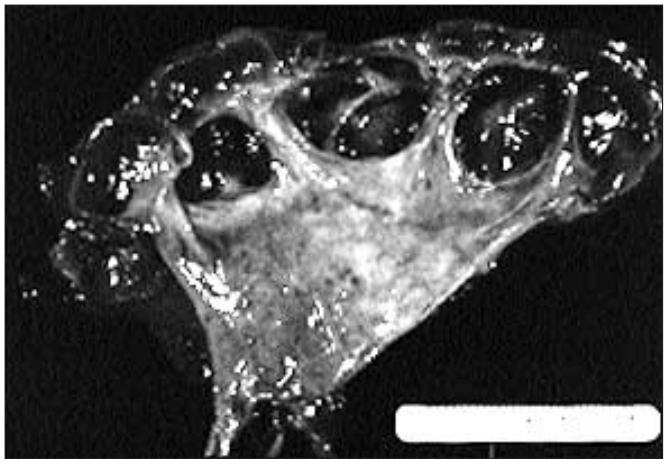

FIGURE 6-26
Gross appearance of a hydronephrotic kidney caused by vesicoureteral reflux.

Obstructive Nephropathy

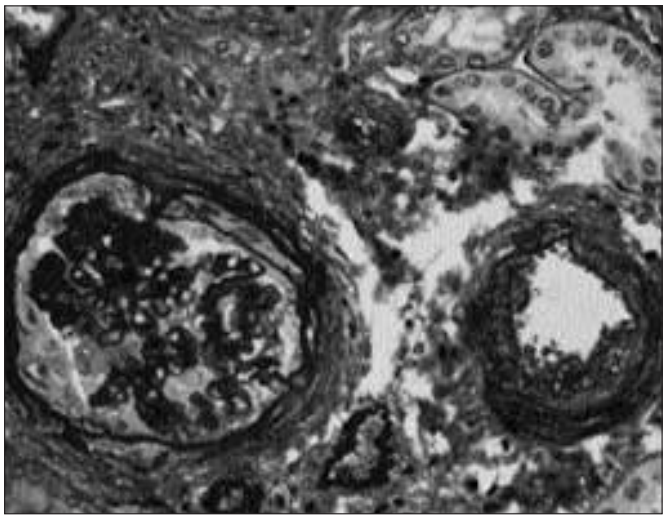

FIGURE 6-27

Glomerular lesion of advanced chronic TIN secondary to vesicoureteral reflux in a patient with massive proteinuria. Note the segmental sclerosis of the glomerulus and the reactive proliferation of the visceral epithelial cells. In persons with obstructive nephropathy, the onset of significant proteinuria (>2g/d) is an ominous sign of progressive renal failure. As a rule, most of these patients will have coexistent hypertension, and the renal vasculature will show changes of hypertensive arteriolosclerosis. The glomerular changes are ischemic in nature. In those with significant proteinuria, the lesions are those of focal and segmental glomerulosclerosis and hyalinosis. The affected glomeruli commonly contain immunoglobulin M and C_3 complement on immunofluorescent microscopy. The role of an immune mechanism remains unclear. Autologous (Tamm-Horsfall protein and brush-border antigen) or bacterial antigen derivatives have been incriminated. Adaptive hemodynamic changes (hyperfiltration) in response to a reduction in renal mass, by the glomeruli of remaining intact nephrons of the hydronephrotic kidney, also have been implicated.

Hematopoietic Diseases

Sickle Hemoglobinopathy

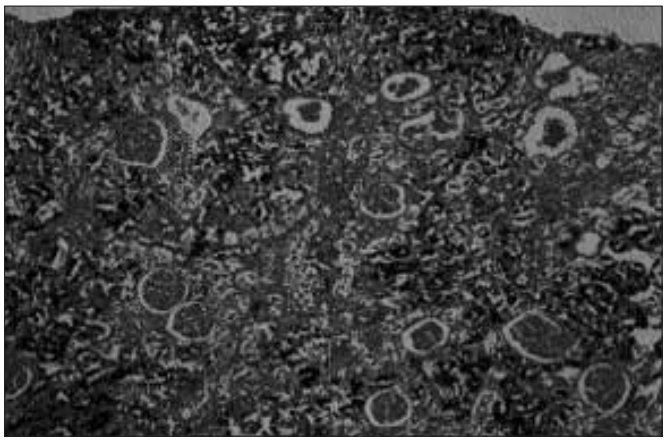

FIGURE 6-28

The kidney in sickle cell disease. Note the tubular deposition of hemosiderin. The principal renal lesion of hemoglobinopathy S is that of chronic TIN. By far more prevalent and severe in patients with sickle cell disease, variable degrees of TIN also are common in those with the sickle cell trait, sickle cell–hemoglobin C disease, or sickle cell–thalassemia disease. The predisposing factors that lead to a propensity of renal involvement are the physicochemical properties of hemoglobin S that predispose its polymerization in an environment of low oxygen tension, hypertonicity, and low pH. These conditions are characteristic of the renal medulla and therefore are conducive to the intraerythrocyte polymerization of hemoglobin S. The consequent erythrocyte sickling accounts for development of the typical vascular occlusive lesions. Although some of these changes occur in the cortex, the lesions begin and are predominantly located in the inner medulla, where they are at the core of the focal scarring and interstitial fibrosis. These lesions account for the common occurrence of papillary necrosis.

Examples of tubular functional abnormalities common and detectable early in the course of the disease are the following: impaired concentrating ability, depressed distal potassium and hydrogen secretion, tubular proteinuria, and decreased proximal reabsorption of phosphate, and increased secretion of uric acid and creatinine.

Hematologic Diseases

Plasma Cell Dyscrasias

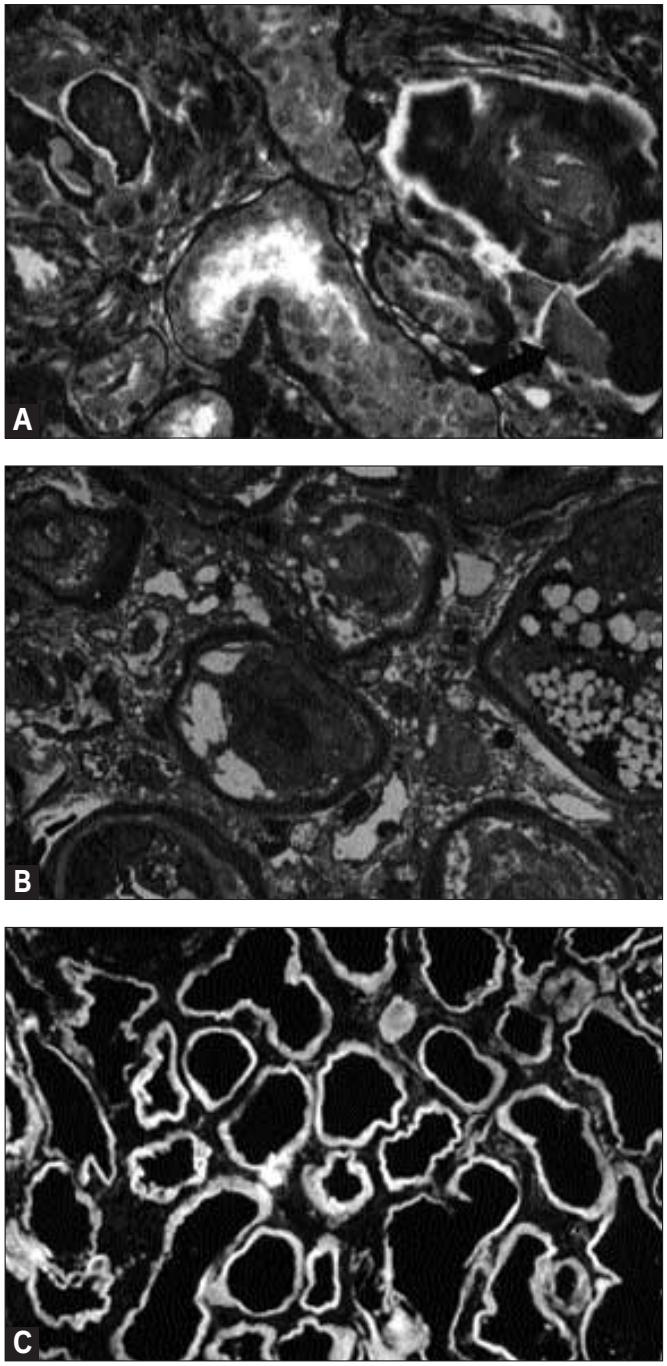

FIGURE 6-29 (*see* Color Plate)

A, Myeloma cast nephropathy. The *arrow* indicates a multinucleated giant cell. **B,** Light chain deposition disease. Note the changes indicative of chronic TIN and light chain deposition along the tubular basement membrane (dark purple). **C,** Immunofluorescent stain for κ light chain deposition along the tubular basement membrane. The renal complications of multiple myeloma are a major risk factor in the morbidity and mortality of this neoplastic disorder. Whereas the pathogenesis of renal involvement is multifactorial (hypercalcemia and hyperuricemia), it is the lesions that result from the excessive production of light chains that cause chronic TIN. These lesions are initiated by the precipitation of the light chain dimers in the distal tubules and result in what has been termed *myeloma cast nephropathy*. The affected tubules are surrounded by multinucleated giant cells. Adjoining tubules show varying degrees of atrophy. The propensity of light chains to lead to myeloma cast nephropathy appears to be related to their concentration in the tubular fluid, the tubular fluid pH, and their structural configuration. This propensity accounts for the observation that increasing the flow rate of urine or its alkalinization will prevent or reverse the casts in their early stages of formation.

Direct tubular toxicity of light chains also may contribute to tubular injury. λ Light chains appear to be more injurious than are κ light chains. Binding of human κ and λ light chains to human and rat proximal tubule epithelial cell brush-border membrane has been demonstrated. Epithelial cell injury associated with the absorption of these light chains in the proximal tubules has been implicated in the pathogenesis of cortical TIN. Another mechanism relates to the perivascular deposition of paraproteins, either as amyloid fibrils that are derived from λ chains or as fragments of light chains that are derived from kappa chains, and produce the so-called light chain deposition disease.

Of the various lesions, myeloma cast nephropathy appears to be the most common, being observed at autopsy in one third of cases, followed by amyloid deposition, which is present in 10% of cases. Light chain deposition is relatively rare, being present in less than 5% of cases.

Metabolic Disorders

Hyperuricemia

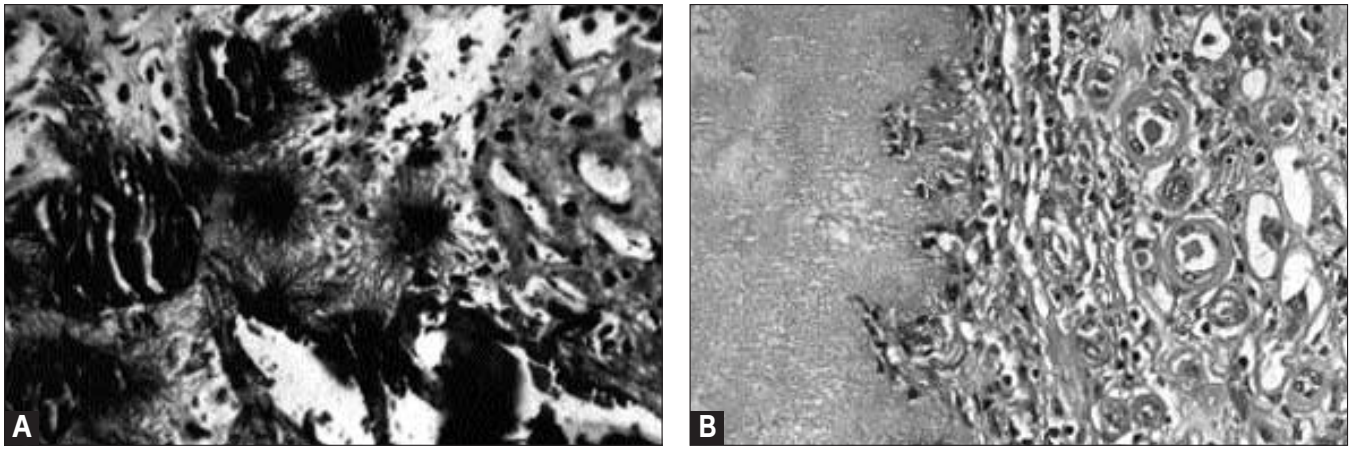

FIGURE 6-30

A, Intratubular deposits of uric acid. **B,** Gouty tophus in the renal medulla. The kidney is the major organ of urate excretion and a primary target organ affected in disorders of its metabolism. Renal lesions result from crystallization of urate in the urinary outflow tract or the renal parenchyma. Depending on the load of urate, one of three lesions result: acute urate nephropathy, uric acid nephrothiasis, or chronic urate nephropathy. Whereas any of these lesions produce tubulointerstitial lesions, it is those of chronic urate nephropathy that account for most cases of chronic TIN.

The principal lesion of chronic urate nephropathy is due to deposition of microtophi of amorphous urate crystals in the interstitium, with a surrounding giant-cell reaction. An earlier change, however, probably is due to the precipitation of birefringent uric acid crystals in the collecting tubules, with consequent tubular obstruction, dilatation, atrophy, and interstitial fibrosis. The renal injury in persons who develop lesions has been attributed to hyperacidity of their urine caused by an inherent abnormality in the ability to produce ammonia. The acidity of urine is important because uric acid is 17 times less soluble than is urate. Therefore, uric acid facilitates precipitation in the distal nephron of persons who do not overproduce uric acid but who have a persistently acidic urine.

The previous notion that chronic renal disease was common in patients with hyperuricemia is now considered doubtful in light of prolonged follow-up studies of renal function in persons with hyperuricemia. Renal dysfunction could be documented only when the serum urate concentration was more than 10 mg/dL in women and more than 13 mg/dL in men for prolonged periods. The deterioration of renal function in persons with hyperuricemia of a lower magnitude has been attributed to the higher than expected occurrence of concurrent hypertension, diabetes mellitus, abnormal lipid metabolism, and nephrosclerosis.

Hyperoxaluria

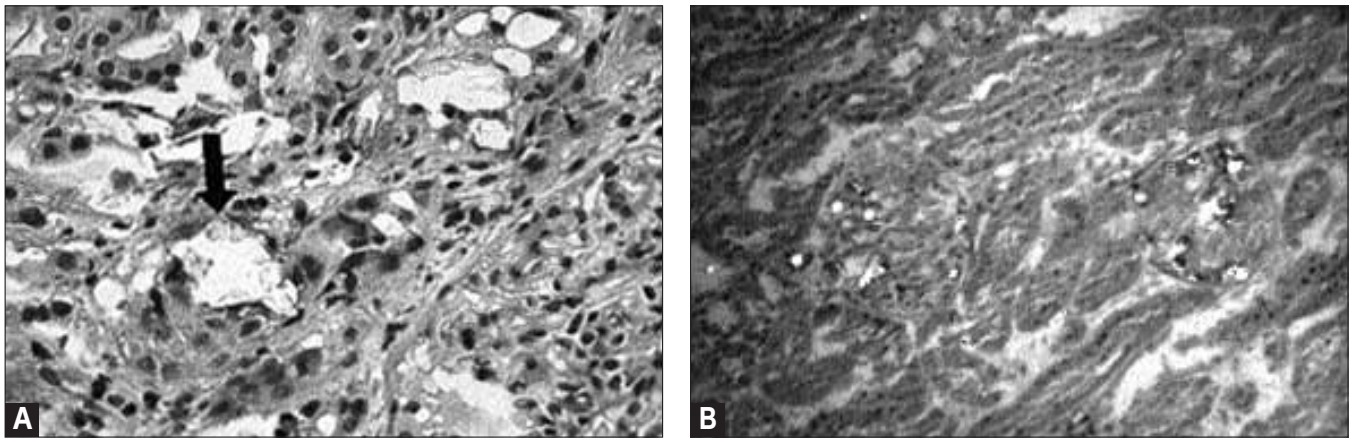

FIGURE 6-31 (*see* Color Plate)

A, Calcium oxalate crystals (arrow) seen on light microscopy. **B,** Dark field microscopy. When hyperoxaluria is sudden and massive (such as after ethylene glycol ingestion) acute renal failure develops. Otherwise, in most cases of hyperoxaluria the overload is insidious and chronic. As a result, interstitial fibrosis, tubular atrophy, and dilation result in chronic TIN with progressive renal failure. The propensity for recurrent calcium oxalate nephrolithiasis and consequent obstructive uropathy contribute to the tubulointerstitial lesions.

Granulomatous Diseases

Malacoplakia

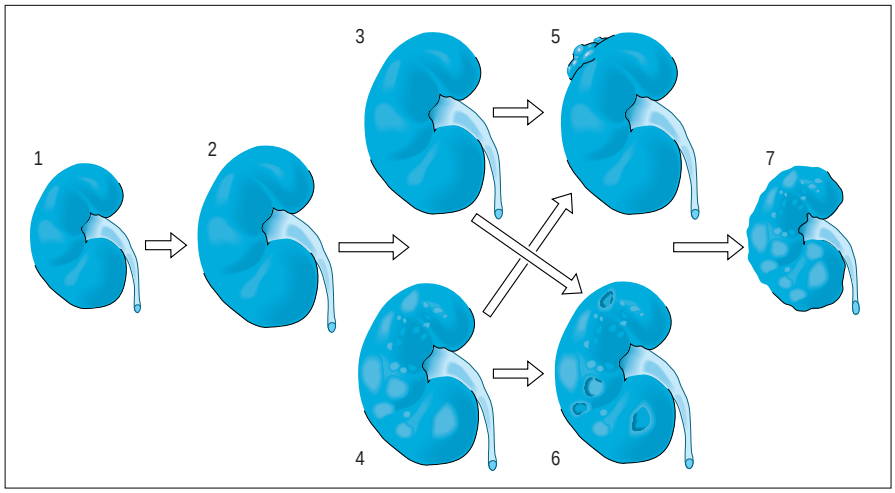

FIGURE 6-32

Schematic representation of the forms and course of renal involvement by malacoplakia: 1, normal kidney; 2, enlarged kidney resulting from interstitial nephritis without nodularity; 3, unifocal nodular involvement; 4, multifocal nodular involvement; 5, abscess formation with perinephric spread of malacoplakia; 6, cystic lesions; and 7, atrophic multinodular kidney after treatment. Interstitial granulomatous reactions are a rare but characteristic hallmark of certain forms of tubulointerstitial disease. The best-known form is that of sarcoidosis. Interstitial granulomatous reactions also have been noted in renal tuberculosis, xanthogranulomatous pyelonephritis, renal malacoplakia, Wegener's granulomatosis, renal candidiasis, heroin abuse, hyperoxaluria after jejunoileal bypass surgery, and an idiopathic form in association with anterior uveitis.

The inflammatory lesions of malacoplakia principally affect the urinary bladder but may involve other organs, most notably the kidneys. The kidney lesions may be limited to one focus or may be multifocal. In three fourths of cases the renal involvement is multifocal, and in one third of cases both kidneys are involved. The lesions are nodular, well-demarcated, and variable in size. They may coalesce, developing foci of suppuration that may become cystic or calcified. The lesions usually are located in the cortex but may be medullary and result in papillary necrosis. (*From* Dobyan and coworkers [7]; with permission.)

Endemic Diseases

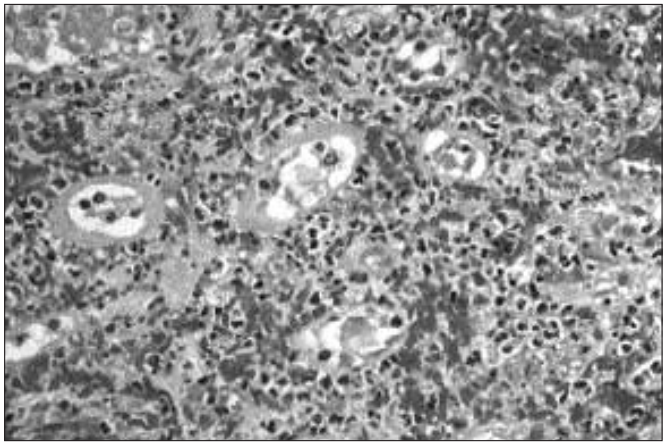

FIGURE 6-33

Hemorrhagic TIN associated with Hantavirus infection. Two endemic diseases in which tubulointerstitial lesions are a predominant component are Balkan nephropathy and nephropathia epidemica. Endemic Balkan nephropathy is a progressive chronic tubulointerstitial nephritis whose occurrence is mostly clustered in a geographic area bordering the Danube River as it traverses Romania, Bulgaria, and the former Yugoslavia. The cause of Balkan nephropathy is unknown; however, it has been attributed to genetic factors, heavy metals, trace elements, and infectious agents. The disease evolves in emigrants from endemic regions, suggesting a role for inheritance or the perpetuation of injury sustained before emigration.

Initially thought to be restricted to Scandinavian countries, and thus termed *Scandinavian acute hemorrhagic interstitial nephritis*, Nephropathia epidemica has been shown to have a more universal occurrence. It therefore has been more appropriately renamed *hemorrhagic fever with renal syndrome*. As a rule the disease presents as a reversible acute tubulointerstitial nephritis but can progress to a chronic form. It is caused by a rodent-transmitted virus of the *Hantavirus* genus of the Bunyaviridae family, the so-called Hantaan virus. Humans appear to be infected by respiratory aerosols contaminated by rodent excreta. Antibodies to the virus are detected in the serum, and viruslike structures have been demonstrated in the kidneys of persons infected with the virus.

Tubulointerstitial nephropathy caused by viral infection also has been reported in polyomavirus, cytomegalovirus, herpes simplex virus, human immunodeficiency virus, infectious mononucleosis, and Epstein-Barr virus.

Hereditary Diseases

Hereditary Nephritis

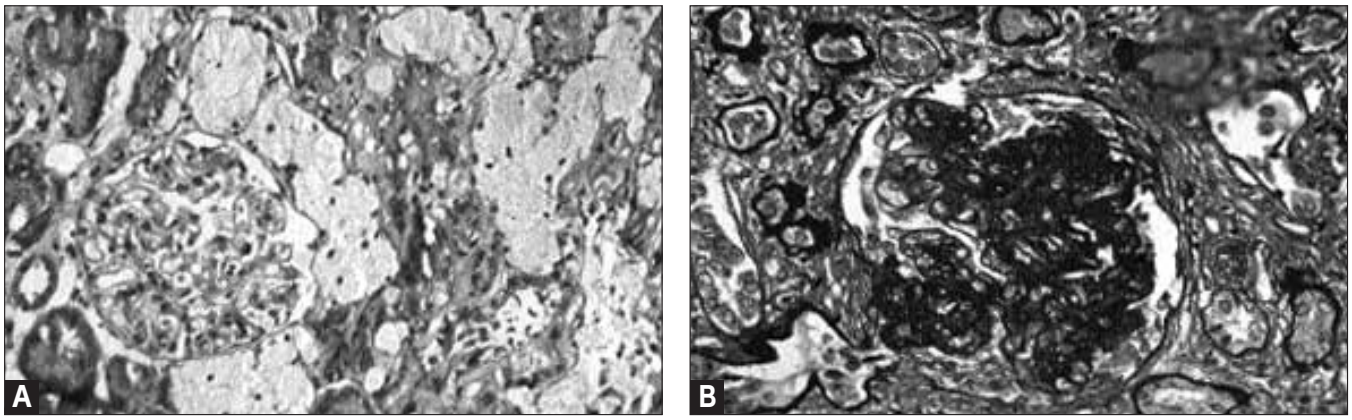

FIGURE 6-34

A, Interstitial foam cells in Alport's syndrome. **B,** Late phase Alport's syndrome showing chronic TIN and glomerular changes in a patient with massive proteinuria. Tubulointerstitial lesions are a prominent component of the renal pathology of a variety of hereditary diseases of the kidney, such as medullary cystic disease, familial juvenile nephronophthisis, medullary sponge kidney, and polycystic kidney disease. The primary disorder of these conditions is a tubular defect that results in the cystic dilation of the affected segment in some patients. Altered tubular basement membrane composition and associated epithelial cell proliferation account for cyst formation. It is the continuous growth of cysts and their progressive dilation that cause pressure-induced ischemic injury, with consequent TIN of the adjacent renal parenchyma.

Tubulointerstitial lesions also are a salient feature of inherited diseases of the glomerular basement membrane. Notable among them are those of hereditary nephritis or Alport's syndrome, in which a mutation in the encoding gene localized to the X chromosome results in a defect in the α-5 chain of type IV collagen.

Papillary Necrosis

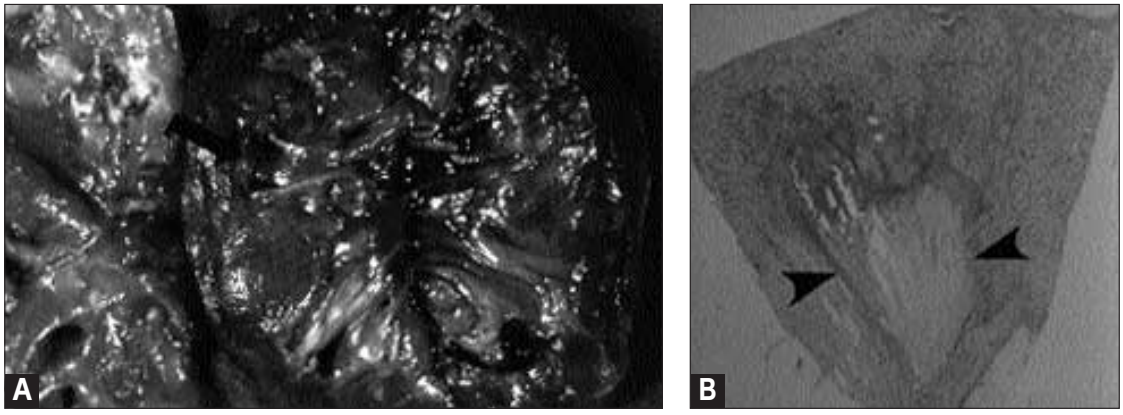

FIGURE 6-35

A, Renal papillary necrosis. The arrow points to the region of a sloughed necrotic papilla. *B*, Whole mount of a necrotic papilla. Arrows delineate focal necrosis principally affecting the medullary inner stripe. Renal papillary necrosis (RPN) develops in a variety of diseases that cause chronic tubulointerstitial nephropathy in which the lesion is more severe in the inner medulla. The basic lesion affects the vasculature with consequent focal or diffuse ischemic necrosis of the distal segments of one or more renal pyramids. In the affected papilla, the sharp demarcation of the lesion and coagulative necrosis seen in the early stages of the disease closely resemble those of infarction. The fact that the necrosis is anatomically limited to the papillary tips can be attributed to a variety of features unique to this site, especially those affecting the vasculature. The renal papilla receives its blood supply from the vasa recta. Measurements of medullary blood flow notwithstanding, it should be noted that much of the blood flow in the vasa recta serves the countercurrent exchange mechanism. Nutrient blood supply is provided by small capillary vessels that originate in each given region. The net effect is that the blood supply to the papillary tip is less than that to the rest of the medulla, hence its predisposition to ischemic necrosis.

The necrotic lesions may be limited to only a few of the papillae or may involve several of the papillae in either one or both kidneys. The lesions are bilateral in most patients. In patients with involvement of one kidney at the time of initial presentation, RPN will develop in the other kidney within 4 years, which is not unexpected because of the systemic nature of the diseases associated with RPN. RPN may be unilateral in patients in whom predisposing factors (such as infection and obstruction) are limited to one kidney.

Azotemia may be absent even in bilateral papillary necrosis, because it is the total number of papillae involved that ultimately determines the level of renal insufficiency that develops. Each human kidney has an average of eight pyramids, such that even with bilateral RPN affecting one papilla or two papillae in each kidney, sufficient unaffected renal lobules remain to maintain an adequate level of renal function.

As a rule, RPN is a disease of an older age group, the average age of patients being 53 years. Nearly half of cases occur in persons over 60 years of age. More than 90% of cases occur in persons over 40 years of age, except for those caused by sickle cell hemoglobinopathy. RPN is much less common in children, in whom the chronic conditions associated with papillary necrosis are rare. However, RPN does occur in children in association with hypoxia, dehydration, and septicemia.

Total Papillary Necrosis

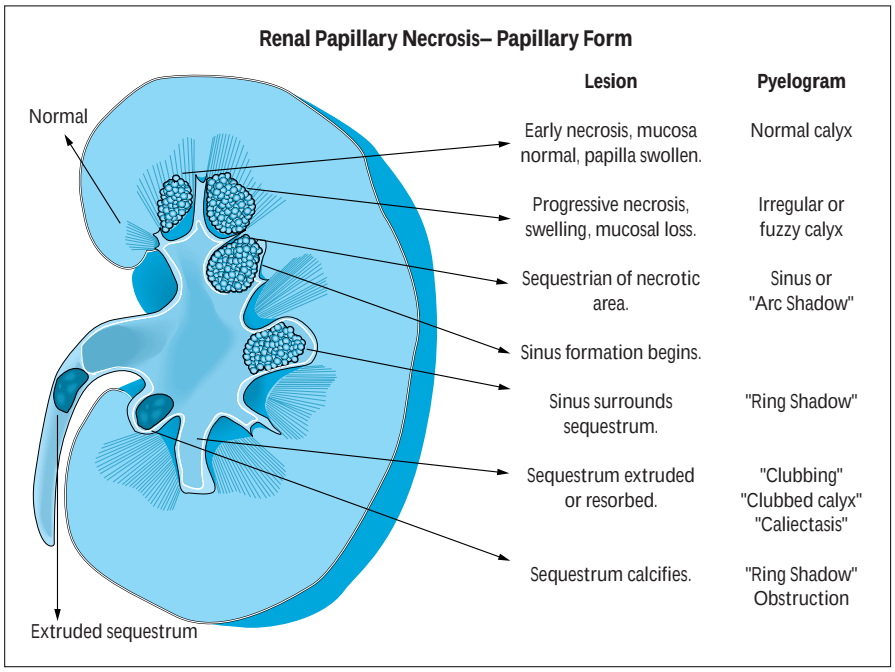

FIGURE 6-36

Schematic of the progressive stages of the papillary form of renal papillary necrosis and their associated radiologic changes seen on intravenous pyelography. Papillary necrosis occurs in one of two forms. In the medullary form, also termed *partial papillary necrosis*, the inner medulla is affected; however, the papillary tip and fornices remain intact. In the papillary form, also termed *total papillary necrosis*, the calyceal fornices and entire papillary tip are necrotic. In total papillary necrosis shown here, the lesion is characterized from the outset by necrosis, demarcation, and sequestration of the papillae, which ultimately slough into the pelvis and may be recovered in the urine. In most of these cases, however, the necrotic papillae are not sloughed but are either resorbed or remain *in situ*, where they becomes calcified or form the nidus of a calculus. In these patients, excretory radiologic examination and computed tomography scanning are diagnostic. Unfortunately, these changes may not be evident until the late stages of RPN, when the papillae already are shrunken and sequestered. In fact, even when the papillae are sloughed out, excretory radiography can be negative.

The passage of sloughed papillae is associated with lumbar pain, which is indistinguishable from ureteral colic of any cause and is present in about half of patients. Oliguria occurs in less than 10% of patients. A definitive diagnosis of RPN can be made by finding portions of necrotic papillae in the urine. A deliberate search should be made for papillary fragments in urine collected during or after attacks of colicky pain of all suspected cases, by straining the urine through filter paper or a piece of gauze. The separation and passage of papillary tissue may be associated with hematuria, which is microscopic in some 40% to 45% of patients and gross in 20%. The hematuria can be massive, and occasionally, instances of exsanguinating hemorrhage requiring nephrectomy have been reported. (*From* Eknoyan and coworkers [8]; with permission.)

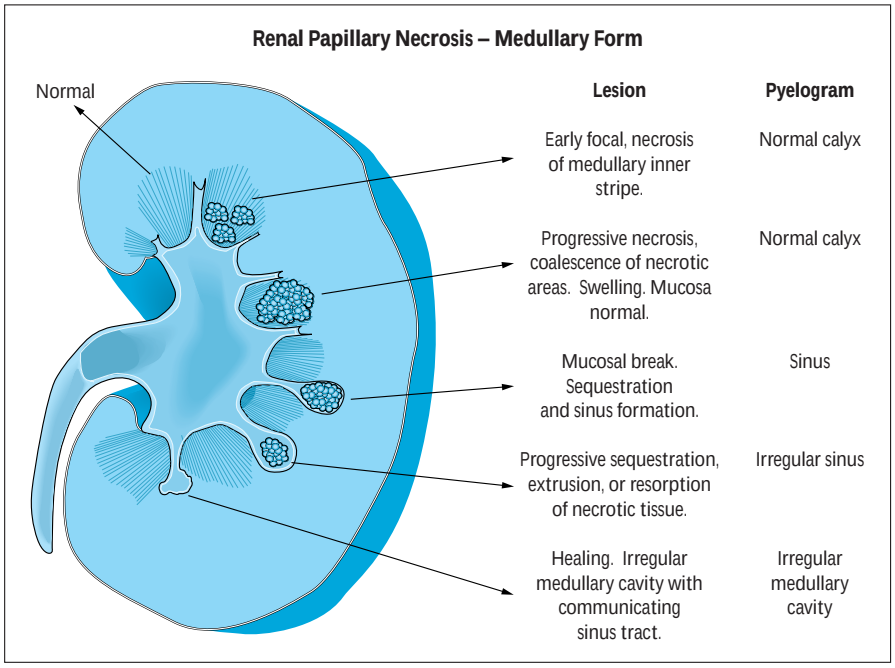

FIGURE 6-37

Schematic of the progressive stages of the medullary form of renal papillary necrosis and their associated radiologic appearance seen on intravenous pyelography. In partial papillary necrosis the lesion begins as focal necrosis within the substance of the medullary inner stripe. The lesion progresses by coagulative necrosis to form a sinus to the papillary tip, with subsequent extrusion or resorption of the sequestered necrotic tissue. The medullary form of papillary necrosis is commonly encountered in persons with sickle cell hemoglobinopathy. The incidence of radiographically demonstrative papillary necrosis is as high as 33% to 65% in such persons.

CONDITIONS ASSOCIATED WITH RENAL PAPILLARY NECROSIS

- Diabetes mellitus
- Urinary tract obstruction
- Pyelonephritis
- Analgesic nephropathy
- Sickle hemoglobinopathy
- Rejection of transplanted kidney
- Vasculitis
- Miscellaneous

FIGURE 6-38

Diabetes mellitus is the most common condition associated with papillary necrosis. The occurrence of capillary necrosis is likely more common than is generally appreciated, because pyelography (the best diagnostic tool for detection of papillary necrosis) is avoided in these patients because of dye-induced nephrotoxicity. When sought, papillary necrosis has been reported in as many as 25% of cases. Analgesic nephropathy accounts for 15% to 25% of papillary necrosis in the United States but accounts for as much as 70% of cases in countries in which analgesic abuse is common. Papillary necrosis also has been reported in patients receiving nonsteroidal anti-inflammatory drugs.

Sickle hemoglobinopathy is another common cause of papillary necrosis, which, when sought by intravenous pyelography, is detected in well over half of cases.

Infection is usually but not invariably a concomitant finding in most cases of RPN. In fact, with few exceptions, most patients with RPN ultimately develop a urinary tract infection, which represents a complication of papillary necrosis: that is, the infection develops after the primary underlying disease has initiated local injury to the renal medulla, with foci of impaired blood flow and poor tubular drainage. Infection contributes significantly to the symptomatology of RPN, because fever and chills are the presenting symptoms in two thirds of patients and a positive urine culture is obtained in 70%. However, RPN is not an extension of severe pyelonephritis. In most patients with florid acute pyelonephritis, RPN does not occur.

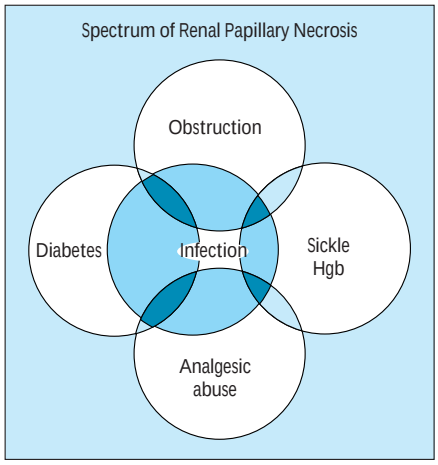

FIGURE 6-39

Spectrum and overlap of diseases principally associated with renal papillary necrosis (RPN). Although each disease can cause RPN, it is their coexistence (darkly shaded areas) that increases the risk, which is even greater after the onset of infection (lightly shaded areas). In most cases of RPN, more than one of the conditions associated with RPN is present. Thus, in most cases, the lesion seems to be multifactorial in origin. The pathogenesis of the lesion may be considered the result of an overlapping phenomenon, in which a combination of detrimental factors appear to operate in concert to cause RPN. As such, whereas each of the conditions alone can cause RPN, the coexistence of more than one predisposing factor in any one person significantly increases the risk for RPN. The contribution of any one of these factors to RPN would be expected to differ among individuals and at various periods during the course of the disease. To the extent that the natural course of RPN itself predisposes patients to development of infection of necrotic foci and obstruction by sloughed papillae, it may be difficult to assign a primary role for any of these processes in an individual patient. Furthermore, the occurrence of any of these factors (necrosis, obstruction, or infection) may itself initiate a vicious cycle that can lead to another of these factors and culminate in RPN.

References

1. Bohman S: The ultrastructure of the renal interstitium. *Contemp Issues Nephrol* 10:1–34, 1983.
2. Lemley KV, Kriz W: Anatomy of the renal interstitium. *Kidney Int* 1991, 39:370–381.
3. Eknoyan G: Chronic tubulointerstitial nephropathies. In *Diseases of the Kidney*, edn 6. Edited by Schrier RW, Gottschalk CW. Boston: Little Brown; 1997:1983–2015.
4. Palmer BF: The renal tubule in the progression of chronic renal failure. *J Invest Med* 1997, 45:346–361.
5. Schainuck LI, Striker GE, Cutler RE, Benditt EP: Structural-functional correlations in renal disease II. The correlations. *Hum Pathol* 1970, 1:631–641.
6. DeBroe ME, Elseviers MM: Analgesic nephropathy. *N Engl J Med* 1998, 338:446–451.
7. Dobyan DC, Truong LD, Eknoyan G: Renal malacoplakia reappraised. *Am J Kidney Dis* 1993, 22:243–252.
8. Eknoyan G, Qunibi WY, Grissom RT, *et al.*: Renal papillary necrosis: an update. *Medicine* 1982, 61:55–73.

Selected Bibliography

Renal Interstitium

Neilson EG: Symposium on the cell biology of tubulointerstitium. *Kidney Int* 1991, 39:369–556.

Strutz F, Mueller GA: Symposium on Renal Fibrosis: prevention and progression. *Kidney Int* 1996, 49(suppl 54):1–90.

Chronic Tubulointerstitial Nephritis

Eknoyan G, McDonald MA, Appel D, Truong LD: Chronic tubulointerstitial nephritis: correlation between structural and functional findings. *Kidney Int* 1990, 38:736–743.

Jones CL, Eddy AA: Tubulointerstitial nephritis. *Ped Nephrol* 1992, 6:572–586.

Nath KA: Tubulointerstitial changes as a major determinant in progression of renal damage. *Am J Kidney Dis* 1992, 20:1–17.

Pathogenesis

Bohle A, Muller GA, Wehrmann M *et al.*: Pathogenesis of chronic renal failure in the primary glomerulopathies, renal vasculopathies and chronic interstitial nephritides. *Kidney Int* 1996, 49(suppl 54):2–9.

Dodd S: The pathogenesis of tubulointerstitial disease and mechanisms of fibrosis. *Curr Top Pathol* 1995, 88:117–143.

Haggerty DT, Allen DM: Processing and presentation of self and foreign antigens by the renal proximal tubule. *J Immunol* 1992, 148:2324–2331.

Nath KA: Reshaping the interstitium by platelet-derived growth factor. Implications for progressive renal disease. *Am J Path* 1996, 148:1031–1036.

Sedor JR: Cytokines and growth factors in renal injury. *Semin Nephrol* 1992, 12:428–440.

Wilson CB: Nephritogenic tubulointers-titial antigens. *Kidney Int* 1991, 39:501–517.

Yamato T, Noble NA, Miller DE, Border WA: Sustained expression of TGF-B1 underlies development of progressive kidney fibrosis. *Kidney Int* 1994, 45:916–927.

Correlation with Renal Failure

D'Amico G, Ferrario F, Rastaldi MP: Tubulointerstitial damage in glomerular diseases: its role in the progression of renal damage. *Am J Kidney Dis* 1995, 26:124–132.

Eddy AA: Experimental insights into tubulointerstitial disease accompanying primary glomerular lesions. *J Am Soc Nephrol* 1994, 5:1273–1287.

Magil AB: Tubulointerstitial lesions in human membranous glomerulonephritis: relationship to proteinuria. *Amer J Kidney Dis* 1995, 25:375–379.

Analgesic Nephropathy

Henrich WL, Agodoa LE, Barrett B, Bennett WM *et al.*: Analgesics and the Kidney. Summary and Recommendations to the Scientific Advisory Board of the National Kidney Foundation. *Am J Kidney Dis* 1996, 27:162–165

Nanra RS: Pattern of renal dysfunction in analgesic nephropathy. Comparison with glomerulonephritis. *Nephrol Dialysis Transpl* 1992, 7:384–390.

Noels LM, Elseviers NM, DeBroe ME: Impact of legislative measures of the sales of analgesics and the subsequent prevalence of analgesic nephropathy: a comparative study in France, Sweden and Belgium. *Nephrol Dial Transplant* 1995, 10:167–174.

Perneger TV, Whelton PK, Klag MJ: Risk of kidney failure associated with the use of acetaminophen, aspirin, and nonsteroidal anti-inflammatory drugs. *N Engl J Med* 1994, 331:1675–1679.

Sandler DP, Burr FR, Weinberg CR: Nonsteroidal anti-inflammatory drugs and risk of chronic renal failure. *Ann Intern Med* 1991, 115:165–172.

Sandler DP, Smith JC, Weinberg CR *et al.*: Analgesic use and chronic renal disease. *N Engl J Med* 1989, 320:1238–1243.

Drugs

Boton R, Gaviria M, Battle DC: Prevalence, pathogenesis, and treatment of renal dysfunction associated with chronic lithium therapy. *Am J Kidney Dis* 1990, 10:329–345.

Myer BD, Newton L: Cyclosporine induced chronic nephropathy: an obliterative microvascular renal injury. *J Am Soc Nephrol* 1991, 2(suppl 1):4551.

Heavy Metals

Batuman V: Lead nephropathy, gout, hypertension. *Am J Med Sci* 1993, 305:241–247.

Batuman V, Maesaka JK, Haddad B *et al.*: Role of lead in gouty nephropathy. *N Engl J Med* 1981, 304:520–523.

Fowler BA: Mechanisms of kidney cell injury from metals. *Environ Health Perspec* 1993, 100:57–63.

Hu H: A 50-year follow-up of childhood plumbism. Hypertension, renal function and hemoglobin levels among survivors. *Am J Dis Child* 1991, 145:681–687.

Staessen JA, Lauwerys RR, Buchet JP *et al.*: Impairment of renal function with increasing lead concentrations in the general population. *N Engl J Med* 1992, 327:151–156.

Vedeen RP: Environmental renal disease: lead. cadmium, and Balkan endemic nephropathy. *Kidney Int* 34(suppl):4–8.

Ischemic Vascular Disease

Freedman BI, Ishander SS, Buckalew VM *et al.*: Renal biopsy findings in presumed hypertensive nephrosclerosis. *Am J Nephrol* 1994, 14:90–94.

Meyrier A, Simon P: Nephroangiosclerosis and hypertension: things are not as simple as you might think. *Nephrol Dial Transplant* 1996, 11:2116–1220.

Schlesinger SD, Tankersley MR, Curtis JJ: Clinical documentation of end stage renal disease due to hypertension. *Am J Kidney Dis* 1994, 23:655–660.

Obstructive Nephropathy

Arant BS Jr: Vesicoureteric reflux and renal injury. *Am J Kidney Dis* 1991, 17:491–511.

Diamond JR: Macrophages and progressive renal disease in experimental hydronephrosis. *Am J Kidney Dis* 1995, 26:133–140.

Klahr S: New insight into consequences and mechanisms of renal impairment in obstructive nephropathy. *Am J Kidney Dis* 1991, 18:689–699.

Hematologic Diseases

Allon M: Renal abnormalities in sickle cell disease. *Arch Intern Med* 1990, 150:501–504.

Falk RJ, Scheinmann JI, Phillips G *et al.*: Prevalence and pathologic features of sickle cell nephropathy and response to inhibition of angiotensin converting enzyme. *N Engl J Med* 1992, 326:910–915.

Ivanyi B: Frequency of light chain deposition nephropathy relative to renal amyloidosis and Bence Jones cast nephropathy in a necropsy study of patients with myeloma. *Arch Pathol Lab Med* 1990, 114:986–987.

Rota S, Mougenot B, Baudouin M: Multiple myeloma and severe renal failure: a clinicopathologic study of outcome and prognosis in 34 patients. *Medicine* 1987, 66:126–137.

Sanders PW, Herrera GA, Kirk KA: Spectrum of glomerular and tubulointerstitial renal lesions associated with monotypical immunoglobulin light chain deposition. *Lab Invest* 1991, 64:527–537.

Metabolic Disorders

Chaplin AJ: Histopathological occurrence and characterization of calcium oxalate. A review. *J Clin Pathol* 1977, 30:800–811.

Foley RJ, Weinman EJ: Urate nephropathy. *Am J Med Sci* 1984, 288:208–211.

Hanif M, Mobarak MR, Ronan A: Fatal renal failure caused by diethylene glycol in paracetamol elixir: the Bangladesh epidemic. *Br Med J* 1995, 311:88–91.

Schneider JA, Lovell H, Calhoun F: Update on nephropathic cystinosis. *Ped Nephrol* 1990, 4:645–653.

Zawada ET, Johnson VH, Bergstein J: Chronic interstitial nephritis. Its occurrence with oxalosis and antitubular basement membrane antibodies after jejunal bypass. *Arch Pathol Ub Med* 1981, 105:379–383.

Granulomatous Diseases

Mignon F, Mery JP, Mougenot B, *et al*.: Granulomatous interstitial nephritis. *Adv Nephrol* 1984, 13:219–245.

Viero RM, Cavallo T: Granulomatous interstitial nephritis. *Hum Pathol* 1995, 26:1345–1353.

Viral Infections

Ito M, Hirabayashi N, Uno Y: Necrotizing tubulointerstitial nephritis associated with adenovirus infection. *Human Pathol* 1991, 22:1225–1231.

Papadimitriou M.: Hantavirus nephropathy. *Kidney Int* 1995, 48:887–902.

Hereditary Diseases

Fick GM, Gabow PA: Hereditary and acquired cystic disease of the kidney. *Kidney Int* 1994, 46:951–964.

Gabow PA, Johnson AM, Kaehny VM: Factors affecting the progression of renal disease in autosomal-dominant polycystic kidney disease. *Kidney Int* 1992, 41:1311–1319.

Gregory MC, Atkin CL: Alports syndrome, Fabry's disease and nail patella syndrome. In *Diseases of the Kidney*, edn 6. Edited by Schrier RW, Gottschalk CW. Boston: Little Brown; 1997:561–590.

Papillary Necrosis

Griffin MD, Bergstralk EJ, Larson TS: Renal papillary necrosis. A sixteen year clinical experience. *J Am Soc Nephrol* 1995, 6:248–256.

Sabatini S, Eknoyan G, editors: Renal papillary necrosis. *Semin Nephrol* 1984, 4:1–106.

Urinary Tract Infection

Alain Meyrier

The concern of renal specialists for urinary tract infections (UTIs) had declined with the passage of time. This trend is now being reversed, owing to new imaging techniques and to substantial progress in the understanding of host-parasite relationships, of mechanisms of bacterial uropathogenicity, and of the inflammatory reaction that contributes to renal lesions and scarring.

UTIs account for more than 7 million visits to physicians' offices and well over 1 million hospital admissions in the United States annually [1]. French epidemiologic studies evaluated its annual incidence at 53,000 diagnoses per million persons per year, which represents 1.05% to 2.10% of the activity of general practitioners. In the United States, the annual number of diagnoses of pyelonephritis in females was estimated to be 250,000 [2].

The incidence of UTI is higher among females, in whom it commonly occurs in an anatomically normal urinary tract. Conversely, in males and children, UTI generally reveals a urinary tract lesion that must be identified by imaging and must be treated to suppress the cause of infection and prevent recurrence. UTI can be restricted to the bladder (essentially in females) with only superficial mucosal involvement, or it can involve a solid organ (the kidneys in both genders, the prostate in males). Clinical signs and symptoms, hazards, imaging, and treatment of various types of UTIs differ. In addition, the patient's background helps to further categorize UTIs according to age, type of urinary tract lesion(s), and occurrence in immunocompromised patients, especially with diabetes or pregnancy. Such various forms of UTI explain the wide spectrum of treatment modalities, which range from ambulatory, single-dose antibiotic treatment of simple cystitis in young females, to rescue nephrectomy for pyonephrosis in a diabetic with septic shock. This chapter categorizes the various forms of UTI, describes progress in diagnostic imaging and treatment, and discusses recent data on bacteriology and immunology.

CHAPTER 7

Diagnosis

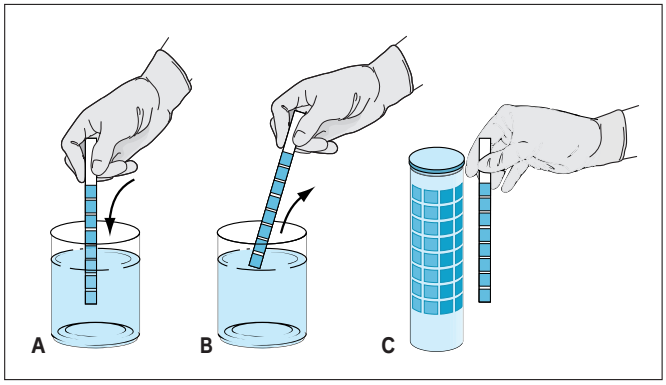

FIGURE 7-1

Urine test strips. Normal urine is sterile, but suprapubic aspiration of the bladder, which is by no means a routine procedure, would be the only way of proving it. Urinary tract infection (UTI) cannot be identified simply by the presence of bacteria in a voided specimen, as micturition flushes saprophytic urethral organisms along with the urine. Thus a certain number of colony-forming units of uropathogens are to be expected in the urine sample. Midstream collection is the most common method of urine sampling used in adults. When urine cannot be studied without delay, it must be stored at 4°C until it is sent to the bacteriology laboratory. The urine test strip is the easiest means of diagnosing UTI qualitatively. This test detects leukocytes and nitrites. Simultaneous detection of the two is highly suggestive of UTI. This test is 95% sensitive and 75% specific, and its negative predictive value is close to 96% [3]. The test does not, however, detect such bacteria as *Staphyloccocus saprophyticus*, a strain responsible for some 3% to 7% of UTIs. Thus, treating UTI solely on the basis of test strip risks failure in about 15% of simple community-acquired infections and a much larger proportion of UTIs acquired in a hospital.

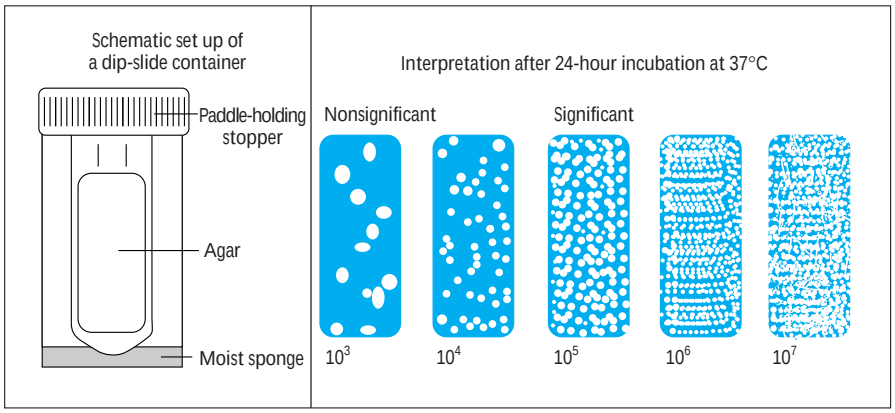

FIGURE 7-2

Culture interpretation. Urinalysis must examine bacterial and leukocyte counts (per milliliter). An approximate way of estimating bacterial counts in the urine uses a dip-slide method: a plastic paddle covered on both sides with culture medium is immersed in the urine, shaken, and incubated overnight.

The most specific results, however, are provided by laboratory analysis, which allows precise counting of bacteria and leukocytes. Normal values for a midstream specimen are less than or equal to 10^5 *Escherichia coli* organisms and 10^4 leukocytes per milliliter. These classical "Kass criteria," however, are not always reliable. In some cases of incipient cystitis the number of *E. coli* per milliliter can be lower, on the order of 10^2 to 10^4 [4]. When fecal contamination has been ruled out, growth of bacteria that are not normally urethral saprophytes indicates infection. This is the case for *Pseudomonas, Klebsiella, Enterobacter, Serratia*, and *Moraxella*, among others, especially in a hospital setting or after urologic procedures.

CAUSES OF ASEPTIC LEUKOCYTURIA

Self-medication before urine culture
Sample contamination by cleansing solution
Vaginal discharge
Urinary stone
Urinary tract tumor
Chronic interstitial nephritis (especially due to analgesics)
Fastidious microorganisms requiring special culture medium (*Ureaplasma urealyticum, Chlamydia, Candida*)

FIGURE 7-3

Leukocyturia. A significant number of leukocytes (more than 10,000 per milliliter) is also required for the diagnosis of urinary tract infection, as it indicates urothelial inflammation. Abundant leukocyturia can originate from the vagina and thus does not necessarily indicate aseptic urinary leukocyturia [1]. Bacterial growth without leukocyturia indicates contamination at sampling. Significant leukocyturia without bacterial growth (aseptic leukocyturia) can develop from various causes, among which self-medication before urinalysis is the most common.

Bacteriology

A. MAIN MICROBIAL STRAINS RESPONSIBLE FOR URINARY TRACT INFECTION

Microbial Strain	First Episode or Delayed Relapse	Relapse Due to Early Reinfection
Escherichia coli	71%–79%	60%
Proteus mirabilis	1.1%–9.7%	15%
Klebsiella	—	20%
Enterobacter	1.0%–9.2%	—
Enterococcus	1.0%–3.2%	—
Staphylococcus saprophyticus	3%–7%	—
Other species	2%–6%	5%

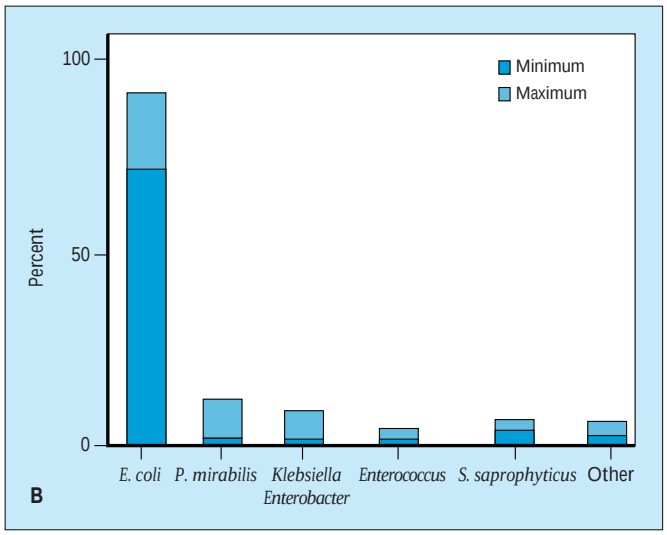

FIGURE 7-4

Principal pathogens of urinary tract infection (UTI). **A** and **B**, Most pathogens responsible for UTI are enterobacteriaceae with a high predominance of *Escherichia coli*. This is especially true of spontaneous UTI in females (cystitis and pyelonephritis). Other strains are less common, including *Proteus mirabilis* and more rarely gram-positive microbes. Among the latter, *Staphylococcus saprophyticus* deserves special mention, as this gram-positive pathogen is responsible for 5% to 15% of such primary infections, is not detected by the leukocyte esterase dipstick, and is resistant to antimicrobial agents that are active on gram-negative rods.

C, Acute simple pyelonephritis is a common form of upper UTI in females and results from the encounter of a parasite and a host. In the absence of urologic abnormality, this renal infection is mostly due to uropathogenic strains of bacteria [5,6], a majority of cases to community-acquired *E. coli*. The clinical picture consists of fever, chills, renal pain, and a general discomfort. Tissue invasion is associated with a high erythrocyte sedimentation rate and C-reactive protein level well above 2 mg/dL.

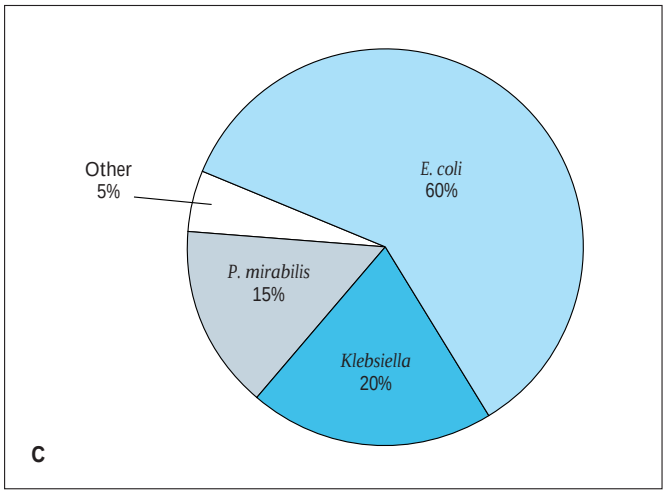

Virulence Factors of Uropathogenic Strains

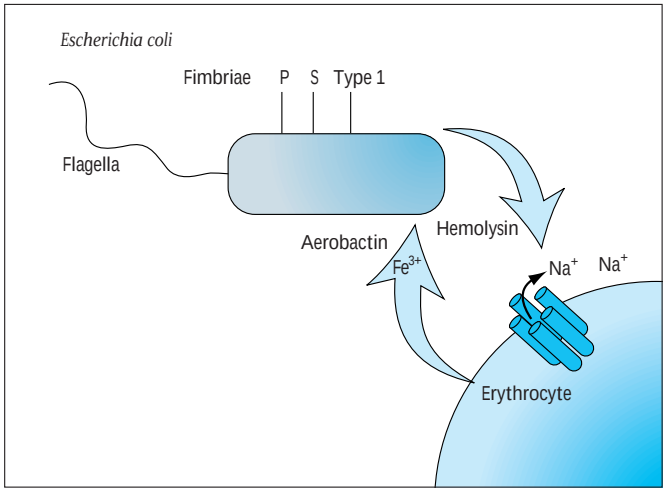

FIGURE 7-5

Bacterial uropathogenicity plays a major role in host-pathogen interactions that lead to urinary tract infection (UTI). For *Escherichia coli*, these factors include flagella necessary for motility, aerobactin necessary for iron acquisition in the iron-poor environment of the urinary tract, a pore-forming hemolysin, and, above all, presence of adhesins on the bacterial fimbriae, as well as on the bacterial cell surface. (*From* Mobley *et al.* [7]; with permission.)

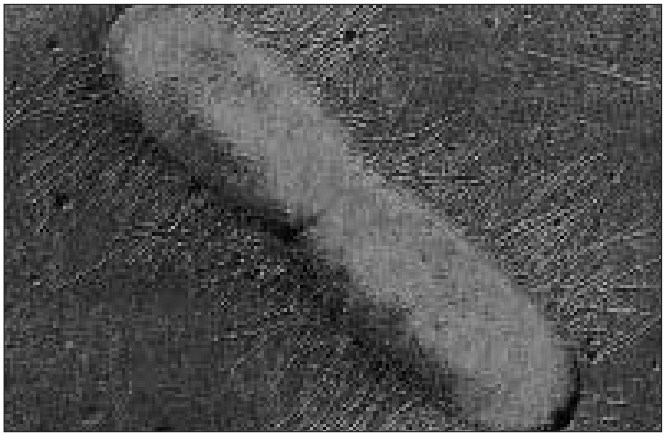

FIGURE 7-6

An electron microscopic view of an *Escherichia coli* organism showing the fimbriae (or pili) bristling from the bacterial cell.

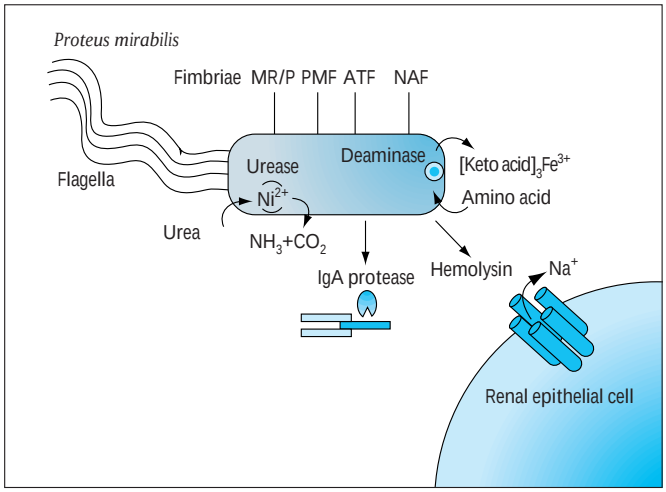

FIGURE 7-7

Proteus mirabilis is endowed with other nonfimbrial virulence factors, including the property of secreting urease, which splits urea into NH_3 and CO_2.

FIGURE 7-8

Staghorn calculi. Ammonium generation alkalinizes the urine, creating conditions favorable for build-up of voluminous struvite stones, which can progressively invade the entire pyelocalyceal system, forming staghorn calculi. These stones are an endless source of microbes, and the urinary tract obstruction perpetuates infection.

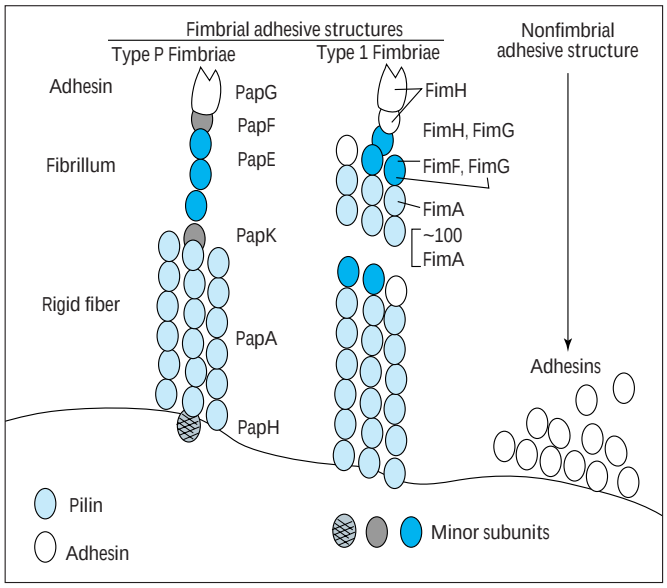

FIGURE 7-9

Schematic representation of morphology and composition of type P and type 1 adhesive structures. Bacterial adhesins are paramount in fostering attachment of the bacteria to the mucous membranes of the perineum and of the urothelium. There are several molecular forms of adhesins. The most studied is the pap G adhesin, which is located at the tip of the bacterial fimbriae (or pili). This lectin recognizes binding site conformations provided by oligosaccharide sequences present on the mucosal surface [8].

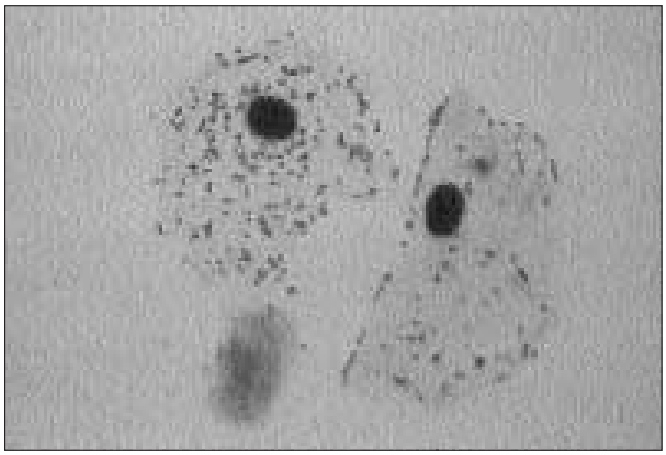

FIGURE 7-10

Uropathogenic strains of *Escherichia coli* readily adhere to epithelial cells. This figure shows two epithelial cells incubated in urine infected with *E. coli*–carrying pap adhesins. Numerous bacteria are scattered on the epithelial cell membranes. About half of all cases of cystitis are due to uropathogenic strains of *E. coli*–carrying adhesins. Females with primary pyelonephritis and no urologic abnormality harbor a uropathogenic strain in almost 100% of cases [5].

APPROPRIATE ANTIBIOTICS FOR URINARY TRACT INFECTIONS

Antibiotics	General Indications	Pregnancy	Prophylaxis
Aminoglycosides	+	+*	-
Aminopenicillins	+†	+	-
Carboxypenicillins	+	+	-
Ureidopenicillins	+	+	-
Quinolones	+‡	-	+
Fluoroquinolones	+§	-	+
Cephalosporins			
First generation	+¶	+	+‡
Second generation	+	+	-
Third generation	+	+	-
Monobactams	+	+	-
Carbapenem	+	+	-
Cotrimoxazole	+	-	+‡
Fosfomycin trometamole	+**	-	-
Nitroturantoin	+††	-	+

* Aminoglycosides should not be prescribed during pregnancy except for very severe infection and for the shortest possible duration.
With the exception of amoxicillin plus clavulanic acid, aminopenicillins should not be prescribed as first-line treatment, owing to the frequency of primary resistance to this class of antibiotics.
‡ According to antibiotic sensitivity tests.
§ Fluoroquinolones carry a risk of tendon rupture (especially Achilles tendon).
¶ Oral administration only.
** Single-dose treatment of cystitis.
†† Simple cystitis; not pyelonephritis or prostatitis.

FIGURE 7-11

Appropriate antibiotics for urinary tract infections (UTI). An appropriate antibiotic for treating UTI must be bactericidal and conform to the following general specifications: 1) its pharmacology must include, in case of oral administration, rapid absorption and attainment of peak serum concentrations; 2) its excretion must be predominantly renal; 3) it must achieve high concentrations in the renal or prostate tissue; 4) it must cover the usual spectrum of enterobacteria with reasonable chance of being effective on an empirical basis. Excluding special considerations for childhood and pregnancy, several classes of antibiotics fulfill these specifications and can be used alone or in combination. The choice also depends on market availability, cost, patient tolerance, and potential for inducing emergence of resistant strains.

Classification of Urinary Tract Infection

Upper versus lower urinary tract infection

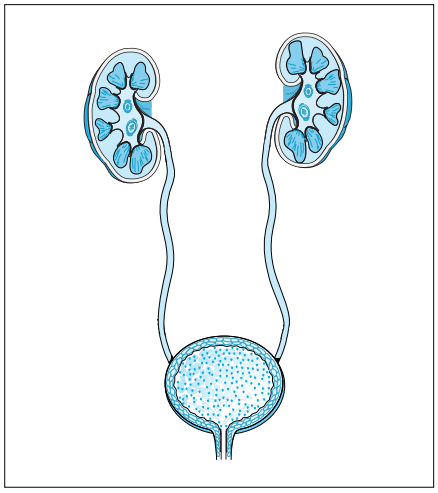

FIGURE 7-12

Cystitis in a female patient. In case of urinary tract infection (UTI), distinguishing between lower and upper tract infection is classical, but the distinction is also beside the point. The real point is to determine whether infection is confined to the bladder mucosa, which is the case in simple cystitis in females, or whether it involves solid organs (*ie*, prostatitis or pyelonephritis). The dots in this figure symbolize the presence of bacteria and leukocytes (*ie*, infection) in the relevant organ. Here, infection is confined to the bladder mucosa, which can be severely inflamed and edematous. This could be reflected radiographically by mucosal wrinkling on the cystogram. In some cases inflammation is severe enough to be accompanied by bladder purpura, which induces macroscopic hematuria but is not a particular grave sign.

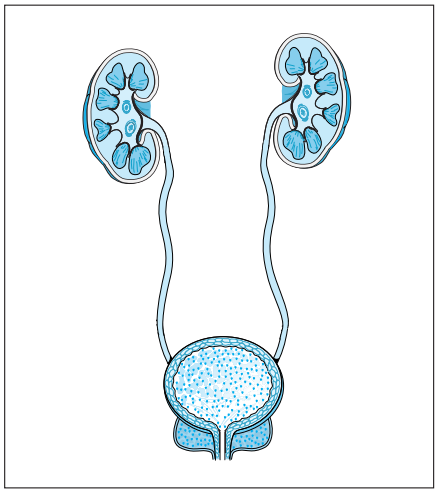

FIGURE 7-13

Prostatitis. Anatomically, prostatitis involves the lower urinary tract, but invasion of prostate tissue affords easy passage of pathogens to the prostatic venous system—and, usually, poor penetration by antibiotics. Presence of bacteria in the bladder is also symbolized in this picture, but owing to free communication between bladder urine and prostate tissue, it can be accepted that pure cystitis does not exist in males.

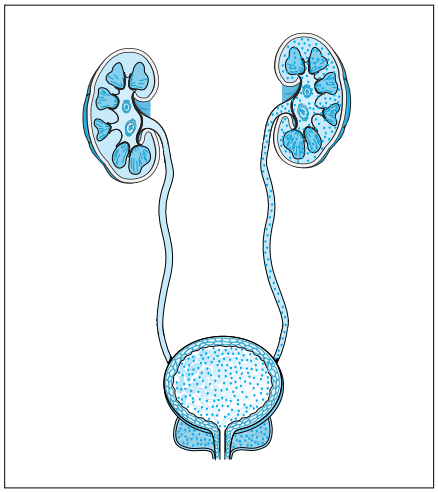

FIGURE 7-14

Acute prostatitis can be complicated by ascending infection, that is, pyelonephritis.

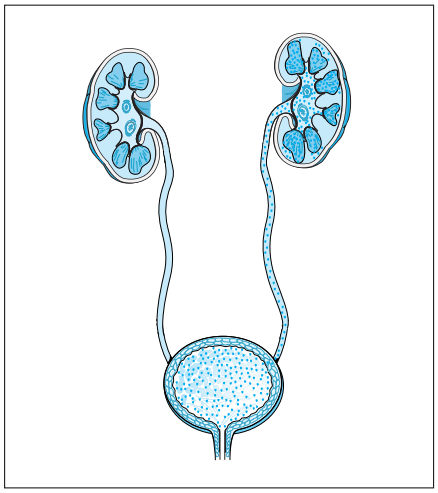

FIGURE 7-15

Pyelonephritis in females. Essentially, this is an ascending infection caused by uropathogens. From the perineum the bacteria gain access to the bladder, ascending to the renal pelvocalyceal system and thence to the renal medulla, from which they spread toward the cortex. It has been shown that "pyelitis" cannot be considered a pathologic entity, as renal pelvis infection is invariably associated with nearby contamination of the renal medulla.

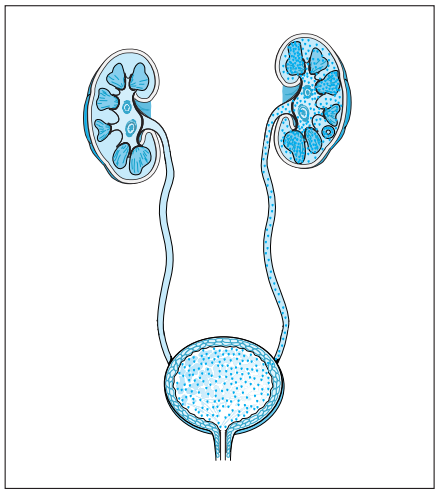

FIGURE 7-16
Renal abscess formation. As specified elsewhere, renal abscess due to enterobacteriaceae (as opposed to hematogenous renal abscess, often of staphylococcal origin) can be considered a severe form of pyelonephritis with renal tissue liquefaction, ending in a walled-off cavity.

CRITERIA FOR TISSUE INVASION

Clinical

Kidney or prostate infection is marked by fever over 38°C, chills, and pain. The patient appears acutely ill.

Laboratory

Tissue invasion is invariably accompanied by an erythrocyte sedimentation rate over 20 mm/h and serum C-reactive protein levels over 2.0 mg/dL. Blood cultures grow in 30%–50% of cases, which in an immunocompetent host indicates simply bacteremia, not septicemia. This reflects easy permeability between the urinary and the venous compartments of the kidney.

Imaging

When indicated, ultrasound imaging, tomodensitometry, and scintigraphy provide objective evidence of pyelonephritis. In case of vesicoureteral reflux, urinary tract infection necessarily involves the upper urinary tract.

FIGURE 7-17
Criteria for tissue invasion.

Primary versus secondary urinary tract infection

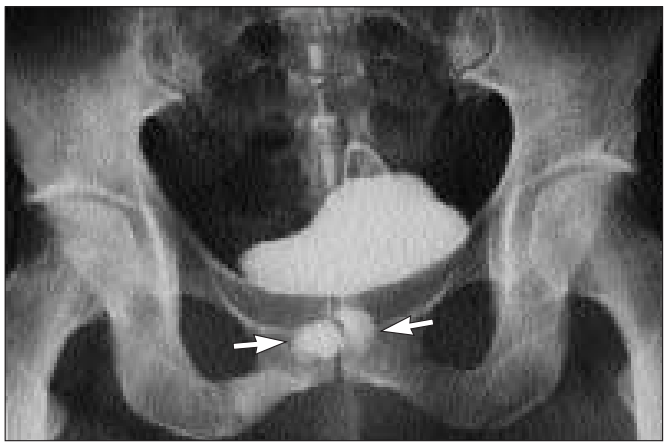

FIGURE 7-18
An episode of urinary tract infection (UTI) should prompt consideration of whether it involves a normal urinary tract or, alternatively, if it is a complication of an anatomic malformation. This is especially true of relapsing UTI in both genders, and this hypothesis should be systematically raised in males and in children.

Recurrent cystitis in females can be explained by hymeneal scars that pull open the urethral outlet during intercourse. Although rarely, other malformations that promote recurrent female cystitis are occasionally discovered, such as urethral diverticula (*arrows*). Finally, it should be recalled that recurrent or chronic cystitis in an older woman can also reveal an unsuspected bladder tumor.

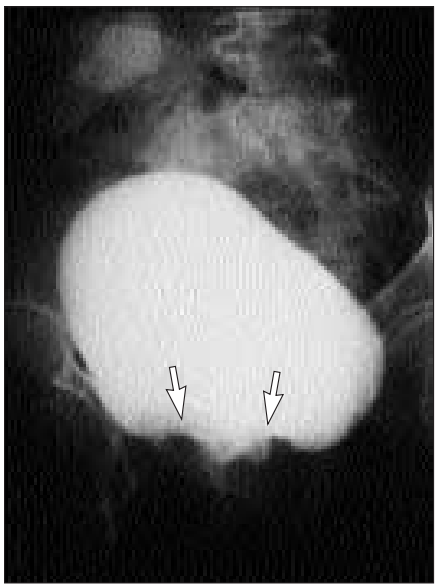

FIGURE 7-19
Cystogram of a 65-year-old woman. A voluminous bladder tumor (*arrows*) infiltrates the bladder floor and the initial segment of the urethra.

FIGURE 7-20
Urethrocystogram of a man following acute prostatitis. In males, acute prostatitis may reveal urethral stenosis. Urethral stenosis is a good explanation for acute prostatitis. The beaded appearance of the stenosis (*arrow*) suggests an earlier episode of gonorrheal urethritis.

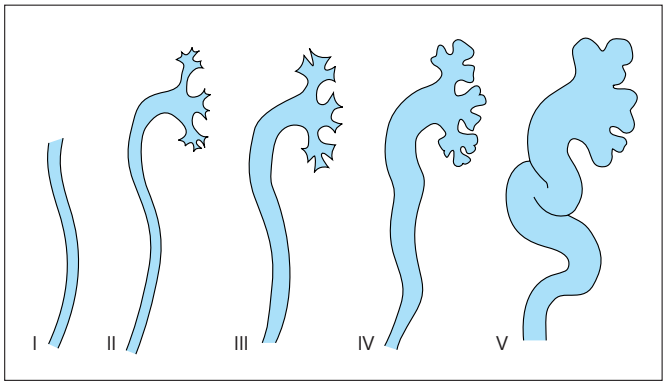

FIGURE 7-21
The severity of vesicoureteral reflux (VUR) as graded in 1981 by the International Reflux Study Committee. When children have pyelonephritis, the possibility of VUR should always be considered. Childhood vesicoureteral reflux is five times more common in girls than in boys. It has a genetic background: several cases occasionally occur in the same family. Unless detected and corrected early, especially the most severe forms of this class and when urine is infected (one episode of pyelonephritis suffices), childhood VUR is a major cause of cortical scarring, renal atrophy, and in bilateral cases chronic renal insufficiency. The International Reflux Study classifies reflux grades as follows: I) ureter only; II) ureter, pelvis, and calyces, no dilation, and normal calyceal fornices; III) mild or moderate dilation or tortuosity of ureter and mild or moderate dilation of renal pelvis but no or slight blunting of fornices; IV) moderate dilation or tortuosity of ureter and moderate dilation of renal pelvis and calyces, complete obliteration of sharp angle of fornices but maintenance of papillary impressions in majority of calyces; V) gross dilation and tortuosity of ureter, gross dilation of renal pelvis and calyces. Papillary impressions are no longer visible in the majority of calyces. (*From* International Reflux Study Committee [9]; with permission.)

FIGURE 7-22
Cystogram demonstrating left ureteral reflux (**A**). The consequences on the left kidney (**B**) consist of calyceal distension and a clubbed appearance due to the destruction of the papillae and of the adjacent renal tissue. The calyceal cavities are very close to the renal capsule, indicating complete cortical atrophy. This picture is typical of chronic pyelonephritis secondary to vesicoureteral reflux.

FIGURE 7-23

In case of bilateral, neglected vesicoureteral reflux, chronic pyelonephritis is bilateral and asymmetric. Here, the right kidney is globally atrophic. A typical cortical scar is seen on the outer aspect of the left kidney. The lower pole, however, is fairly well-preserved with nearly normal parenchymal thickness.

FIGURE 7-24

When intravenous pyelography discloses two ureters, the one draining the lower pyelocalyceal system crosses the upper ureter and opens into the bladder less obliquely than normally, allowing reflux of urine and explaining repeated attacks of pyelonephritis followed by atrophy of the lower pole of the kidney. Retrograde cystography is indicated for repeated episodes of pyelonephritis and when intravenous pyelography or computed tomography renal examination discovers cortical scars. In adults, retrograde cystography is obtained by direct catheterization of the bladder.

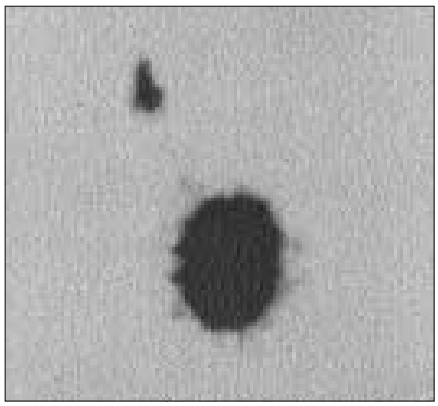

FIGURE 7-25
(*see* Color Plate)

In children, isotopic cystography allows a diagnosis of vesicoureteral reflux with much less radiation than if cystography were carried out with iodinated contrast medium.

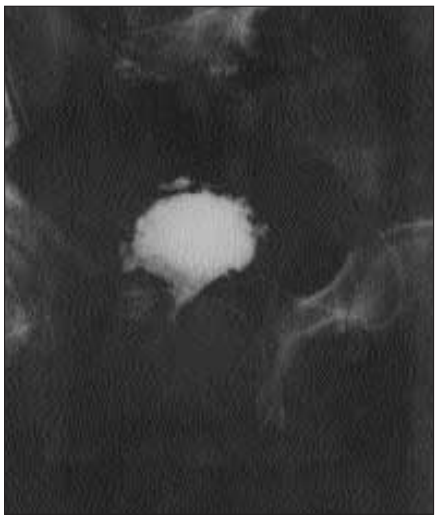

FIGURE 7-26

In the paraplegic, and more generally in patients with spinal disease, neurogenic bladder is responsible for stasis, bladder distension, and diverticula. These functional and anatomic factors explain the frequency of chronic urinary tract infection complicated with bladder and upper urinary tract infectious stones.

Imaging

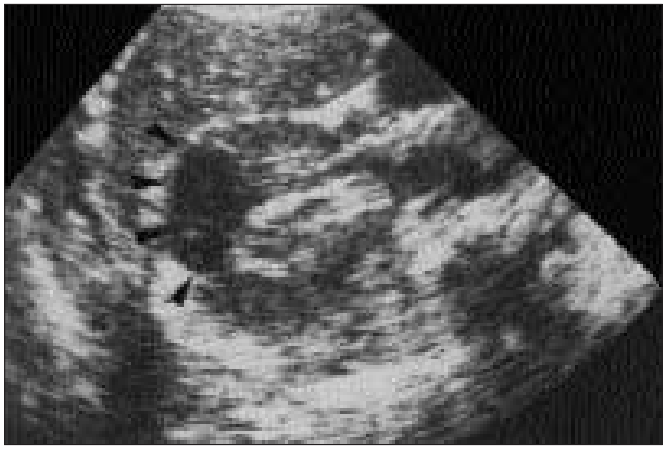

FIGURE 7-27

When acute pyelonephritis occurs in a sound, immunocompetent female with no history of urologic disease, imaging can be limited to a plain abdominal film (to rule out renal and ureteral stones) and renal ultrasonography. Ultrasonography typically discloses a swollen kidney with loss of corticomedullary differentiation, denoting renal inflammatory edema. Images corresponding to the infected zones are more dense than normal renal tissue (*arrows*).

FIGURE 7-28

The ultrasound procedure occasionally discloses the cavity of a small renal abscess, a common complication of acute pyelonephritis, even in simple forms.

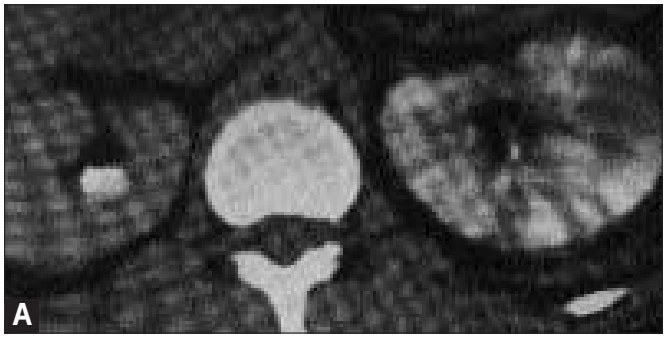

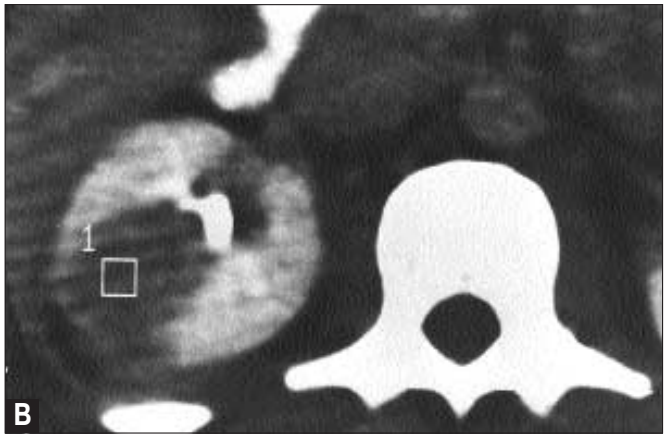

FIGURE 7-29

Computed tomodensitometry. Simple pyelonephritis does not require much imaging; however, it should be remembered that there is no correlation between the severity of the clinical picture and the renal lesions. Therefore, a diagnosis of "simple" pyelonephritis at first contact can be questioned when response to treatment is not clear after 3 or 4 days. This is an indication for uroradiologic imaging, such as renal tomodensitometry followed by radiography of the urinary tract while it is still opacified by the contrast medium.

The typical picture of acute pyelonephritis observed after contrast medium injection [10] consists of hypodensities of the infected areas in an edematous, swollen kidney. The pathophysiology of hypodense images has been elucidated by animal experiments in the primates [11] which have shown that renal infection with uropathogenic *Escherichia coli* induces intense vasoconstriction.

Computed tomodensitometric images of acute pyelonephritis can take various appearances. The most common findings consist of one or several wedge-shaped or streaky zones of low attenuation extending from papilla to cortex, **A**. Hypodense images can be round, **B**. On this figure, the infected zone reaches the renal cortex and is accompanied with adjacent perirenal edema. Several such

(Continued on next page)

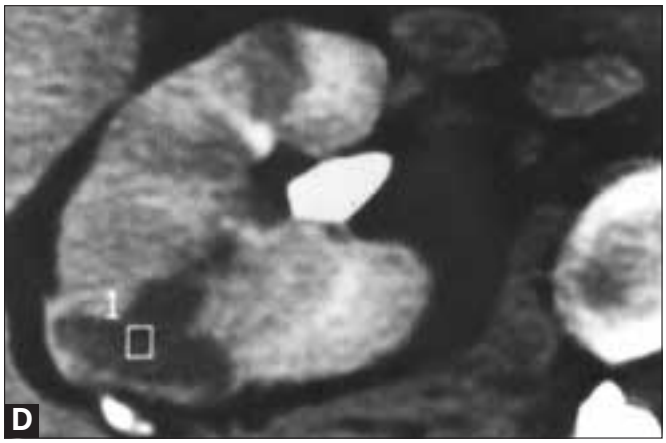

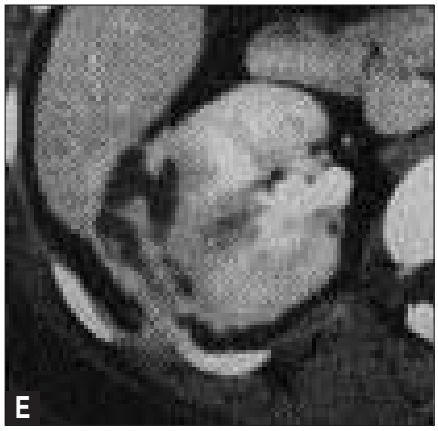

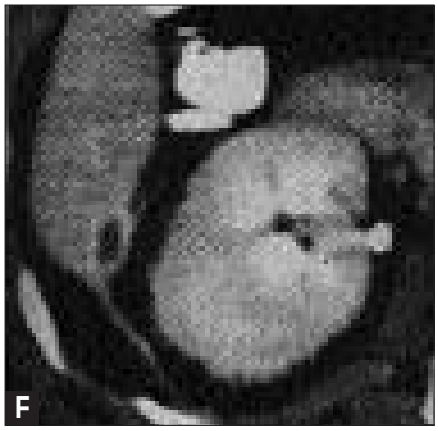

FIGURE 7-29 *(Continued)*
images can coexist in the same kidney, **C**. Marked juxtacortical, circumscribed hypodense zones, bulging under the renal capsule, **D**, usually correspond to lesions close to liquefaction and should be closely followed, as they can lead to abscess formation and opening into the perinephric space, **E** and **F.** (**E** and **F** *from* Talner *et al.* [10]; with permission.)

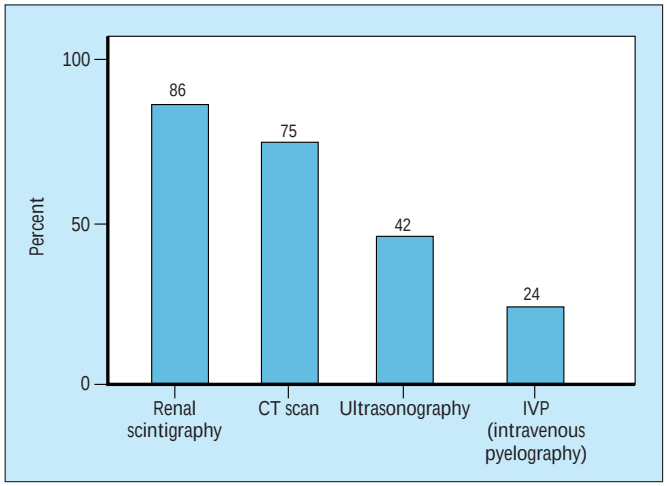

FIGURE 7-30
Comparative sensitivity of four diagnostic imaging techniques for acute pyelonephritis. Renal cortical scintigraphy using ^{99m}Tc-dimethyl succinic acid (DMSA) or ^{99m}Tc-gluconoheptonate (GH) is very sensitive for diagnosing acute pyelonephritis. It entails very little irradiation as compared with conventional radiography using contrast medium. Some nephrologists consider ^{99m}Tc-DMSA cortical scintigraphy as the first-line diagnostic imaging method for renal infection in children. It is interesting to compare its sensitivity with that of more conventional imaging methods. (*From* Meyrier and Guibert [5]; with permission.)

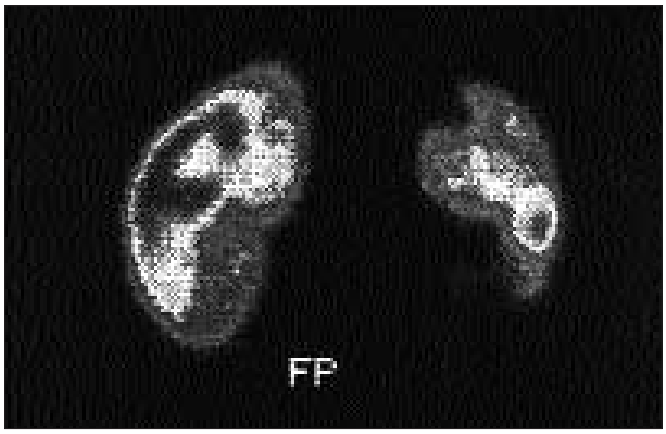

FIGURE 7-31 (*see* Color Plate)

^{99m}Tc-DMSA cortical imaging of simple pyelonephritis in a female. The clinical signs implicated the right kidney. (Contrary to conventional radiology, the right kidney appears on the right of the image.) The false colors indicate cortical renal blood supply from red (normal) to blue (ischemia). The right kidney is obviously involved with pyelonephritis, especially its poles. However, contrary to the results of computed tomography, which indicated right-sided pyelonephritis only, a focus of infection also occupies the lower pole of the right kidney. This picture illustrates the greater sensitivity of renal scintigraphy for diagnosing renal infection. It also indicates that clinically unilateral acute pyelonephritis can, in fact, be bilateral.

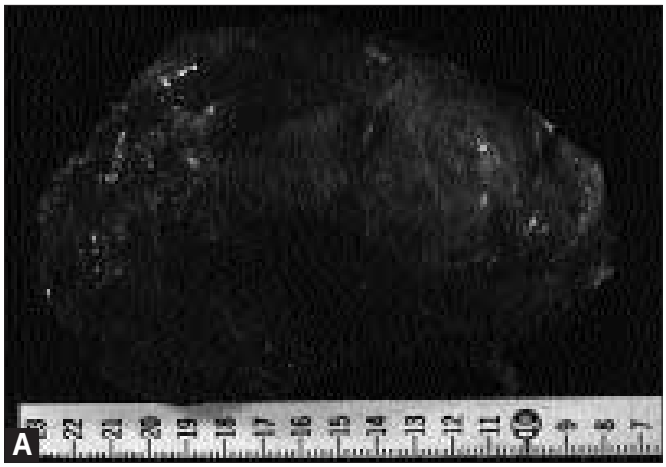

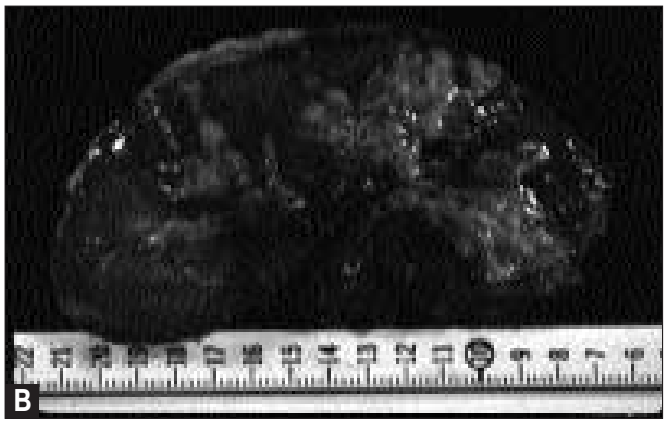

FIGURE 7-32

Renal pathology in acute pyelonephritis. Renal pathology of human acute pyelonephritis is quite comparable to what is observed in experimental pyelonephritis in primates [11]. However, our knowledge of renal pathology in this condition in humans is based mainly on the most catastrophic cases, which required nephrectomy, like the diabetes patient whose kidney is shown here. **A**, The surgically removed kidney is swollen, and its surface shows whitish zones. **B**, A section of the same organ shows white suppurative areas (scattered with small abscesses) extending eccentrically from the medulla to the cortex. There also were sloughed papillae (*see* Fig. 7-37).

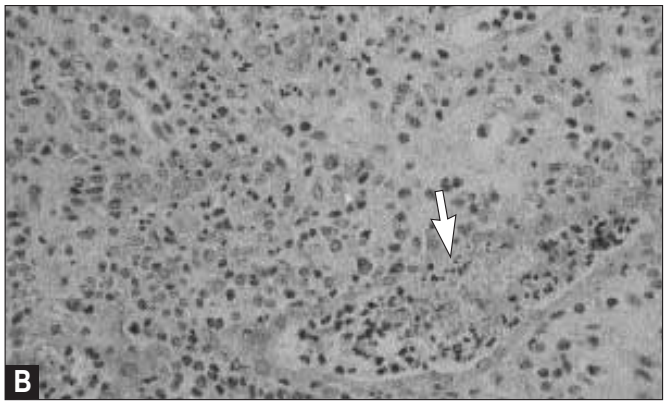

FIGURE 7-33

Histologic appearance of pyelonephritic kidney. **A**, The renal tissue is severely edematous and interspersed with inflammatory cells and hemorrhagic streaks. **B**, On another section, severe inflammation, comprising a majority of polymorphonuclear leukocytes, induces tubular destruction and is accompanied by a typical infectious cast in a tubular lumen (*arrow*).

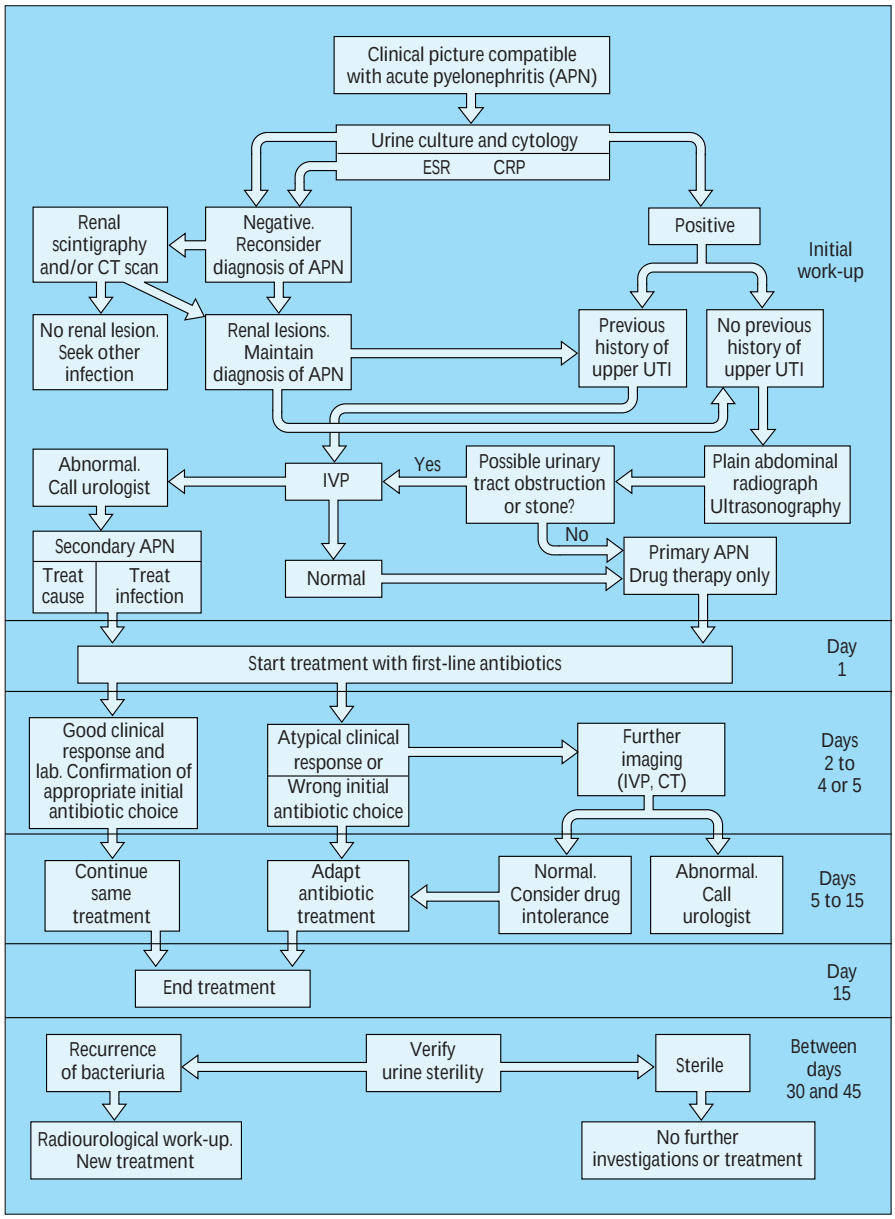

FIGURE 7-34

A general algorithm for the investigation and treatment of acute pyelonephritis. Treatment of acute pyelonephritis is based on antibiotics selected from the list in Figure 7-11. Preferably, initial treatment is based on parenteral administration. It is debatable whether common forms of simple pyelonephritis initially require both an aminoglycoside and another antibiotic. Initial parenteral treatment for an average of 4 days should be followed by about 10 days of oral therapy based on bacterial sensitivity tests. It is strongly recommended that urine culture be carried out some 30 to 45 days after the end of treatment, to verify that bacteriuria has not recurred. APN—acute pyelonephritis; ESR—erythrocyte sedimentation rate; CRP—C-reactive protein; UTI—urinary tract infection; IVP—intravenous pyelography. (*From* Meyrier and Guibert [5]; with permission.)

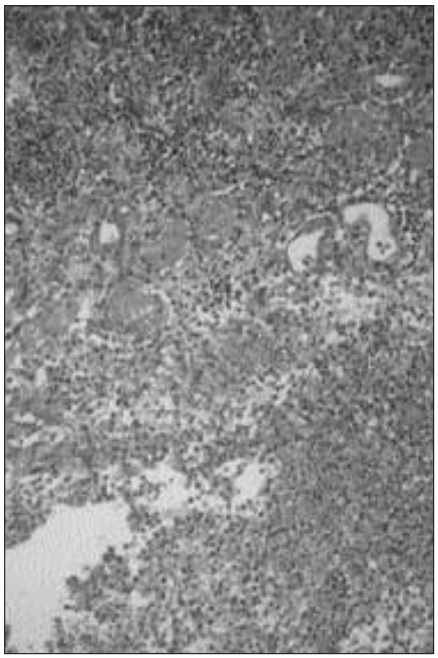

FIGURE 7-35 (*see* Color Plate)

Renal abscess. Like acute pyelonephritis, one third of cases of renal abscess occur in a normal urinary tract; in the others it is a complication of a urologic abnormality. The clinical picture is that of severe pyelonephritis. In fact, it can be conceptualized as an unfavorably developing form of acute pyelonephritis that progresses from presuppurative to suppurative renal lesions, leading to liquefaction and formation of a walled-off cavity. The diagnosis of renal abscess is suspected when, despite adequate treatment of pyelonephritis (described in Fig. 7-34), the patient remains febrile after day 4. Here, necrotic renal tissue is visible close to the abscess wall. The tubules are destroyed, and the rest of the preparation shows innumerable polymorphonuclear leukocytes within purulent material.

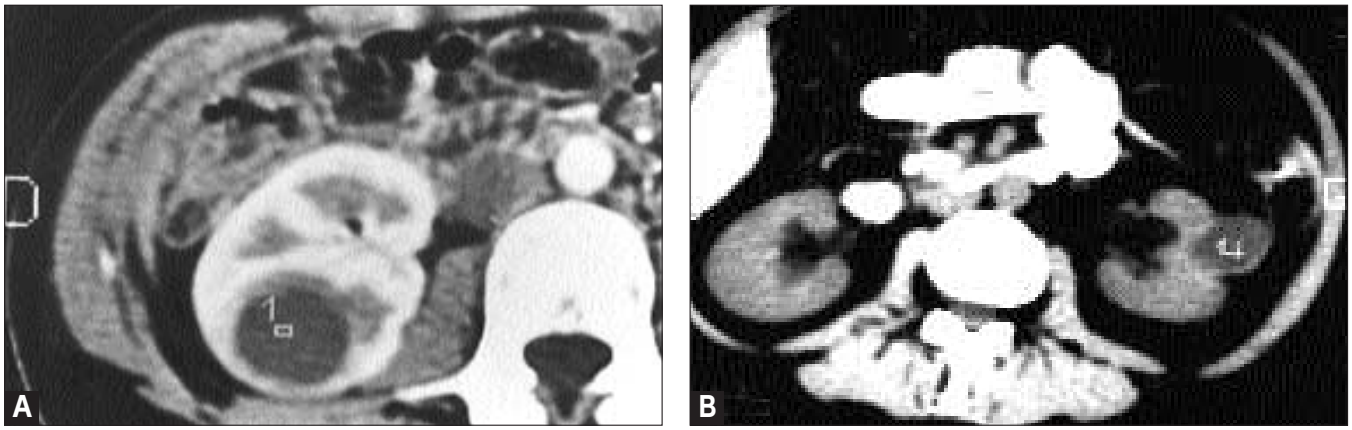

FIGURE 7-36

Renal computed tomography (CT). In addition to ultrasound examination, CT is the best way of detecting and localizing a renal abscess. The abscess cavity can be contained entirely within the renal parenchyma, **A**, or bulge outward under the renal capsule, risking rupture into Gerota's space, **B**.

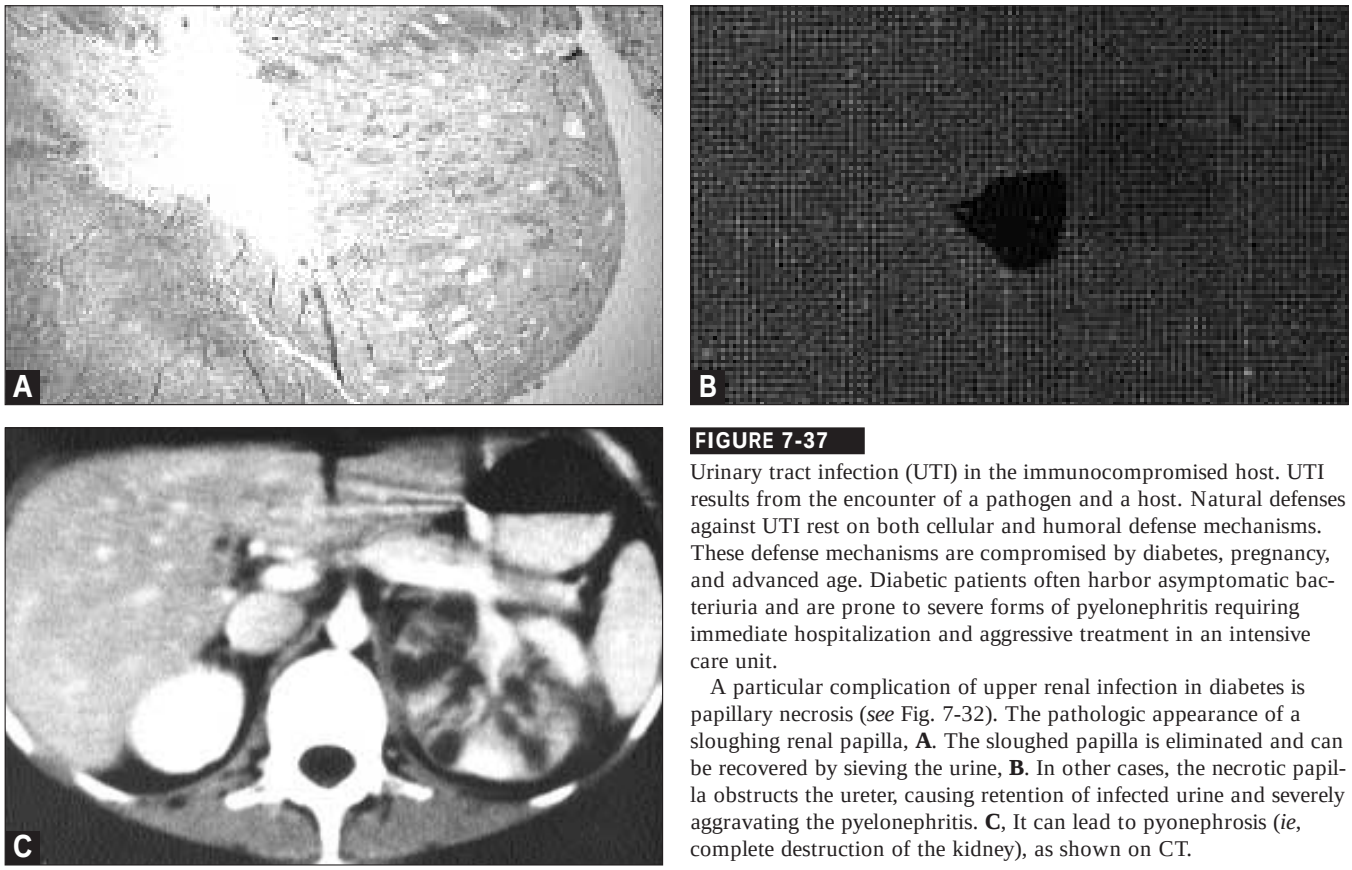

FIGURE 7-37

Urinary tract infection (UTI) in the immunocompromised host. UTI results from the encounter of a pathogen and a host. Natural defenses against UTI rest on both cellular and humoral defense mechanisms. These defense mechanisms are compromised by diabetes, pregnancy, and advanced age. Diabetic patients often harbor asymptomatic bacteriuria and are prone to severe forms of pyelonephritis requiring immediate hospitalization and aggressive treatment in an intensive care unit.

A particular complication of upper renal infection in diabetes is papillary necrosis (*see* Fig. 7-32). The pathologic appearance of a sloughing renal papilla, **A**. The sloughed papilla is eliminated and can be recovered by sieving the urine, **B**. In other cases, the necrotic papilla obstructs the ureter, causing retention of infected urine and severely aggravating the pyelonephritis. **C**, It can lead to pyonephrosis (*ie*, complete destruction of the kidney), as shown on CT.

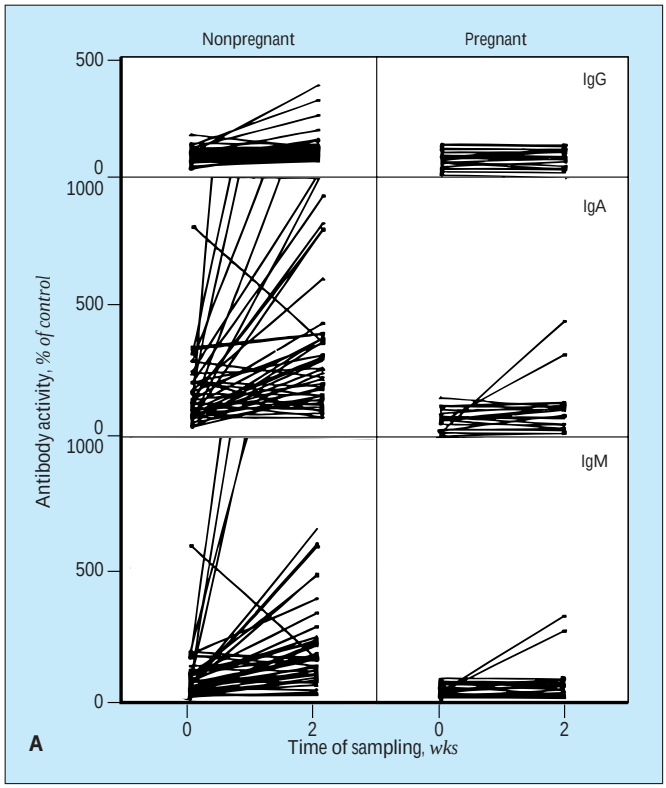

FIGURE 7-38

Urinary tract infection (UTI) in an immunocompromised host. Pregnancy is associated with suppression of the host's immune response, in the form of reduced cytotoxic T-cell activity and reduced circulating immunoglobulin G (IgG) levels. Asymptomatic bacteriuria is common during pregnancy and represents a major risk of ascending infection complicated by acute pyelonephritis.

(Continued on next page)

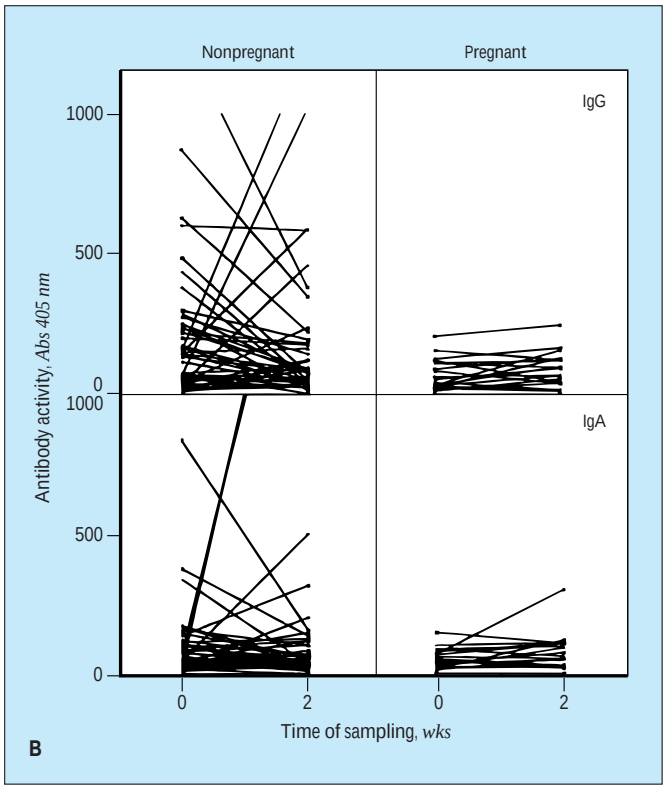

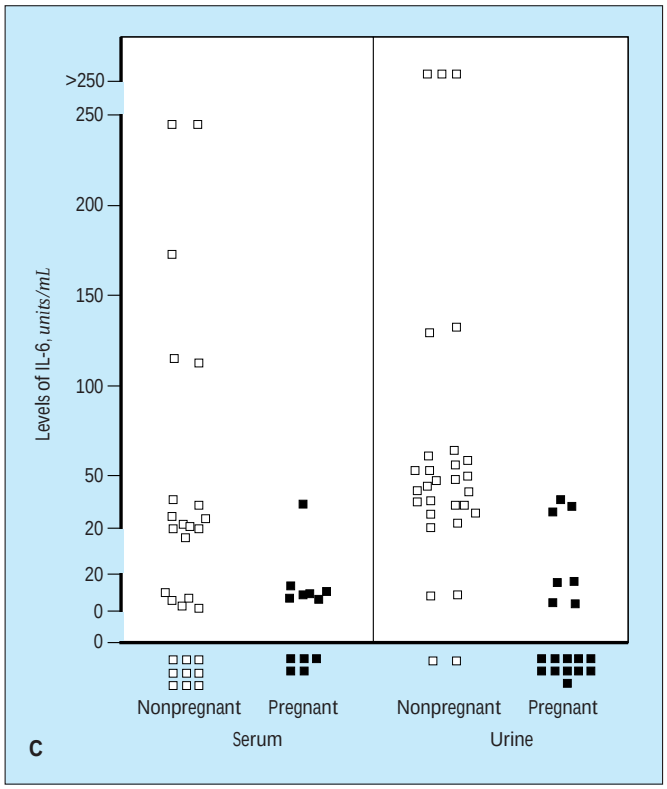

FIGURE 7-38 *(Continued)*

Petersson and coworkers [12] recently demonstrated that the susceptibility of the pregnant woman to acute UTI is accompanied by reduced serum antibody activity (IgG, IgA, IgM), reduced urine antibody activity (IgG, IgA), and low interleukin 6 (IL-6) response, **A–C**, respectively. The last may indicate that pregnant women have a generally reduced level of mucosal inflammation. These factors may be crucial for explaining the frequency and the severity of acute pyelonephritis during pregnancy. (*From* Petersson *et al.* [12]; with permission.)

FIGURE 7-39

Acute prostatitis as visualized sonographically. Acute prostatitis is common after urethral or bladder infection (usually by *Escherichia coli* or *Proteus* organisms). Another cause is prostate hematogenous contamination, especially by *Staphylococcus*. Signs and symptoms of acute prostatitis, in addition to fever, chills, and more generally the signs and symptoms of tissue invasion by infection described above, are accompanied by dysuria, pelvic pain, and septic urine. Acute prostatitis is an indication for direct ultrasound (US) examination of the prostate by endorectal probe. In this case of acute prostatitis in a young male, US examination disclosed a prostatic abscess (1) complicating acute prostatitis in the right lobe (2). Acute prostatitis is an indication for thorough radiologic imaging of the whole urinary tract, giving special attention to the urethra. Urethral stricture may favor prostate infection (*see* Fig. 7-20).

Special Forms of Renal Infection

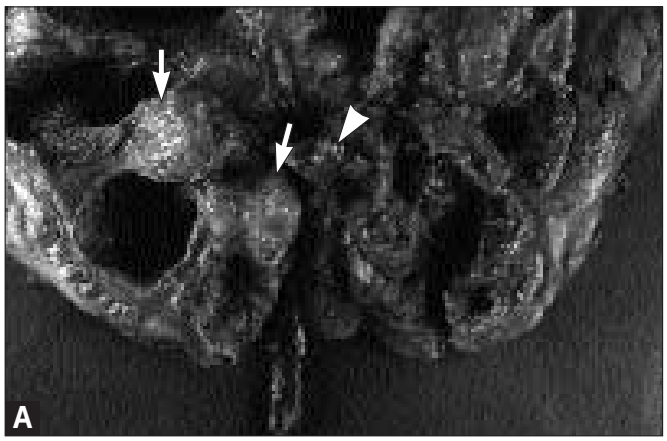

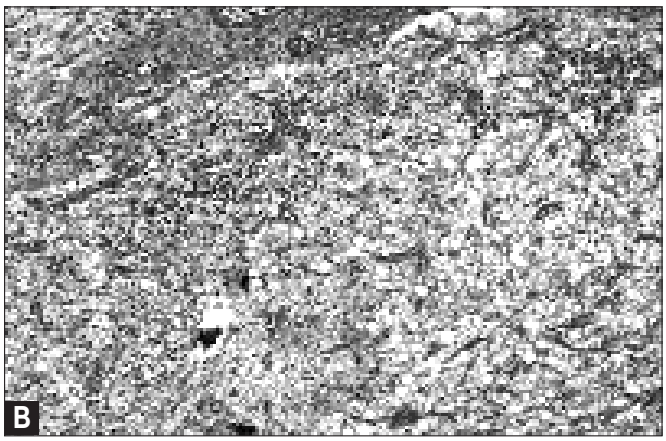

FIGURE 7-40 (*see* Color Plate)
Xanthogranulomatous pyelonephritis (XPN). XPN is a special form of chronic renal inflammation caused by an abnormal immune response to infected obstruction [13]. This case in a middle-aged woman with a long history of renal stones is typical. For several months she complained of flank pain, fever, fatigue, anorexia and weight loss. Laboratory workup found inflammatory anemia and increased erythrocyte sedimentation rate and C-reactive protein levels. Urinalysis showed pyuria and culture grew *Escherichia coli*. CT scan of the right kidney showed replacement of the renal tissue by several rounded, low-density areas and detected an obstructive renal stone. Nephrectomy was performed. **A**, The obstructive renal stone is shown by an arrowhead. The renal cavities are dilated. The xanthogranulomatous tissue (*arrows*) consists of several round, pseudotumoral masses with a typical yellowish color due to presence of lipids. In some instances such xanthogranulomatous tissue extends across the capsule into the perirenal fat and fistulizes into nearby viscera such as the colon or duodenum. **B**, Microscopic view of the xanthogranulomatous tissue. This part of the lesion is made of lipid structures composed of innumerable clear droplets.

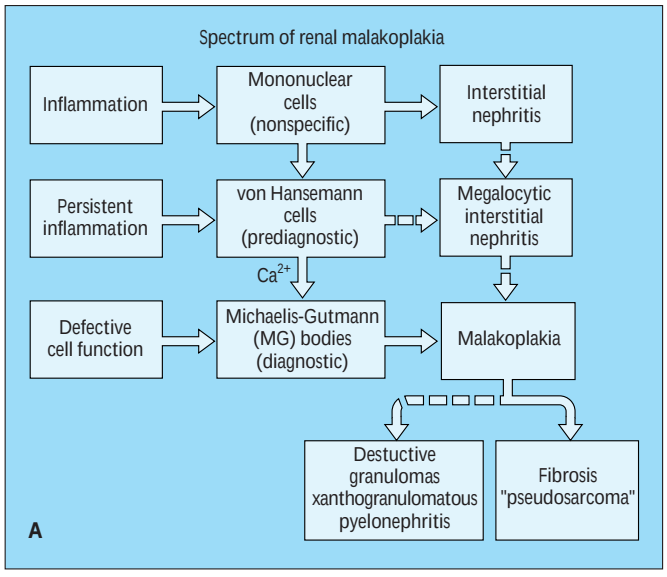

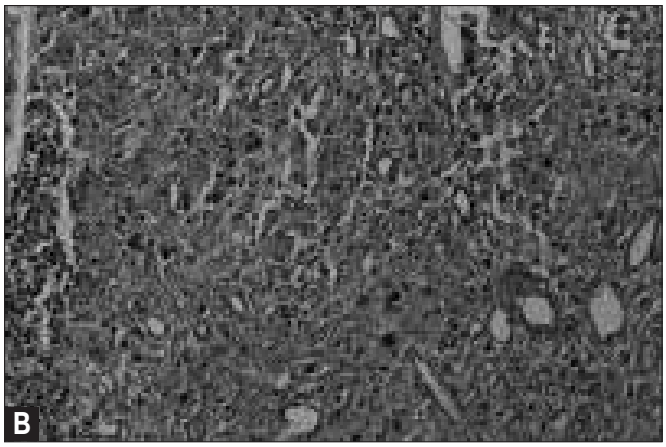

FIGURE 7-41
Malakoplakia. Malakoplakia (or malacoplakia), like xanthogranulomatous pyelonephritis, is also a consequence of abnormal macrophage response to gram-negative bacteria, **A**. Malakoplakia occurs in association with chronic UTI [14]. In more than 20% of cases, affected persons have some evidence of immunosuppression, especially corticosteroid therapy for autoimmune disease. In 13% of the published cases, malakoplakia involved a transplanted kidney. The female-male ratio is 3:1. Lesions can involve the kidney, the bladder, or the ureter and form pseudotumors. **B**, Histologically, malakoplakia is distinguished by large, pale, periodic acid–Schiff–positive macrophages (von Hansemann cells) containing calcific inclusions (Michaelis-Gutmann bodies). The larger ones are often free in the interstitium. Malakoplakia, an unusual form of chronic tubulointerstitial nephritis, must be recognized by early renal biopsy and can resolve, provided treatment consisting of antibiotics with intracellular penetration is applied for several weeks. (**B**, *Courtesy of* Gary S. Hill, MD.)

References

1. Stamm WE, Hooton TM: Management of urinary tract infections in adults. *N Engl J Med* 1993, 329:1328–1334.
2. Pinson AG, Philbrick JT, Lindbeck GH, Schorling JB: ED management of acute pyelonephritis in women: A cohort study. *Am J Emerg Med* 1994, 12:271–278.
3. Pappas PG: Laboratory in the diagnosis and management of urinary tract infections. *Med Clin North Am* 1991, 75:313–325.
4. Kunin CM, VanArsdale White L, Tong HH: A reassessment of the importance of "low-count" bacteriuria in young women with acute urinary symptoms. *Ann Intern Med* 1993, 119:454–460.
5. Meyrier A, Guibert J: Diagnosis and drug treatment of acute pyelonephritis. *Drugs* 1992, 44:356–367.
6. Meyrier A: Diagnosis and management of renal infections. *Curr Opin Nephrol Hypertens* 1996, 5:151–157.
7. Mobley HLT, Island MD, Massad G: Virulence determinants of uropathogenic *Escherichia coli* and *Proteus mirabilis*. *Kidney Int* 1994, 46(Suppl. 47):S129–S136.
8. Roberts JA, Marklund BI, Ilver D, *et al.*: The Gal(α 1-4)Gal–specific tip adhesin of *Escherichia coli* P-fimbriae is needed for pyelonephritis to occur in the normal urinary tract. *Proc Natl Acad Sci USA* 1994, 91:11889–11893.
9. International Reflux Study Committee: Medical versus surgical treatment of primary vesicoureteral reflux. *J Urol* 1981, 125:277.
10. Talner LB, Davidson AJ, Lebowitz RL, *et al.*: Acute pyelonephritis: Can we agree on terminology? *Radiology* 1994, 192:297–306.
11. Roberts JA: Etiology and pathophysiology of pyelonephritis. *Am J Kidney Dis* 1991, 17:1–9.
12. Petersson C, Hedges S, Stenqvist K, *et al.*: Suppressed antibody and interleukin-6 responses to acute pyelonephritis in pregnancy. *Kidney Int* 1994, 45:571–577.
13. Case records of the Massachusetts General Hospital. *N Engl J Med* 1995, 332:174–179.
14. Dobyan DC, Truong LD, Eknoyan G: Renal malacoplakia reappraised. *Am J Kidney Dis* 1993, 22:243–252.

Reflux and Obstructive Nephropathy

James M. Gloor
Vicente E. Torres

Reflux nephropathy, or renal parenchymal scarring associated with vesicoureteral reflux (VUR), is an important cause of renal failure. Some studies have shown that in up to 10% of adults and 30% of children requiring renal replacement therapy for end-stage renal disease, reflux nephropathy is the cause of the renal failure. Reflux nephropathy is thought to result from the combination of VUR of infected urine into the kidney by way of an incompetent ureterovesical junction valve mechanism and intrarenal reflux. Acute inflammatory responses to the infection result in renal parenchymal damage and subsequent renal scarring. Loss of functioning renal mass prompt compensatory changes in renal hemodynamics that, over time, are maladaptive and result in glomerular injury and sclerosis.

Clinically, reflux nephropathy may cause hypertension, proteinuria, and decreased renal function when the scarring is extensive. The identification of VUR raises the theoretic possibility of preventing reflux nephropathy. The inheritance pattern of VUR clearly is suggestive of a strong genetic influence. Familial studies of VUR are consistent with autosomal dominant transmission, and linkage to the major histocompatibility genes has been reported. Identification of infants with reflux detected on the basis of abnormalities seen on prenatal ultrasound examinations before urinary tract infection occurs may provide an opportunity for prevention of reflux nephropathy. In persons with VUR detected at the time of diagnosis of a urinary tract infection, avoidance of further infections may prevent renal injury. Nevertheless, the situation is far from clear. Most children with reflux nephropathy already have renal scars demonstrable at the time of the urinary tract infection that prompts the diagnosis of VUR. Most children found to have VUR do not develop further renal scarring after diagnosis, even after subsequent urinary tract infections. Other children may develop renal scars in the absence of further urinary tract infections. The best treatment of

CHAPTER 8

VUR has not yet been firmly established. No clear advantage has been demonstrated for surgical correction of VUR versus medical therapy with prophylactic antibiotics after 5 years of follow-up examinations. New surgical techniques such as the submucosal injection of bioinert substances may have a role in select cases.

The term *obstructive nephropathy* is used to describe the functional and pathologic changes in the kidney that result from obstruction to the flow of urine. Obstruction to the flow of urine usually is accompanied by hydronephrosis, an abnormal dilation of the renal pelvis, and calices. However, because hydronephrosis can occur without functional obstruction, the terms *obstructive nephropathy* and *hydronephrosis* are not synonymous. Hydronephrosis is found at autopsy in 2% to 4% of cases. Obstructive nephropathy is responsible for approximately 4% of end-stage renal failure. Obstruction to the flow of urine can occur anywhere in the urinary tract and has many different causes.

CAUSES OF OBSTRUCTIVE NEPHROPATHY

- Intraluminal
  - Calculus, clot, renal papilla, fungus ball
- Intrinsic
  - Congenital:
    - Calyceal infundibular obstruction
    - Ureteropelvic junction obstruction
    - Ureteral stricture or valves
    - Posterior urethral valves
    - Anterior urethral valves
    - Urethral stricture
    - Meatal stenosis
    - Prune-belly syndrome
  - Neoplastic:
    - Carcinoma of the renal pelvis, ureter, or bladder
    - Polyps
- Extrinsic
  - Congenital (aberrant vessels):
    - Congenital hydrocalycosis
    - Ureteropelvic junction obstruction
    - Retrocaval ureter
  - Neoplastic tumors:
  - Benign tumors:
    - Benign prostatic hypertrophy
    - Pelvic lipomatosis
    - Cysts
  - Primary retroperitoneal tumors:
    - Mesodermal origin (*eg*, sarcoma)
    - neurogenic origin (*eg*, neurofibroma)
    - Embryonic remnant (*eg*, teratoma)
  - Retroperitoneal extension of pelvic or abdominal tumors:
    - Uterus, cervix
    - Bladder, prostate
    - Rectum, sigmoid colon
  - Metastatic tumor:
    - Lymphoma
  - Inflammatory:
    - Retroperitoneal fibrosis
    - Inflammatory bowel disease
    - Diverticulitis
    - Infection or abscess
  - Gynecologic:
    - Pregnancy
    - Uterine prolapse
    - Surgical disruption or ligation
- Functional
  - Neurogenic bladder
  - Drugs(anticholinergics, antidepressants, calcium channel blockers)

FIGURE 8-1

Obstructive nephropathy is responsible for end-stage renal failure in approximately 4% of persons. Obstruction to the flow of urine can occur anywhere in the urinary tract. Obstruction can be caused by luminal bodies; mural defects; extrinsic compression by vascular, neoplastic, inflammatory, or other processes; or dysfunction of the autonomic nervous system or smooth muscle of the urinary tract. The functional and clinical consequences of urinary tract obstruction depend on the developmental stage of the kidney at the time the obstruction occurs, severity of the obstruction, and whether the obstruction affects one or both kidneys.

Anatomy of Vesicoureteric Reflux

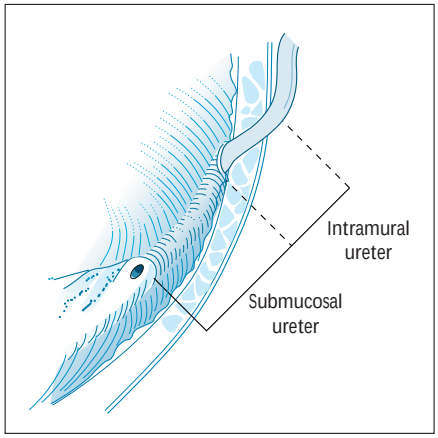

FIGURE 8-2

Anatomy of the ureterovesical junction. The ureterovesical junction permits free antegrade urine flow from the upper urinary tract into the bladder and prevents retrograde urinary reflux from the bladder into the ureter and kidney. Passive compression of the distal submucosal portion of the ureter against the detrusor muscle as a result of bladder filling impedes vesicoureteral reflux (VUR). An active mechanism preventing reflux also has been proposed in which contraction of longitudinally arranged distal ureteral muscle fibers occludes the ureteral lumen, impeding retrograde urine flow [1–3]. (*From* Politano [4]; with permission.)

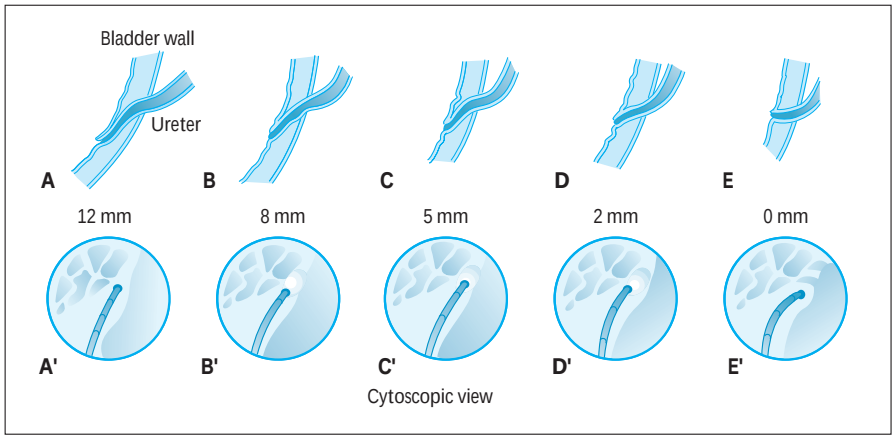

FIGURE 8-3

Tissue sagittal sections (*upper panels*) and cystoscopic appearances (*lower panels*) of the ureterovesical junction illustrating varying submucosal tunnel lengths. The length of the submucosal segment of the distal ureter is an important factor in determining the effectiveness of the ureteral valvular mechanism in preventing vesicoureteral reflux (VUR). In children without VUR, the ratio of tunnel length to ureteral diameter is significantly greater than in children with VUR [5,6]. (*From* Kramer [7]; with permission.)

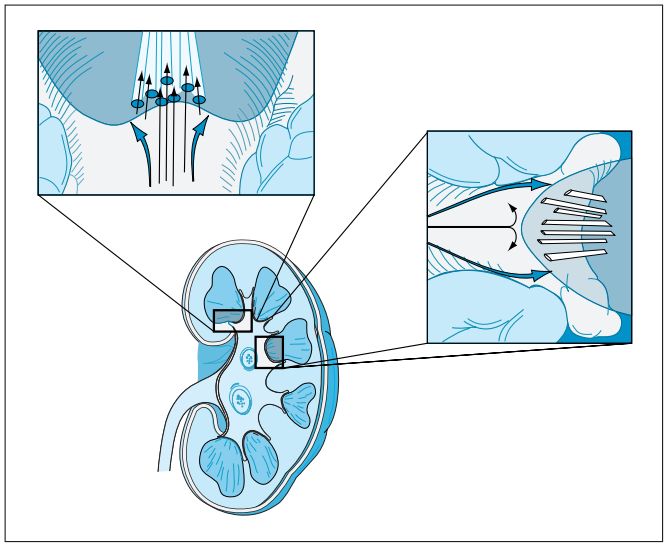

FIGURE 8-4

Simple and compound papillae are illustrated [8,9]. Two types of renal papillae have been identified. Simple papillae are the most common type. They have slitlike papillary duct openings on their convex surface. These papillae are compressed by increases in pelvic pressure, preventing urine from entering the papillary ducts (intrarenal reflux). Compound papillae are formed by the fusion of two or more simple papillae. In compound papillae, some ducts open onto a flat or concave surface at less oblique angles. Increased intrapelvic pressure may permit intrarenal reflux. Compound papillae usually are found in the renal poles.

Pathogenesis of Vesicoureteric Reflux and Reflux Nephropathy

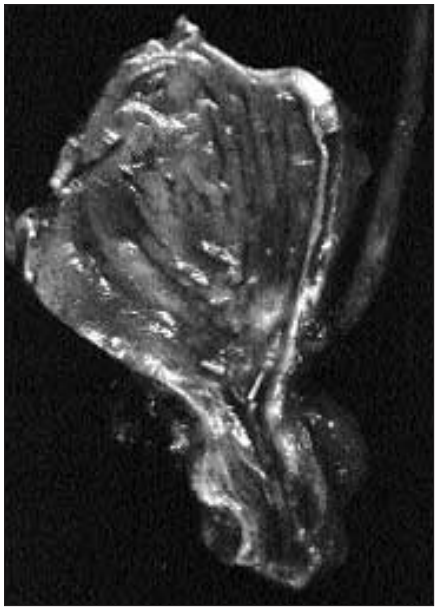

FIGURE 8-5

Experimental vesicoureteric reflux in pigs. This pathology specimen demonstrates surgically induced vesicoureteric reflux in a 2-week-old male piglet. Note that the submucosal canal of one of the ureters has been unroofed.

FIGURE 8-6

Experimental vesicoureteric reflux in pigs: cystourethrogram showing intrarenal reflux. Reflux of radiocontrast medium into the renal parenchyma is seen. The pressure required to produce intrarenal reflux is lower in young children than it is in older children or adults, which is consistent with the observation that reflux scars occur more commonly in younger children [10].

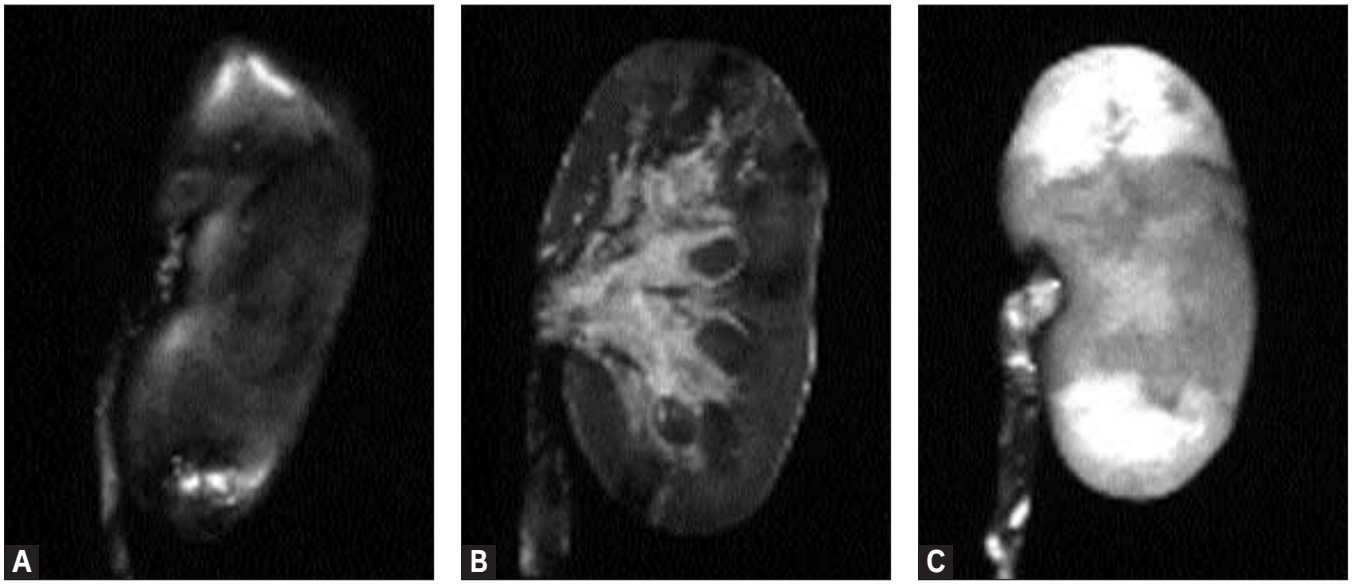

FIGURE 8-7

Experimental vesicoureteric reflux in pigs. The polar location of acute suppurative pyelonephritis and evolution of parenchymal scars. In urinary tract infections, reflux of urine from the renal pelvis into the papillary ducts of compound papillae predominantly

(Continued on next page)

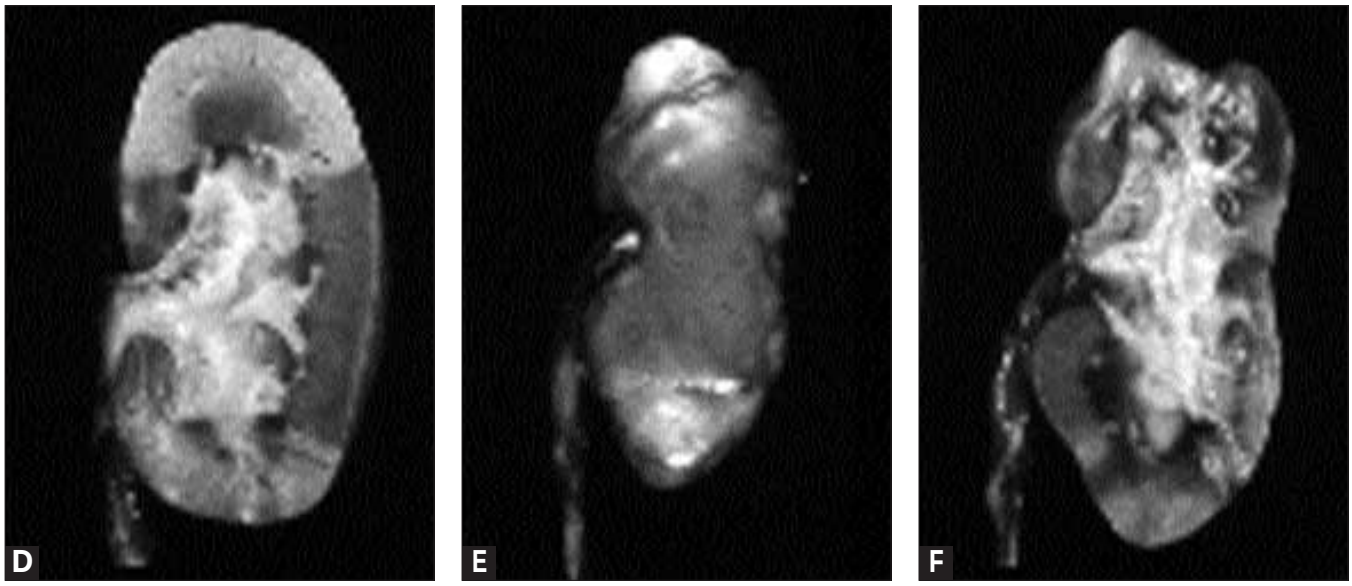

FIGURE 8-7 (*Continued*)
located in the poles (intrarenal reflux) provides bacteria access to the renal parenchyma, resulting in suppurative pyelonephritis and subsequent polar scarring [11,12]. Intact (**A, C, E**) and coronally sectioned (**B, D, F**) kidneys illustrating the three stages of reflux nephropathy: Hemorrhagic with polymorphonuclear cell infiltrate (**A, B**); white, not retracted, with prominent mononuclear cell infiltrate (**C, D**), and retracted scan with prominent fibrosis (**E, F**).

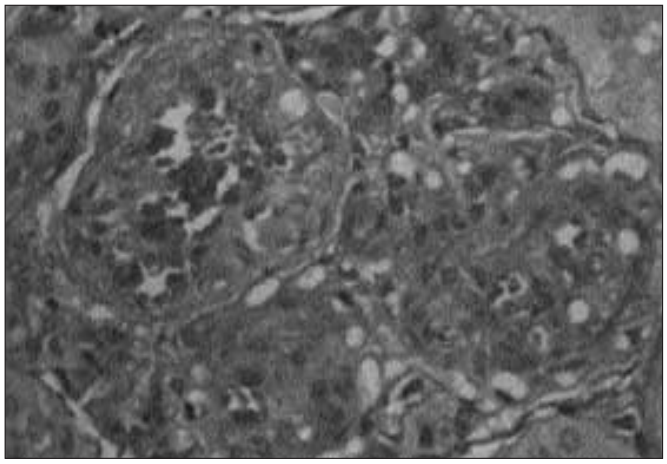

FIGURE 8-8 (*see* Color Plate)
Experimental vesicoureteric reflux (VUR) in pigs: mesangiopathic lesions. Reflux of infected urine can result in glomerular lesions characterized by activation of mesangial cells, mesangial expansion, mesangial hypercellularity, and the presence of large granules. The granules test positive on periodic acid–Schiff reaction and are located inside cells with the appearance of macrophages. These glomerulopathic lesions occur by a process that does not require contiguity with the infected interstitium nor intrarenal reflux. These lesions are not related to reduction of renal mass. Similar glomerular lesions have been identified in piglets after intravenous administration of endotoxin. Whether similar glomerular lesions occur in infants or young children with VUR and reflux nephropathy is not known [13].

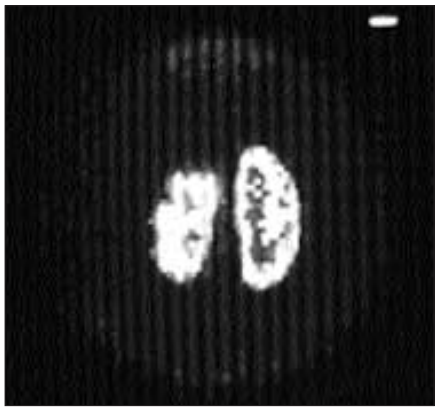

FIGURE 8-9 (*see* Color Plate)
Experimental vesicoureteric reflux (VUR) in pigs: ^{99m}Technetium-dimercaptosuccinic acid (DMSA) scan demonstrating reflux nephropathy. Radionuclide imaging using DMSA has been found to be safe and effective in investigating reflux nephropathy [14]. DMSA is localized to the proximal renal tubules of the renal cortex. Parenchymal scars appear as a defect in the kidney outline, with reduced uptake of DMSA or by contraction of the whole kidney. Currently, DMSA radionuclide renal scanning is the most sensitive modality used to detect renal scars relating to reflux. New areas of renal scarring can be seen earlier with DMSA than with intravenous pyelography [15].

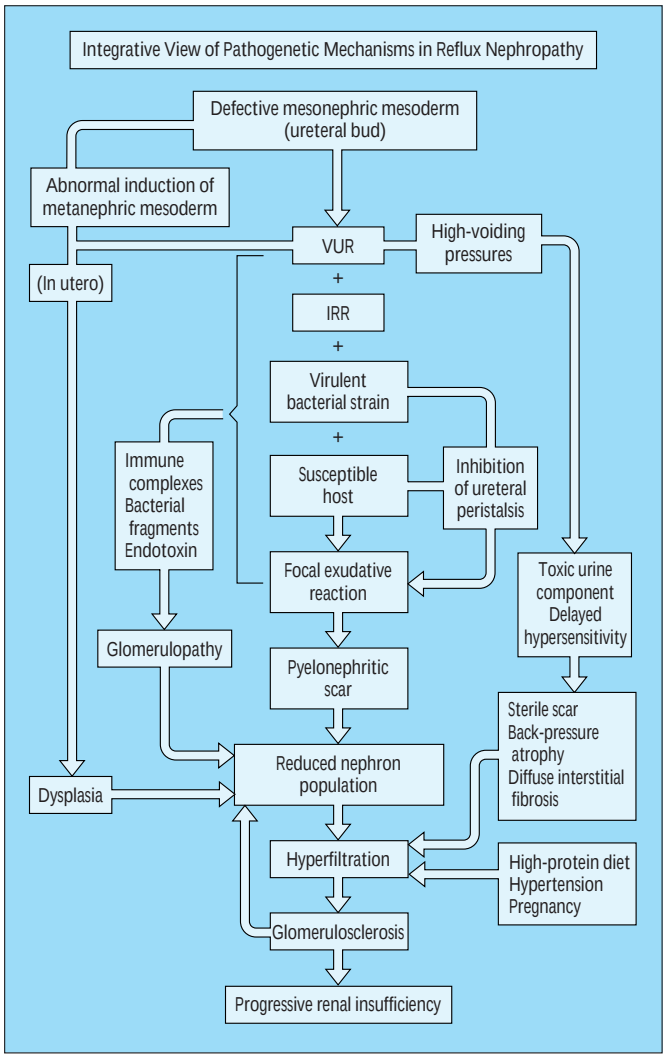

FIGURE 8-10

Integrative view of pathogenetic mechanisms in reflux nephropathy. Abnormalities of ureteral embryogenesis may result in a defective antireflux mechanism, permitting vesicoureteral reflux (VUR), incomplete bladder emptying, urinary stasis, and infection. Bacterial virulence factors modify the pathogenicity of different bacterial strains. Bacterial surface appendages such as fimbriae may interact with epithelial cell receptors of the urinary tract, enhancing bacterial adhesion to urothelium. Endotoxin is capable of inhibiting ureteral peristalsis, contributing to the extension of the infection into the upper urinary tract even in the absence of VUR. Inoculation of the renal parenchyma with bacteria produces an acute inflammatory response, resulting in the release of inflammatory mediators into the surrounding tissue. The acute inflammatory response elicited by the presence of infecting bacteria is responsible for the subsequent renal parenchymal injury. In addition, it is possible that immune complexes, bacterial fragments, and endotoxin resulting from infection may produce a glomerulopathy.

Even in the absence of urinary tract infection, VUR associated with elevated intravesical pressure is capable of producing renal parenchymal scars. The developing kidney appears to be particularly susceptible. Renal tubular distention resulting from high intrapelvic pressure may exert an injurious effect on renal tubular epithelium. Compression of the surrounding peritubular capillary network by distended renal tubules may produce ischemia. During micturition, elevated intravesical pressure is transmitted to the renal pelvis and renal tubule. This transient pressure elevation may produce tubular disruption. Extravasation of urine into the surrounding parenchyma results in an immune-mediated interstitial nephritis and further renal injury.

The reduction in functional renal mass produced by the interaction of the pathogenetic factors listed here induces compensatory hemodynamic changes in renal blood flow and the glomerular filtration rate. Over time, these compensatory changes may be maladaptive, may produce hyperfiltration and glomerulosclerosis, and may eventuate in renal insufficiency. (*From* Kramer [16]; with permission.)

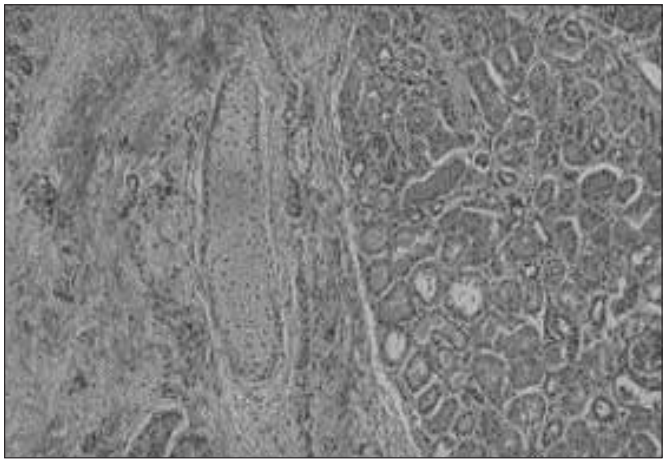

FIGURE 8-11

Vesicoureteral reflux and renal dysplasia. An abnormal ureteral bud resulting from defective ureteral embryogenesis may penetrate the metanephric blastema at a site other than that required for optimum renal development, potentially resulting in renal dysplasia or hypoplasia [17].

Diagnosis of Vesicoureteric Reflux and Reflux Nephropathy

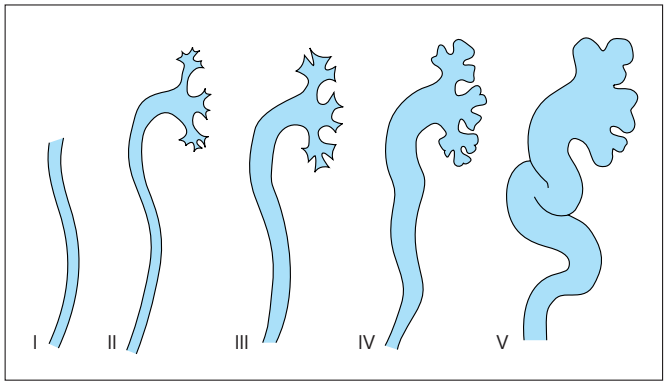

FIGURE 8-12

International system of radiographic grading of vesicoureteral reflux (VUR). The severity of VUR is most frequently classified according to the International Grading System of Vesicoureteral Reflux, using a standardized technique for performance of voiding cystourethrography. The definitions of this system are illustrated in Figure 8-4 and are as follows. In grade I, reflux only into the ureter occurs. In grade II, reflux into the ureter, pelvis, and calyces occurs. No dilation occurs, and the calyceal fornices are normal. In grade III, mild or moderate dilation, tortuosity, or both of the ureter are observed, with mild or moderate dilation of the renal pelvis. No or only slight blunting of the fornices is seen. In grade IV, moderate dilation, tortuosity, or both of the ureter occur, with moderate dilation of the renal pelvis and calyces. Complete obliteration of the sharp angle of the fornices is observed; however, the papillary impressions are maintained in most calyces. In grade V, gross dilation and tortuosity of the ureter occur; gross dilation of the renal pelvis and calyces is seen. The papillary impressions are no longer visible in most calyces [18].

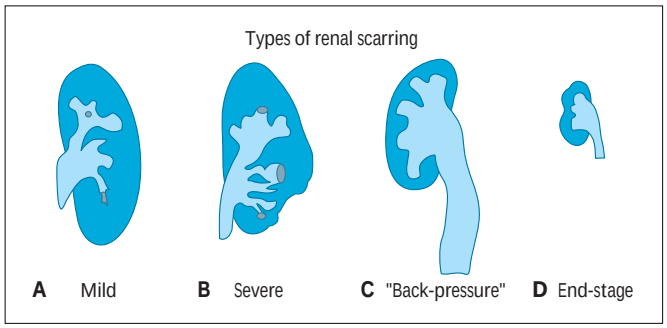

FIGURE 8-13

Grading of renal scarring associated with vesicoureteral reflux. Reflux renal parenchymal scarring detected on intravenous pyelography can be classified according to the system adopted by the International Reflux Study Committee consisting of four grades of severity. In grade 1, mild scarring in no more than two locations is seen. More severe and generalized scarring is seen in grade 2 but with normal areas of renal parenchyma between scars. In grade 3, or so-called backpressure type, contraction of the whole kidney occurs and irregular thinning of the renal cortex is superimposed on widespread distortion of the calyceal anatomy, similar to changes seen in obstructive uropathy. Grade 4 is characterized by end-stage renal disease and a shrunken kidney having very little renal function [19].

Parenchymal scarring detected by radionuclide renal scintigraphy is classified similarly. **A**, In grade 1, no more than two scarred areas are detected. **B**, In grade 2, more than two affected areas are seen, with some areas of normal parenchyma between them. **C**, Grade 3 renal scarring is characterized by general damage to the entire kidney, similar to obstructive nephropathy. **D**, In grade 4, a contracted kidney in end-stage renal failure is seen, with less than 10% of total overall function [14].

FIGURE 8-14

Voiding cystourethrogram demonstrating bilateral grade 5 vesicoureteral reflux. Voiding cystourethrography is performed by filling the bladder with radiocontrast material and observing for reflux under fluoroscopy, either during the phase of bladder filling or during micturition. Contrast material is infused through a small urethral catheter under gravity flow.

FIGURE 8-15

Radionuclide cystogram demonstrating bilateral vesicoureteral reflux (VUR). This method using ^{99m}technetium pertechnetate is useful in detecting VUR. Advantages of radionuclide cystography include lower radiation exposure, less interference with overlying bowel contents and bones, and higher sensitivity in detection of VUR. Radionuclide cystography is useful in follow-up examinations of patients known to have VUR, as a screening test in asymptomatic siblings of children with reflux and girls with urinary tract infections, and in serial examinations of children with neuropathic bladders at risk for developing VUR. Disadvantages of this method include less anatomic detail and inadequacy in evaluating the male urethra, making it unsuitable for screening boys for urinary tract infections [7].

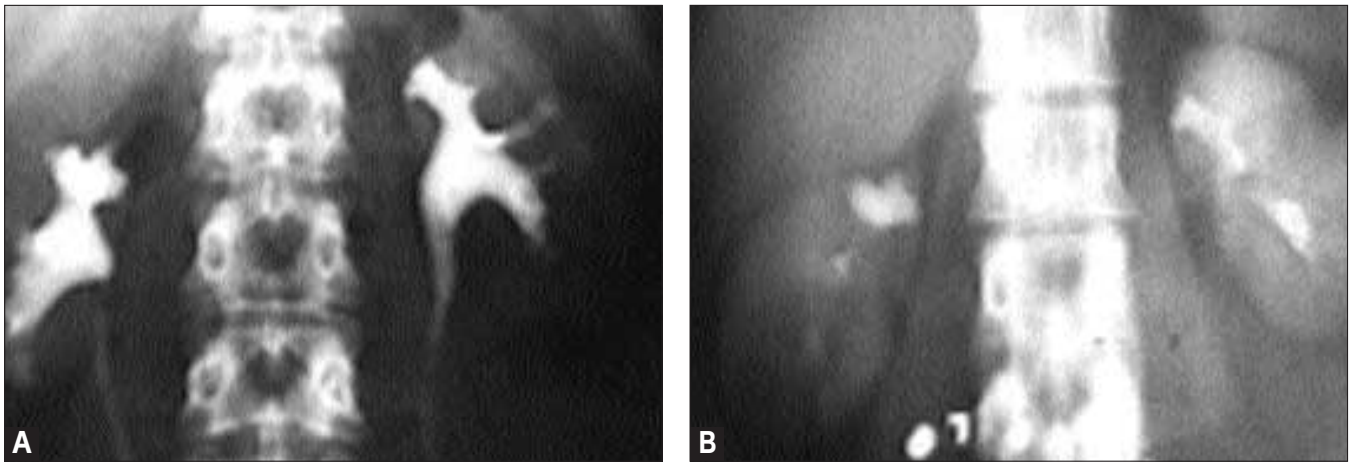

FIGURE 8-16

A, Intravenous pyelogram and, **B**, nephrotomogram demonstrating grade 2 reflux nephropathy. Historically, this testing modality has been the one most commonly used to evaluate reflux nephropathy [7]. Irregular renal contour, parenchymal thinning, small renal size, and calyceal blunting all are radiographic signs of reflux nephropathy on intravenous pyelography [17]. Radiographic changes may not be visible immediately after renal infection, because scars may not be fully developed for several years [20]. The advantages of intravenous pyelography in evaluating reflux nephropathy include precision in delineating renal anatomic detail and providing baseline measurements for future follow-up evaluations, renal growth, and scar formation.

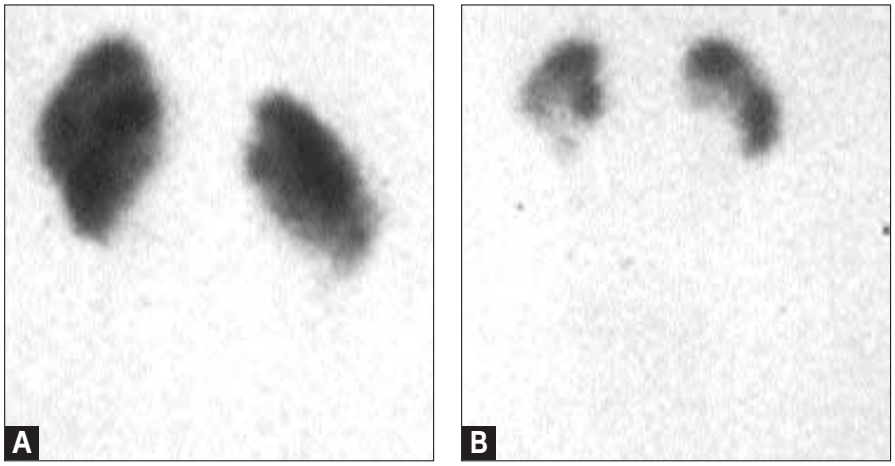

FIGURE 8-17

A, Posterior and, **B**, anterior views of ^{99m}technetium-dimercaptosuccinic acid (DMSA) renal scan showing bilateral grade 2 reflux nephropathy. This nephropathy is characterized by focal areas of decreased radionuclide uptake predominantly affecting the lower renal poles.

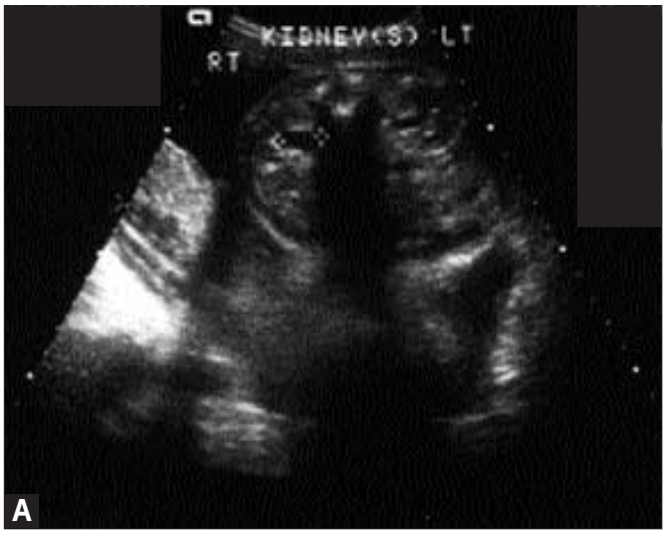

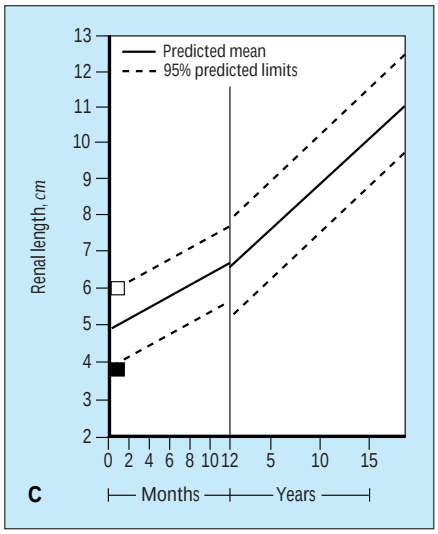

FIGURE 8-18

Prenatal detection of vesicoureteral reflux (VUR). **A**, Ultrasonography showing mild fetal hydronephrosis. **B**, Postnatal voiding cystourethrogram (VCUG) showing grade 4 VUR. **C**, Graph showing small renal size in the same infant. Vesicoureteral reflux has been identified in neonates in whom prenatal ultrasonography examination reveals hydronephrosis [21–28]. Normal infants do not have VUR, even when born prematurely [29,30]. The severity of reflux often is not predictable on the basis of appearance on ultrasonography [22,31]. Hydronephrosis greater than 4 mm and less than 10 mm in the anteroposterior dimension on ultrasound examination after 20 weeks' gestational age has been termed *mild fetal hydronephrosis*. Mild fetal hydronephrosis is associated with VUR in a significant percentage of infants [26,31]. Despite the absence of a previous urinary tract infection, many kidneys affected prenatally exhibit decreased function [22,24,32,33]. Unlike the focal parenchymal scars seen in infection-associated reflux nephropathy, the parenchymal abnormalities seen in prenatal VUR are most commonly manifested by a generalized decrease in renal size (reflux nephropathy grade 3 or 4) [34,35].

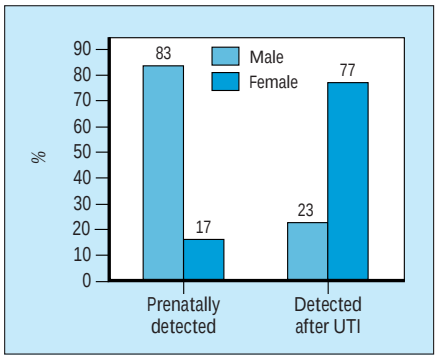

FIGURE 8-19

Prenatal detection of vesicoureteral reflux (VUR): gender distribution versus VUR detected after urinary tract infection (UTI). VUR detected as part of the evaluation of prenatal hydronephrosis is most commonly identified in boys. In an analysis of six published studies of VUR diagnosed in a total of 124 infants with antenatally detected hydronephrosis, 83% of those affected were boys [33]. Conversely, VUR detected after a UTI most commonly affects girls. In the International Reflux Study in Children (IRSC) and Southwest Pediatric Nephrology Study Group (SWPNSG) investigations of VUR detected in a total of 380 children after UTI, 77% of those affected were girls [20,36].

Clinical Course of Vesicoureteric Reflux

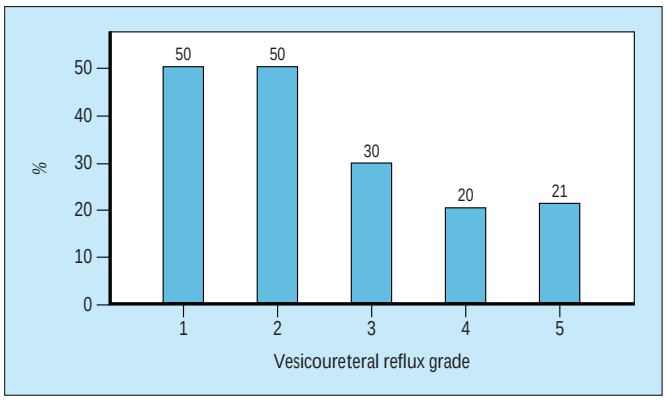

FIGURE 8-20

Resolution of vesicoureteral reflux (VUR) detected prenatally at follow-up examinations over 2 years. Spontaneous resolution of VUR can occur in infants with reflux detected during the postnatal evaluation of prenatal urinary tract abnormalities. In an analysis of six investigations of VUR detected neonatally with a follow-up period of 2 years, resolution was seen in 50% of infants with grades I and II. High-grade reflux (grades IV to V) resolved in only 20% [33].

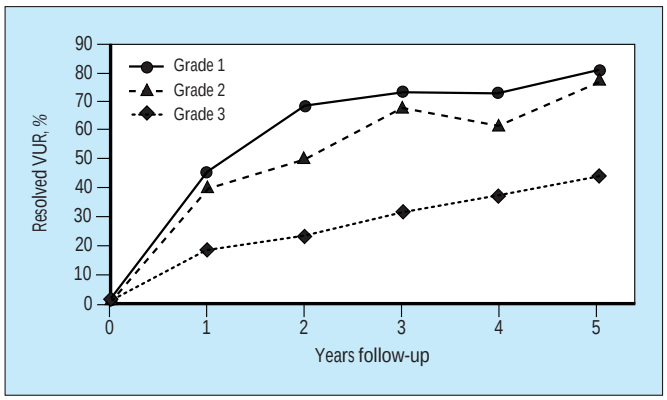

FIGURE 8-21

Resolution of vesicoureteral reflux (VUR) detected postnatally after urinary tract infection: mild to moderate VUR. The Southwest Pediatric Nephrology Study Group (SWPNSG) prospectively observed 113 patients aged 4 months to 5 years with grades I to III VUR detected after urinary tract infection. The SWPNSG reported on 59 children followed up with serial excretory urograms and voiding cystourethrography for 5 years. Mild (grade I and II) VUR resolved after 5 years in the ureters of 80% of these children, and in most cases within 2 to 3 years. Grade III VUR resolved in only 46% of ureters in children with VUR [20].

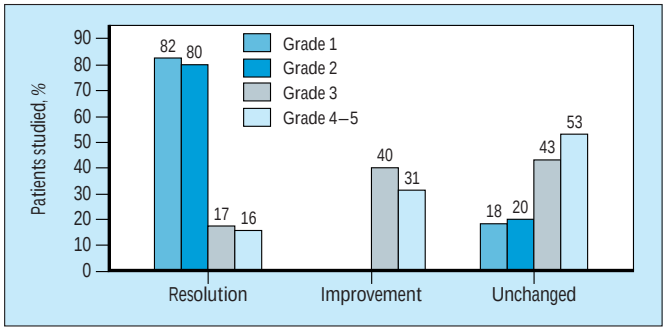

FIGURE 8-22

Resolution of vesicoureteral reflux (VUR) detected postnatally after urinary tract infection at follow-up examinations over 5 years. Mild to moderate VUR spontaneously resolves in a significant percentage of children, whereas high-grade reflux resolves only rarely. The Southwest Pediatric Nephrology Study Group (SWPNSG) found that grades I and II VUR resolved in 80% of children with refluxing ureters at follow-up examinations over 5 years. In the Birmingham Reflux Study Group (BRSG), International Reflux Study in Children (IRSC), and SWPNSG investigations of high-grade VUR (grades III to V) in children, improvement in reflux severity was seen in 30% to 40% of affected ureters. Spontaneous resolution was rare and occurred in only 16% to 17% of children with refluxing ureters at follow-up examinations over 5 years [20,37,38].

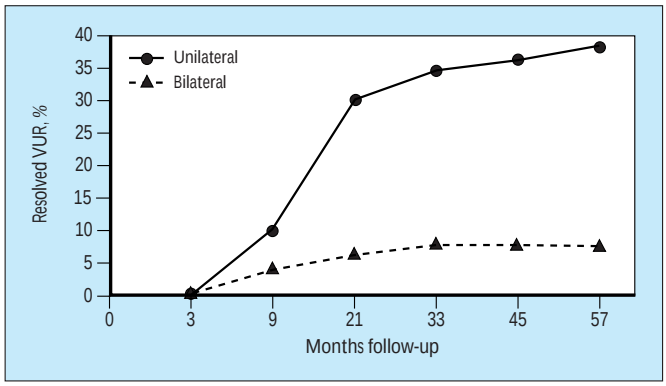

FIGURE 8-23

Resolution of grades III to V vesicoureteral reflux (VUR) detected postnatally after urinary tract infection: bilateral versus unilateral VUR. Spontaneous resolution of high-grade VUR is much more likely to occur in unilateral reflux. The International Reflux Study in Children (IRSC) showed that grades III to V VUR resolved in children in whom both kidneys were affected nearly five times as often (39%) as in those in whom VUR was bilateral (8%). In bilateral VUR, spontaneous resolution did not occur after 2 years of observation [38].

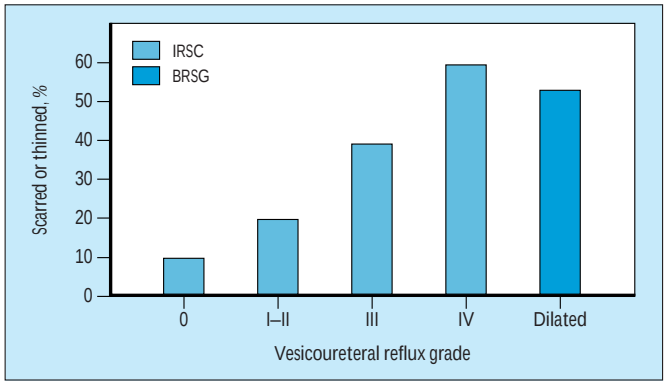

FIGURE 8-24

Frequency of parenchymal scarring at the time of diagnosis of vesicoureteral reflux (VUR). Many children in whom VUR is detected after a urinary tract infection already have evidence of renal parenchymal scarring. In two large prospective studies the frequency of scars seen in persons with VUR increased with VUR severity. The International Reflux Study in Children (IRSC) studied 306 children under 11 years of age with grades III to V VUR [36]. The frequency of parenchymal scarring or thinning increased from 10% in children with nonrefluxing renal units (in children with contralateral VUR) to 60% in those with severely refluxing grade V kidneys. In another large prospective study, the Birmingham Reflux Study Group (BRSG) reported renal scarring in 54% of 161 children under 14 years of age with severe VUR resulting in ureteral dilation (greater than grade 3 using the classification system adopted by the International Reflux Study in Children group) at the time reflux was detected [39]. Participants in these studies were children previously diagnosed as having had urinary tract infection.

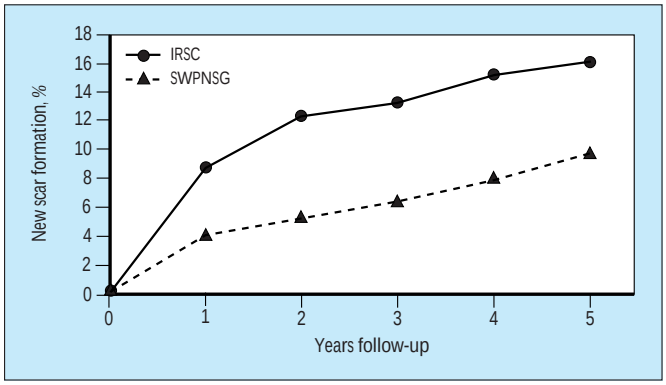

FIGURE 8-25

Development of parenchymal scarring after diagnosis of vesicoureteral reflux (VUR). Parenchymal scarring occurs after diagnosis and initiation of therapy as well. The Southwest Pediatric Nephrology Study Group (SWPNSG) followed up 59 children with mild to moderate VUR (grades I to III) diagnosed after urinary tract infection [20]. None of the children studied had parenchymal scarring on intravenous pyelography at the time of diagnosis. Parenchymal scars were seen to develop in 10% of children over the course of 5 years of follow-up examinations, including some children without documented urinary tract infections during the period of observation. In this group, renal scarring occurred nearly three times more commonly in grade 3 VUR than it did in grades 1 and 2 VUR. In the International Reflux Study in Children (IRSC) (European group), a prospective study of high-grade VUR (grades III and IV), new scars developed in 16% of 236 children after 5 years' observation [40].

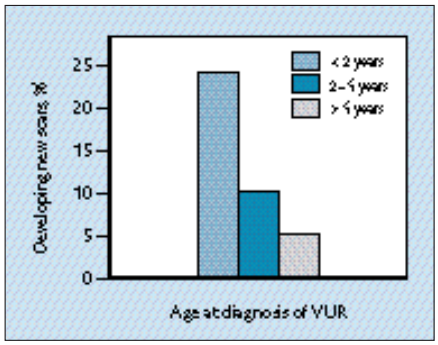

FIGURE 8-26

Development of new renal scars versus age at diagnosis of vesicoureteral reflux (VUR). The frequency of new scar formation appears to be inversely related to age. The International Reflux Study in Children (IRSC) examined children with high-grade VUR and found that new scars developed in 24% under 2 years of age, 10% from 2 to 4 years of age, and 5% over 4 years of age [40].

Treatment of Vesicoureteric Reflux

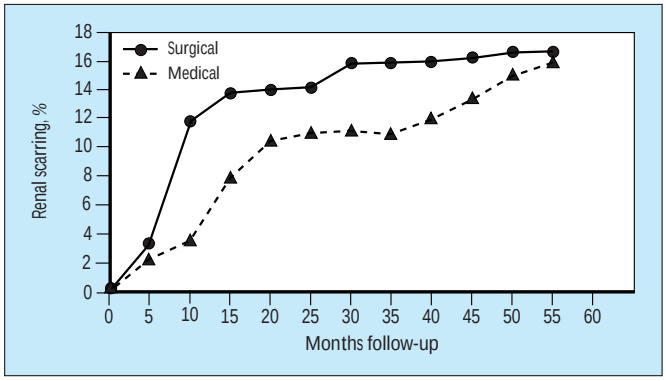

FIGURE 8-27

Effectiveness of medical versus surgical treatment: new scar formation at follow-up examinations over 5 years in children with high-grade vesicoureteral reflux (VUR). The International Reflux Study in Children (IRSC) (European group) was designed to compare the effectiveness of medical versus surgical therapy of VUR in children diagnosed after urinary tract infection. Surgery was successful in correcting VUR in 97.5% of 231 reimplanted ureters in 151 children randomized to surgical therapy. Medical therapy consisted of long-term antibiotic uroprophylaxis using nitrofurantoin, trimethoprim, or trimethoprim-sulfa. No statistically significant advantage was demonstrable for either treatment modality with respect to new scar formation after 5 years of observation in either study. New scars were identified in 20 of the 116 children treated surgically (17%) and 19 of the 155 children treated medically (16%) at follow-up examinations over 5 years. Those children treated surgically who developed parenchymal scars generally did so within the first 2 years after ureteral repeat implantation, whereas scarring occurred throughout the observation period in the group that did not have surgery. VUR persisted in 80% of children randomized to medical treatment after follow-up examinations over 5 years.

The results of the IRSC paralleled the findings of the Birmingham Reflux Study Group (BRSG) investigation of medical versus surgical therapy for VUR in 161 children. After 2 years of observation, progressive or new scar formation was seen in 16% of children with refluxing ureters in the group treated surgically and 19% in the group treated medically. In contrast to the IRSC, however, new scar formation was rare after 2 years of observation in both groups [37,40].

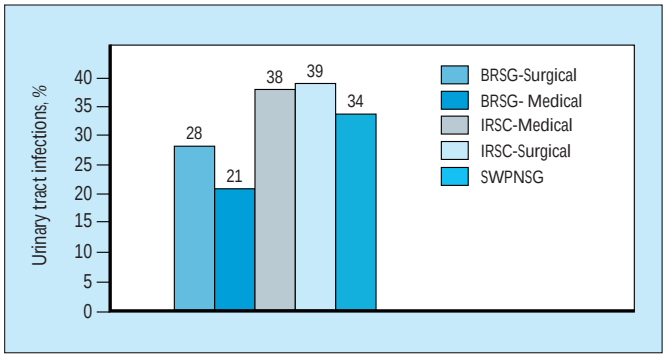

FIGURE 8-28

Effectiveness of medical versus surgical treatment: incidence of urinary tract infections. Vesicoureteral reflux (VUR) predisposes affected persons to urinary tract infection owing to incomplete bladder emptying and urinary stasis. Medical therapy with uroprophylactic antibiotics and surgical correction of VUR have as a goal the prevention of urinary tract infection. In three prospective studies of 400 children with VUR (Southwest Pediatric Nephrology Study Group [SWPNSG], International Reflux Study in Children [IRSC], Birmingham Reflux Study Group [BRSG]) treated either medically or surgically and who were observed over 5 years the rate of infection was similar, ranging from 21% to 39%. The rate of infection was no different between the group treated medically and that treated surgically [20,37,39].

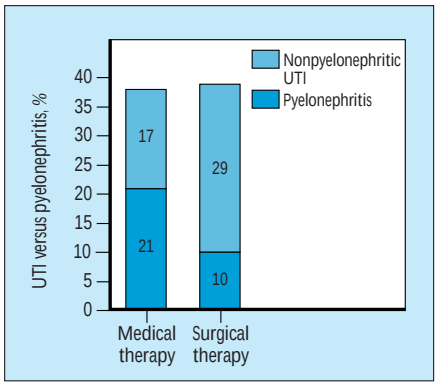

FIGURE 8-29

Effectiveness of medical versus surgical treatment: incidence of urinary tract infection versus pyelonephritis in severe vesicoureteral reflux (VUR). Although the incidence of urinary tract infections (UTIs) is the same in surgically and medically treated children with VUR, the severity of infection is greater in those treated medically. The International Reflux Study in Children (IRSC) (European group) studied 306 children with VUR and observed them over 5 years; 155 were randomized to medical therapy, and 151 had surgical correction of their reflux. Although the incidence of UTI statistically was no different between the groups (38% in the medical group, 39% in the surgical group), children treated medically had an incidence of pyelonephritis twice as high (21%) as those treated surgically (10%) [41].

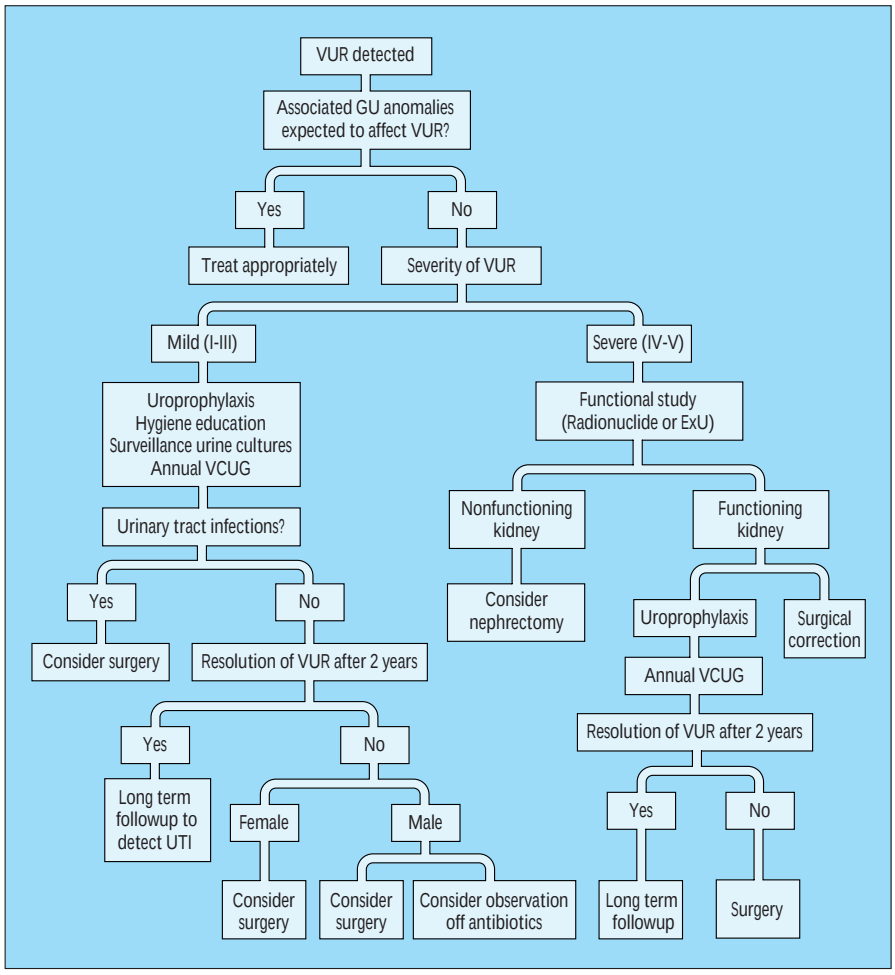

FIGURE 8-30

Proposed treatment of vesicoureteral reflux (VUR) in children. This algorithm provides an approach to evaluate and treat VUR in children. In VUR associated with other genitourinary anomalies, therapy for reflux should be part of a comprehensive treatment plan directed toward correcting the underlying urologic malformation. Children with mild VUR should be treated with prophylactic antibiotics, attention to perineal hygiene and regular bowel habits, surveillance urine cultures, and annual voiding cystourethrogram (VCUG). Children with recurrent urinary tract infection on this regimen should be considered for surgical correction. In children in whom VUR resolves spontaneously, a high index of suspicion for urinary tract infection should be maintained, and urine cultures should be obtained at times of febrile illness without ready clinical explanation.

In persons in whom mild VUR fails to resolve after 2 to 3 years of observation, consideration should be given to voiding pattern. A careful voiding history and an evaluation of urinary flow rate may reveal abnormalities in bladder function that impede resolution of reflux. Correction of dysfunctional voiding patterns may result in resolution of VUR. In the absence of dysfunctional voiding, it is controversial whether older women with persistent VUR are best served by surgical correction or close observation with uroprophylactic antibiotic therapy and surveillance urine cultures, especially during pregnancy. Males with persistent low-grade VUR may be candidates for close observation with surveillance urine cultures while not receiving antibiotic therapy, especially if they are over 4 years of age and circumcised. Circumcision lowers the incidence of urinary tract infection. In severe VUR the function of the affected kidney should be evaluated with a functional study (radionuclide renal scan). High-grade VUR in nonfunctioning kidneys is unlikely to resolve spontaneously, and nephrectomy may be indicated to decrease the risk of urinary tract infection and avoid the need for uroprophylactic antibiotic therapy. In patients with functioning kidneys who have high-grade VUR, the likelihood for resolution should be considered. Severe VUR, especially if bilateral, is unlikely to resolve spontaneously. Proceeding directly to repeat implantation may be indicated in some cases. Medical therapy with uroprophylactic antibiotics and serial VCUG may also be used, reserving surgical therapy for those in whom resolution fails to occur.

Complications of Reflux Nephropathy

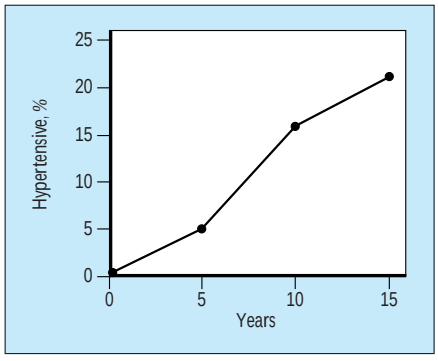

FIGURE 8-31

Development of hypertension in 55 normotensive subjects with reflux nephropathy at follow-up examinations over 15 years. The incidence of hypertension in persons with reflux nephropathy increases with age and appears to develop most commonly in young adults within 10 to 15 years of diagnosis. In a cohort of 55 normotensive persons with reflux nephropathy observed for 15 years, 5% became hypertensive after 5 years. This percentage increased to 16% at 10 years, and 21% at 15 years. The grading system for severity of scarring was different from the system adopted by the International Reflux Study Committee. Nevertheless, using this system, 78% of persons in the group could be classified as having reflux nephropathy severity scores between 1 and 4 [42].

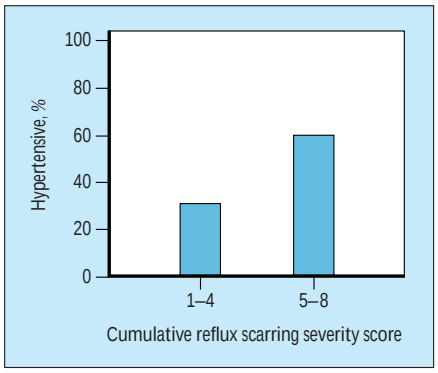

FIGURE 8-32

Frequency of hypertension versus severity of parenchymal scarring. The frequency of hypertension in persons with vesicoureteral reflux–related renal scars is higher than in the normal population. In adults with reflux nephropathy the incidence of hypertension can be correlated with the severity of renal scarring. Adding the individual grade of reflux (0–4) for the two kidneys results in a scale ranging from 0 (no scars) to 8 (severe bilateral scarring). Persons with cumulative scores of parenchymal scarring from 1 to 4 have a 30% incidence of hypertension, whereas 60% of those with scarring scores ranging from 5 to 8 have hypertension [42,43].

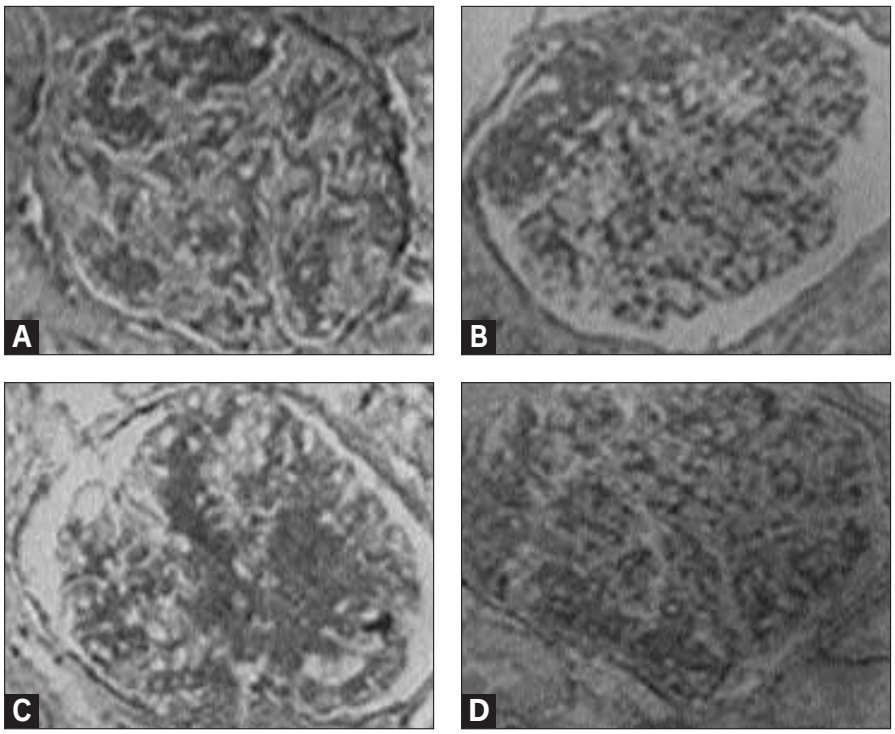

FIGURE 8-33

Glomerular hypertrophy and focal segmental glomerulosclerosis (FSGS) in severe reflux nephropathy. Reflux nephropathy resulting in reduced renal functional mass induces compensatory changes in glomerular and vascular hemodynamics. These changes initially maintain the glomerular filtration rate but are maladaptive over time. **A–D**, Compensatory hyperfiltration results in renal injury manifested histologically by glomerular hypertrophy and FSGS and clinically as persistent proteinuria [44]. In reflux nephropathy, proteinuria is a poor prognostic sign, indicating that renal injury has occurred. The severity of proteinuria is inversely proportional to functioning renal mass and the glomerular filtration rate and directly proportional to the degree of global glomerulosclerosis. Surgical correction of vesicoureteral reflux has not been found to prevent further deterioration of renal function after proteinuria has developed. Hyperfiltration resulting from decreased renal mass continues and produces progressive glomerulosclerosis and loss of renal function. Evidence exists that inhibition of the renin-angiotensin system through the use of angiotensin-converting enzyme inhibitors decreases the compensatory hemodynamic changes that produce hyperfiltration injury. Thus, these inhibitors may be effective in slowing the progress of renal failure in reflux nephropathy.

Pathogenesis of Obstructive Nephropathy

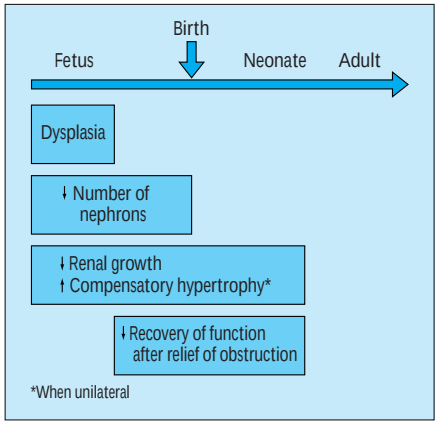

FIGURE 8-34

Consequences of urinary tract obstruction for the developing kidney in animals. The effects of urinary tract obstruction on the developing kidney depend on the time of onset, location, and degree of obstruction. Ureteral obstruction during early pregnancy results in disorganization of the renal parenchyma (dysplasia) and a reduction in the number of nephrons. Partial or complete ureteral obstruction in neonates causes vasoconstriction, glomerular hypoperfusion, impaired ipsilateral renal growth, and interstitial fibrosis. The degree of impairment of the ipsilateral kidney, in the case of partial unilateral ureteral obstruction, and of compensatory hypertrophy of the contralateral kidney, in the case of partial or complete unilateral ureteral obstruction, is inversely related to the age of the animal at the time of obstruction. The older the animal, the less the impairment of the ipsilateral kidney and the less the compensatory growth of the contralateral kidney. In addition, the recovery of renal function after relief of urinary tract obstruction also decreases with the age of the animal [45].

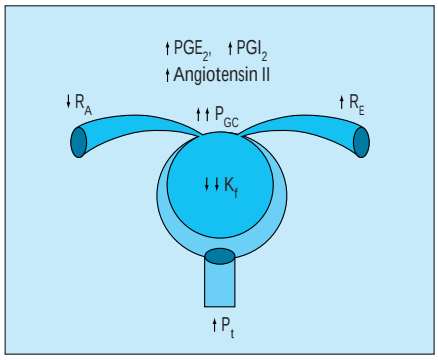

FIGURE 8-35

Renal hemodynamic response to mild partial ureteral obstruction. Renal blood flow and the glomerular filtration rate may not change in mild partial ureteral obstruction, despite a significant reduction in glomerular capillary ultrafiltration coefficient (Kf). This is due to the increase in glomerular capillary hydraulic pressure (P_{GC}) caused by a prostaglandin E2–induced reduction of afferent arteriolar resistance (R_A) and an angiotensin II–induced elevation of efferent arteriolar resistance (R_E). It is likely that other vasoactive factors, such as thromboxane A2, also play a role, particularly in more severe ureteral obstruction accompanied by reductions in renal blood flow and glomerular filtration rate [46]. PGE2—prostaglandin E2; PGI2—prostaglandin I2; Pt—tubule hydrostatic pressure.

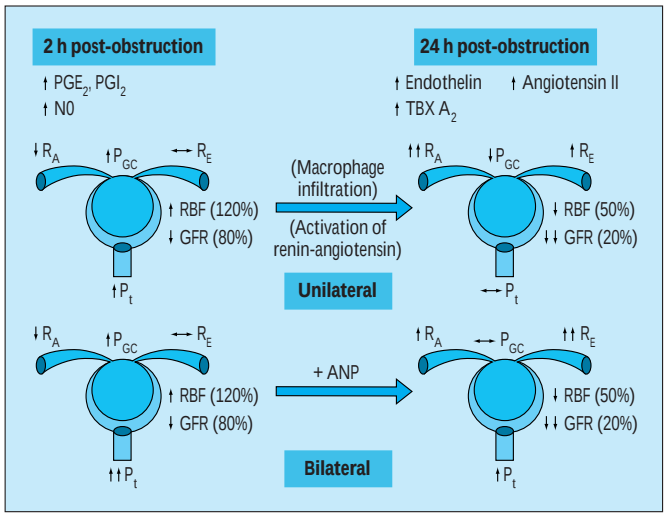

FIGURE 8-36

Acute renal hemodynamic response to unilateral or bilateral complete ureteral obstruction. In the first 2 hours after unilateral complete ureteral obstruction, there is a reduction in preglomerular vascular resistance and an increase in renal blood flow mediated by increased production of prostaglandin E2 (PGE2), prostacyclin, and nitric oxide (NO). The increase in renal blood flow (RBF) and glomerular capillary pressure maintain the glomerular filtration rate (GFR) at approximately 80% of normal, despite an increase in intratubular pressure. As the ureteral obstruction persists, activation of the renin-angiotensin system and increased production of thromboxane A2 (TBXA2) and endothelin result in progressive vasoconstriction, with reductions in renal blood flow and glomerular capillary pressure. The glomerular filtration rate decreases to approximately 20% of baseline, despite normalization of the intratubular pressures. The hemodynamic changes in the early phase (0–2 h) of bilateral ureteral obstruction are similar to those observed after unilateral obstruction. As bilateral obstruction persists, however, there is an accumulation of atrial natriuretic peptide (ANP) that does not occur after unilateral obstruction. The increased ANP levels attenuate the afferent and enhance the efferent vasoconstrictions, with maintenance of normal glomerular capillary and elevated tubular pressures. Despite these differences in hemodynamic changes between unilateral and bilateral ureteral obstruction, the reductions in renal blood flow and glomerular filtration rate 24 hours after obstruction are similar [47–49]. P_{GC}—glomerular capillary hydraulic pressure; PGI2—prostaglandin I2; Pt—tubule hydrostatic pressure; R_A—afferent arteriolar resistance; R_E—efferent arteriolar resistance.

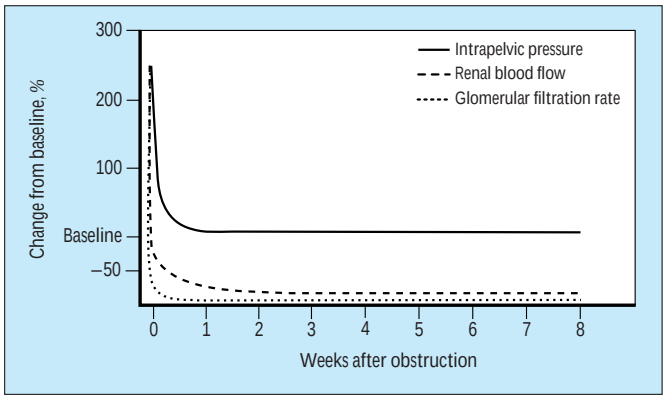

FIGURE 8-37

Chronic renal hemodynamic response to complete unilateral ureteral obstruction. During complete ureteral obstruction, renal blood flow progressively decreases. Renal blood flow is 40% to 50% of normal after 24 hours, 30% at 6 days, 20% at 2 weeks, and 12% at 8 weeks [48].

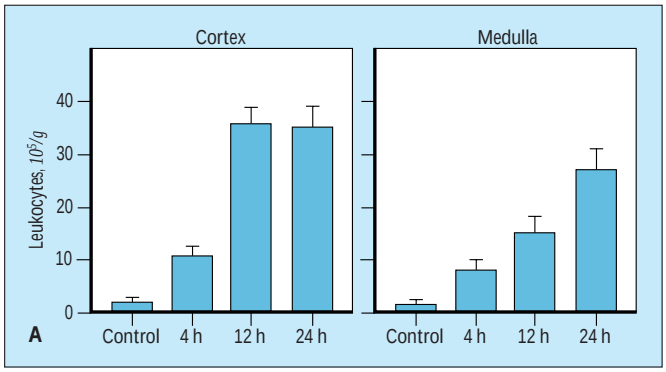

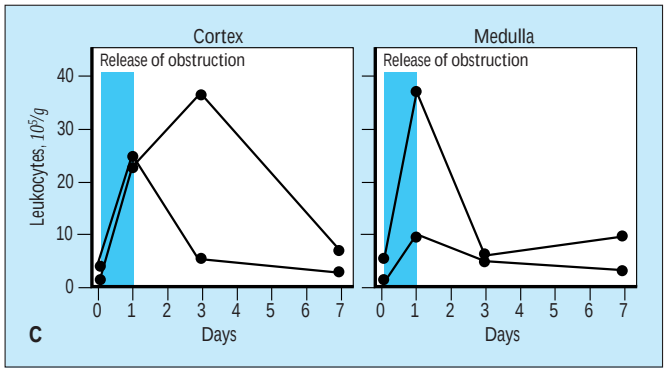

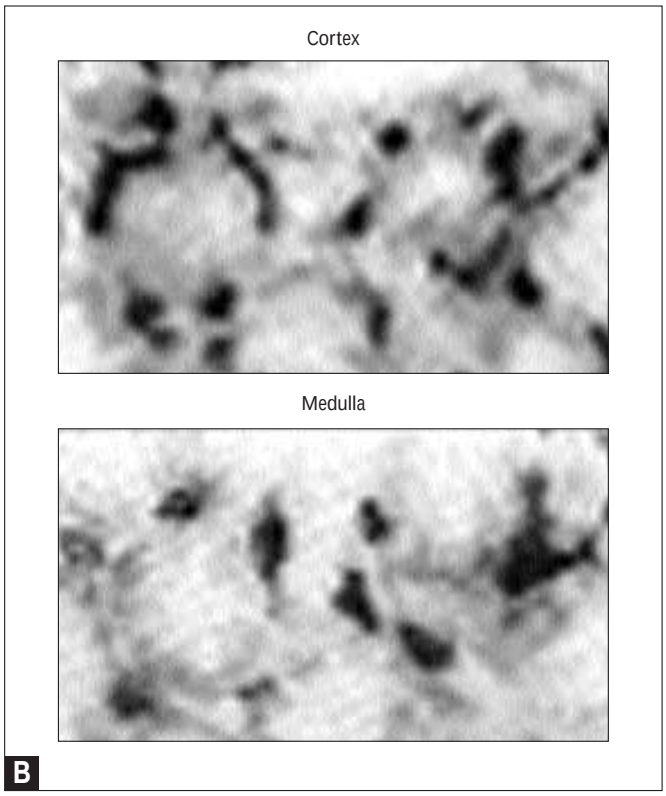

FIGURE 8-38

Development of interstitial cellular infiltrates in the renal cortex and medulla after ureteral obstruction. After ureteral obstruction there is a rapid influx of macrophages and suppressor T lymphocytes in the cortex and medulla (**A**) that is accompanied by an increase in urinary thromboxane B2 and a decrease in the glomerular filtration rate. The production of thromboxane A2 by the infiltrating macrophages (**B**) contributes to the renal vasoconstriction of chronic urinary tract obstruction. After release of the obstruction the cellular infiltration is slowly reversible, requiring several days to revert to near normal levels (**C**) [50,51].

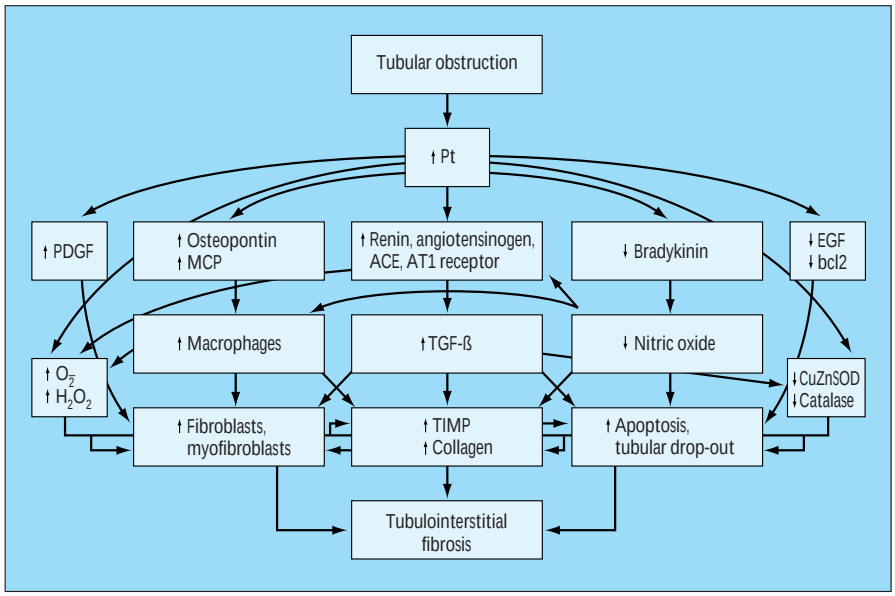

FIGURE 8-39

Pathogenesis of tubulointerstitial fibrosis in obstructive nephropathy. This pathogenesis has been extensively studied. Increased expression of renin, angiotensinogen, angiotensin-converting enzyme (ACE), and the angiotensin II type 1 (AT1) receptor occurs in the obstructed kidney. Angiotensin II can induce the synthesis of transforming growth factor β (TGF-β), a cytokine that stimulates extracellular matrix synthesis and inhibits its degradation. Obstructive nephropathy is accompanied by downregulation of the kallikrein-kinin system and nitric oxide production that can be reversed by administration of a converting enzyme inhibitor or of L-arginine. The rapid upregulation of chemotactic factors such as monocyte chemoattractant peptide 1 (MCP-1) and osteopontin in the tubular epithelial cells, in response to increased intratubular pressure, contributes to the recruitment of macrophages. Macrophages produce fibroblast growth factor and induce fibroblast proliferation and myofibroblast transformation. The downregulation of epidermal growth factor (EGF), Bcl 2, and antioxidant enzymes and the increased production of superoxide and hydrogen peroxide (H_2O_2) contribute to an increased rate of apoptosis and tubular dropout [51– 57]. PDGF–platelet-derived growth factor; SOD—superoxide dismutase; TIMP—tissue inhibitor of metalloproteinases.

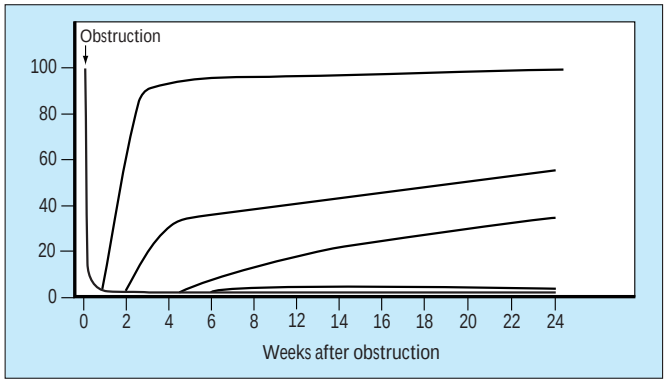

FIGURE 8-40

Recovery of renal function after relief of complete unilateral ureteral obstruction of variable duration. The recovery of the ipsilateral glomerular filtration rate after relief of a unilateral complete ureteral obstruction has been best studied in dogs and depends on the duration of the obstruction. Complete recovery occurs after 1 week of obstruction. The degree of recovery after 2 and 4 weeks of obstruction is only of 58% and 36%, respectively. No recovery occurs after 6 weeks of obstruction [58]. Rare reports of recovery of renal function in patients with longer periods of unilateral ureteral obstruction may represent high-grade partial obstruction rather than complete obstruction or may reflect differences in lymphatic drainage and renal anatomy between the human and canine kidneys [59].

Clinical Manifestations of Obstructive Nephropathy

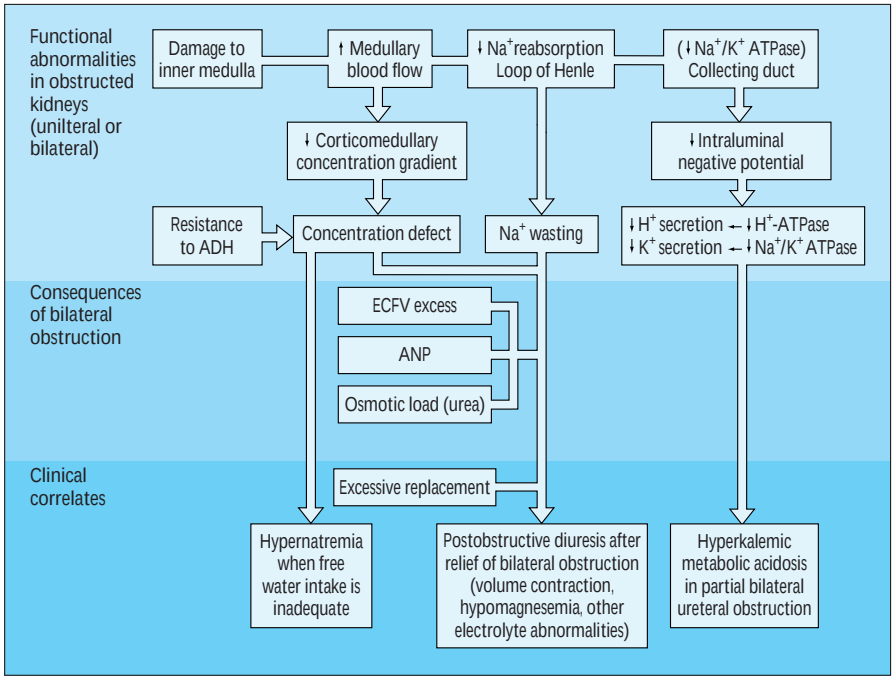

FIGURE 8-41

Clinical correlates of abnormalities of tubular function in obstructive nephropathy. Acute ureteral obstruction stimulates tubular reabsorption, resulting in increased urine osmolality and reduced urine sodium concentration [60]. In contrast, obstructive nephropathy is characterized by a reduced ability to concentrate the urine, reabsorb sodium, and secrete hydrogen ions (H^+) and potassium. In unilateral obstructive nephropathy, these functional abnormalities do not have a clinical correlate because of the reduced glomerular filtration rate and immaterial contribution of the obstructed kidney to total renal function. Hyperkalemic metabolic acidosis and, when the intake of free water is not adequate, hypernatremia can occur in patients with partial bilateral ureteral obstruction or partial ureteral obstruction in a solitary kidney. Similarly, postobstructive diuresis can occur only after relief of bilateral ureteral obstruction or ureteral obstruction in a solitary kidney but not after relief of unilateral obstruction [61–67]. ADH>\#209>antidiuretic hormone; ANP—atrial natriuretic peptide; ECFV—extracellular fluid volume; Na-K ATPase—sodium-potassium adenosine triphosphatase.

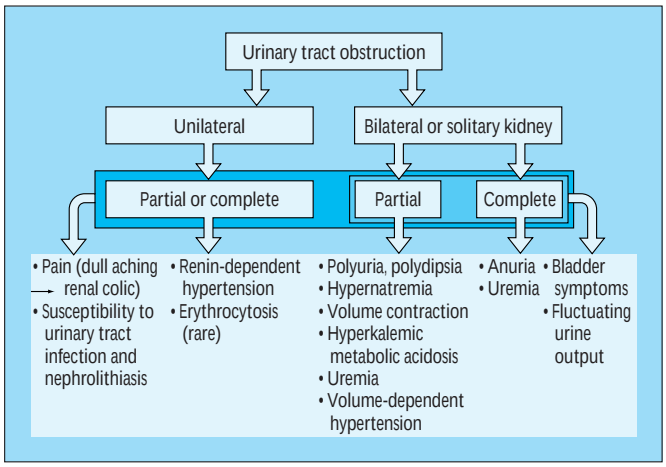

FIGURE 8-42

Clinical manifestations of obstructive nephropathy. These manifestations depend on the cause of the obstruction, its anatomic location, its severity, and its rate of development [61,68,69].

Diagnosis of Obstructive Nephropathy

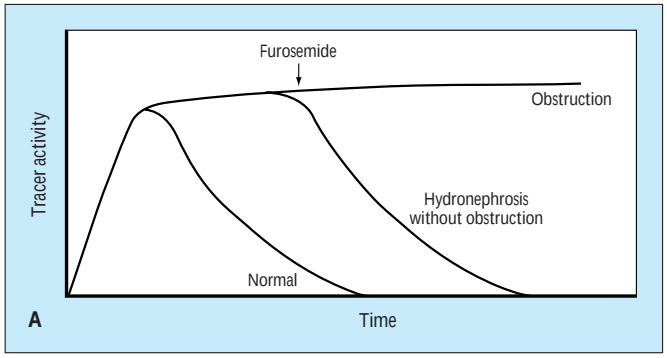

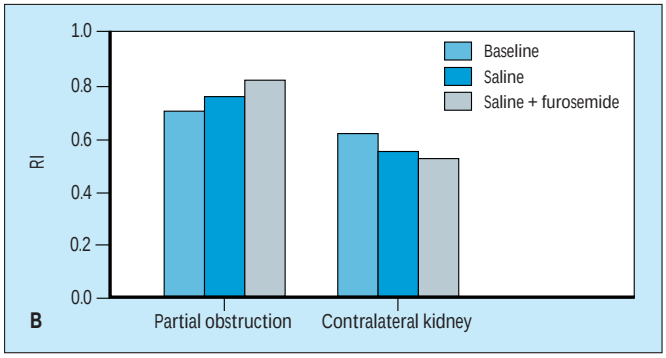

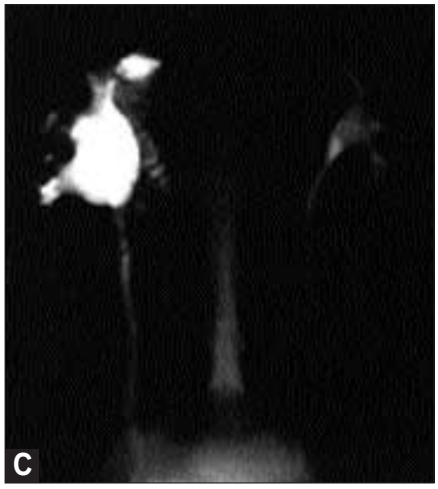

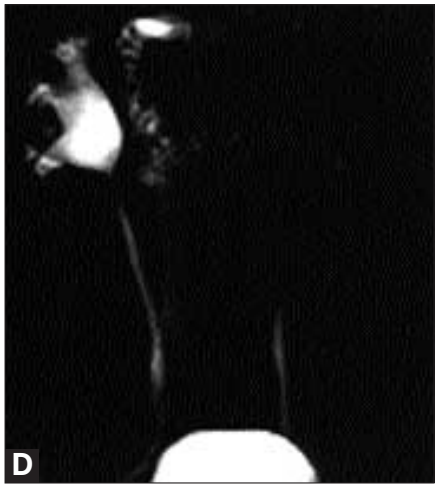

FIGURE 8-43

Diagnosis of obstructive nephropathy. **A**, Diuresis renography. **B**, Doppler ultrasonography. **C, D**, Magnetic resonance urogram utilizing a single shot fast spin echo technique with anterior-posterior projection (**C**) and left posterior oblique projection (**D**). Images demonstrate a widely patent right ureteropelvic junction in a patient with abdominal pain and suspected ureteropelvic junction obstruction. Administration of gadolinium is not required for this technique. Note also the urine in the bladder, cerebrospinal fluid in the spinal canal, and fluid in the small bowel.

Ultrasonography is the procedure of choice to determine the presence or absence of a dilated renal pelvis or calices and to assess the degree of associated parenchymal atrophy. Nevertheless, obstruction rarely can occur without hydronephrosis, when the ureter and renal pelvis are encased in a fibrotic process and unable to expand. In contrast, mild dilation of the collecting system of no functional significance is not unusual. Even obvious hydronephrosis in some cases may not be associated with functional obstruction [70]. Diuresis renography is helpful when the functional significance of the dilation of the collecting system is in question [71,72]. Renal Doppler ultrasonography before and after administration of normal saline and furosemide also has been used to differentiate obstructive from nonobstructive pyelocaliectasis [73]. Other techniques such as excretory urography, computed tomography, and retrograde or antegrade ureteropyelography are helpful to determine the cause of the urinary tract obstruction. The utility of excretory urography is limited in patients with advanced renal insufficiency. In these cases magnetic resonance urography can provide coronal imaging of the renal collecting systems and ureters similar to that of conventional urography without the use of iodinated contrast. RI— resistive index. (**C, D**, Courtesy of B. F. King, MD.)

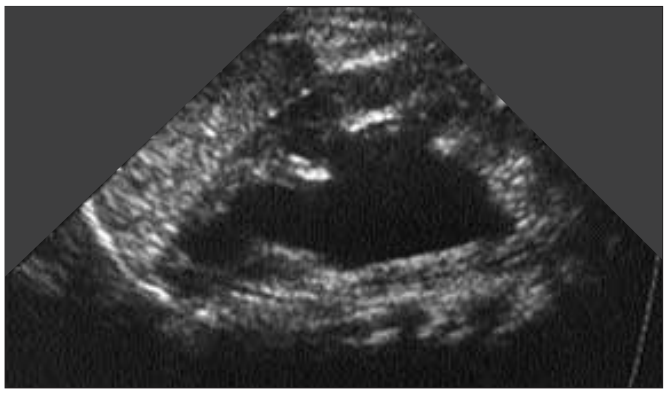

FIGURE 8-44

Diagnosis of obstructive nephropathy by postnatal renal ultrasonography, showing hydronephrosis in ureteropelvic junction obstruction. Renal ultrasonography is a sensitive test to detect hydronephrosis. The absence of ureteral dilation is consistent with obstruction at the level of the ureteropelvic junction.

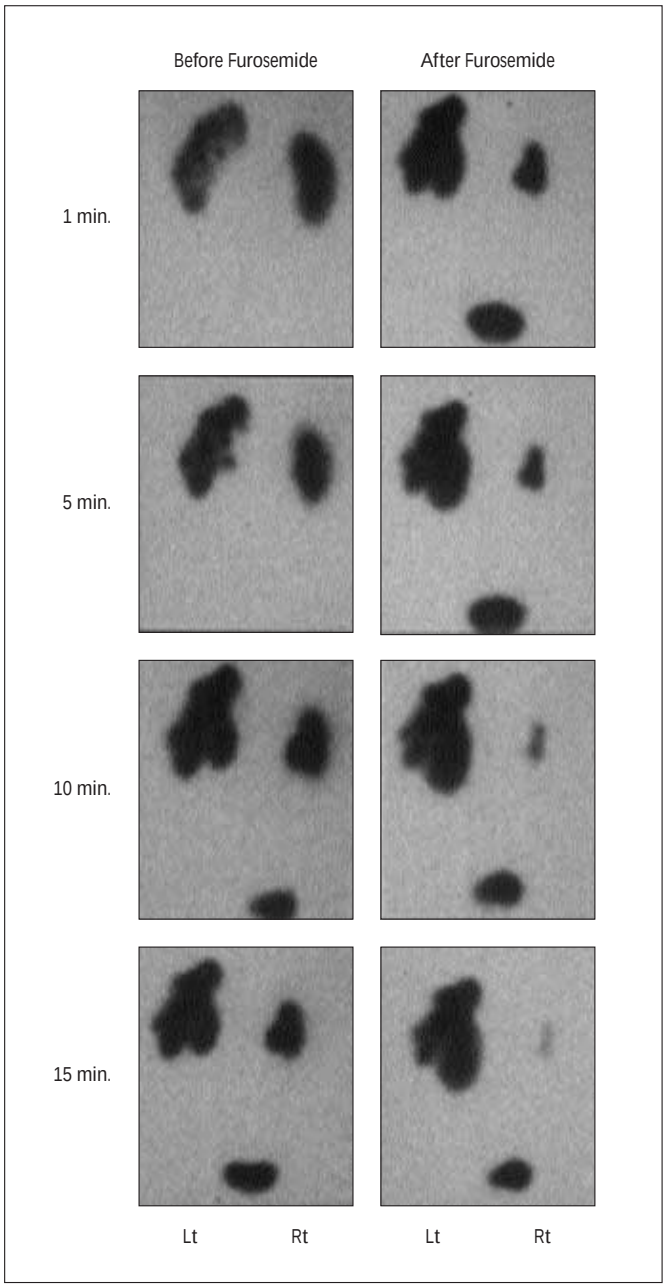

FIGURE 8-45

Mercaptoacetyltriglycine-3 renal scan with furosemide in a newborn with left ureteropelvic junction obstruction. A diuretic renal scan using ^{99m}technetium-mercaptoacetyltriglycine (^{99m}Tc-MAG-3) showing differential renal function (47% right kidney; 53% left kidney) at 1 to 2 minutes after radionuclide administration is seen. A significant amount of radionuclide remains in each kidney 15 minutes after administration. After administration of furosemide, however, the isotope is seen to disappear rapidly from the right kidney (t1/2 of radioisotope washout in 4.9 minutes) but persists in the hydronephrotic left kidney (t1/2 in 50.1 minutes). A t1/2 of the radioisotope in less than 10 minutes is thought to reflect a lack of significant obstruction. A t1/2 of over 20 minutes is suggestive of obstruction. Intermediate values of washout are indeterminate. The most appropriate therapy for infants with delayed renal pelvic radioisotope washout and diagnosis of ureteropelvic junction obstruction is controversial. Some authors advocate pyeloplasty to alleviate the obstruction based on renal scan results, whereas others advocate withholding surgery unless renal function deteriorates or hydronephrosis progresses.

Posterior Urethral Valves

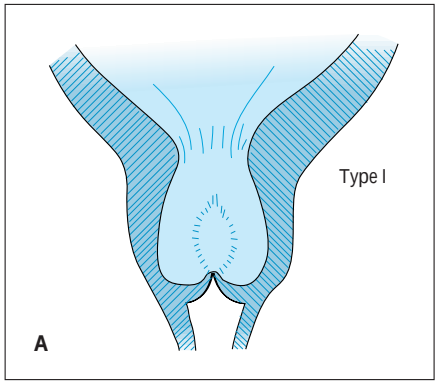

FIGURE 8-46

Posterior urethral valves. **A**, Illustrative diagram. **B**, Pathology specimen. Valvular obstruction at the posterior urethra is the most common cause of lower urinary tract obstruction in boys. Anatomically, the lesion most commonly is comprised of an oblique diaphragm with a slitlike perforation arising from the posterior urethra distal to the verumontanum and inserting at the midline anterior urethra. (*From* Kaplan and Scherz [74]; with permission.)

FIGURE 8-47

Excretory urogram of a patient with posterior urethral valves. Bladder outlet obstruction results in bladder wall thickening, trabeculation, and formation of diverticula. Increased intravesical pressure may result in vesicoureteral reflux, as is seen on the left. Obstruction resulting in increased intrarenal pressure may result in rupture at the level of a renal fornix, producing a urinoma, or perirenal collection of urine, as seen on the right.

FIGURE 8-48

Voiding cystourethrogram (VCUG) demonstrating posterior urethral valves and dilation of the posterior urethra. Urethral valves are best detected by VCUG. The obstructing valves are seen as oblique or perpendicular folds with proximal urethral dilation and elongation. Distal to the valves the urinary stream is diminished. Alleviating the bladder outlet obstruction is indicated, either by lysis of the valves themselves or by way of vesicostomy, in small infants until sufficient growth occurs to make valve resection technically feasible.

Ureterovesical Junction Obstruction

FIGURE 8-49
Excretory urogram showing ureterovesical junction obstruction in a 2-year-old girl.

Retroperitoneal Fibrosis

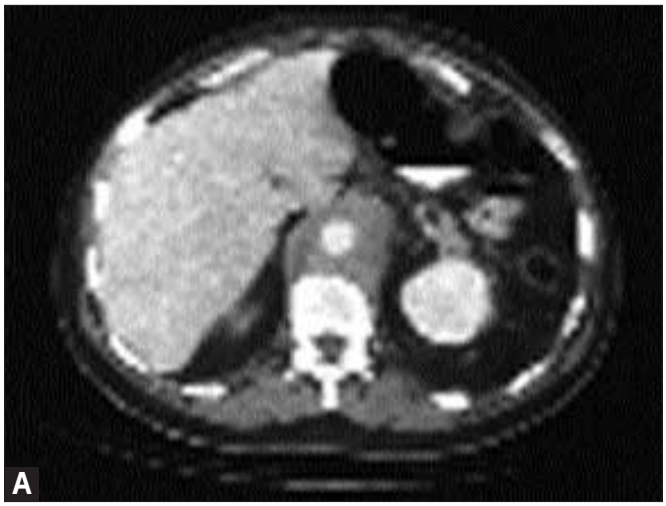

FIGURE 8-50
A–H, Idiopathic retroperitoneal fibrosis: computed tomography scans of the abdomen before (left panels, note right ureteral stent and mild left ureteropyelocaliectasis) and 7 years after ureterolysis (right panels, note omental interposition). Retroperitoneal fibrosis is characterized by the accumulation of inflammatory and fibrotic tissue around the aorta, between the renal hila and the pelvic brim. Most cases are idiopathic; the remainder are associated with immune-mediated connective tissue diseases, ingestion of drugs such as methysergide, abdominal aortic aneurysms, or malignancy. Idiopathic retroperitoneal fibrosis can be associated with mediastinal fibrosis, sclerosing cholangitis, Riedel's thyroiditis, and fibrous pseudotumor of the orbit. In the clinical setting, patients with idiopathic retroperitoneal fibrosis exhibit systemic symptoms such as malaise, anorexia and weight loss, and abdominal or flank pain. Renal insufficiency is often seen and is caused by bilateral ureteral obstruction. Laboratory test results usually demonstrate anemia and an elevated sedimentation rate. The treatment is directed to the release of the ureteral obstruction, which initially can be achieved by placement of ureteral stents. Administration of corticosteroids is helpful to control the systemic manifestations of the disease and

(Continued on next page)

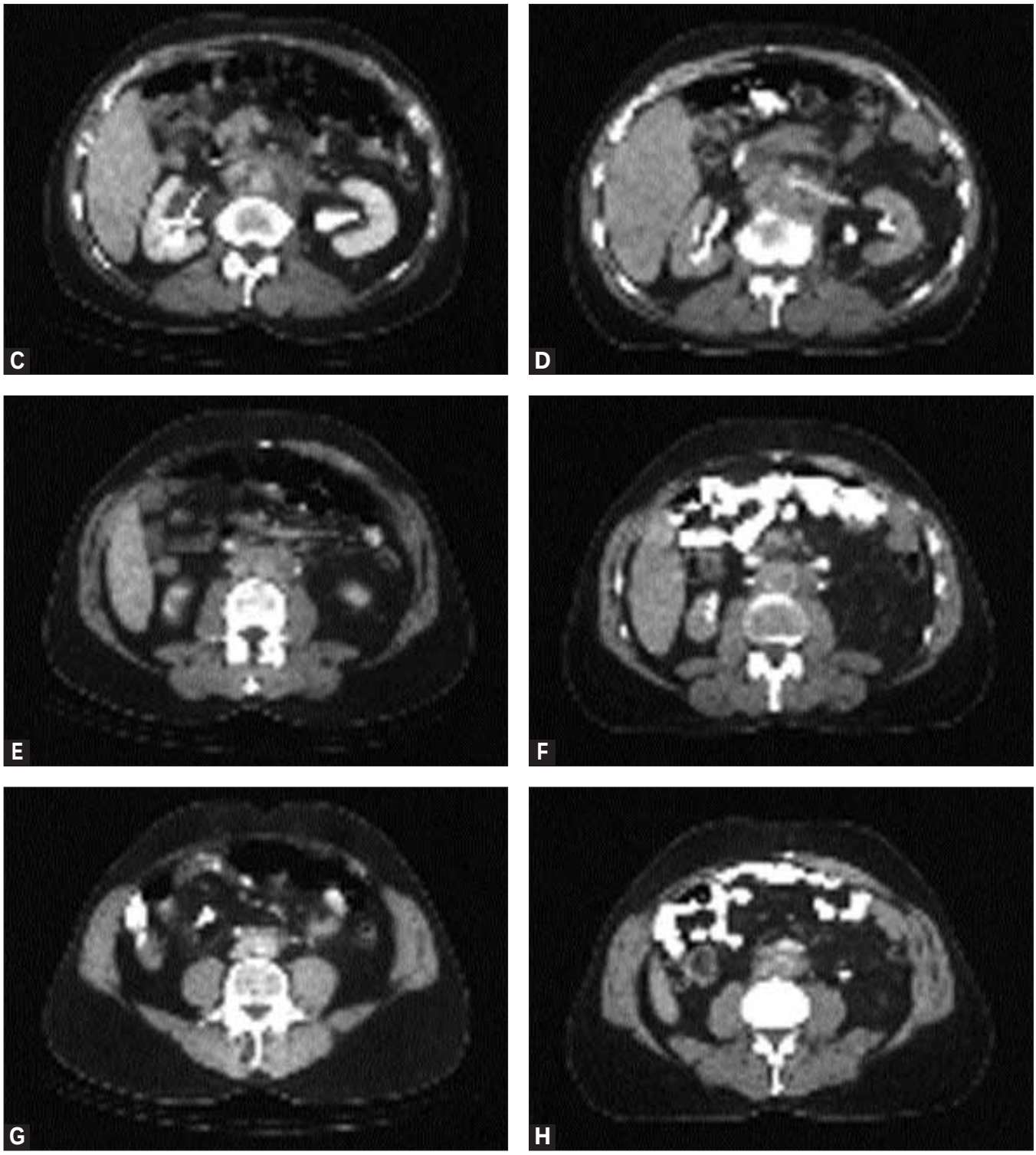

FIGURE 8-50 *(Continued)*

often to reduce the bulk of the tumor and relieve the ureteral obstruction. Administration of corticosteroids, however, should be considered only when malignancy and retroperitoneal infection can be ruled out. As in other chronic renal diseases, administration of corticosteroids should be kept at the minimal level capable of controlling symptoms. Surgical ureterolysis, which consists of freeing the ureters from the fibrotic mass, lateralizing them, and wrapping them in omentum to prevent repeat obstruction, is often necessary. Other immunosuppressive agents have been used rarely when the systemic manifestations of the disease cannot be controlled with safe doses of corticosteroids. In most cases the long-term outcome of idiopathic retroperitoneal fibrosis is satisfactory [75–77].

References

1. Roshani H, Dabhoiwala NF, Verbeek FJ, Lamers WH: Functional anatomy of the human ureterovesical junction. *Anat Rec* 1996, 245:645–651.
2. Noordzij JW, Dabhoiwala NF: A view on the anatomy of the ureterovesical junction. *Scand J Urol Nephrol* 1993, 27:371–380.
3. Thomson AS, Dabhoiwala NF, Verbeek FJ, Lamers WH: The functional anatomy of the ureterovesical junction. *Br J Urol* 1994, 73:284–291.
4. Politano VA: Vesico-ureteral reflux. In *Urologic Surgery*, edn 2. Edited by Glenn JF. New York: Harper and Row Publishers, 1975:272–293.
5. Paquin AJ: Ureterovesical junction: the description and evaluation of a technique. *J Urol* 1959, 82:573.
6. Stephens FD, Lenaghan D: The anatomical basis and dynamics of vesicoureteral reflux. *J Urol* 1962, 87:669.
7. Kramer, SA: Vesicoureteral reflux. In *Clinical Pediatric Urology*, edn 3. Edited by Kelalis PP, King LR, Belman AB. Philadelphia: WB Saunders Company, 1992:441–499.
8. Ransley PG, Risdon RA: Renal papillary morphology in infants and young children. *Urol Res* 1975, 3:111–113.
9. Ransley PG, Risdon RA: Renal papillary morphology and intrarenal reflux in the young pig. *Urol Res* 1975, 3:105–109.
10. Funston MR, Cremin BJ: Intrarenal reflux-papillary morphology and pressure relationships in children's necropsy kidneys. *Br J Radiol* 1978, 51:665–670.
11. Ransley PG, Risdon RA: Reflux nephropathy: effects of antimicrobial therapy on the evolution of the early pyelonephritic scar. *Kidney Int* 1981, 20:733–742.
12. Torres VE, Kramer SA, Holley KE, *et al.*: Effect of bacterial immunization on experimental reflux nephropathy. *J Urol* 1984, 131:772.
13. Torres VE, Kramer SA, Holley KE, *et al.*: Interaction of multiple risk factors in the pathogenesis of experimental reflux nephropathy in the pig. *J Urol* 1985, 133:131–135.
14. Goldraich NP, Goldraich IH, Anselmi OE, Ramos OL: Reflux nephropathy: the clinical picture in South Brazilian children. *Control Nephrol* 1984, 39:52–67.
15. Scherz HC, Downs TM, Caeser R: The selective use of dimercaptosuccinic acid renal scans in children with vesicoureteral reflux. *J Urol* 1994, 152:628–631.
16. Kramer SA: Experimental vesicoureteral reflux. *Dialogues Pediatr Urol* 1984, 7:1.
17. Hinchliffe SA, Chan Y, Jones H, *et al.*: Renal hypoplasia and postnatally acquired cortical loss in children with vesicoureteral reflux. *Pediatr Nephrol*1992, 6:439–444.
18. Lebowitz RL, Olbing H, Parkkulainen K, *et al.*: International system of radiographic grading of vesicoureteral reflux. *Pediatr Radiol* 1985, 15:105.
19. Smellie JM, Edwards D, Hunter N, *et al.*: Vesico-ureteric reflux and renal scarring. *Kidney Int* 1975, 8:s65–s72.
20. Arant BS: Medical management of mild and moderate vesicoureteral reflux: followup studies of infants and young children. A preliminary report of the Southwest Pediatric Nephrology Study Group. *J Urol* 1992, 148:1683–1687.
21. Steele BT, Robitaille P, DeMaria J, Grignon A: Follow-up evaluation of prenatally recognized vesicoureteric reflux. *J Pediatr* 1989, 115:95–96.
22. Najmaldin A, Burge DM, Atwell JD: Reflux nephropathy secondary to intrauterine vesicoureteric reflux. *J Pediatr Surg* 1990, 25:387–390.
23. Marra G, Barbieri G, Dell'Agnola CA, *et al.*: Congenital renal damage associated with primary vesicoureteral reflux detected prenatally in male infants. *J Pediatr* 1994, 124:726–730.
24. Anderson PAM, Rickwood AMK: Features of primary vesicoureteric reflux detected by prenatal sonography. *Br J Urol* 1991, 67:267–271.
25. Stocks A, Richards D, Frentzen B, Richard G: Correlation of prenatal renal pelvic anteroposterior diameter with outcome in pregnancy. *J Urol* 1996, 155:1050–1052.
26. Adra AM, Mejides AA, Dennaoui MS, *et al.*: Fetal pyelectasis: Is it always "physiological"? [abstract]. *Am J Obstet Gynecol* 1995, 172:359.
27. Morin L, Cendron M, Garmel SH, *et al.*: Minimal fetal hydronephrosis: natural history and implications for treatment. *Am J Obstet Gynecol* 1995, 172:354.
28. Zerin JM, Ritchey MJ, Chang ACH: Incidental vesicoureteral reflux in neonates with antenatally detected hydronephrosis and other abnormalities. *Radiology* 1993, 187:157–160.
29. Peters PC, Johnson DE, Jackson JHJ: The incidence of vesicoureteral reflux in the premature child. *J Urol* 1967, 97:259–260.
30. Lich R Jr, Howerton LW Jr, Goode LS, Davis LA: The ureterovesical junction of the newborn. *J Urol* 1964, 92:436–438.
31. Marra G, Barbieri G, Moioli C, *et al.*: Mild fetal hydronephrosis indicating vesicoureteric reflux. *Arch Dis Child* 1994, 70:F147–150.
32. Wallin L, Bajc M: The significance of vesicoureteric reflux on kidney development assessed by dimercaptosuccinate renal scintigraphy. *Br J Urol* 1994, 73:607–611.
33. Elder JS: Commentary: importance of antenatal diagnosis of vesicoureteral reflux. *J Urol* 1992, 148:1750–1754.
34. Crabbe DCG, Thomas DFM, Gordon AC, *et al.*: Use of ^{99m}technetium-dimercaptosuccinic acid to study patterns of renal damage associated with prenatally detected vesicoureteral reflux. *J Urol* 1992, 148:1229–1231.
35. Sheridan M, Jewkes F, Gough DCS: Reflux nephropathy in the first year of life: role of infection. *Pediatr Surg Int* 1991, 6:214–216.
36. Weiss R, Tamminen-Mobius T, Koskimies O, *et al.*: Characteristics at entry of children with severe primary vesicoureteral reflux recruited for a multicenter international therapeutic trial comparing medical and surgical management. *J Urol* 1992, 148:1644–1649.
37. Taylor CM, White RHR: Prospective trial of operative vs. non-operative treatment of severe vesicoureteric reflux in children: five years' observation. *Br Med J* 1987, 295:237–241.
38. Tamminen-Mobius T, Brunier E, Ebel K-D, *et al.*: Cessation of vesicoureteral reflux for 5 years in infants and children allocated to medical treatment. *J Urol* 1992, 148:1662–1666.
39. Astley R, Clark RC, Corkery JJ, *et al.*: Prospective trial of operative vs. non-operative treatment of severe vesicoureteric reflux: two years' observation in 96 children. *Br Med J* 1983, 287:171–174.
40. Olbing H, Claesson I, Ebel K-D, *et al.*: Renal scars and parenchymal thinning in children with vesicoureteral reflux: a 5-year report of the International Reflux Study in Children (European branch). *J Urol* 1992, 148:1653–1656.
41. Jodal U, Koskimies O, Hanson E, *et al.*: Infection pattern in children with vesicoureteral reflux randomly allocated to operation or long-term antibacterial prophylaxis. *J Urol* 1992, 148:1650–1652.
42. Goonasekera CDA, Shah V, Wade A, *et al.*: 15-year follow-up of renin and blood pressure in reflux nephropathy. *Lancet* 1996, 347:640–643.
43. Torres V, Malek RS, Svensson JP: Vesicoureteral reflux in the adult: nephropathy, hypertension, and stones. *J Urol* 1983, 130:41–44.
44. Torres V, Velosa J, Holley KE, *et al.*: The progression of vesicoureteral reflux nephropathy. *Ann Intern Med* 1980, 92:776–784.
45. Chevalier RL: Effects of ureteral obstruction on renal growth. *Semin Nephrol* 1995, 15:353–360.

46. Ichikawa I, Brenner BM: Local intrarenal vasoconstrictor-vasodilator interactions in mild partial ureteral obstruction. *Am J Physiol* 1979, 236:F131–140.
47. Dal Canton A: Effects of 24-hour unilateral ureteral obstruction on glomerular hemodynamics in rat kidney. *Kidney Int* 1979, 15:457.
48. Klahr S: Pathophysiology of obstructive nephropathy: a 1991 update. *Semin Nephrol* 1991, 11:156.
49. Marin-Grez M, Fleming JT: Atrial natriuretic peptide causes preglomerular vasodilatation and post-glomerular vasoconstriction in rat kidney. *Nature* 1986, 324:473.
50. Schreiner GF, Harris KPG, Purkerson ML, Klahr S: Immunological aspects of acute ureteral obstruction: immune cell infiltrate in the kidney. *Kidney Int* 1988, 34:487–493.
51. Diamond JR: Macrophages and progressive renal disease in experimental hydronephrosis. *Am J Kidney Dis* 1995, 26:133–140.
52. Chevalier RL: Growth factors and apoptosis in neonatal ureteral obstruction. *J Am Soc Nephrol* 1996, 7:1098–1105.
53. Ishidoya S, Morrisey J, McCracken R, Klahr S: Delayed treatment with enalapril halts tubulointerstitial fibrosis in rats with obstructive uropathy. *Kidney Int* 1996, 49:1110–1119.
54. Morrisey J, Ishidoya S, McCracken R, Klahr S: Nitric oxide generation ameliorates the tubulointerstitial fibrosis of obstructive nephropathy. *J Am Soc Nephrol* 1996, 7:2202–2212.
55. Ricardo SD, Ding G, Eufemio M, Diamond JR: Antioxidant expression in experimental hydronephrosis: role of mechanical stretch and growth factors. *Am J Physiol* 1997, 272:F789–F798.
56. Wright EJ, McCaffrey TA, Robertson AP, *et al.*: Chronic unilateral ureteral obstruction is associated with interstitial fibrosis and tubular expression of transforming growth factor-beta.*Lab Invest* 1996, 74:528–537.
57. Yanagisawa H: Dietary protein restriction normalized eicosanoid production in isolated glomeruli from rats with bilateral ureteral obstruction.*Kidney Int* 1994, 46:245.
58. Vaughn EDJ, Gillenwater JY: Recovery following complete chronic unilateral ureteral occlusion: functional, radiographic and pathologic alterations. *J Urol* 1971, 106:27–35.
59. Shapiro SR: Recovery of renal function after prolonged unilateral ureteral obstruction. *J Urol* 1976, 115:136–40.
60. Miller TR: Urinary diagnostic studies in acute renal failure: a prospective study. *Ann Intern Med* 1978, 89:47.
61. Batlle DC, Arruda JAL, Kurtzman NA: Hyperkalemic distal renal tubular acidosis associated with obstructive uropathy. *N Engl J Med* 1981, 304:373.
62. Campbell HT, Bello-Reuss E, Klahr S: Hydraulic water permeability and transepithelial voltage in the isolated perfused rabbit cortical collecting tubule following acute unilateral ureteral obstruction. *J Clin Invest* 1985, 75:219.
63. Hanley MJ, Davidson K: Isolated nephron segments from rabbit models of obstructive uropathy. *J Clin Invest* 1982, 69:165.
64. Hwang S: Transport defects of rabbit inner medullary collecting duct cells in obstructive uropathy. *Am J Physiol* 1993, 264:F808.
65. Hwang S: Transport defects of rabbit medullary thick ascending limb cells in obstructive uropathy. *J Clin Invest* 1993, 91:21.
66. Kimura H, Mujais SK: Cortical collecting duct Na-K pump in obstructive uropathy. *Am J Physiol* 1990, 258:F1320.
67. Muto S, Asano Y: Electrical properties of the rabbit cortical collecting duct from obstructed kidneys after unilateral ureteral obstruction. *J Clin Invest* 1994, 94:1846.
68. Davis BB, Preuss HG, Murdaugh HVJ: Hypomagnesemia following the diuresis of post-renal obstruction and renal transplant. *Nephron* 1975, 14:275.
69. Landsberg L: Hypernatremia complicating partial urinary tract obstruction. *N Engl J Med* 1970, 283:746.
70. Whitherow RO, Whitaker RH: The predictive accuracy of antegrade pressure flow studies in equivocal upper tract obstruction. *Br J Urol* 1981, 53:496.
71. Koff SA, Thrall JN, Keyes JW: Diuretic radionuclide urography. A noninvasive method for evaluating nephroureteral dilatation. *J Urol* 1979, 122:451.
72. Whitfield HN: Furosemide intravenous urography in the diagnosis of pelviureteric junction obstruction. *Br J Urol* 1979, 51:445.
73. Shokeir AA, Nijman RJM, El-Azab M, Provoost AP: Partial ureteral obstruction: effect of intravenous normal saline and furosemide on the resistive index. *J Urol* 1997, 157:1074–1077.
74. Kaplan GW, Scherz HC: Infravesicle obstruction. In *Clinical Pediatric Urology*, edn 3. Edited by Kelalis PP, King LR, Belman AB. Philadelphia: WB Saunders Company; 1992:821–864.
75. Gilkeson GS, Allen NB: Retroperitoneal fibrosis: a true connective tissue disease. *Rheum Dis North Am* 1996, 22:23–38.
76. Kottra JJ, Dunnick NR: Retroperitoneal fibrosis. *Radiol Clin North Am* 1996, 34:1259–1275.
77. Massachusetts General Hospital: Case records–case 27–1996: *N Engl J Med* 1996, 335:650–655.

Cystic Diseases of the Kidney

Yves Pirson
Dominique Chauveau

A kidney cyst is a fluid-filled sac arising from a dilatation in any part of the nephron or collecting duct. A sizable fraction of all kidney diseases—perhaps 10% to 15%—are characterized by cysts that are detectable by various imaging techniques. In some, cysts are the prominent abnormality; thus, the descriptor *cystic* (or *polycystic*). In others, kidney cysts are an accessory finding, or are only sometimes present, so that some question whether they are properly classified as cystic diseases of the kidney. In fact, the commonly accepted complement of cystic kidney diseases encompasses a large variety of disorders of different types, presentations, and courses. Dividing cystic disorders into genetic and "nongenetic" conditions makes sense, not only conceptually but clinically: in the former cystic involvement of the kidney often leads to renal failure and is most often associated with extrarenal manifestations of the inherited defect, whereas in the latter cysts rarely jeopardize renal function and generally are not part of a systemic disease.

In the first section of this chapter we deal with nongenetic (*ie*, acquired and developmental) cystic disorders, emphasizing the imaging characteristics that enable correct identification of each entity. Some common pitfalls are described. A large part of the section on genetic disorders is devoted to the most common ones (*eg*, autosomal-dominant polycystic kidney disease), focusing on genetics, clinical manifestations, and diagnostic tools. Even in the era of molecular genetics, the diagnosis of the less common inherited cystic nephropathies relies on proper recognition of their specific renal and extrarenal manifestations. Most of these features are illustrated in this chapter.

CHAPTER 9

General Features

PRINCIPAL CYSTIC DISEASES OF THE KIDNEY

Nongenetic	Genetic
Acquired disorders	Autosomal-dominant
Simple renal cysts (solitary or multiple)	**Autosomal-dominant polycystic kidney disease**
Cysts of the renal sinus (or peripelvic lymphangiectasis)	**Tuberous sclerosis complex**
Acquired cystic kidney disease (in patients with chronic renal impairment)	**von Hippel-Lindau disease**
Multilocular cyst (or multilocular cystic nephroma)	Medullary cystic disease
Hypokalemia-related cysts	Glomerulocystic kidney disease
Developmental disorders	Autosomal-recessive
Medullary sponge kidney	**Autosomal-recessive polycystic kidney disease**
Multicystic dysplastic kidney	**Nephronophthisis**
Pyelocalyceal cysts	X-linked
	Orofaciodigital syndrome, type I

FIGURE 9-1

Principal cystic diseases of the kidney. Classification of the renal cystic disorders, with the most common ones printed in **bold type**. (*Adapted from* Fick and Gabow [1]; Welling and Grantham [2]; Pirson, *et al.* [3].)

IMAGING CHARACTERISTICS OF THE MOST COMMON RENAL CYSTIC DISEASES

Disease	Kidney Size	Cyst Size	Cyst Location	Liver
Simple renal cysts	Normal	Variable (mm–10 cm)	All	Normal
Acquired renal cystic disease	Most often small, sometimes large	0.5–2 cm	All	Normal
Medullary sponge kidney	Normal or slightly enlarged	mm	Precalyceal	Normal (most often)
ADPKD	Enlarged	Variable (mm–10 cm)	All	Cysts (most often)
ARPKD	Enlarged	mm increase with age	All	CHF
NPH	Small	mm–2 cm (when present)	Medullary	Normal

FIGURE 9-2

Characteristics of the most common renal cystic diseases detectable by imaging techniques (ultrasonography, computed tomography, magnetic resonance). In the context of family history and clinical findings, these allow the clinician to establish a definitive diagnosis in the vast majority of patients. ADPKD—autosomal-dominant polycystic kidney disease; ARPKD—autosomal-recessive polycystic kidney disease; CHF—congenital hepatic fibrosis; NPH—nephronophthisis.

Nongenetic Disorders

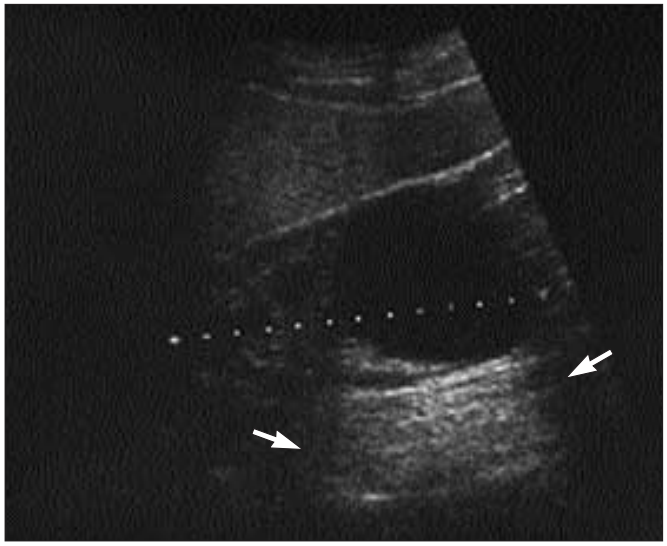

FIGURE 9-3

Solitary simple cyst. Large solitary cyst found incidentally at ultrasonography (longitudinal scan) in the lower pole of the right kidney. Criteria for the diagnosis of simple cyst include absence of internal echoes, rounded outline, sharply demarcated, smooth walls, bright posterior wall echo (*arrows*). The latter occur because less sound is absorbed during passage through cyst than through the adjacent parenchyma. If these criteria are not satisfied, computed tomography can rule out complications and other diagnoses.

PREVALENCE OF SIMPLE RENAL CYSTS DETECTED BY ULTRASONOGRAPHY

	Prevalence, %							
	≥1 Cyst		≥2 Cysts*		≥3 Cysts*		≥1 Cyst in Each Kidney	
Age group, y	M	F	M	F	M	F	M	F
15–29	0	0	0	0	0	0	0	0
30–49	2	1	0	1	0	1	0	1
50–69	15	7	2	1	1	1	2	1
≥70	32	15	17	8	6	3	9	3

*Unilateral or bilateral. M—male; F—Female.

FIGURE 9-4

Prevalence of simple renal cysts detected by ultrasonography according to age in an Australian population of 729 persons prospectively screened by ultrasonography. The prevalence increases with age and is higher in males. Cyst size also increases with age. Most simple cysts are located in the cortex. (*From* Ravine *et al.* [4]; with permission.)

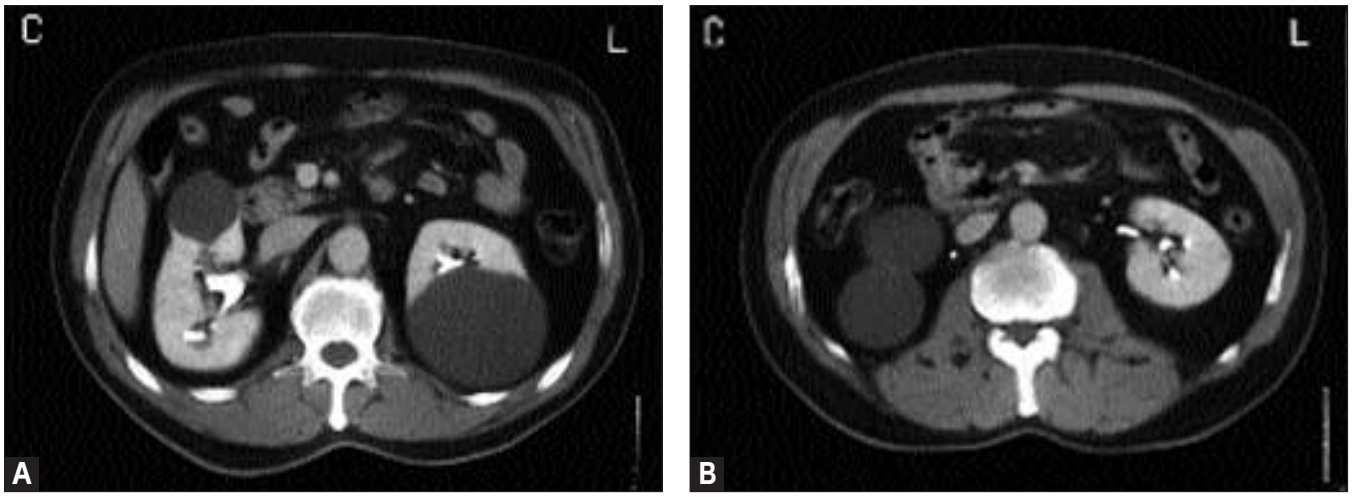

FIGURE 9-5

A and **B**, Multiple simple cysts (one 7 cm in diameter in the lower pole of the left kidney and three 4 to 5 cm in diameter in the right kidney) detected by contrast-enhanced computed tomography (CT). Additional millimetric cysts might be suspected in both kidneys. Each cyst exhibits the typical features of an uncomplicated simple cyst on CT: 1) homogeneous low density, unchanged by contrast medium; 2) rounded outline; 3) very thin (most often indetectable) wall; 4) distinct delineation from adjacent parenchyma.

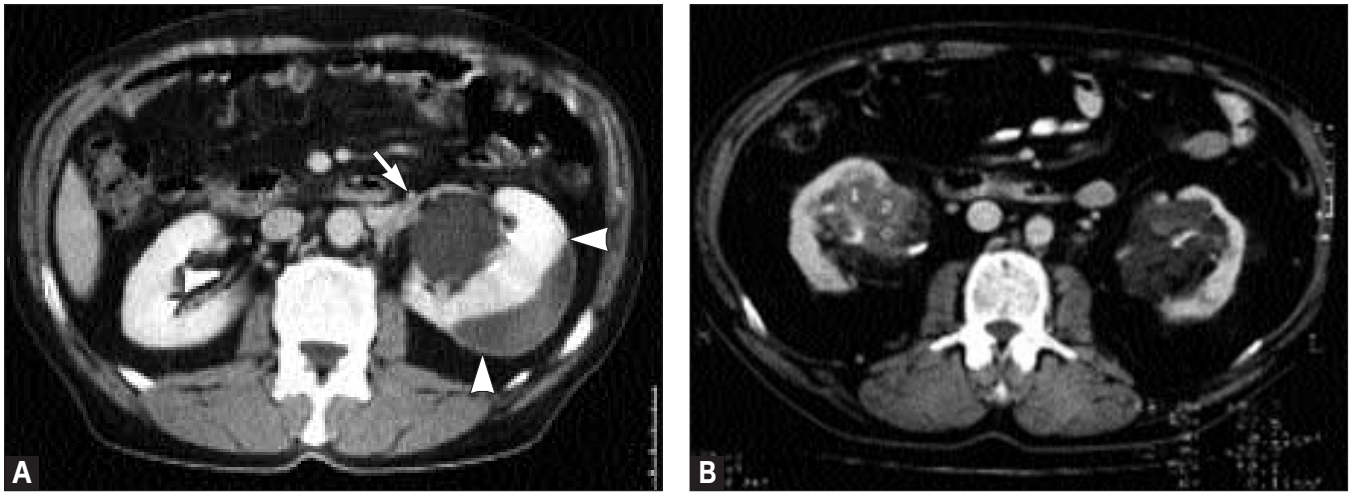

FIGURE 9-6

A, Contrast-enhanced computed tomography (CT) shows a simple, 3-cm wide cyst of the renal sinus (*arrows*) found during investigation of renal calculi. Note subcapsular hematoma (*arrowheads*) detected after lithotripsy. **B**, Contrast-enhanced CT shows bilateral multiple cysts of the renal sinus, leading to chronic compression of the pelvis and subsequent renal atrophy. Ultrasonographic appearance mimicked hydronephrosis. Also known as hilar lymphangiectasis or peripelvic (or parapelvic) cysts, this acquired disorder consists of dilated hilar lymph channels. Its frequency is about 1% in autopsy series. Although usually asymptomatic, cysts of the renal sinus can cause severe urinary obstruction, **B**.

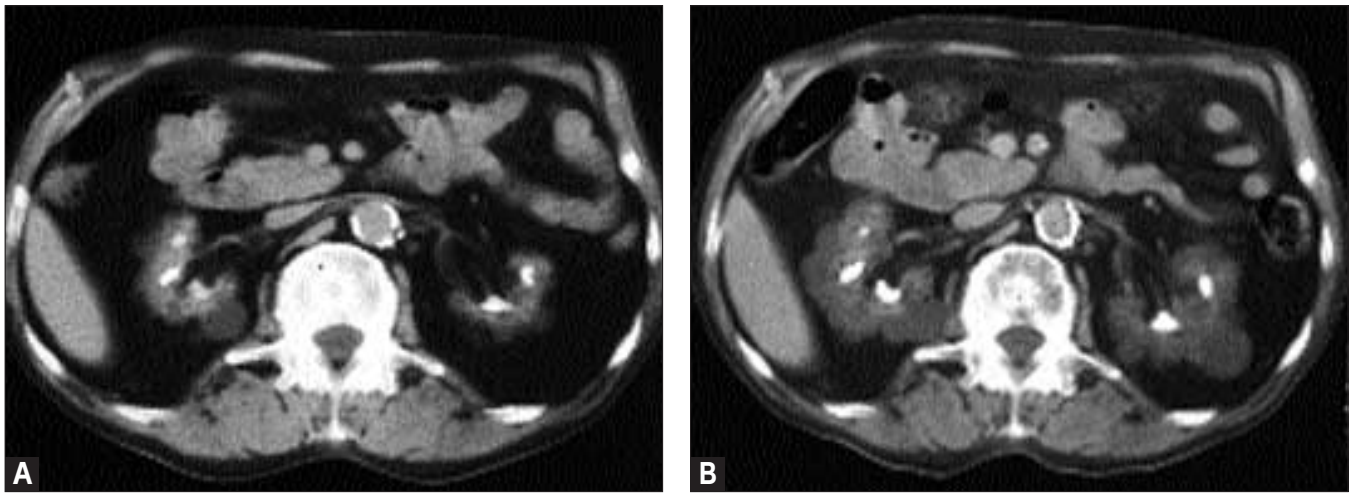

FIGURE 9-7

A, Acquired cystic kidney disease (ACKD) detected by contrast-enhanced computed tomography (CT) in a 71-year-old man on hemodialysis for 4 years. **A**, Note the several intrarenal calcifications, which are not unusual in dialysis patients. ACKD is characterized by the development of many cysts in the setting of chronic uremia. It can occur at any age, including childhood, whatever the original nephropathy. The diagnosis is based on detection of at least three to five cysts in each kidney in a patient who has chronic renal failure but not hereditary cystic disease. The prevalence of ACKD averages 10% at onset of dialysis treatment and subsequently increases, to reach 60% and 90% at 5 and 10 years into hemodialysis and peritoneal dialysis, respectively [5]. In the early stage, kidneys are small or even shrunken and cysts are usually smaller than 0.5 cm. Cyst numbers and kidney volume increase with time, as seen on this patient's scan (**B**) repeated 8 years into dialysis. Advanced ACKD can mimic autosomal-dominant polycystic disease. ACKD sometimes regresses after successful transplantation; it can involve chronically rejected kidney grafts. Although ACKD is usually asymptomatic it may be complicated by bleeding—confined to the cysts or extending to either the collecting system (causing hematuria) or the perinephric spaces—and associated with renal cell carcinoma. (*Courtesy of* M. Jadoul.)

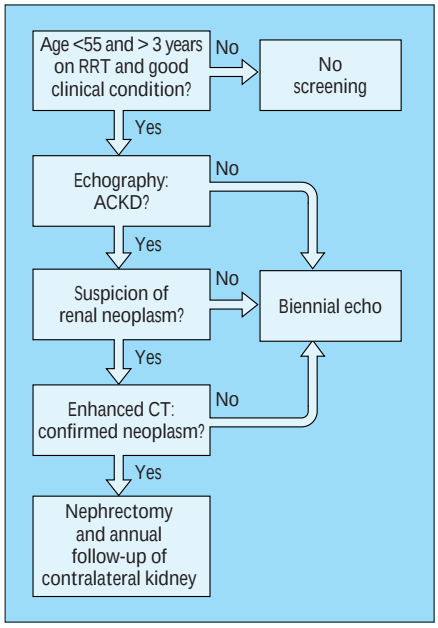

FIGURE 9-8

Screening for acquired cystic kidney disease (ACKD) and renal neoplasms in patients receiving renal replacement therapy (RRT). The major clinical concern with ACKD is the risk of renal cell carcinoma, often the tubulopapillary type, associated with this disorder: the incidence is 50-times greater than in the general population. Moreover, ACKD-associated renal carcinoma is more often bilateral and multicentric; however, only a minority of them evolve into invasive carcinomas or cause metastases [5]. There is no doubt that imaging should be performed when a dialysis patient has symptoms such as flank pain and hematuria, the question of periodic screening for ACKD and neoplasms in asymptomatic dialysis patients is still being debated. Using decision analysis incorporating morbidity and mortality associated with nephrectomy in dialysis patients, Sarasin and coworkers [6] showed that only the youngest patients at risk for ACKD benefit from periodic screening. On the basis of this analysis, it has been proposed that screening be restricted to patients younger than 55 years, who have been on dialysis at least 3 years and are in good general condition. Recognized risk factors for renal cell carcinoma in ACKD are male gender, uremia of long standing, large kidneys, and analgesic nephropathy.

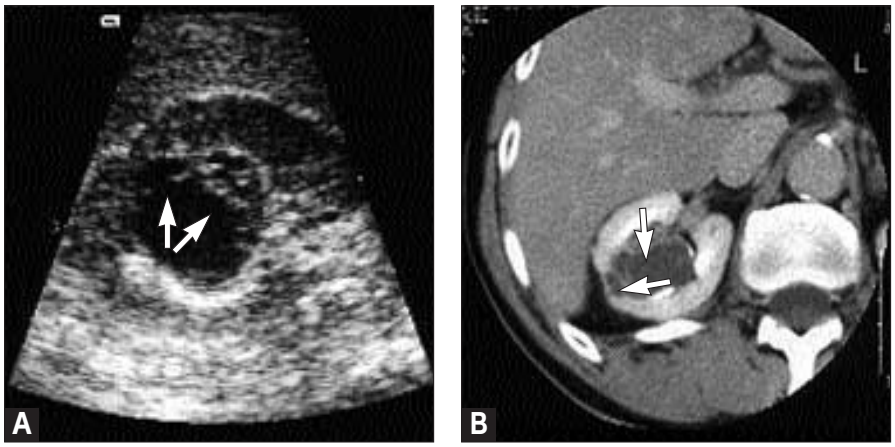

FIGURE 9-9

Multilocular cyst (or multilocular cystic nephroma) of the right kidney, detected by ultrasonography (**A**) and contrast-enhanced CT-scan (**B**). Both techniques show the characteristic septa (*arrow*) dividing the mass into multiple sonolucent locules. This rare disorder is usually a benign tumor, though some lesions have been found to contain foci of nephroblastoma or renal clear cell carcinoma. The imaging appearance is actually indistinguishable from those of the cystic forms of Wilms' tumor and renal clear cell carcinoma. (*Courtesy of* A. Dardenne.)

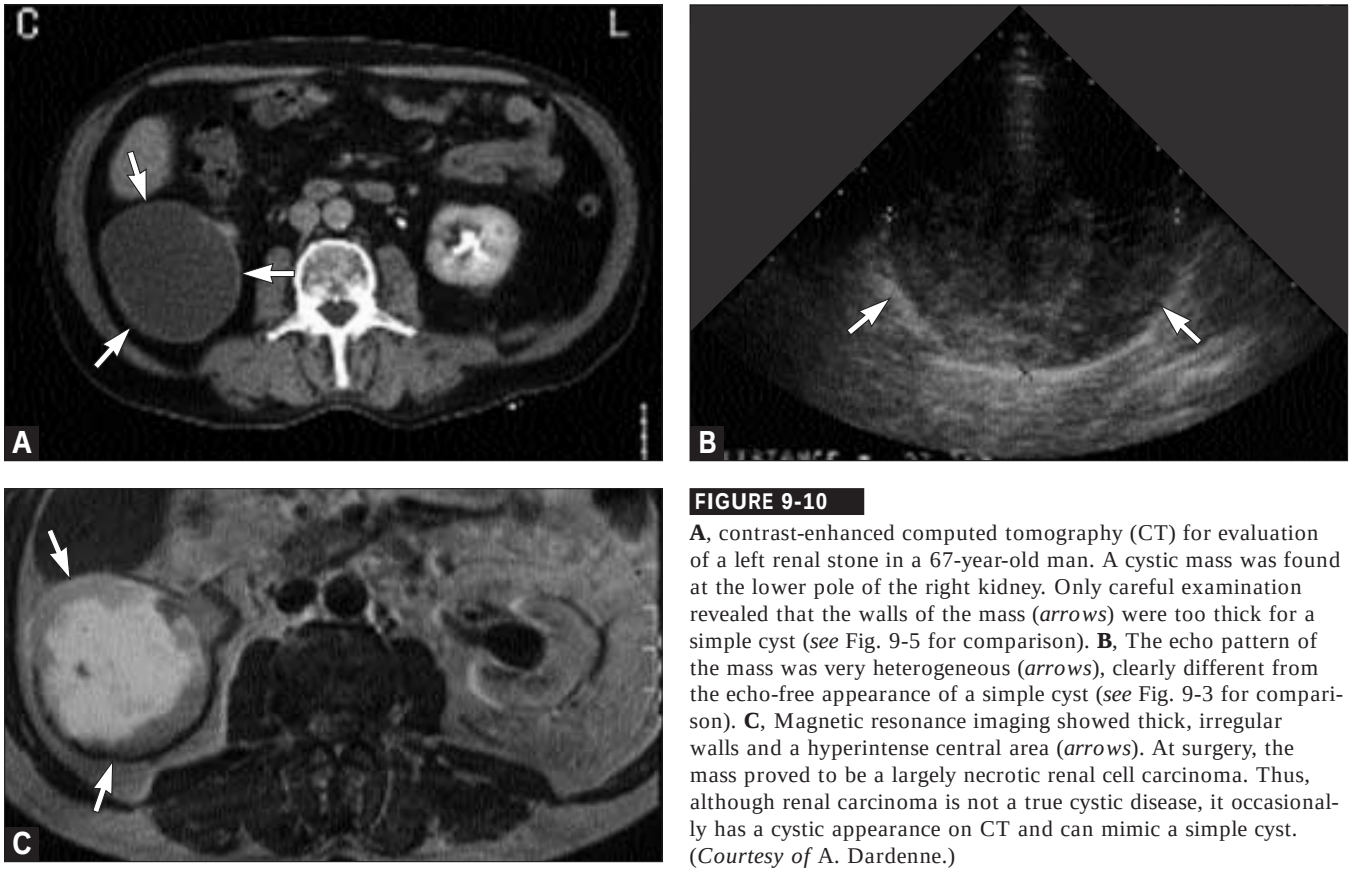

FIGURE 9-10

A, contrast-enhanced computed tomography (CT) for evaluation of a left renal stone in a 67-year-old man. A cystic mass was found at the lower pole of the right kidney. Only careful examination revealed that the walls of the mass (*arrows*) were too thick for a simple cyst (*see* Fig. 9-5 for comparison). **B**, The echo pattern of the mass was very heterogeneous (*arrows*), clearly different from the echo-free appearance of a simple cyst (*see* Fig. 9-3 for comparison). **C**, Magnetic resonance imaging showed thick, irregular walls and a hyperintense central area (*arrows*). At surgery, the mass proved to be a largely necrotic renal cell carcinoma. Thus, although renal carcinoma is not a true cystic disease, it occasionally has a cystic appearance on CT and can mimic a simple cyst. (*Courtesy of* A. Dardenne.)

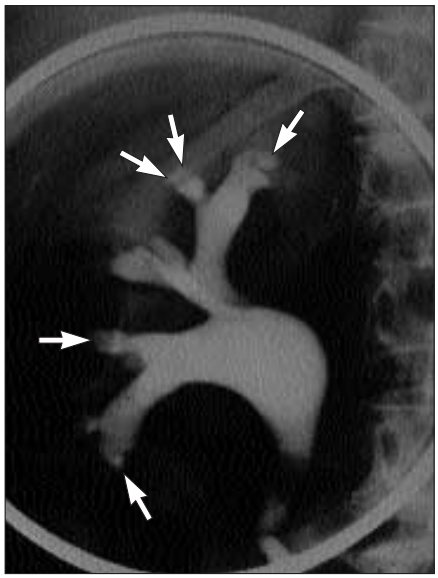

FIGURE 9-11

Medullary sponge kidney (MSK) diagnosed by intravenous urography in 53-year-old woman with a history of recurrent kidney stones. Pseudocystic collections of contrast medium in the papillary areas (*arrows*) are the typical feature of MSK. They result from congenital dilatation of collecting ducts (involving part or all of one or both kidneys), ranging from mild ectasia (appearing on urography as linear striations in the papillae, or papillary "blush") to frank cystic pools, as in this case (giving a spongelike appearance on section of the kidney). MSK has an estimated prevalence of 1 in 5000 [2]. It predisposes to stone formation in the dilated ducts: on plain films, clustering of calcifications in the papillary areas is very suggestive of the condition. MSK may be associated with a variety of other congenital and inherited disorders, including corporeal hemihypertrophy, Beckwith-Wiedemann syndrome (macroglossia, omphalocele, visceromegaly, microcephaly, and mental retardation), polycystic kidney disease (about 3% of patients with autosomal-dominant polycystic kidney disease have evidence of MSK), congenital hepatic fibrosis, and Caroli's disease [7].

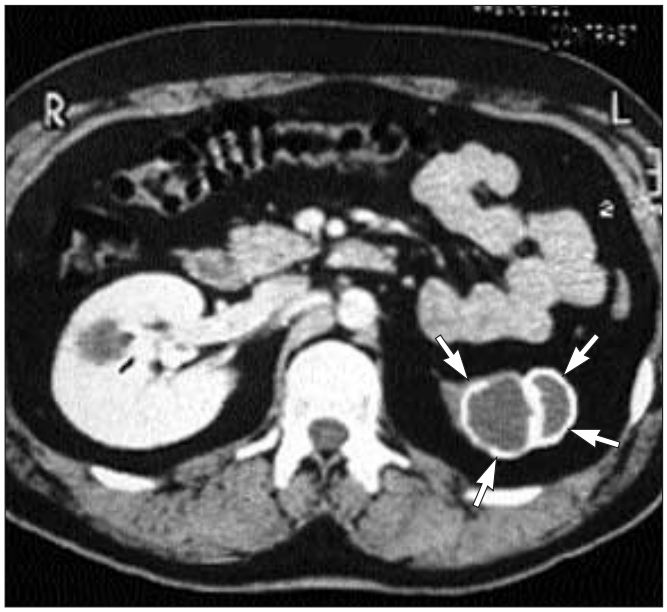

FIGURE 9-12

Multicystic dysplastic kidney (MCDK) found incidentally by enhanced CT in a 34-year-old patient. The dysplastic kidney is composed of cysts with mural calcifications (*arrows*). Note the compensatory hypertrophy of the right kidney and the incidental simple cysts in it. MCDK consists of a collection of cysts frequently described as resembling a bunch of grapes and an atretic ureter. No function can be demonstrated. Only unilateral involvement is compatible with life. Usually, the contralateral kidney is normal and exhibits compensatory hypertrophy. In some 30% of cases, however, it is also affected by some congenital abnormalities such as dysplasia or pelviureterical junction obstruction. In fact, among the many forms of renal dysplasia, MCDK is thought to represent a cystic variety.

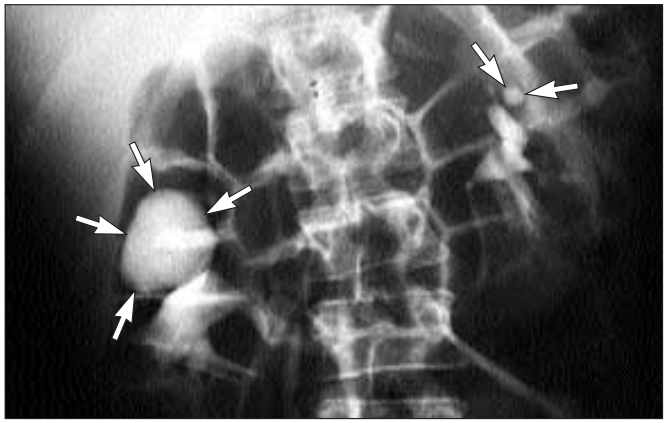

FIGURE 9-13

Intravenous urography demonstrates multiple calyceal diverticula (*arrows*) in a 38-year-old woman who complained of intermittent flank pain. Previously, the ultrasonographic appearance had suggested the existence of polycystic kidney disease. Although usually smaller than 1 cm in diameter, pyelocalyceal diverticula occasionally are much larger, as in this case. They predispose to stone formation. Since ultrasonography is the preferred screening tool for cystic renal diseases, clinicians must be aware of both its pitfalls (exemplified in this case and in the case of parapelvic cysts; *see* Fig. 9-6) and its limited power to detect very small cysts.

Genetic disorders

GENETICS OF ADPKD

Gene	Chromosome	Product	Patients with ADPKD, %
PKD1	16	Polycystin 1	80–90
PKD2	4	Polycystin 2	10–20
PKD3	?	?	Very few

FIGURE 9-14

Genetics of autosomal-dominant polycystic kidney disease (ADPKD). ADPKD is by far the most frequent inherited kidney disease. In white populations, its prevalence ranges from 1 in 400 to 1 in 1000. ADPKD is characterized by the development of multiple renal cysts that are variably associated with extrarenal (mainly hepatic and cardiovascular) abnormalities [1,2,3]. It is caused by mutations in at least three different genes. PKD1, the gene responsible in approximately 85% of the patients, located on chromosome 16, was cloned in 1994 [8]. It encodes a predicted protein of 460 kD, called polycystin 1. The vast majority of the remaining cases are accounted for by a mutation in PKD2, located on chromosome 4 and cloned in 1996 [9]. The PKD2 gene encodes a predicted protein of 110 kD called polycystin 2. Phenotypic differences between the two main genetic forms are detailed in Figure 9-19. The existence of (at least) a third gene is suggested by recent reports.

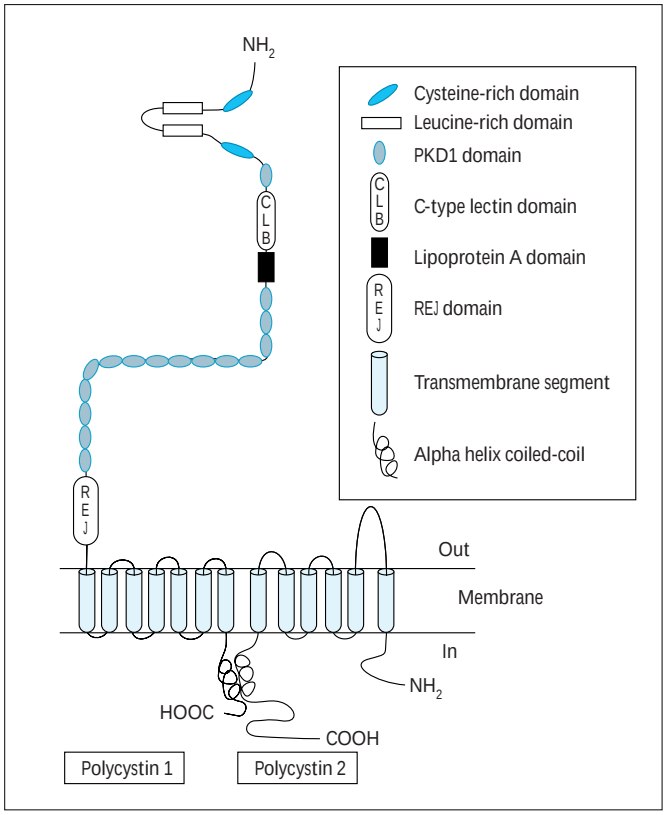

FIGURE 9-15

Autosomal-dominant polycystic kidney disease: predicted structure of polycystin 1 and polycystin 2 and their interaction. Polycystin 1 is a 4302-amino acid protein, which anchors itself to cell membranes by seven transmembrane domains [10]. The large extracellular portion includes two leucine-rich repeats usually involved in protein-protein interactions and a C-type lectin domain capable of binding carbohydrates. A part of the intracellular tail has the capacity to form a coiled-coil motif, enabling either self-assembling or interaction with other proteins. Polycystin 2 is a 968-amino acid protein with six transmembrane domains, resembling a subunit of voltage-activated calcium channel. Like polycystin 1, the C-terminal end of polycystin 2 comprises a coiled-coil domain and is able to interact in vitro with PKD2 [11]. This C-terminal part of polycystin 2 also includes a calcium-binding domain. On these grounds, it has been hypothesized that polycystin 1 acts like a receptor and signal transducer, communicating information from outside to inside the cell through its interaction with polycystin 2. This coordinated function could be crucial during late renal embryogenesis. It is currently speculated that both polycystins play a role in the maturation of tubule epithelial cells. Mutation of polycystins could thus impair the maturation process, maintaining some tubular cells in a state of underdevelopment. This could result in both sustained cell proliferation and predominance of fluid secretion over absorption, leading to cyst formation (*see* Fig. 9-16 and references 12 and 13 for review). (*From* Hughes *et al.* [10] and Germino [12].)

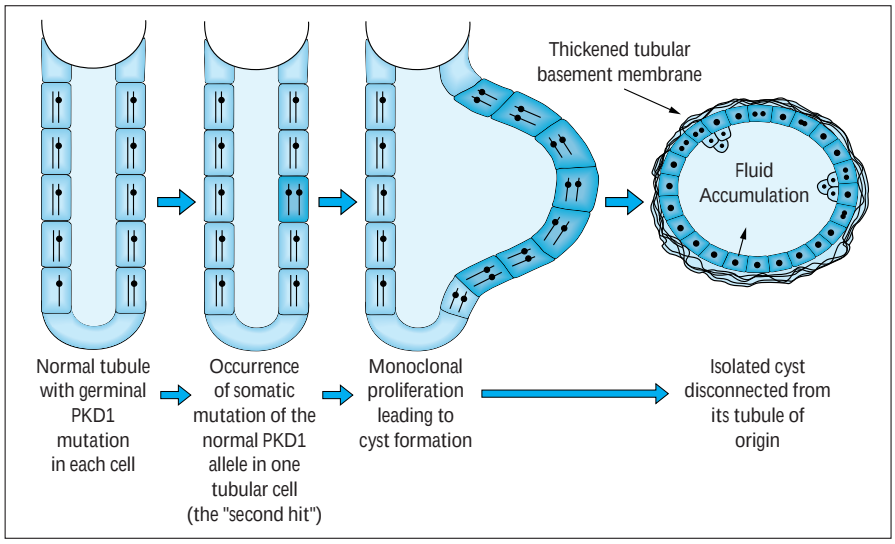

FIGURE 9-16

Hypothetical model for cyst formation in autosomal-dominant polycystic kidney disease (ADPKD), relying on the "two-hit" mechanism as the primary event. The observation that only a minority of nephrons develop cysts, despite the fact that every tubular cell harbors germinal PKD1 mutation, is best accounted for by the two-hit model. This model implies that, in addition to the germinal mutation, a somatic (acquired) mutation involving the normal PKD1 allele is required to trigger cyst formation (*ie*, a mechanism similar to that demonstrated for tumor suppressor genes in tuberous sclerosis complex and von Hippel-Lindau disease). The hypothesis is supported by both the clonality of most cysts and the finding of loss of heterozygosity in some of them [12].

Cell immaturity resulting from mutated polycystin would lead to uncontrolled growth, elaboration of abnormal extracellular matrix, and accumulation of fluid. Aberrant cell proliferation is demonstrated by the existence of micropolyps, identification of mitotic phases, and abnormal expression of proto-oncogenes. Abnormality of extracellular matrix is evidenced by thickening and lamination of the tubular basement membrane; involvement of extracellular matrix would explain the association of cerebral artery aneurysms with ADPKD. As most cysts are disconnected from their tubule of origin, they can expand only through net transepithelial fluid secretion, just the reverse of the physiologic tubular cell function [13]. Figure 9-17 summarizes our current knowledge of the mechanisms that may be involved in intracystic fluid accumulation.

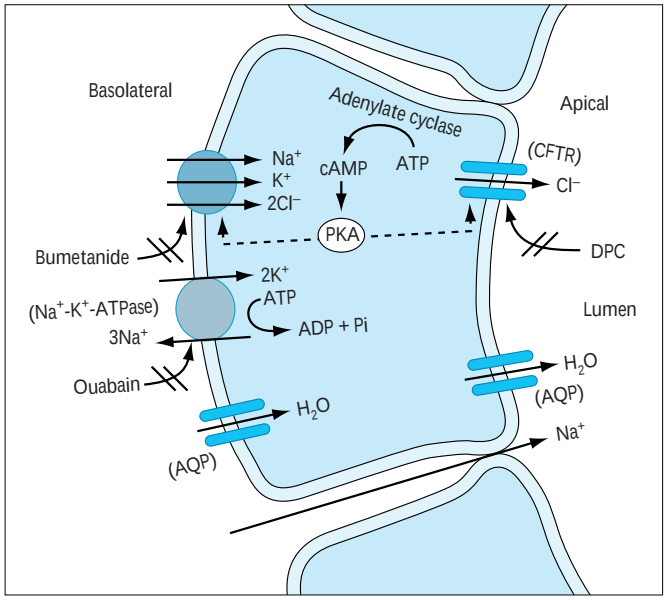

FIGURE 9-17

Autosomal-dominant polycystic kidney disease (ADPKD): mechanisms of intracystic fluid accumulation [13,14]. The primary mechanism of intracystic fluid accumulation seems to be a net transfer of chloride into the lumen. This secretion is mediated by a bumetanide-sensitive Na^+-K^+-$2Cl^-$ cotransporter on the basolateral side and cystic fibrosis transmembrane regulator (CFTR) chloride channel on the apical side. The activity of the two transporters is regulated by protein kinase A (PKA) under the control of cyclic adenosine monophosphate (AMP). The chloride secretion drives movement of sodium and water into the cyst lumen through electrical and osmotic coupling, respectively. The pathway for transepithelial Na^+ movement has been debated. In some experimental conditions, part of the Na^+ could be secreted into the lumen via a mispolarized apical Na^+-K^+-ATPase ("sodium pump"); however, it is currently admitted that most of the Na^+ movement is paracellular and that the Na^+-K^+-ATPase is located at the basolateral side. The movement of water is probably transcellular in the cells that express aquaporins on both sides and paracellular in others [13, 14]. AQP—aquaporine; DPC—diphenylamine carboxylic acid.

ADPKD: CLINICAL MANIFESTATIONS

Manifestation	Prevalence, %	Reference
Renal		
Hypertension	Increased with age (80 at ESRD)	[15]
Pain (acute and chronic)	60	[3,16]
Gross hematuria	50	[3,16]
Urinary tract infection	Men 20; women 60	[3]
Calculi	20	[17]
Renal failure	50 at 60 y	[18]
Hepatobiliary (see Fig. 9–23)		
Cardiovascular		
Cardiac valvular abnormality	20	[16]
Intracranial arteries		
Aneurysm	8	[3]
Dolichoectasia	2	[19]
? Ascending aorta dissection	Rare	
? Coronary arteries aneurysm	Rare	
Other		
Pancreatic cysts	9	[20]
Arachnoid cysts	8	[21]
Hernia		
Inguinal	13	[22]
Umbilical	7	[22]
Spinal Meningeal Diverticula	0.2	[23]

FIGURE 9-18

Main clinical manifestations of autosomal-dominant polycystic kidney disease (ADPKD). Renal involvement may be totally asymptomatic at early stages. Arterial hypertension is the presenting clinical finding in about 20% of patients. Its frequency increases with age. Flank or abdominal pain is the presenting symptom in another 20%. The differential diagnosis of acute abdominal is detailed in Figure 9-22. Gross hematuria is most often due to bleeding into a cyst, and more rarely to stone. Renal infection, a frequent reason for hospital admission, can involve the upper collecting system, renal parenchyma or renal cyst. Diagnostic data are obtained by ultrasonography, excretory urography and CT: use of CT in cyst infection is described in Figure 9-21. Frequently, stones are radiolucent or faintly opaque, because of their uric acid content. The main determinants of progression of renal failure are the genetic form of the disease (*see* Fig. 9-19) and gender (more rapid progression in males). Hepatobiliary and intracranial manifestations are detailed in Figures 9-23 to 9-26. Pancreatic and arachnoid cysts are most usually asymptomatic. Spinal meningeal diverticula can cause postural headache. ESRD—end-stage renal disease.

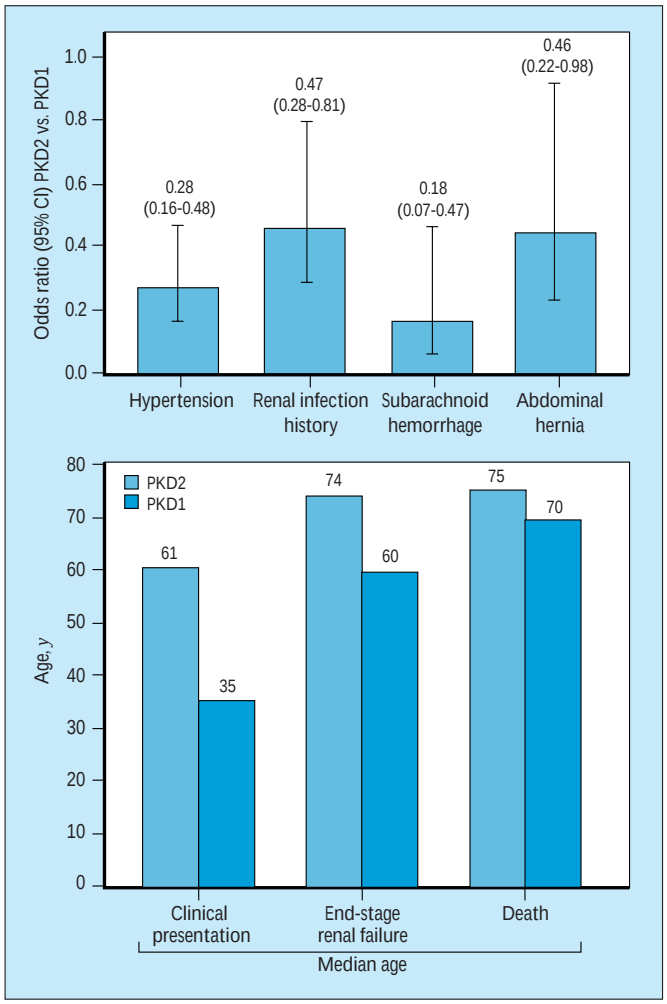

FIGURE 9-19

Autosomal-dominant polycystic kidney disease (ADPKD): phenotype PKD2 versus PKD1. Families with a PKD2 mutation have a milder phenotype than those with a PKD1 mutation. In this study comparing 306 PKD2 patients (from 32 families) with 288 PKD1 patients (17 families), PKD2 patients were, for example, less likely to be hypertensive, to have a history of renal infection, to suffer a subarachnoid hemorrhage, and to develop an abdominal hernia. As a consequence of the slower development of clinical manifestations, PKD2 patients were, on average, 26 years older at clinical presentation, 14 years older when they started dialysis, and 5 years older when they died. Early-onset ADPKD leading to renal failure in childhood has been reported only in the PKD1 variety. (*Data from* Hateboer [24].)

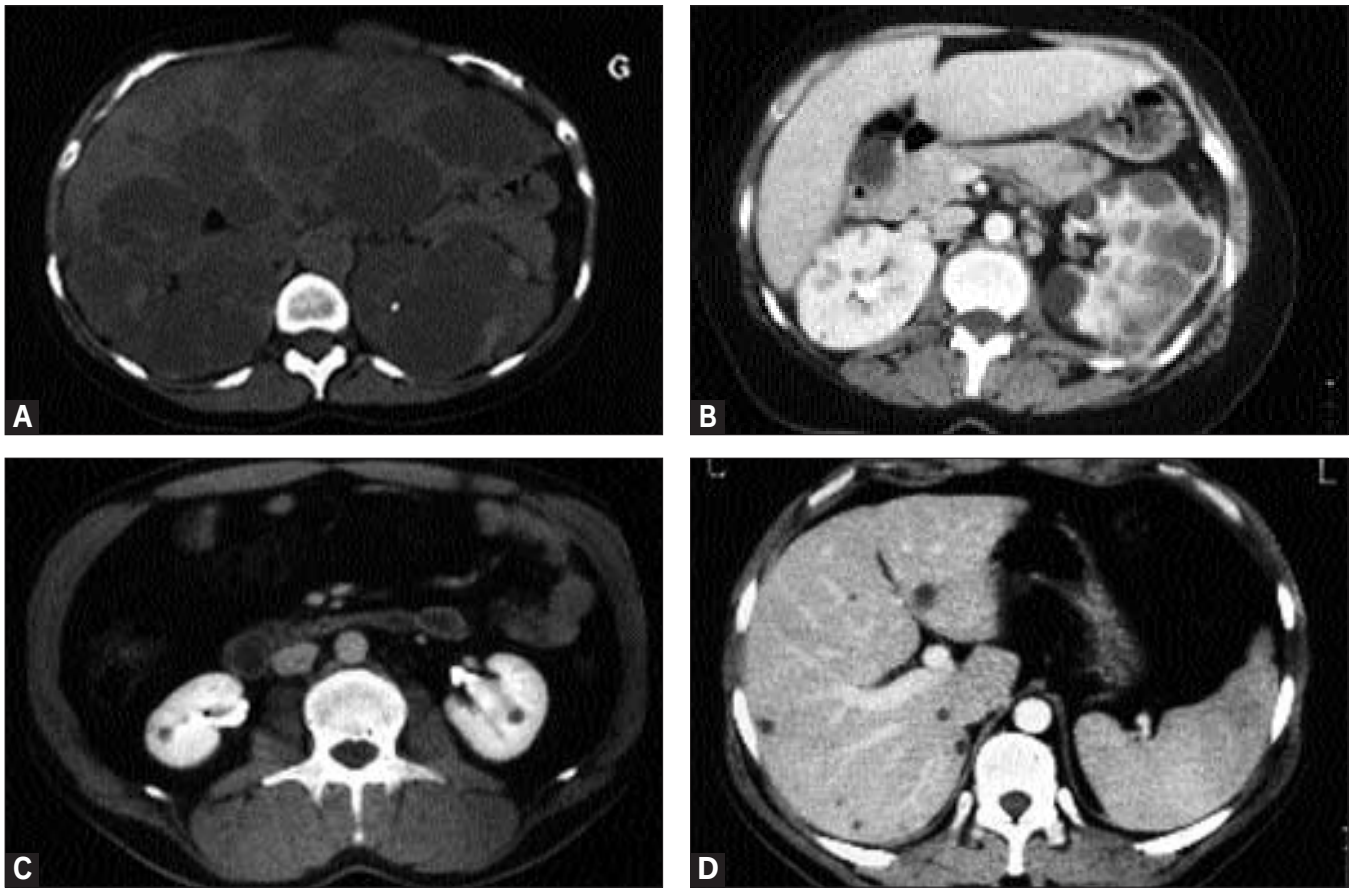

FIGURE 9-20

Autosomal-dominant polycystic kidney disease (ADPKD): kidney involvement. Examples of various cystic involvements of kidneys in ADPKD. Degree of involvement depends on age at presentation and disease severity. **A**, With advanced disease as in this 54-year-old woman, renal parenchyma is almost completely replaced by innumerable cysts. Note also the cystic involvement of the liver. **B**, Marked asymmetry in the number and size of cysts between the two kidneys may be observed, as in this 36-year-old woman. In the early stage of the disease, making the diagnosis may be more difficult (*see* Fig. 9-28 for the minimal sonographic criteria to make a diagnosis of ADPKD in PKD1 families). **C, D**, Contrast-enhanced CT is more sensitive than ultrasonography in the detection of small cysts. The presence of liver cysts helps to establish the diagnosis, as in this 38-year-old man with PKD2 disease and mild kidney involvement.

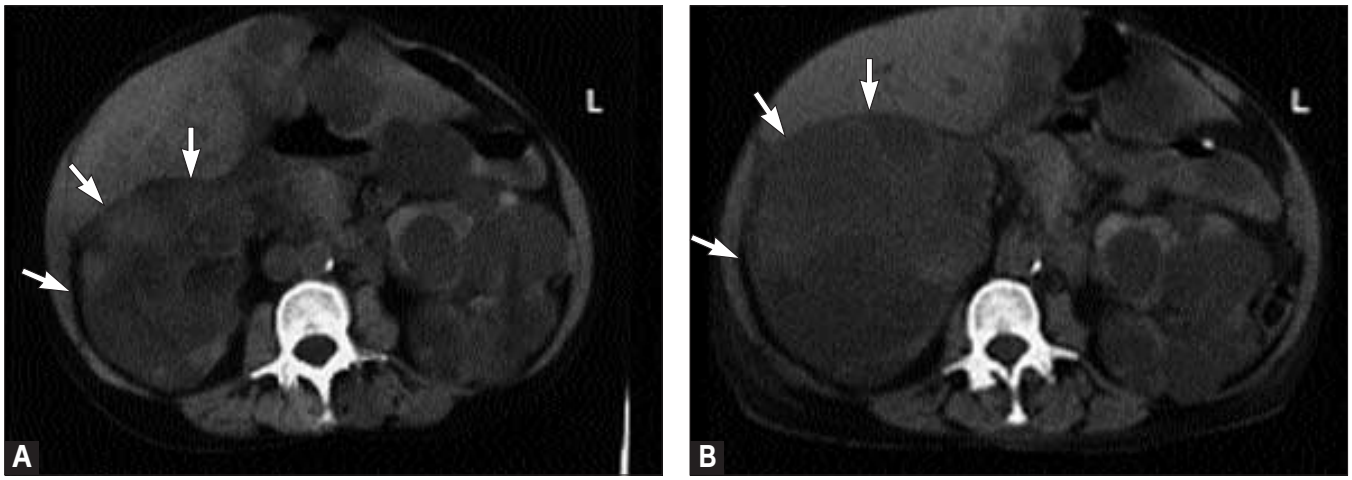

FIGURE 9-21

Autosomal-dominant polycystic kidney disease (ADPKD): kidney cyst infection. Course of severe cyst infection in the right kidney of a patient with ADPKD who was admitted for fever and acute right flank pain. Blood culture was positive for *Escherichia coli*. **A**, CT performed on admission showed several heterogeneous cysts in the right kidney (*arrows*). Infection did not respond to appropriate antibiotherapy (fluoroquinolone). **B**, CT repeated 17 days later showed considerable enlargement of the infected cysts (*arrows*). Percutaneous drainage failed to control infection, and nephrectomy was necessary. This case illustrates the potential severity of cyst infection and the contribution of sequential CT in the diagnosis and management of complicated cysts.

ADPKD: SPECIFIC CAUSES OF ACUTE ABDOMINAL PAIN

Cause	Frequency	Fever
Renal		
Cyst Bleeding	++++	Mild (<38°C, maximum 2 days) or none
Stone	++	With pyonephrosis
Infection	+	High; prolonged with cyst involved
Liver Cyst		
Infection	Rare	High, prolonged
Bleeding	Very Rare	Mild (<38°C, maximum 2 days) or none

FIGURE 9-22

Autosomal-dominant polycystic kidney disease (ADPKD): specific causes of acute abdominal pain. The most frequent cause of acute abdominal pain related to ADPKD is intracyst bleeding. Depending on the amount of bleeding, it may cause mild, transient fever. It may or may not cause gross hematuria. Cyst hemorrhage is responsible for most high-density cysts and cyst calcifications demonstrated by CT. Spontaneous resolution is the rule. Excretory urography or enhanced CT is needed mostly to locate obstructive, faintly opaque stones. Stones may be treated by percutaneous or extracorporal lithotripsy.

Renal infection may involve the upper collecting system, renal parenchyma, or cyst. Parenchymal infection is evidenced by positive urine culture and prompt response to antibiotherapy; cyst infection by the development of a new area of renal tenderness, quite often a negative urine culture (but a positive blood culture), and a slower response to antibiotherapy. CT demonstrates the heterogeneous contents and irregularly thickened walls of infected cysts. Cyst infection warrants prolonged anti-biotherapy [3]. An example of severe, intractable cyst infection is shown in Figure 9-21.

ADPKD: HEPATOBILIARY MANIFESTATIONS

Finding	Frequency
Asymptomatic liver cysts	Very common; increased prevalence with age (up to 80% at age 60)
Symptomatic polycystic liver disease	Uncommon (male/female ratio: 1/10)
Complicated cysts (hemorrhage, infection)	
Massive hepatomegaly	
Chronic pain/discomfort	
Early satiety	
Supine dyspnea	
Abdominal hernia	
Obstructive jaundice	
Hepatic venous outflow obstruction	
Congenital hepatic fibrosis	Rare (not dominantly transmitted)
Idiopathic dilatation of intrahepatic or extrahepatic biliary tract	Very rare
Cholangiocarcinoma	Very rare

FIGURE 9-23

Autosomal-dominant polycystic kidney disease (ADPKD): hepatobiliary manifestations. Liver cysts are the most frequent extrarenal manifestation of ADPKD. Their prevalence increases dramatically from the third to the sixth decade of life, reaching a plateau of 80% thereafter [25, 26]. They are observed earlier and are more numerous and extensive in women than in men. Though usually mild and asymptomatic, cystic liver involvement occasionally is massive and symptomatic (*see* Figure 9-24). Rare cases have been reported of congenital hepatic fibrosis or idiopathic dilatation of the intrahepatic or extrahepatic tract associated with ADPKD [25, 26].

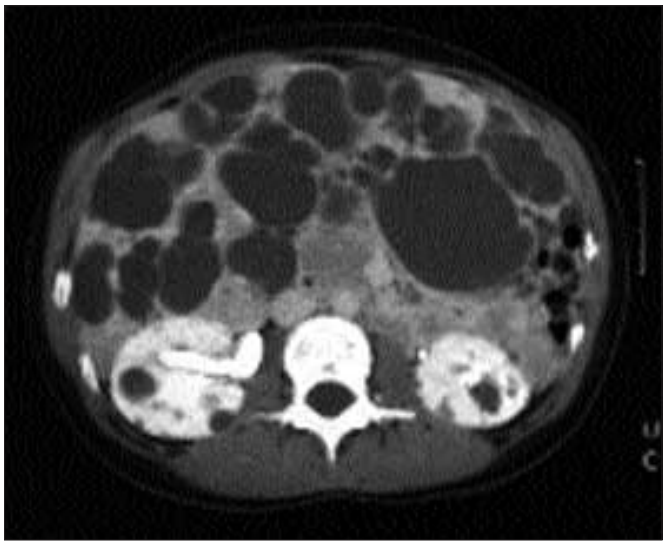

FIGURE 9-24

Autosomal-dominant polycystic kidney disease (ADPKD): polycystic liver disease. Contrast-enhanced CT in a 32-year-old woman with ADPKD, showing massive polycystic liver disease contrasting with mild kidney involvement.

Massive polycystic liver disease can cause chronic pain, early satiety, supine dyspnea, abdominal hernia, and, rarely, obstructive jaundice, or hepatic venous outflow obstruction. Therapeutic options include cyst sclerosis and fenestration, hepatic resection, and, ultimately, liver transplantation [25, 26].

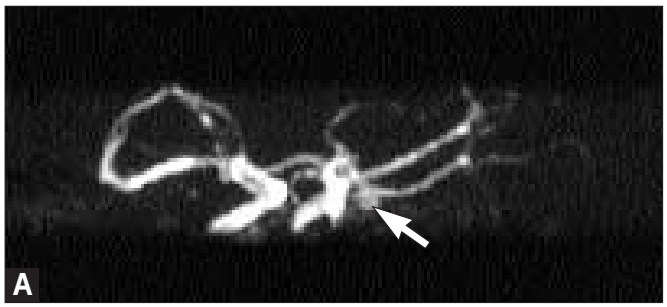

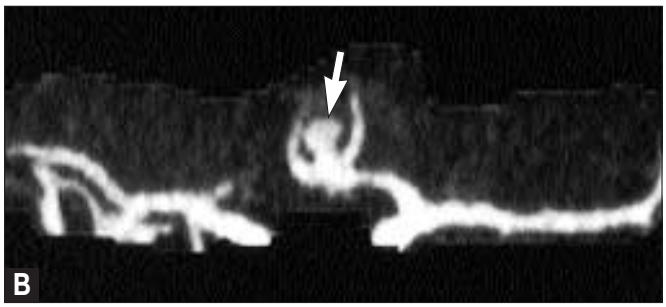

FIGURE 9-25

Autosomal-dominant polycystic kidney disease (ADPKD): intracranial aneurysm detection. Magnetic resonance angiography (MRA), **A**, and spiral computed tomography (CT) angiography, **B**, in two different patients, both with ADPKD, show an asymptomatic intracranial aneurysm (ICA) on the posterior communicating artery (*arrow*), **A**, and the anterior communicating artery (*arrow*), **B**, respectively.

The prevalence of asymptomatic ICA in ADPKD is 8%, as compared with 1.2% in the general population. It reaches 16% in ADPKD patients with a family history of ICA [27]. The risk of ICA rupture in ADPKD is ill-defined. ICA rupture entails 30% to 50% mortality. It is generally manifested by subarachnoid hemorrhage, which usually presents as an excruciating headache. In this setting, the first-line diagnostic procedure is CT. Management should proceed under neurosurgical guidance [27].

Given the severe prognosis of ICA rupture and the possibility of prophylactic treatment, screening ADPKD patients for ICA has been considered. Screening can be achieved by either MRA or spiral CT angiography. Current indications for screening are presented in Figure 9-26. (*Courtesy of* T. Duprez and F. Hammer.)

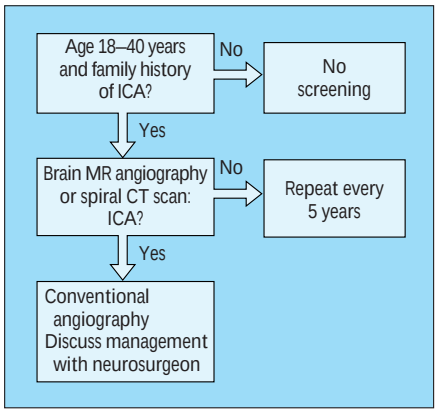

FIGURE 9-26

Autosomal-dominant polycystic kidney disease (ADPKD): intracranial aneurysm (ICA) screening. On the basis of decision analyses (taking into account ICA prevalence, annual risk of rupture, life expectancy, and risk of prophylactic treatment), it is currently proposed to screen for ICA 18 to 40-year-old ADPKD patients with a family history of ICA [25, 27]. Screening could also be offered to patients in high-risk occupations and those who want reassurance. Guidelines for prophylactic treatment are the same ones used in the general population: the neurosurgeon and the interventional radiologist opt for either surgical clipping or endovascular occlusion, depending on the site and size of ICA.

ADPKD: PRESYMPTOMATIC DIAGNOSIS

Presymptomatic diagnosis

- Is *advisable* in families when early management of affected patients would be altered (*eg*, because of history of intracranial aneurysm)
- Should be made *available* to persons at risk who are 18 years or older who request the test
- Should be *preceded by information* about the possibility of inconclusive results and the consequences of the diagnosis:
  - If negative, reassurance
  - If positive, regular medical follow-up, possible psychological burden, risk of disqualification from employment and insurances

FIGURE 9-27

Autosomal-dominant polycystic kidney disease (ADPKD): presymptomatic diagnosis. Presymptomatic diagnosis is aimed at both detecting affected persons (to provide follow-up and genetic counseling) and reassuring unaffected ones. Until a specific treatment for ADPKD is available, presymptomatic diagnosis in children is not advised except in rare families where early-onset disease is typical. Presymptomatic diagnosis is recommended when a family is planned and when early management of affected patients would be altered. The mainstay of screening is ultrasonography; diagnostic echographic criteria according to age in PKD1 families are depicted in Figure 9-28, and diagnosis by gene linkage in Figure 9-29.

ADPKD: ULTRASONOGRAPHIC DIAGNOSTIC CRITERIA

Age	Cysts
15–29	2, uni- or bilateral
30–59	2 in each kidney
≥60	4 in each kidney

Minimal number of cysts to establish a diagnosis of ADPKD in PKD1 families at risk.

FIGURE 9-28

Autosomal-dominant polycystic kidney disease (ADPKD): ultrasonographic diagnostic criteria. Ultrasound diagnostic criteria for the PKD1 form of ADPKD, as established by Ravine's group on the basis of both a sensitivity and specificity study [4, 28]. Note that the absence of cyst before age 30 years does not rule out the diagnosis, the false-negative rate being inversely related to age. When ultrasound diagnosis remains equivocal, the next step should be either contrast-enhanced CT (more sensitive than ultrasonography in the detection of small cysts) or gene linkage (*see* Figure 9-29). A similar assessment is not yet available for the PKD2 form. (*From* Ravine *et al.* [28]; with permission.)

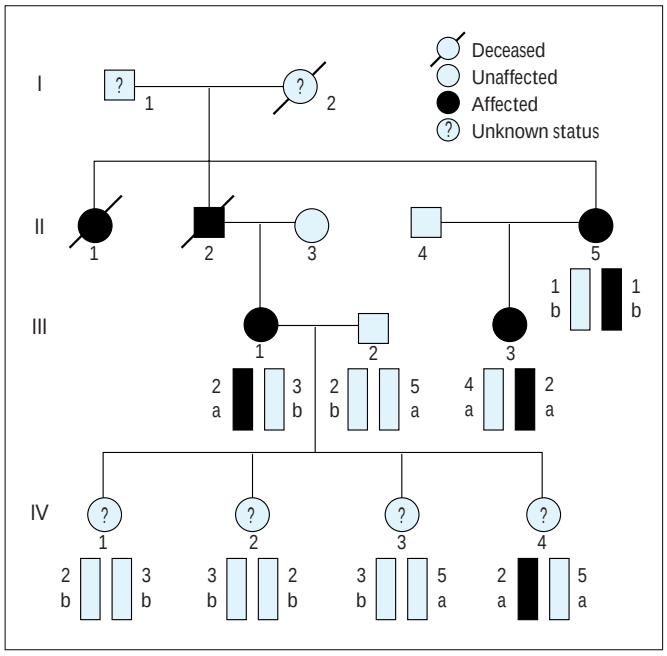

FIGURE 9-29

Example of the use of gene linkage to identify ADPKD gene carriers among generation IV of a PKD1 family. Two markers flanking the PKD1 gene were used. The first one (3' HVR) has six possible alleles (1 through 6) and the other (p 26.6) is biallelic (a, b). In this family, the haplotype 2a is transmitted with the disease (see affected persons II5, III1, and III3). Thus, IV4 has a 99% chance of being a carrier of the mutated PKD1 gene, whereas her sisters (IV1, IV2, IV3) have a 99% chance of being disease free.

Until direct gene testing for PKD1 and PKD2 is readily available, genetic diagnosis will rest on gene linkage. Such analysis requires that other affected and unaffected family members (preferably from two generations) be available for study. Use of markers on both sides of the tested gene is required to limit potential errors due to recombination events. Linkage to PKD1 is to be tested first, as it accounts for about 85% of cases.

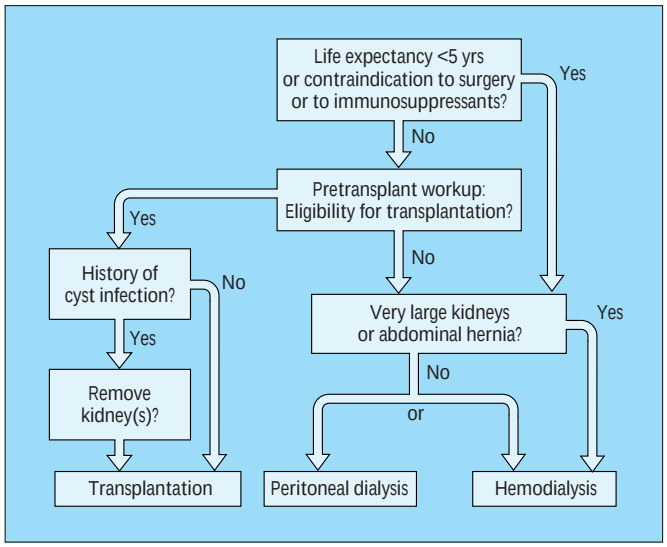

FIGURE 9-30

Autosomal-dominant polycystic kidney disease (ADPKD): renal replacement therapy. Transplantation nowadays is considered in any ADPKD patient with a life expectancy of more than 5 years and with no contraindications to surgery or immunosuppression. Pretransplant workup should include abdominal CT, echocardiography, myocardial stress scintigraphy, and, if needed (*see* Figure 9-26), screening for intracranial aneurysm. Pretransplant nephrectomy is advised for patients with a history of renal cyst infection, particularly if the infections were recent, recurrent, or severe. Patients not eligible for transplantation may opt for hemodialysis or peritoneal dialysis. Although kidney size is rarely an impediment to peritoneal dialysis, this option is less desirable for patients with very large kidneys, because their volume may reduce the exchangeable surface area and the tolerance for abdominal distension. Outcome for ADPKD patients following renal replacement therapy is similar to that of matched patients with another primary renal disease [29, 30].

CLINICAL FEATURES

Finding	Frequency, %	Age at onset, y
Skin		
Hypomelanotic macules	90	Childhood
Facial angiofibromas	80	5–15
Forehead fibrous plaques	30	≥5
"Shagreen patches" (lower back)	30	≥10
Periungual fibromas	30	≥15
Central nervous system		
Cortical tubers	90	Birth
Subependymal tumors (may be calcified)	90	Birth
focal or generalized seizures	80	0–1
Mental retardation/ behavioral disorder	50	0–5
Kidney		
Angiomyolipomas	60	Childhood
Cysts	30	Childhood
Renal cell carcinoma	2	Adulthood
Eye		
Retinal hamartoma	50	Childhood
Retinal pigmentary abnormality	10	Childhood
Liver (angiomyolipomas, cysts)	40	Childhood
Heart (rhabdomyoma)	2	Childhood
Lung (lymphangiomyomatosis; affects females)	1	≥20

FIGURE 9-31

Tuberous sclerosis complex (TSC): clinical features. TSC is an autosomal-dominant multisystem disorder with a minimal prevalence of 1 in 10,000 [30, 31]. It is characterized by the development of multiple hamartomas (benign tumors composed of abnormally arranged and differentiated tissues) in various organs. The most common manifestations are dermatologic (*see* Fig. 9-32) and neurologic (*see* Fig. 9-33). Renal involvement occurs in 60% of cases and includes cysts (*see* Fig. 9-34). Retinal involvement, occurring in 50% of cases, is almost always asymptomatic. Liver involvement, occurring in 40% of cases, includes angiomyolipomas and cysts. Involvement of other organs is much rarer [31, 32].

FIGURE 9-32 (*see* Color Plate)

Tuberous sclerosis complex (TSC): skin involvement. Facial angiofibromas, forehead plaque, **A**, and ungual fibroma, **B**, characteristic of TSC. Previously (and inappropriately) called *adenoma sebaceum*, facial angiofibromas are pink to red papules or nodules, often concentrated in the nasolabial folds. Forehead fibrous plaques appear as raised, soft patches of red or yellow skin. Ungual fibromas appear as peri- or subungual pink tumors; they are found more often on the toes than on the fingers and are more common in females. Other skin lesions include hypomelanotic macules and "shagreen patches" (slightly elevated patches of brown or pink skin). (*Courtesy of* A. Bourloud and C. van Ypersele.)

FIGURE 9-33

Tuberous sclerosis complex (TSC): central nervous system involvement. Brain CT shows several subependymal, periventricular, calcified nodules characteristic of TSC. Subependymal tumors and cortical tubers are the two characteristic neurologic features of TSC. Calcified nodules are best seen on CT, whereas noncalcified tumors are best detected by magnetic resonance imaging. Clinical manifestations are seizures (including infantile spasms) occurring in 80% of infants, and varying degrees of intellectual disability or behavioral disorder, reported in 50% of children [32].

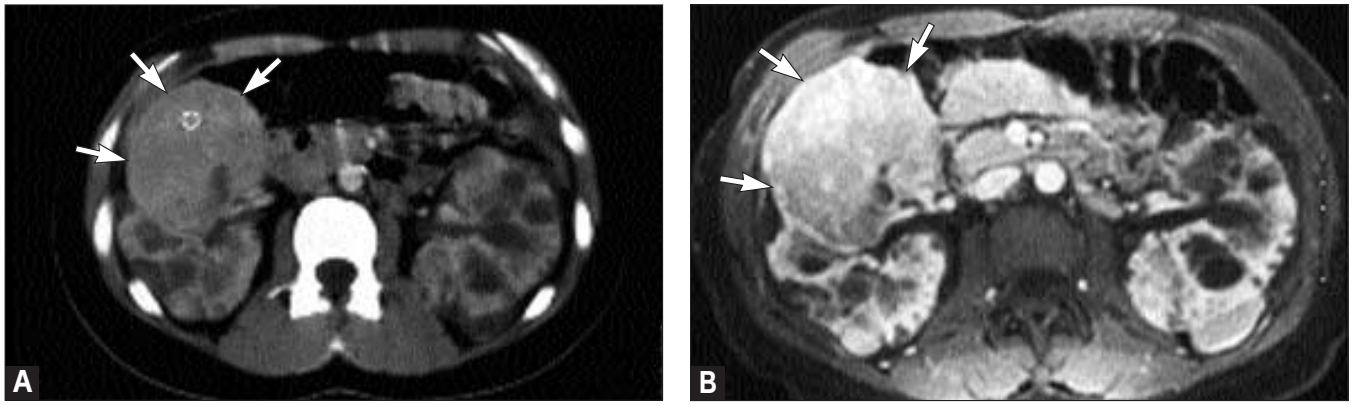

FIGURE 9-34

Tuberous sclerosis complex (TSC): kidney involvement. Contrast-enhanced CT, **A**, and gadolinium-enhanced T1 weighted magnetic resonance images, **B**, of a 15-year-old woman with TSC, show both a large, hypodense, heterogeneous tumor in the right kidney (*arrows*) characteristic of angiomyolipoma (AML) and multiple bilateral kidney cysts. Kidney cysts had been detected at birth.

AML is a benign tumor composed of atypical blood vessels, smooth muscle cells, and fat tissue. While single AML is the most frequent kidney tumor in the general population, multiple and bilateral AMLs are characteristic of TSC. In TSC, AMLs develop at a younger age in females; frequency and size of the tumors increase with age. Diagnosis of AML by imaging techniques (ultrasonography [US], CT, magnetic resonance imagine [MRI]) relies on identification of fat into the tumor, but it is not always possible to distinguish between AML and renal cell carcinoma. The main complication of AML is bleeding with subsequent gross hematuria or potentially life-threatening retroperitoneal hemorrhage.

Cysts seem to be restricted to the TSC2 variety (*see* Fig. 9-35) [33]. Their extent varies widely from case to case. Occasionally, polycystic kidneys are the presenting manifestation of TSC2 in early childhood: in the absence of renal AML, the imaging appearance is indistinguishable from ADPKD. Polycystic kidney involvement leads to hypertension and renal failure that reaches end stage before age 20 years. Though the frequency of renal cell carcinoma in TSC is small, the incidence is increased as compared with that of the general population. (*Courtesy of* J. F. De Plaen and B. Van Beers.)

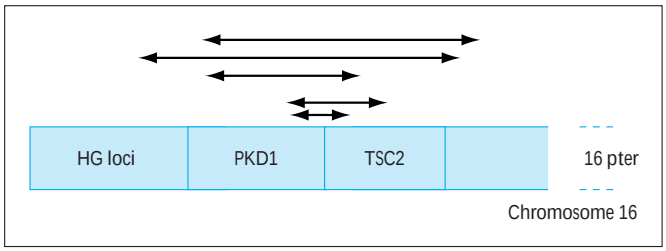

FIGURE 9-35

Tuberous sclerosis complex (TSC): genetics. Representative examples of various contiguous deletions of the PKD1 and TSC2 genes in five patients with TSC and prominent renal cystic involvement (the size of the deletion in each patient is indicated).

TSC is genetically heterogeneous. Two genes have been identified. The TSC1 gene is on chromosome 9, and TSC2 lies on chromosome 16 immediately adjacent and distal to the PKD1 gene. Half of affected families show linkage to TSC1 and half to TSC2. Nonetheless, 60% of TSC cases are apparently sporadic, likely representing new mutations (most are found in the TSC2 gene) [34]. The proteins encoded by the TSC1 and TSC2 genes are called hamartin and tuberin, respectively. They likely act as tumor suppressors; their precise cellular role remains largely unknown. The diseases caused by type 1 and type 2 TSC are indistinguishable except for renal cysts, which, so far, have been observed only in TSC2 patients [33], and for intellectual disability, which is more common in TSC2 patients [34]. (*Adapted from* Sampson, *et al.* [33].)

VHL: ORGAN INVOLVEMENT

Findings	Frequency, %	Mean age (range) at diagnosis, y
Central nervous system		30 (9–71)
Hemangioblastoma		
Cerebellar	60	
Spinal cord	20	
Endolymphatic sac tumor	Rare	
Eye/Retinal hemangioblastoma	60	25 (8–70)
Kidney		
Clear cell carcinoma	40	40 (18–70)
Cysts	30	35 (15–60)
Adrenal glands/ Pheochromocytoma	15	20 (5–60)
Pancreas		30 (13–70)
Cysts	40	
Microcystic adenoma	4	
Islet cell tumor	2	
Carcinoma	1	
Liver (cysts)	Rare	?

FIGURE 9-36

Von Hippel-Lindau disease (VHL): organ involvement. VHL is an autosomal-dominant multisystem disorder with a prevalence rate of roughly 1 in 40,000 [32, 35]. It is characterized by the development of tumors, benign and malignant, in various organs. VHL-associated tumors tend to arise at an earlier age and more often are multicentric than the sporadic varieties. Morbidity and mortality are mostly related to central nervous system hemangioblastoma and renal cell carcinoma. Involvement of cerebellum, retinas, kidneys, adrenal glands, and pancreas is illustrated (*see* Figures 9-37 to 9-41).

The VHL gene is located on the short arm of chromosome 3 and exhibits characteristics of a tumor suppressor gene. Mutations are now identified in 70% of VHL families [36].

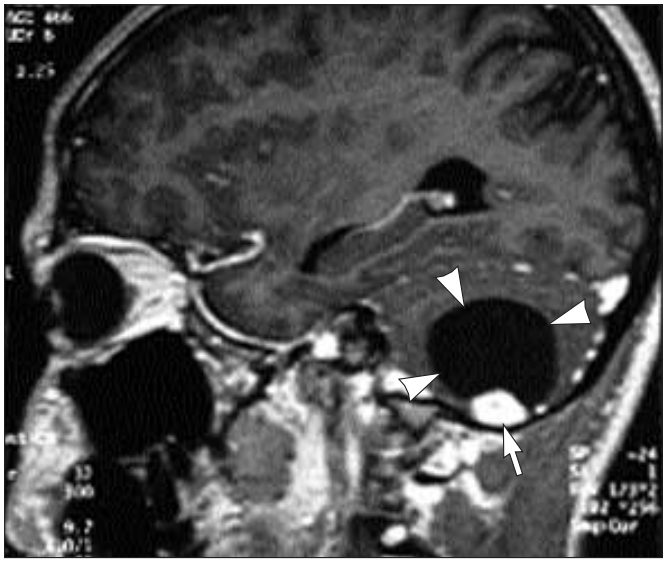

FIGURE 9-37

Von Hippel-Lindau disease (VHL): central nervous system involvement. Gadolinium-enhanced brain magnetic resonance image of a patient with VHL, shows a typical cerebellar hemangioblastoma, appearing as a highly vascular nodule (*arrow*) in the wall of a cyst (*arrowheads*) located in the posterior fossa. Hemangioblastomas are benign tumors whose morbidity is due to mass effect. Cerebellar hemangioblastomas may present with symptoms of increased intracranial pressure. Spinal cord involvement may be manifested as syringomyelia. (*Courtesy of* S. Richard.)

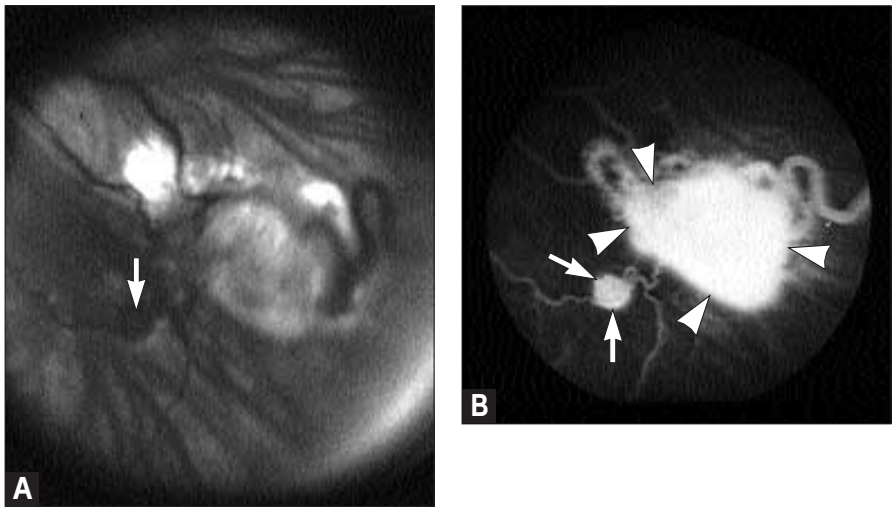

FIGURE 9-38 (*see* Color Plate)
Von Hippel-Lindau disease (VHL): retinal involvement. Ocular fundus, **A**, and corresponding fluorescein angiography, **B**, in a patient with VHL, shows two typical retinal hemangioblastomas. The smaller tumor (*arrow*) appears at the fundus as an intense red spot, whereas the larger (*arrow heads*) appears as a pink-orange lake with dilated, tortuous afferent and efferent vessels. Small peripheral lesions are usually asymptomatic, whereas large central tumors can impair vision. (*Courtesy of* B. Snyers.)

FIGURE 9-39
Von Hippel-Lindau disease (VHL): kidney involvement. Contrast-enhanced CT of a patient with VHL, showing the polycystic aspect of the kidneys. Renal involvement of VHL includes cysts (simple, atypical, and cystic carcinoma) and renal cell carcinoma [36, 37]. The latter is the leading cause of death from VHL. Occasionally, polycystic kidney involvement may mimic autosomal-dominant polycystic kidney disease. Both cystic involvement and sequelae of surgery can lead to renal failure. Nephron-sparing surgery is recommended [37].

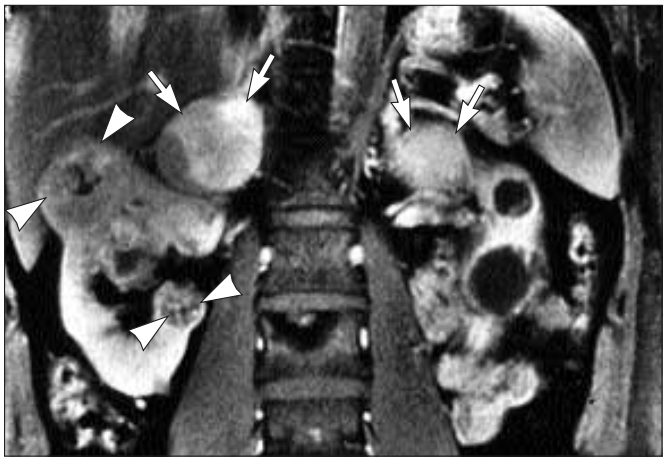

FIGURE 9-40
Von Hippel-Lindau disease (VHL): adrenal gland involvement. Gadolinium-enhanced abdominal magnetic resonance image of a patient with VHL shows bilateral pheochromocytoma (*arrows*). Renal lesions include cysts and solid carcinomas (*arrow heads*). Pheochromocytoma may be the first manifestation of VHL. It tends to cluster within certain VHL families [36]. (*Courtesy of* H. Neumann.)

FIGURE 9-41

Von Hippel-Lindau disease (VHL): pancreas involvement. Contrast-enhanced abdominal CT in a patient with VHL shows multiple cysts in both pancreas (especially the tail, *arrows*) and kidneys. The majority of pancreatic cysts are asymptomatic. When they are numerous and large, they can induce diabetes mellitus or steatorrhea. Other, rare pancreatic lesions include microcystic adenoma, islet cell tumor, and carcinoma.

VHL: SCREENING PROTOCOL

Study	Affected persons	Relatives at risk
Physical examination	Annual	Annual
24-h Urine collection for metadrenaline and normetadrenaline	Annual	Annual
Funduscopy	Annual	Annual (age 5 to 60)
Gadolinium MRI brain scan	Every 3 y (from age 10)	Every 3 y (age 15 to 60)
Abdomen	Annual gadolinium MRI	Annual echography or gadolinium MRI (age 15 to 60)

FIGURE 9-42

Von Hippel-Lindau disease. As most manifestations of VHL are potentially treatable, periodic examination of affected patients is strongly recommended. Though genetic testing is now very useful for presymptomatic identification of affected persons, it must be remembered that a mutation in the VHL gene currently is detected in only 70% of families. For persons at risk in the remaining families, a screening program is also proposed.

FIGURE 9-43

Medullary cystic disease (MCD). Contrast-enhanced CT in a 35-year-old man with MCD. Multiple cysts are seen in the medullary area. Two daughters were also found to be affected. MCD is a very rare autosomal-dominant disorder characterized by medullary cysts detectable by certain imaging techniques (preferably computed tomography) and progressive renal impairment leading to end-stage disease between 20 and 40 years of age. Dominant inheritance and early detection of kidney cysts distinguish MCD from autosomal-recessive nephronophthisis (*see* Fig. 9-48), even though the two may be indistinguishable on histologic examination.

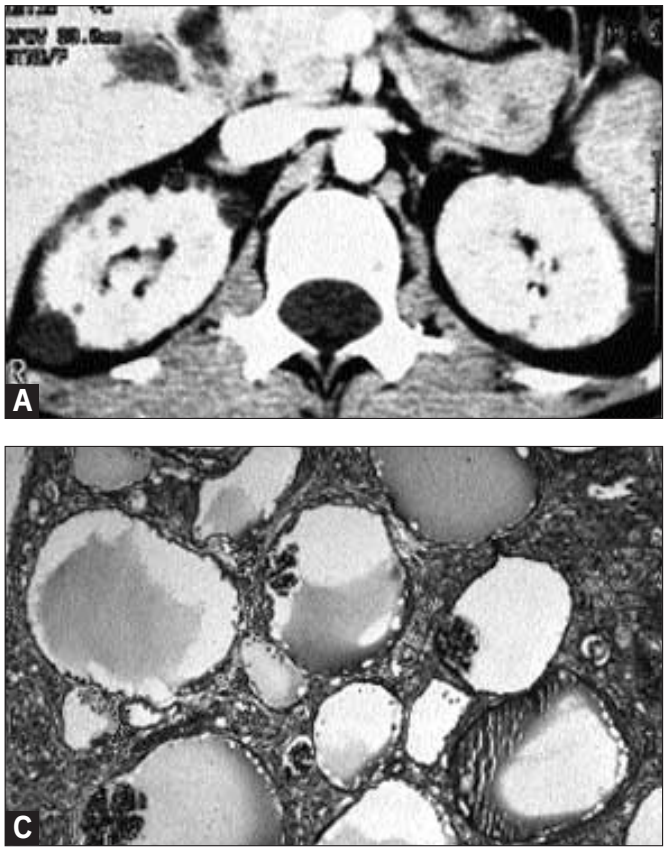

FIGURE 9-44

Glomerulocystic kidney disease (GCKD). Contrast-enhanced CT, **A**, in a 23-year-old woman with the sporadic form of GCKD shows multiple cysts, typically small cortical ones. This cystic pattern was verified in the nephrectomy specimen, **B**, obtained 8 months later at the time of kidney transplantation, and GCKD was confirmed by histopathologic examination with Masson's trichrome stain. **C**, Cysts consisted of a dilatation of Bowman's space surrounding a primitive-looking glomerulus.

GCKD may be sporadic or genetically dominant. Among the familial cases, some patients are infants who have early-onset autosomal-dominant polycystic disease. In others (children or adults) the disease is unrelated to PKD1 and PKD2 and may or not progress to end-stage renal failure [38]. (*Courtesy of* D. Droz.)

ARPKD: CLINICAL MANIFESTATIONS

- Renal
  - Antenatal (ultrasonographic changes)
    - Oligohydramnios with empty bladder
    - Increased renal volume and echogenicity
  - Neonatal period
    - Dystocia and oligohydramnios
    - Enlarged kidneys
    - Renal failure
    - Respiratory distress with pulmonary hypoplasia (possibly fatal)
  - Infancy of childhood
    - Nephromegaly (may regress with time)
    - Hypertension (often severe in the first year of life)
    - Chronic renal failure (slowly progressive, with a 60% probability of renal survival at 15 years of age and 30% at 25 years of age)
- Hepatic
  - Portal fibrosis
  - Intrahepatic biliary tract ectasia

FIGURE 9-45

Autosomal-recessive polycystic kidney disease (ARPKD): clinical manifestations. ARPKD is characterized by the development of cysts originating from collecting tubules and ducts, invariably associated with congenital hepatic fibrosis. Its prevalence is about 1 in 40,000 [39]. In the most severe cases, with marked oligohydramnios and an empty bladder, the diagnosis may be suspected as early as the 12th week of gestation. Some neonates die from either respiratory distress or renal failure. In most survivors, the disease is recognized during the first year of life. The ultrasonographic (US) kidney appearance is depicted in Figure 9-46. Excretory urography shows medullary striations owing to tubular ectasia. Kidney enlargement may regress with time. End-stage renal failure develops before age 25 in 70% of patients.

Liver involvement consists of portal fibrosis (*see* Fig. 9-47) and intrahepatic bilary ectasia, frequently resulting in portal hypertension (leading to hypersplenism and esophageal varices) and less often in cholangitis, respectively. US may show dilatation of the biliary ducts, and even cysts. The respective severity of kidney and liver involvement vary widely between families and even in a single kindred.

A comparison of the diagnostic features of autosomal-dominant polycystic kidney disease (ADPKD) and ARPKD is summarized in Figure 9-2. Renal US of the parents of a child with ARPKD is, of course, normal. It should be noted that congenital hepatic fibrosis is found in rare cases of ADPKD with early-onset renal disease. The gene responsible for ARPKD has been mapped to chromosome 6. There is no evidence of genetic heterogeneity [40].

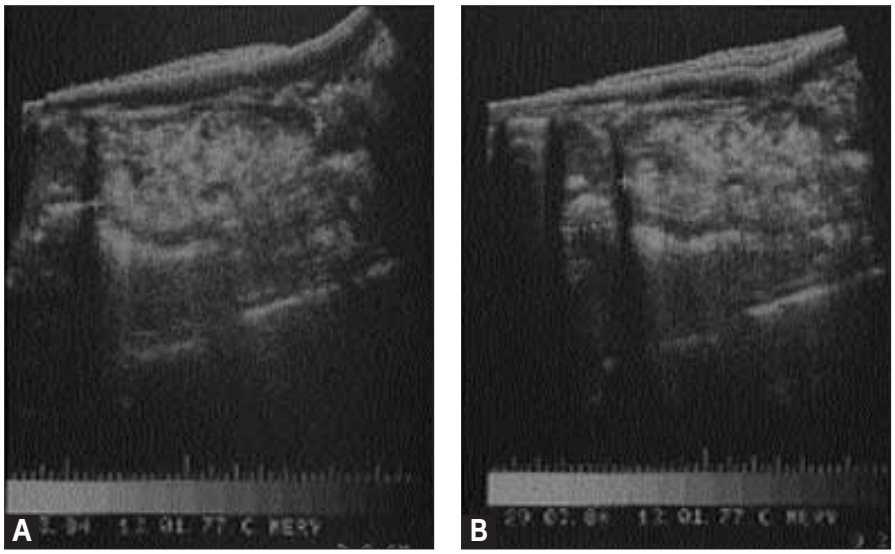

FIGURE 9-46

A and **B**, Autosomal-recessive polycystic kidney disease (ARPKD): renal imaging. On ultrasonography of a child with ARPKD the kidneys appear typically enlarged and uniformly hyperechogenic (owing to the presence of multiple small cysts), and demarcations of cortex, medulla, and sinus are lost. The ultrasonographic appearance is different in older children, because cysts can grow and become round; then they resemble the appearance of ADPKD. Figure 9-2 describes how to differentiate the two conditions. (*Courtesy of* P. Niaudet.)

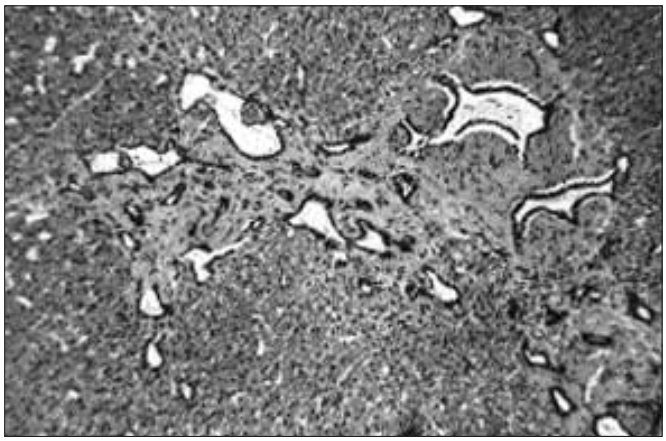

FIGURE 9-47

Autosomal-recessive polycystic kidney disease (ARPKD): liver histology. Liver biopsy specimen from a child with ARPKD shows typical congenital hepatic fibrosis (hematoxylin eosin safran [HES] stain). This portal space is enlarged by fibrosis, and the number of biliary channels is increased, many of them being enlarged and all being irregular in outline. (*Courtesy of* S. Gosseye.)

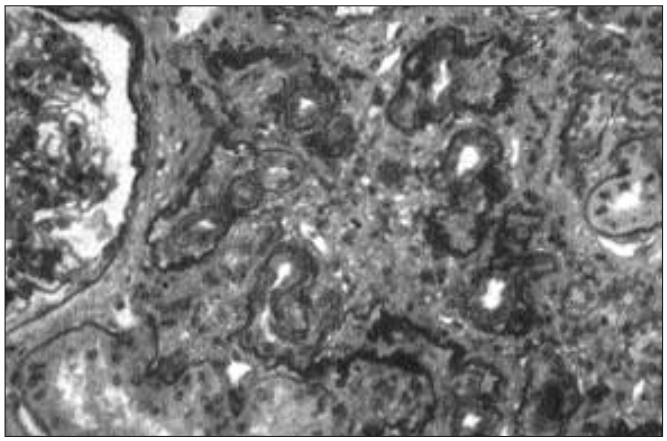

FIGURE 9-48

Nephronophthisis (NPH): renal involvement. Kidney biopsy specimen visualized by light microscopy with periodic acid–Schiff stain, in a patient with juvenile NPH of an early stage. Note the typical thickening and disruption of the tubular basement membrane (appearing in red); the histiolymphocytic infiltration present at this stage is progressively replaced by interstitial fibrosis.

NPH is an autosomal recessive disorder, accounting for 10% to 15% of all children admitted for end-stage renal failure. Although classified as a renal cystic disorder, NPH is characterized by chronic diffuse tubulointerstitial nephritis; the presence of cysts at the corticomedullary boundary (thus, the alternative term "medullary cystic disease," now preferably reserved for the autosomal-dominant form; *see* Fig. 9-43) is a late manifestation of the disease. Clinical features include early polyuria-polydypsia, unremarkable urinalysis, frequent absence of hypertension, and eventually, end-stage renal failure at a median age of 13 (range 3 to 23) years. Ultrasonographic features are summarized in Figure 9-2; medullary cysts are sometimes detected. Associated disorders are detailed in Figure 9-49. A gene called NPH1 that has been identified on chromosome 2 accounts for about 80% of cases [41, 42]. In two thirds of them, a large homozygous deletion is detected in this gene [43]. (*Courtesy of* P. Niaudet.)

NPH: EXTRARENAL INVOLVEMENT

- Retinitis pigmentosa (Senior-Loken syndrome)
- Multiple organ involvement, including
  - Liver fibrosis
  - Other rare features
    - Skeletal changes (cone-shaped epiphyses)
    - Cerebellar ataxia
    - Mental retardation

FIGURE 9-49

Nephronophthisis (NPH): extrarenal involvement. Extrarenal involvement occurs in 20% of NPH cases. The most frequent finding is tapetoretinal degeneration (known as Senior-Loken syndrome), which often results in early blindness or progressive visual impairment. Other rare manifestations include liver (hepatomegaly, hepatic fibrosis), bone (cone-shaped epiphysis), and central nervous system (mental retardation, cerebellar ataxia) abnormalities, quite often in association.

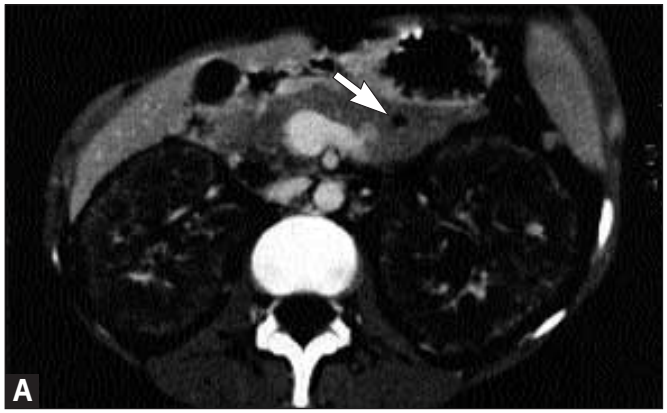

FIGURE 9-50

Orofaciodigital syndrome (OFD). Contrast-enhanced CT, **A**, and the hands, **B**, of a 26-year-old woman with OFD type 1 (OFD1) [43]. Multiple cysts involve both kidneys. Note that they are smaller and more uniform than in ADPKD and that renal contours are preserved. Some cysts were also detected in liver and pancreas (*arrow*). Syndactyly was surgically corrected, and the digits of the hands are shortened (brachydactyly).

OFD1 is a rare X-linked, dominant disorder, diagnosed almost exclusively in females, as affected males die in utero. Characteristic dysmorphic features include oral (hyperplastic frenulum, cleft tongue, cleft palate or lip, malposed teeth), facial (asymmetry, broad nasal root), and digit (syn-brachy-polydactyly) abnormalities. Mental retardation is present in about half the cases. Kidneys may be involved by multiple (usually small) cysts, mostly of glomerular origin; renal failure occurs between the second and the seventh decade of life. Recognition of the dysmorphic features is the key to the diagnosis [44, 45]. (*Courtesy of* F. Scolari.)

References

1. Fick GM, Gabow PA: Hereditary and acquired cystic disease of the kidney. *Kidney Int* 1994, 46:951–964.
2. Welling LW, Grantham JJ: Cystic and developmental diseases of the kidney. In *The Kidney*. Edited by Brenner M. Philadelphia:WB Saunders Company; 1996:1828–1863.
3. Pirson Y, Chauveau D, Grünfeld JP: Autosomal dominant polycystic kidney disease. In *Oxford Textbook of Clinical Nephrology*. Edited by Davison AM, Cameron JS, Grünfeld JP, *et al*. Oxford:Oxford University Press; 1998:2393–2415.
4. Ravine D, Gibson RN, Donlan J, Sheffield LJ: An ultrasound renal cyst prevalence survey: Specificity data for inherited renal cystic diseases. *Am J Kidney Dis* 1993, 22:803–807.
5. Levine E: Acquired cystic kidney disease. *Radiol Clin North Am* 1996, 34:947–964.
6. Sarasin FP, Wong JB, Levey AS, Meyer KB: Screening for acquired cystic kidney disease: A decision analytic perspective. *Kidney Int* 1995, 48:207–219.
7. Hildebrandt F, Jungers P, Grünfeld JP: Medullary cystic and medullary sponge renal disorders. In *Diseases of the Kidney*. Edited by Schrier RW, Gottschalk CW. Boston: Little Brown; 1997:499–520.
8. The European Polycystic Kidney Disease Consortium: The polycystic kidney disease 1 gene encodes a 14 kb transcript and lies within a duplicated region on chromosome 16. *Cell* 1994, 77:881–894.
9. Mochizuki T, Wu G, Hayashi T, *et al*.: PKD2, a gene for polycystic kidney disease that encodes an integral membrane protein. *Science* 1996, 272:1339–1342.
10. Hughes J, Ward CJ, Peral B, *et al*.: The polycystic kidney disease 1 (PKD1) gene encodes a novel protein with multiple cell recognition domains. *Nature Genet* 1995, 10:151–160.

11. Qian F, Germino FJ, Cai Y, *et al*.: PKD1 interacts with PKD2 through a probable coiled-coil domain. *Nature Genet* 1997, 16:179–183.
12. Germino GG: Autosomal dominant polycystic kidney disease: a two-hit model. *Hospital Pract* 1997, 81–102.
13. Grantham JJ: The etiology, pathogenesis, and treatment of autosomal dominant polycystic kidney disease: Recent advances. *Am J Kidney Dis* 1996, 28:788–803.
14. Devuyst O, Beauwens R: Ion transport and cystogenesis: The paradigm of autosomal dominant polycystic kidney disease. *Adv Nephrol* 1998, (in press).
15. Parfrey PS, Barrett BJ: Hypertension in autosomal dominant polycystic kidney disease. *Curr Opin Nephrol Hypertens* 1995, 4:460–464.
16. Gabow PA: Autosomal dominant polycystic kidney disease. *N Engl J Med* 1993, 329:332–342.
17. Torres WE, Wilson DM, Hattery RR, Segura JW: Renal stone disease in autosomal dominant polycystic kidney disease. *Am J Kidney Dis* 1993, 22:513–519.
18. Choukroun G, Itakura Y, Albouze G, *et al*.: Factors influencing progression of renal failure in autosomal dominant polycystic kidney disease. *J Am Soc Nephrol* 1995, 6:1634–1642.
19. Schievink WI, Torres VE, Wiebers DO, Huston J III: Intracranial arterial dolichoectasia in autosomal dominant polycystic kidney disease. *J Am Soc Nephrol* 1997, 8:1298–1303.
20. Torra R, Nicolau C, Badenas C, *et al*.: Ultrasonographic study of pancreatic cysts in autosomal dominant polycystic kidney disease. *Clin Nephrol* 1997, 47:19–22.
21. Schievink WI, Huston J III, Torres VA, Marsh WR: Intracranial cysts in autosomal dominant polycystic kidney disease. *J Neurosurg* 1995, 83:1004–1007.
22. Gabow PA: Autosomal dominant polycystic kidney disease—more than a renal disease. *Am J Kidney Dis* 1990, 16:403–413.
23. Schievink WI, Torres VE: Spinal meningeal diverticula in autosomal dominant polycystic kidney disease. *Lancet* 1997, 349:1223–1224.
24. Hateboer N, Dijk M, Torra R, *et al*.: Phenotype PKD2 vs. PKD1; results from the European concerted action. *J Am Soc Nephrol* 1997, 8:373A.
25. Chauveau D, Pirson Y, Le Moine A, *et al*.: Extrarenal manifestations in autosomal dominant polycystic kidney disease. *Adv Nephrol* 1997, 26:265–289.
26. Torres VE: Polycystic liver disease. In *Polycystic Kidney Disease*. Edited by Watson ML, Torres VE. Oxford: Oxford University Press; 1996:500–529.
27. Pirson Y, Chauveau D: Intracranial aneurysms in autosomal dominant polycystic kidney disease. In *Polycystic Kidney Disease*. Edited by Watson ML, Torres VE. Oxford:Oxford University Press; 1996:530–547.
28. Ravine D, Gibson RN, Walker RG, *et al*.: Evaluation of ultrasonographic diagnostic criteria for autosomal dominant polycystic kidney disease 1. *Lancet* 1994, 343:824–827.
29. Pirson Y, Christophe JL, Goffin E: Outcome of renal replacement therapy in autosomal dominant polycystic kidney diseases. *Nephrol Dial Transplant* 1996, 11 (suppl. 6):24–28.
30. Culleton B, Parfrey PS: Management of end-stage renal failure and problems of transplantation in autosomal dominant polycystic kidney disease. In *Polycystic Kidney Disease*. Edited by Watson ML, Torres VE. Oxford:Oxford University Press; 1996:450–461.
31. Torres VE: Tuberous sclerosis complex. In *Polycystic Kidney Disease*. Edited by Watson ML, Torres VE. Oxford:Oxford University Press; 1996:283–308.
32. Huson SM, Rosser EM: The Phakomatoses. In *Principles and Practice of Medical Genetics*. Edited by Rimoin DL, Connor JM, Pyeritz RE. New York:Churchill Livingstone; 1997: 2269–2302.
33. Sampson JR, Maheshwar MM, Aspinwall R, *et al*.: Renal cystic disease in tuberous sclerosis: Role of the polycystic kidney disease 1 gene. *Am J Human Genet* 1997, 61:843–851.
34. Jones AC, Daniells CE, Snell RG, *et al*.: Molecular genetic and phenotypic analysis reveals differences between TSC1 and TSC2 associated familial and sporadic tuberous sclerosis. *Hum Molec Genet* 1997, 6:2155–2161.
35. Michels V: Von Hippel-Lindau disease. In *Polycystic Kidney Disease*. Edited by Watson ML, Torres VE. Oxford:Oxford University Press; 1996:309–330.
36. Neumann HPH, Zbar B: Renal cysts, renal cancer and von Hippel-Lindau disease. *Kidney Int* 1997, 51:16–26.
37. Chauveau D, Duvic C, Chretien Y, *et al*.: Renal involvement in von Hippel-Lindau disease. *Kidney Int* 1996, 50:944–951.
38. Sharp CK, Bergman SM, Stockwin JM, *et al*.: Dominantly transmitted glomerulocystic kidney disease: A distinct genetic entity. *J Am Soc Nephrol* 1997, 8:77–84.
39. Gagnadoux MF, Broyer M: Polycystic kidney disease in children. In *Oxford Textbook of Clinical Nephrology*. Edited by Davison AM, Cameron JS, Grünfeld JP, *et al*. Oxford:Oxford University Press; 1998:2385–2393.
40. Zerres K, Mücher G, Bachner L, *et al*.: Mapping of the gene for autosomal recessive polycystic kidney disease (ARPKD) to chromosome 6p21-cen. *Nature Genet* 1994, 7:429–432.
41. Antignac C, Arduy CH, Beckmann JS, *et al*.: A gene for familial juvenile nephronophthisis (recessive medullary cystic kidney disease) maps to chromosome 2p. *Nature Genet* 1993, 3:342–345.
42. Hildebrandt F, Otto E, Rensing C, *et al*.: A novel gene encoding an SH3 domain protein is mutated in nephronophthisis type 1. *Nature Genet* 1997, 17:149–153.
43. Konrad M, Saunier S, Heidet L, *et al*.: Large homozygous deletions of the 2q13 region are a major cause of juvenile nephronophthisis. *Hum Molec Genet* 1996, 5: 367–371.
44. Scolari F, Valzorio B, Carli O, *et al*.: Oral-facial-digital syndrome type I: An unusual cause of hereditary cystic kidney disease. *Nephrol Dial Transplant* 1997, 12:1247–1250.
45. Feather SA, Winyard PJD, Dodd S, Woolf AS: Oral-facial-digital syndrome type 1 is another dominant polycystic kidney disease: Clinical, radiological and histopathological features of a new kindred. *Nephrol Dial Transplant* 1997, 12:1354–1361.

Toxic Nephropathies

Jean-Louis Vanherweghem

Tubular interstitial structures of the kidney are particularly vulnerable in face of toxic compounds. High concentration of the toxics in de medulla as well as medullary hypoxia and renal hypoperfusion could explain this particularity. Clinical nephrotoxicity involves toxins of diverse origin. The culprits are often registered and non registered drugs either prescribed or purchased over the counter. Other major causes result from occupational and industrial exposures. Sometimes, the identification of the nephrotoxin requires astuteness and long investigations especially in cases of environmental toxins or prolonged intake of unregulated drugs or natural products. A correct diagnosis of the causes is, however, the key for future prevention of renal diseases. The diagnosis of "chronic interstitial nephritis of unknown origin" should, therefore, no longer be used.

CHAPTER

10

Exposure to Nephrotoxins

TOXIC CAUSES OF CHRONIC TUBULOINTERSTITIAL RENAL DISEASES

Metals (Environmental or Occupational Exposure)
- Lead
- Cadmium

Drugs or Additives (Use, Misuse, or Abuse)
- Lithium
- Germanium
- Analgesics
- Cyclosporine
- Mesalazine

Fungus and Plant Toxins (Environmental or Iatrogenic Exposure)
- Ochratoxins
- Aristolochic acids

FIGURE 10-1

Chronic exposure to drugs, occupational hazards, or environmental toxins can lead to chronic interstitial renal diseases. The following are the major causes of chronic interstitial renal diseases: occupational exposure to heavy metals; abuse of over-the-counter analgesics; misuse of germanium; chronic intake of mesalazine for intestinal disorders, lithium for depression, and cyclosporine in renal and nonrenal diseases; and environmental or iatrogenic exposure to fungus or plant nephrotoxins (ochratoxins, aristolochic acids).

Exposure to Metals

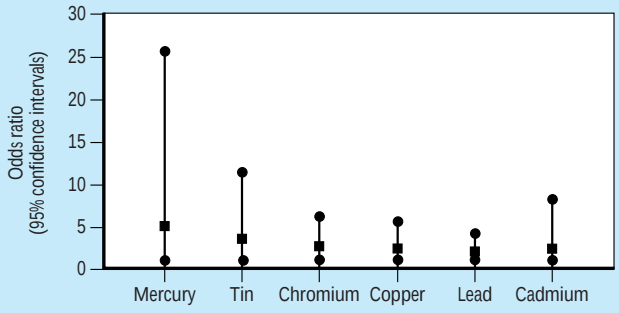

	Odds ratio	C1 >	C1 <
Mercury	5130	1020	25,700
Tin	3720	1220	11,300
Chromium	2770	1210	6330
Copper	2540	1160	5530
Lead	2110	1230	4360
Cadmium	2200	900	8250

FIGURE 10-2

Occupational exposure to metals and risks for chronic renal failure. Comparison of the occupational histories of 272 patients with chronic renal failure with those of a matched control group having normal renal function has shown an increased risk of chronic renal failure after exposure to mercury, tin, chromium, copper, and lead. In this study the increased risk with exposure to cadmium was not statistically significant. *Squares* indicate odds ratios; *circles* indicate CIs. (*Adapted from* Nuyts and coworkers [1]; with permission.)

Lead nephropathy

CAUSES OF LEAD NEPHROPATHY

Environmental
- Eating paint from lead-painted furniture, woodwork, and toys in children
- Lead-contaminated flour
- Home lead-contaminated drinking water from lead pipes
- Drinking of moonshine whiskey

Occupational
- Lead-producing plants: lead smelters, battery plants

FIGURE 10-3

Lead nephropathy associated with environmental and occupational exposure. Epidemiologic observations have established the relationship between lead exposure and renal failure in association with children eating lead paint in their homes, chronic ingestion of lead-contaminated flour, lead-loaded drinking water in homes, and drinking of illegal moonshine whiskey [2,3]. Occupational exposure in lead-producing industries also has been associated with a higher incidence of renal dysfunction.

CLINICAL MANIFESTATIONS OF LEAD NEPHROPATHY

Gout
Arterial hypertension
Renal failure (interstitial type)

FIGURE 10-4

Gout and hypertension are the major clinical manifestations of lead nephropathy. The prominent feature of early hyperuricemia in lead nephropathy may explain the confusion between lead nephropathy and gout nephropathy. Lead urinary excretion after ethylenediamine tetraacetic acid (EDTA)–lead mobilization testing may help with the correct diagnosis [3].

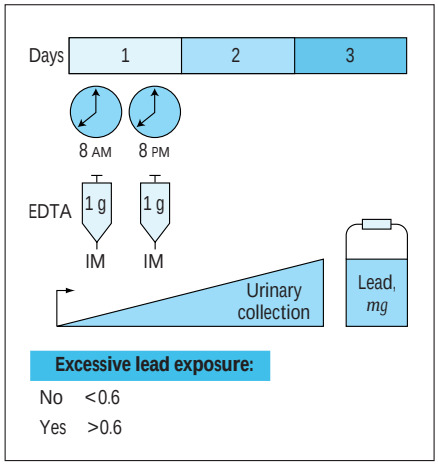

FIGURE 10-5

Ethylenediamine tetraacetic acid (EDTA)–lead mobilization test in lead nephropathy. EDTA (calcium disodium acetate) for detecting lead nephropathy. This test consists of a 24-hour urinary lead excretion over 3 consecutive days after administration of 2 g of EDTA by intramuscular route on the first day in divided doses 12 hours apart. Persons without excessive lead exposure excrete less than 0.6 mg of lead during the day after receiving 2 g of EDTA parenterally. In the presence of renal failure, the excretion is delayed; however, the cumulative total remains less than 0.6 mg over 3 days (*From* Batuman and coworkers [3]; with permission.)

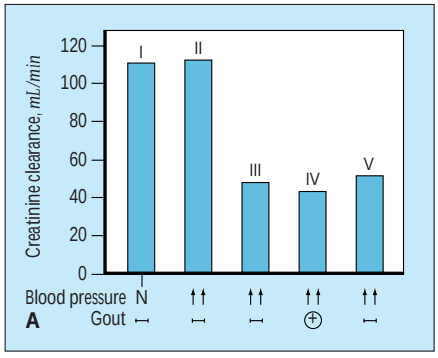

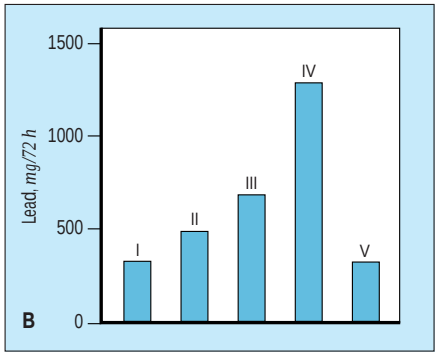

FIGURE 10-6

Ethylenediamine tetraacetic acid (EDTA)–lead mobilization test in chronic renal failure of uncertain origin (**A–C**). In a study of 296 patients without history of lead exposure, the results of this test were abnormal in 15.4% (II) of patients with hypertension and normal renal function and in 56.1% of patients with renal failure of uncertain origin (in 44.1% of the patients without associated gout (III) and in 68.7% of the patients with associated gout (IV), respectively).

(Continued on next page)

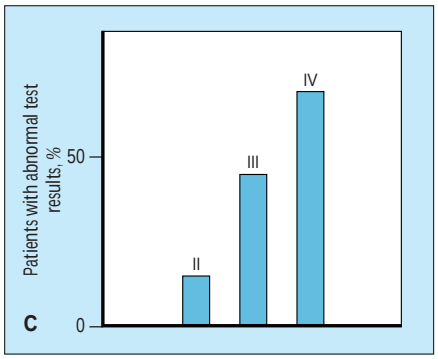

FIGURE 10-6 *(Continued)*
The EDTA–lead mobilization test was normal in normotensive subjects with normal renal function and in patients with chronic renal failure (I) of well-known origin (V). (*Adapted from* Sanchez-Fructuoso and coworkers [4].)

Cadmium nephropathy

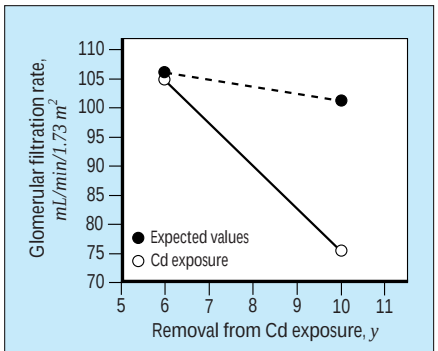

Graph values	I	II	III	IV
NEP	43	53	50	76
CC16	16	17	25	124
RBP	80	122	132	594
ß$_2$-m	73	112	102	834

FIGURE 10-7
Decrease in renal function after 25-year exposure to cadmium (Cd). In workers exposed to cadmium for an average time of 25 years, a progressive decrease in renal function occurs during a 5-year follow-up period, despite removal from cadmium exposure 10 years earlier. On average, the glomerular filtration rate was shown to be decreased to 31 mL/min/1.73 m^2 after 5 years instead of the expected age-related value of 5 mL/min/1.73 m^2. (*Adapted from* Roels and coworkers [5].)

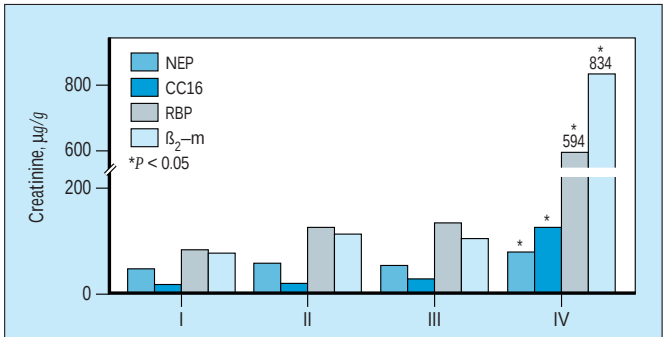

	I	II	III	IV
Creatinine clearance, *mL/min*	103	103	90*	79*
Urinary Cd, µg/g/creatinine	0.55	1.34	3.28*	8.45*

FIGURE 10-8
Tubular markers in cadmium workers. Impairment of renal proximal tubular epithelium induced by cadmium can be documented by an increase in urinary excretion of urinary neutral endopeptidase 24.11 (NEP), an enzyme of the proximal tubule brush borders, as well as by an increase in microproteinuria: Clara cell protein (CC16), retinol-binding protein (RBP) and β_2-microglobulin (β_2-m). The data were obtained from 106 healthy persons working in cadmium smelting plants. These markers could be used for the screening of cadmium workers. (*Adapted from* Nortier and coworkers [6].)

Lithium nephropathy

LITHIUM NEPHROTOXICITY

Reversible polyuria and polydipsia
Persistent nephrogenic diabetes insipidus
Incomplete distal tubular acidosis
Chronic renal failure (chronic interstitial fibrosis)

FIGURE 10-9
Lithium acts both distally and proximally to antidiuretic hormone–induced generation of cyclic adenosine monophosphatase. Polyuria and polydipsia can occur in up to 40% of patients on lithium therapy and are considered harmless and reversible. However, nephrogenic diabetes insipidus may persist months after lithium has been discontinued [7]. Lithium also induces an impairment of distal urinary acidification. Chronic renal failure secondary to chronic interstitial fibrosis may appear in up to 21% of patients on maintenance lithium therapy for more than 15 years [8]. However, these observations are still a matter of debate [7].

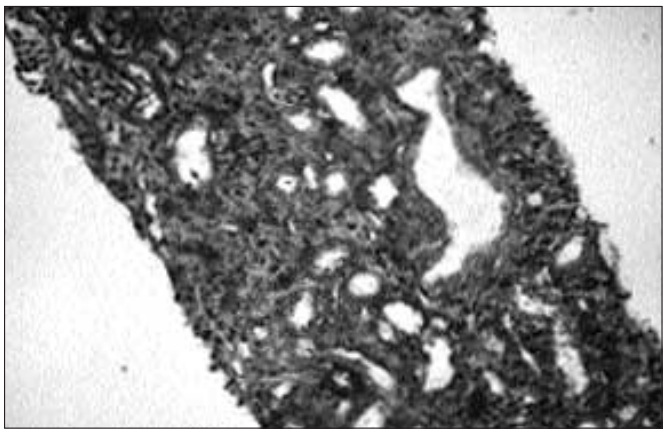

FIGURE 10-10 (*see* Color Plate)
Lithium nephropathy. A 22-year-old female patient was on maintenance lithium therapy (lithium carbonate 750 mg/d) for 5 years. She presented with polyuria (6500 mL/d) and moderate renal failure (creatinine clearance, 60 mL/min). Proteinuria was not present, and the urinary sediment was unremarkable. A renal biopsy showed focal interstitial fibrosis with scarce inflammatory cell infiltrate, tubular atrophy, and characteristic dilated tubule (microcyst formation). Half of the glomeruli (not shown) were sclerotic. (Magnification × 125, periodic acid–Schiff reaction.)

Germanium nephropathy

CIRCUMSTANCES OF CHRONIC RENAL FAILURE SECONDARY TO GERMANIUM SUPPLEMENTS

Ge-dioxyde elixir, food additives, or capsules (used to improve health in normal persons [Japan])
Ge-lactate-citrate (used to rebuild the immune system) in patients with HIV infection (Switzerland)
Ge-lactate-citrate (used to improve health) in patients with cancer (the Netherlands)
Ge-dioxyde elixir (used to restore health) in patients with chronic hepatitis (Japan)

FIGURE 10-11
Germanium (atomic number, 32; atomic weight, 72.59) is contained in soil, plants, and animals as a trace metal. It is widely used in the industrial fields because of its semiconductive capacity. The increased use of natural remedies and trace elements to protect, improve, or restore the health has lead regular supplementation with germanium salts either through food addition or by the means of elixirs and capsules. The chronic supplementation by germanium salts was at the origin of the development of chronic renal failure secondary to a tubulointerstitial nephritis [9–12].

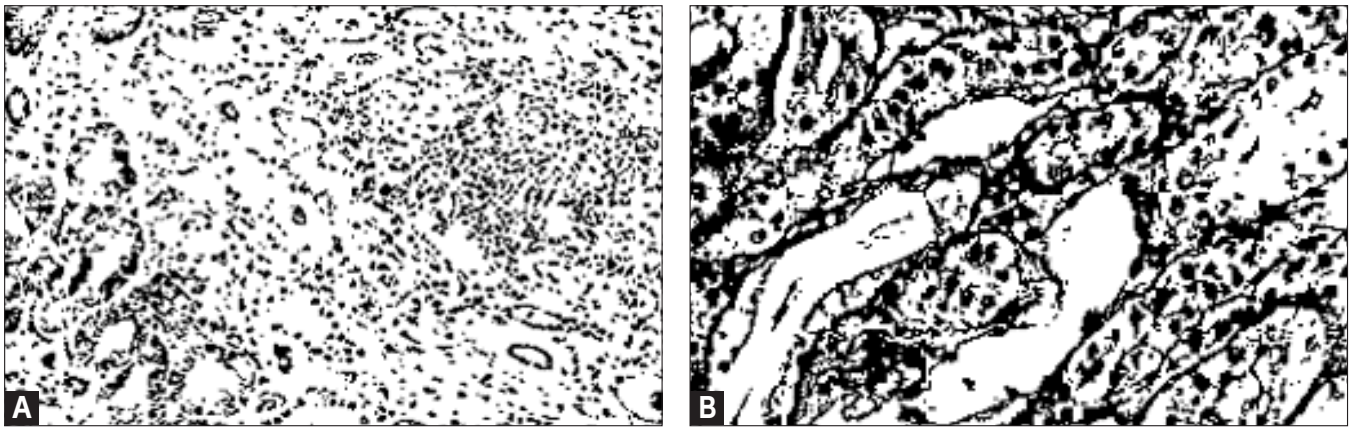

FIGURE 10-12

Light microscopy of renal tissue in a patient with chronic renal failure secondary to the chronic intake of germanium, showing focal tubular atrophy and focal interstitial lymphocyte infiltration. **A,** Hematoxylin and eosin stain. (Magnification × 162.) Renal tubular epithelial cells show numerous dark small inclusions. **B,** Periodic acid–Schiff reaction. (Magnification, × 350). (*From Hess* and coworkers [12]; with permission).

Exposure to Analgesics

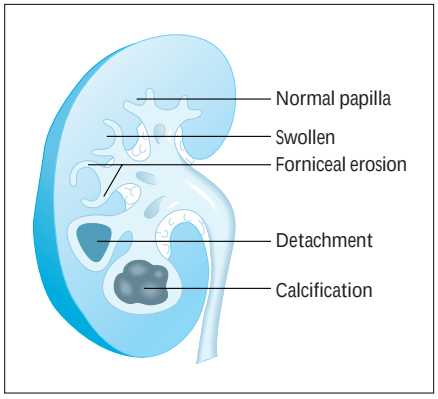

FIGURE 10-13

Analgesic nephropathy and papillary necrosis. The characteristic feature of analgesic nephropathy is the papillary necrosis process that begins with swollen papillae and continues with forniceal erosion, detachment, and calcification of necrotic papillae.

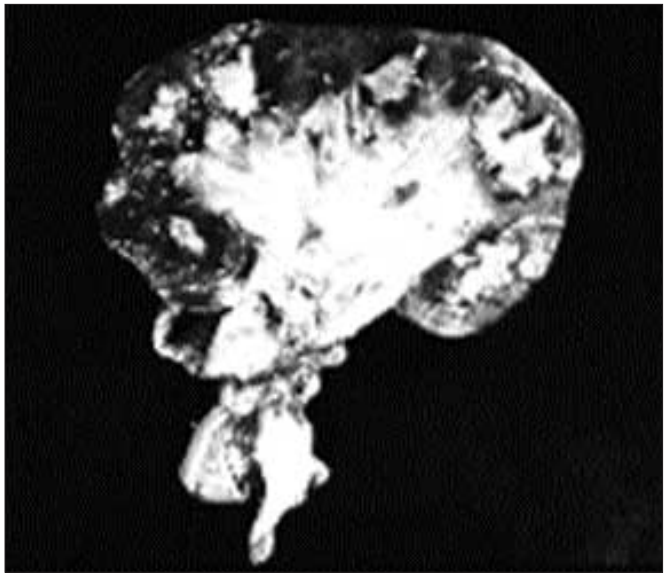

FIGURE 10-14

Pathology of analgesic nephropathy. Nephrectomy showing a kidney reduced in size with necrosed and calcified papillae.

FIGURE 10-15

Radiologic appearance of papillary necrosis in analgesic nephropathy. The pyelogram was obtained by pyelostomy. It shows a swollen papilla (upper calyx), forniceal erosions (middle calyx), and detachment of papilla, or *filling defect* (lower calyx).

CLINICAL FEATURES OF ANALGESIC NEPHROPATHY

Daily consumption of analgesic mixtures	100%
Women	80%
Headache	80%
Gastrointestinal disturbances	35–40%
Urinary tract infection	30–48%
Papillary necrosis (clinical)	20%
Papillary calcifications (computed tomography scan)	65%

FIGURE 10-16

Classic analgesic nephropathy is a slowly progressive disease resulting from the daily consumption over several years of mixtures containing analgesics usually combined with caffeine, codeine, or both. Caffeine and codeine create psychological dependence. Most cases of analgesic nephropathy occur in women. In 80% of the cases, analgesics were taken for persistent headache. Gastrointestinal complaints are also frequent, as are urinary tract infections. Evidence of clinical papillary necrosis (fever and pain) is present in 20% of cases. Calcifications of papillae (detected by computed tomography scan) are present in 65% of persons who abuse analgesics [13].

EPIDEMIOLOGY OF ANALGESIC NEPHROPATHY AMONG ESRD PATIENTS

Australia	20%
Belgium	18%
Canada	6%
Germany	15%
South Africa	22%
Switzerland	20%
United Kingdom	1%
United States	5%

FIGURE 10-17

Worldwide epidemiology of analgesic nephropathy. The frequency of analgesic nephropathy in patients with end-stage renal diseases (ESRD) varies greatly within and among countries [14–16]. The highest prevalence rates of end-stage renal disease from analgesic nephropathy occur in South Africa (22%), Switzerland and Australia (20%), Belgium (18%), and Germany (15%). In Belgium, the prevalence is 36% in the north and 10% in the south. In Great Britain, the rate is 1% nationwide; in Scotland it is 26%. In United States, the rate is 5% nationwide, 13% in North Carolina, and 3% in Washington, DC. In Canada, the rate is 6% nationwide.

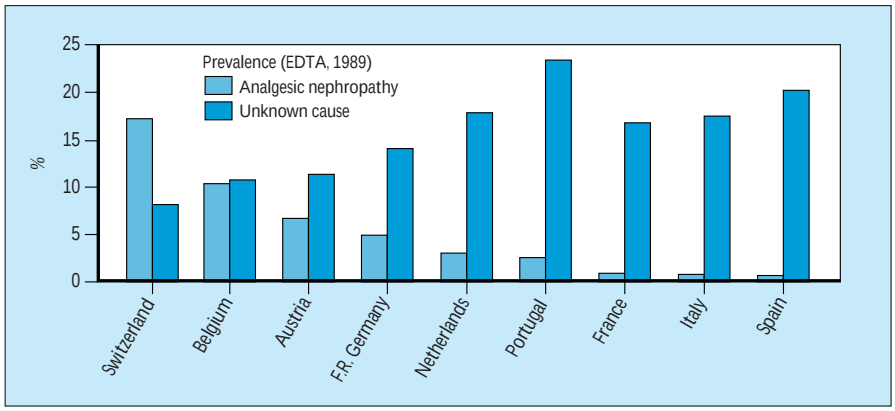

FIGURE 10-18

Prevalence of analgesic nephropathy versus nephropathy with unknown cause. Cross-national comparisons in Europe indicate that the proportion of cases of end-stage renal disease attributed to analgesics varies considerably; however, it is inversely proportional to unknown causes. These findings suggest an underestimation of the prevalence of analgesic nephropathy in several countries, probably owing to the lack of well-defined criteria for diagnosis [13,15]. EDTA—European Dialysis and Transplant Association. (*From* Elseviers and coworkers [13]; with permission).

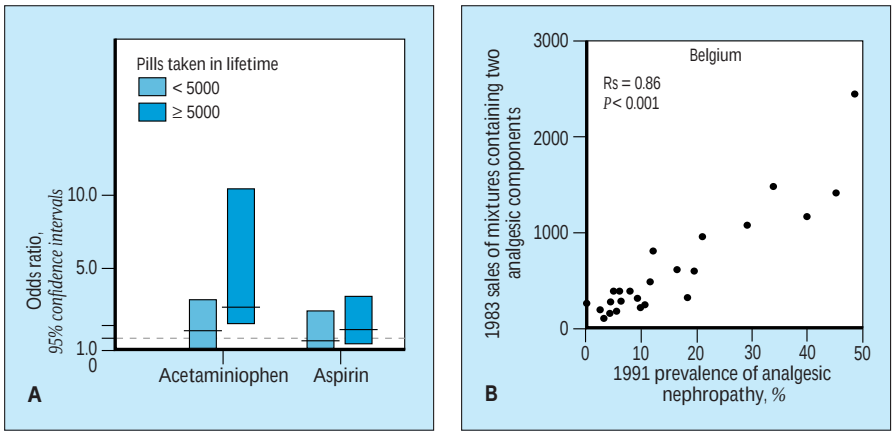

FIGURE 10-19

Risk of analgesic nephropathy associated with specific types of analgesics. The initial reports of analgesic nephropathy chiefly concerned phenacetin mixtures. Phenacetin has been replaced with acetaminophen in analgesia mixtures without significant changes in the cause of analgesic nephropathy in some countries [15]. **A**, The risk factor for end-stage renal disease of unknown cause is increased in relationship to the cumulative intake of acetaminophen as well as nonsteroidal anti-inflammatory drugs but not to aspirin. Moreover, mixtures containing several analgesic compounds were shown to be more nephrotoxic than are simple drugs. **B**, In Belgium, the prevalence of analgesic nephropathy in 1991 was strongly correlated with sales of analgesic mixtures in 1983. Rs—coefficient of correlation. (**A**, *Adapted from* Perneger and coworkers [17]; **B**, *adapted from* Elseviers and De Broe [18]; with permission).

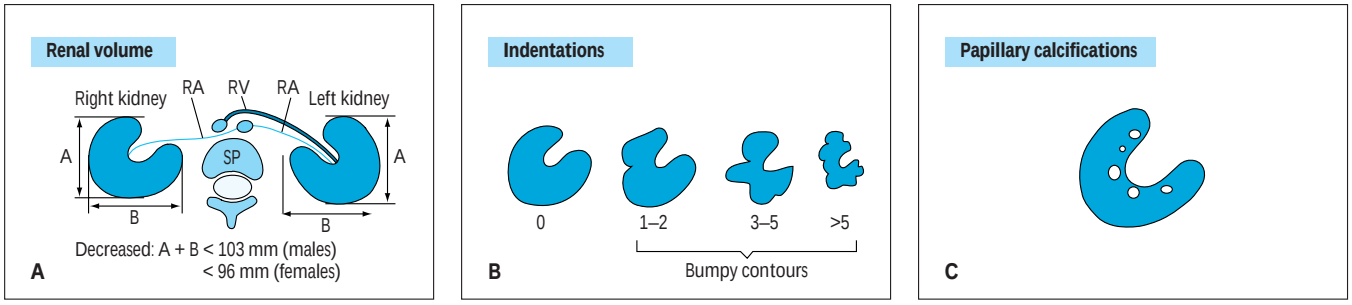

D. PERCENTAGES OF SENSITIVITY AND SPECIFICITY

Criteria	Sensitivity, %	Specificity, %
Decrease in renal size	95	10
Bumpy contours	50	90
Papillary calcifications	87	97

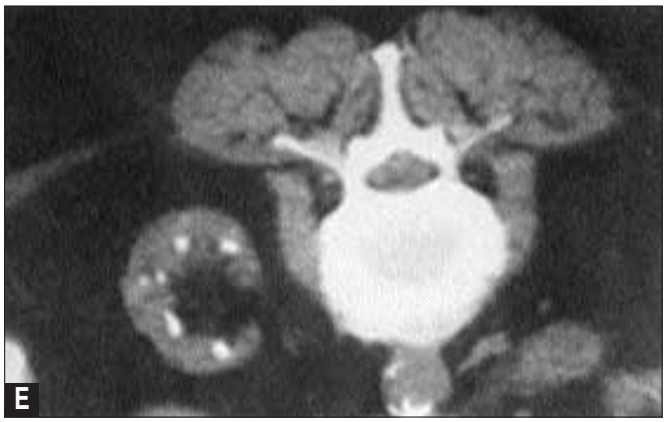

FIGURE 10-20

High performance of computed tomography (CT) scan for diagnosing analgesic nephropathy. Three criteria may be used to diagnose analgesic nephropathy by CT scan: decrease in renal size, measured by the sum of both sides of the rectangle enclosing the kidney at the level of the renal vessels (**A**); indentations counted at the level at which most indentations are present (more than three are qualified of bumpy contours) (**B**); and papillary calcifications (**C**). Percentages of sensitivity and specificity are given for the three criteria (**D**). Example of papillary calcifications on CT scan (**E**). RA—renal artery; RV—renal vein; SP—spine. (*Adapted from* Elseviers and De Broe [19]; with permission).

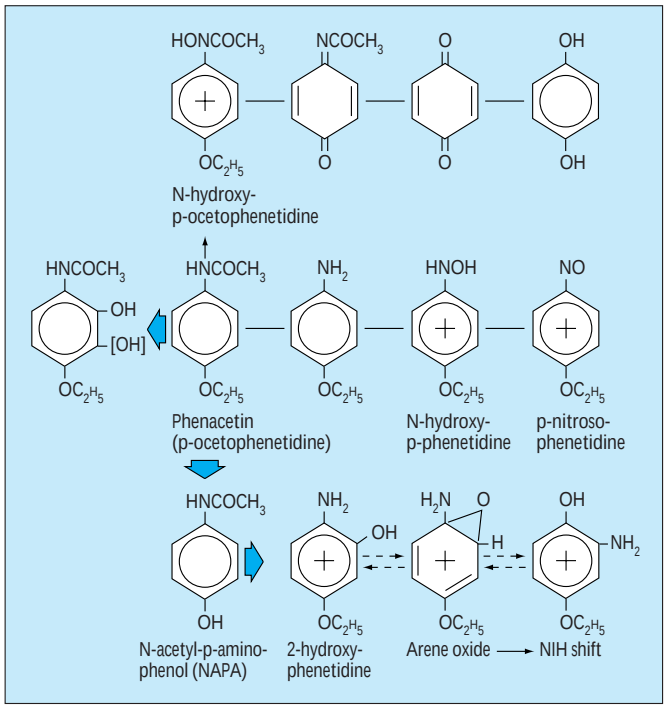

FIGURE 10-21

Malignancies of the urinary tract and their association with analgesic nephropathy. Malignancies of the renal pelvis and ureters were reported in up to 9% of patients with analgesic nephropathy. This high prevalence can be explained by the appearance of carcinogenic substances in the major pathways of the metabolism of phenacetin. Probable carcinogenic substances are indicated by a *plus* sign.

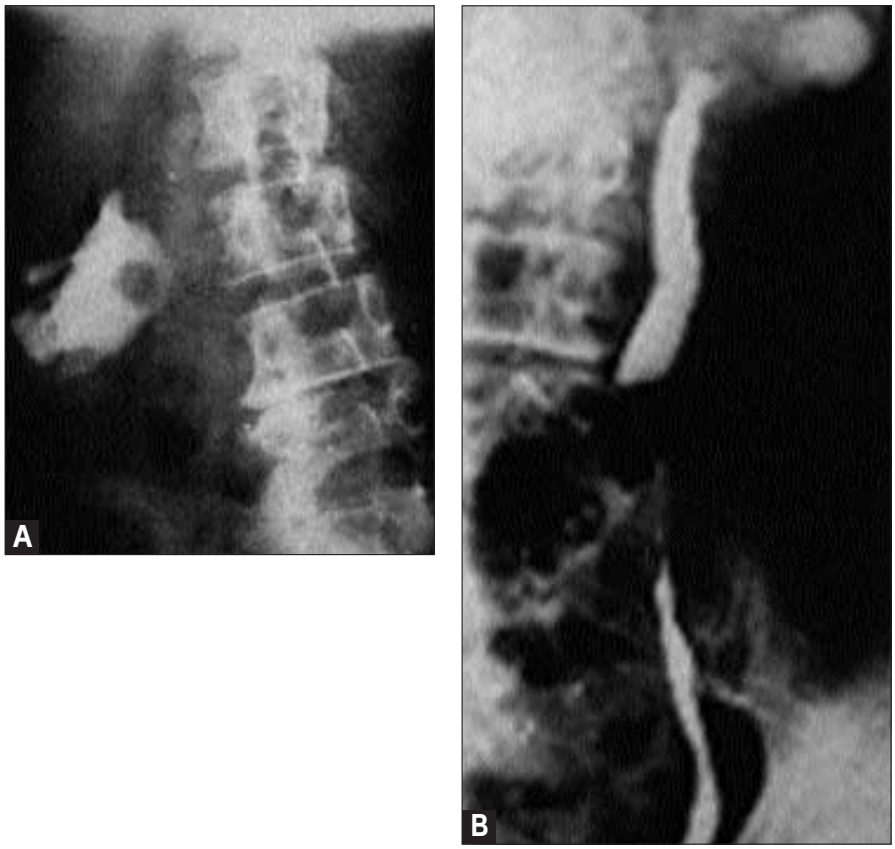

FIGURE 10-22

Malignant uroepithelial tumors of the upper urinary tract in patients with analgesic nephropathy. **A,** Pyelogram showing a filling defect, indicating a tumor of the renal pelvis. **B,** Retrograde pyelography showing a long malignant stricture of the ureter, causing ureteral dilation and hydronephrosis. (*Courtesy of* W Lornoy, MD, OL Vrouwziekenhuis, MD.)

Exposure to Cyclosporine

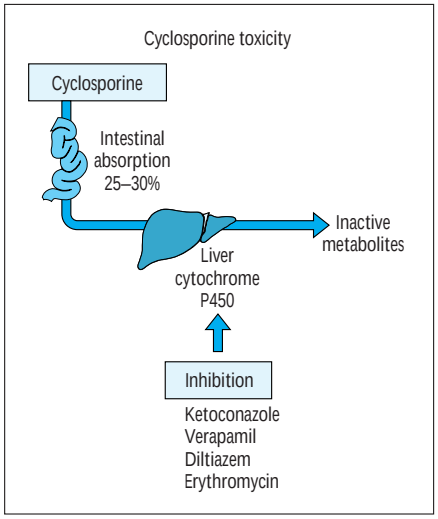

FIGURE 10-23

Toxicity of cyclosporine. Cyclosporine is a neutral fungal hydrophobic 11-amino acid cyclic polypeptide. Cyclosporine is metabolized by hepatic cytochrome P450 to multiple less active and less toxic metabolites. Drugs that inhibit cytochrome P450 enzymes such as ketoconazole, verapamil, diltiazem, and erythromycin increase the concentration of cyclosporine and may thus precipitate renal side effects [20,21].

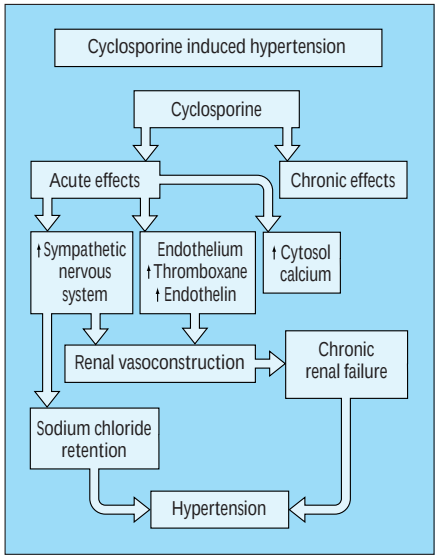

FIGURE 10-24

Cyclosporine and hypertension. Hypertension can develop in 10% to 80% of patients treated with cyclosporine, depending on dosage and length of the exposure. Cyclosporine increases cytosol calcium and, thus, enhances arteriolar smooth muscle responsiveness to vasoconstrictive stimuli. Vasoconstrictive effects of cyclosporine also are mediated by enhanced thromboxane action, sympathetic nerve stimulation, and release of endothelin. Renal vasoconstriction results in salt retention and hypertension. In chronic exposure to cyclosporine, hypertension also is a part of cyclosporine-induced chronic renal failure [22].

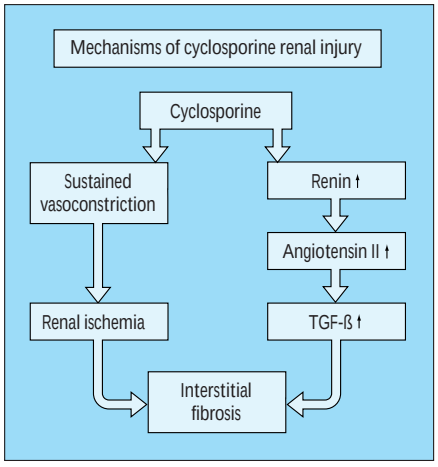

FIGURE 10-25

Pathogenesis of cyclosporine nephropathy. Chronic administration of cyclosporine may induce sustained renal vasoconstriction. Impairment of renal blood flow leads to tubulointerstitial fibrosis. Cyclosporine increases the recruitment of renin-containing cells along the afferent arteriole. Hyperplasia of the juxtaglomerular apparatus increases angiotensin II levels that, in turn, stimulate tumor growth factor-β (TGF-β) secretion, resulting in interstitial fibrosis [20].

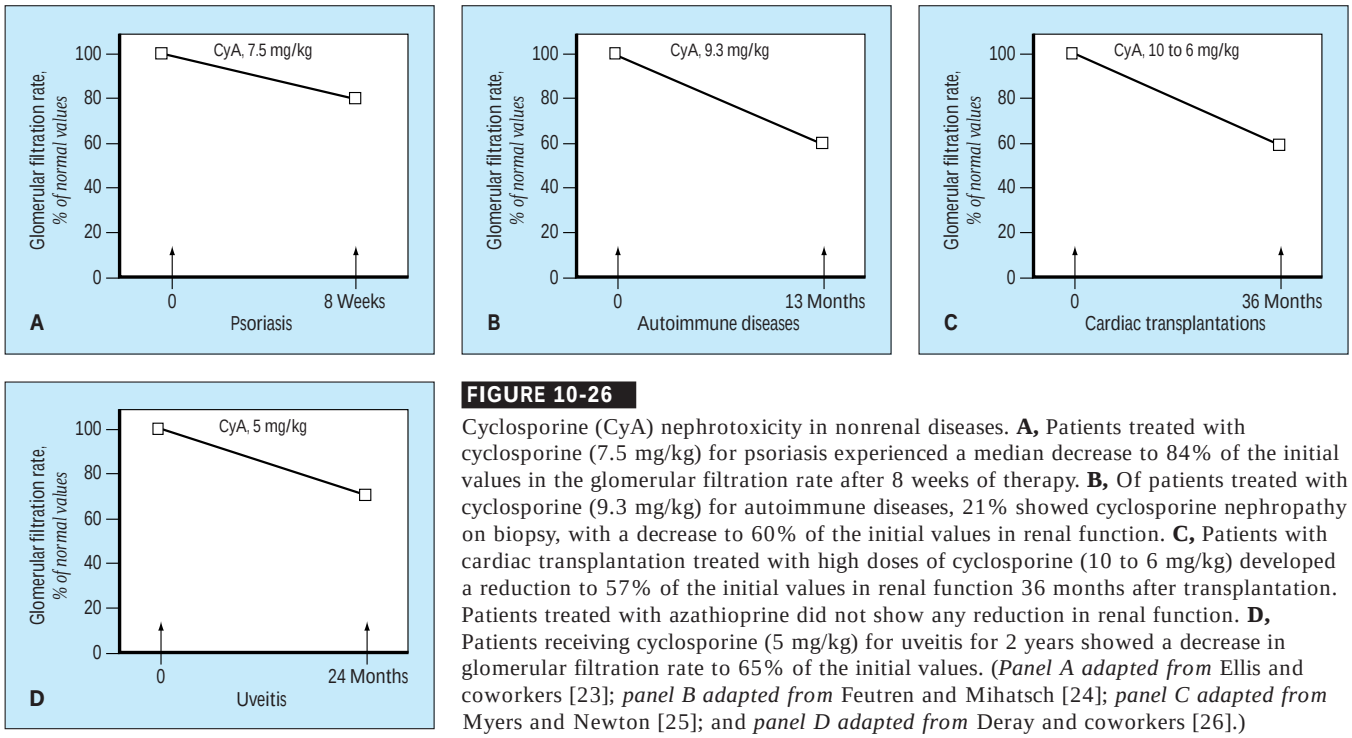

FIGURE 10-26

Cyclosporine (CyA) nephrotoxicity in nonrenal diseases. **A,** Patients treated with cyclosporine (7.5 mg/kg) for psoriasis experienced a median decrease to 84% of the initial values in the glomerular filtration rate after 8 weeks of therapy. **B,** Of patients treated with cyclosporine (9.3 mg/kg) for autoimmune diseases, 21% showed cyclosporine nephropathy on biopsy, with a decrease to 60% of the initial values in renal function. **C,** Patients with cardiac transplantation treated with high doses of cyclosporine (10 to 6 mg/kg) developed a reduction to 57% of the initial values in renal function 36 months after transplantation. Patients treated with azathioprine did not show any reduction in renal function. **D,** Patients receiving cyclosporine (5 mg/kg) for uveitis for 2 years showed a decrease in glomerular filtration rate to 65% of the initial values. (*Panel A adapted from* Ellis and coworkers [23]; *panel B adapted from* Feutren and Mihatsch [24]; *panel C adapted from* Myers and Newton [25]; and *panel D adapted from* Deray and coworkers [26].)

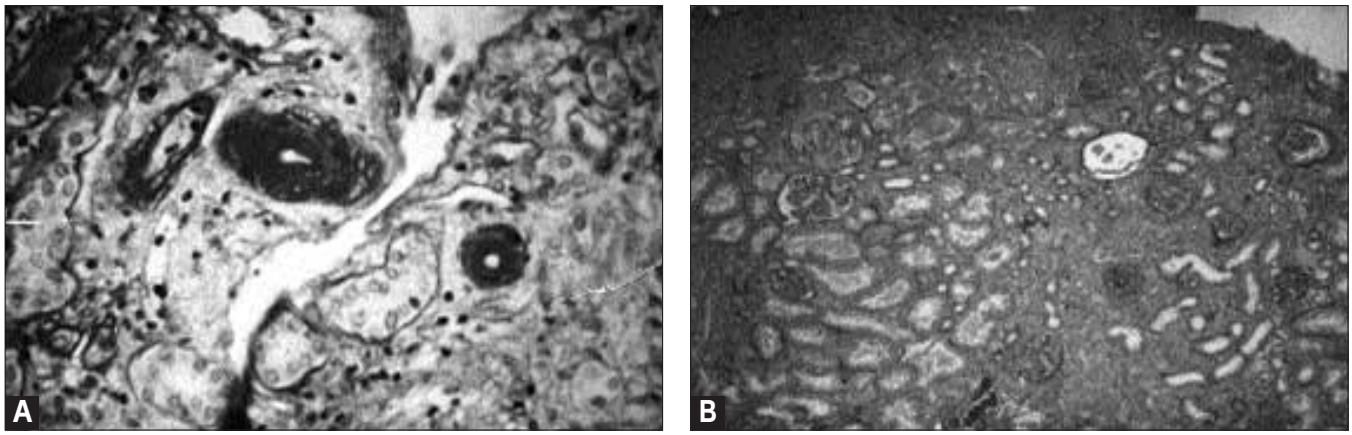

FIGURE 10-27

Morphology of cyclosporine nephropathy on renal biopsy of a patient with cardiac transplantation. Two different types of lesions are seen in cyclosporine nephropathy. **A,** Arteriolopathy: Hyalin, paucicellular thickening of the intima with focal wall necrosis results in narrowing of the vascular lumen (magnification × 300 periodic acid–Schiff reaction). **B,** A striped form of interstitial fibrosis characterized by irregularly distributed areas of stripes of interstitial fibrosis and tubular atrophy in the renal cortex. Tubules in other areas were normal (magnification x 100 periodic acid–Schiff reaction).

Exposure to Aminosalicylic Acid

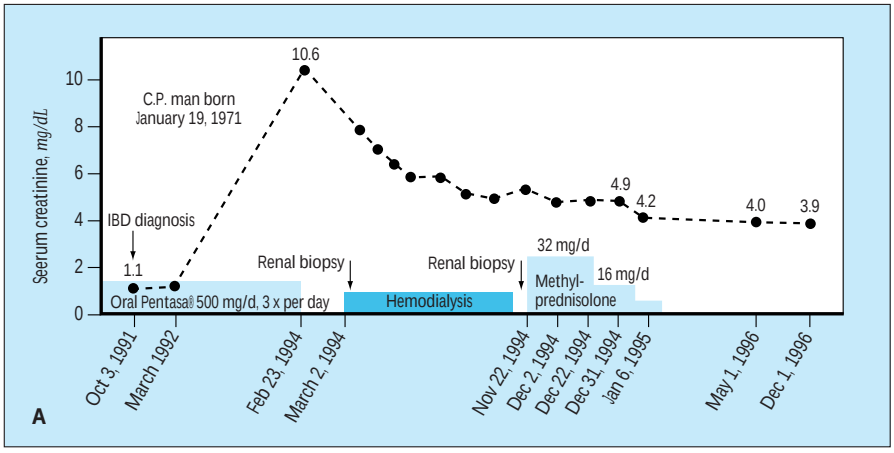

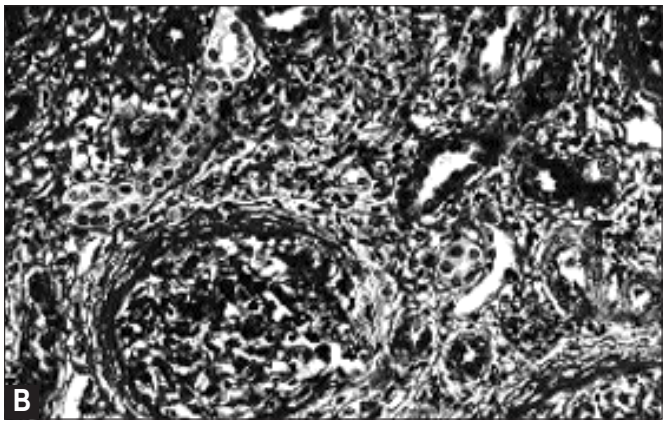

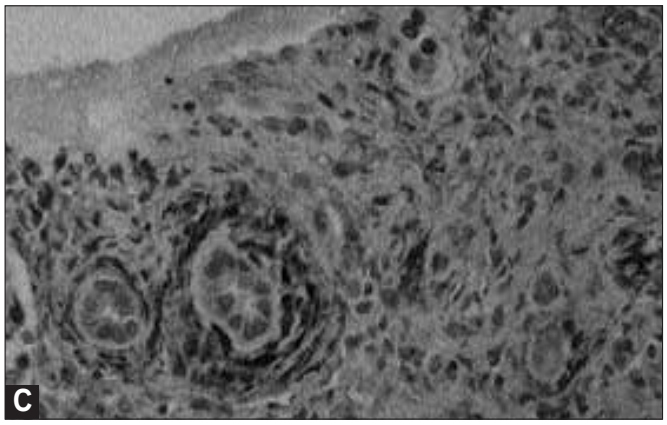

FIGURE 10-28

Aminosalicylic acid and chronic tubulointerstitial nephritis. **A**, A 36-year-old man suffering from Crohn's disease exhibited severe renal failure after 23 months of treatment with 5-aminosalicylic acid (5-ASA, or Pentasa, Hoechst Marion Roussel, Kansas City, MO). **B,** The first renal biopsy showing widening and massive cellular infiltration of the interstitium, tubular atrophy, and relative spacing of glomeruli. **C**, The second renal biopsy 8 months, after discontinuation of the drug and moderate improvement of the renal function, again showing important cellular infiltration of the interstitium tubular atrophy, and fibrosis. Several atrophic tubules are surrounded by one or more layers of α-smooth muscle actin positive cells. The patient had normal renal function on beginning treatment with 5-ASA. After 5 years of 5-ASA therapy, the patient demonstrated severe impaired renal function. The association between the use of 5-ASA and development of chronic tubulointerstitial nephritis in patients with inflammatory bowel disease (IBD) has gained recognition in recent years [27,28]. (*Courtesy of* ME De Broe, MD.)

Exposure to Ochratoxins

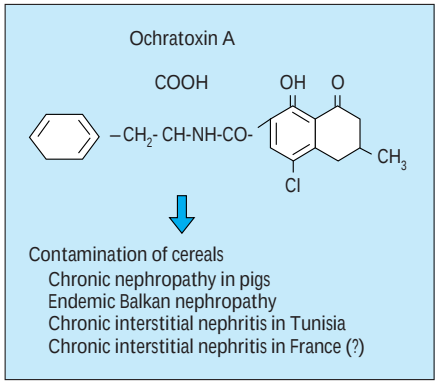

FIGURE 10-29

Ochratoxin nephropathy. Ochratoxin A is a mycotoxin produced by various species of Aspergillus and Penicillium. Ochratoxins contaminate foods (mainly cereals) for humans as well as for cattle. Ochratoxins are mutagenic, oncogenic, and nephrotoxic. Ochratoxins are responsible for chronic nephropathy in pigs and also may be the cause of endemic Balkan nephropathy and some chronic interstitial nephropathies seen in North Africa and France [29].

FIGURE 10-30

Endemic Balkan nephropathy. Endemic nephropathy is encountered in some well-defined areas of the Balkans. Distribution (*dark areas*) is along the affluents of the Danube, in a few areas on the plains and low hills owing to high humidity and rainfall. (*From* Stefanovic and Polenakovic [30]; with permission.)

CLINICAL FEATURES OF BALKAN NEPHROPATHY

- Residence in an endemic area
- Occupational history of farming
- Progressive renal failure
- Microproteinuria of tubular type
- Unremarkable urinary sediment
- Small and shrunken kidneys
- Associated urothelial tumors

FIGURE 10-31

Clinical features in Balkan nephropathy. Balkan nephropathy is characterized by progressive renal failure in residents (generally farmers) living in endemic areas for over 10 years. The urinary sediment is unremarkable and no proteinuria is seen, except for a microproteinuria of tubular type. The kidneys are small and shrunken. Urothelial cancers are frequently associated with Balkan nephropathy [29,30].

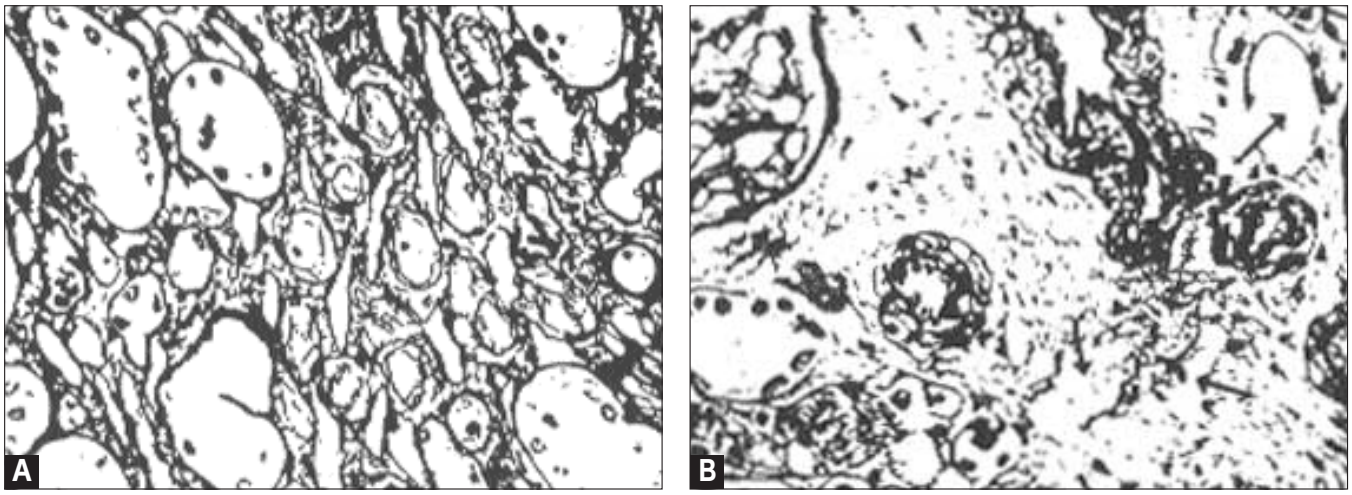

FIGURE 10-32

Pathology of Balkan nephropathy. Balkan nephropathy is characterized by pure interstitial fibrosis with marked tubular atrophy (**A**) and by hyperplasia of the myocythial cells with narrowing of the lumen of the vessel (**B**) (*From* Stefanovic and M. Polenakovic [30]; with permission).

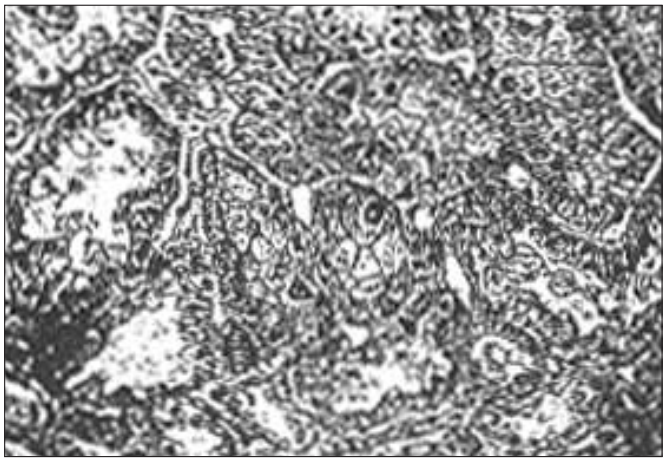

FIGURE 10-33

Pathology of ochratoxin nephropathy. In addition to interstitial fibrosis, large hyperchromatic nuclei in tubular epithelial cells are shown by the *arrow* (interstitial caryomegalic nephropathy). (Masson trichrome stain, magnification x 160.) The renal biopsy was obtained from a woman from France who had renal failure (creatinine clearance 40 mL/min) without significant proteinuria and urinary sediment abnormalities. Ochratoxin levels were 367 and 1810 ng/mL, respectively, in the patient's blood and urine. (*From* Godin and coworkers [29].)

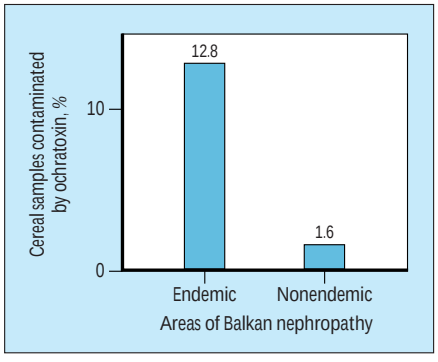

FIGURE 10-34

Balkan nephropathy and ochratoxin A in food. A survey of home-produced foodstuffs in the Balkans has revealed that contamination with ochratoxin A is more frequent in areas in which endemic nephropathy is prevalent (endemic areas) than in areas in which nephropathy is absent. (*Adapted from* Krogh and coworkers [31].)

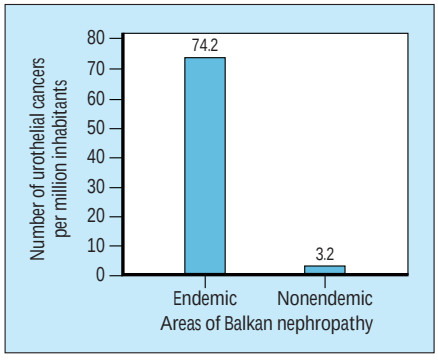

FIGURE 10-35

Balkan nephropathy and urothelial cancers. Urothelial cancers appear as a frequent complication of Balkan nephropathy. An increased prevalence of upper tract urothelial tumors is described in inhabitants of areas in which Balkan nephropathy is endemic. (*Adapted from* Godin and coworkers [29].)

Exposure to Chinese Herbs

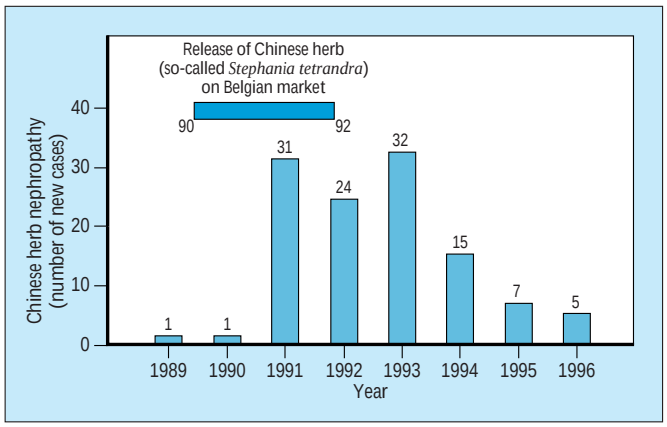

FIGURE 10-36

Epidemiology of Chinese herbs nephropathy. Chinese herbs nephropathy was described for the first time in Belgium in 1993 [32]. A peak incidence of new cases of women with rapidly progressive interstitial nephritis in Brussels during 1992 lead to suspicion of a new cause of renal disease. The relationship between this new renal disease and the recent introduction of Chinese herbs (namely, *Stephania tetrandra*) in a slimming regimen was established [32]. The withdrawal from the market of this herb has decreased the incidence of interstitial nephritis in Brussels, Belgium.

A. CHINESE HERBAL MEDICINE

Chinese Name	Western name	Chemical Marker
Han fang-ji	*Stephania tetrandra*	Tetrandrine
Guang fang-ji	*Aristolochia* fang chi	Aristolochic acid

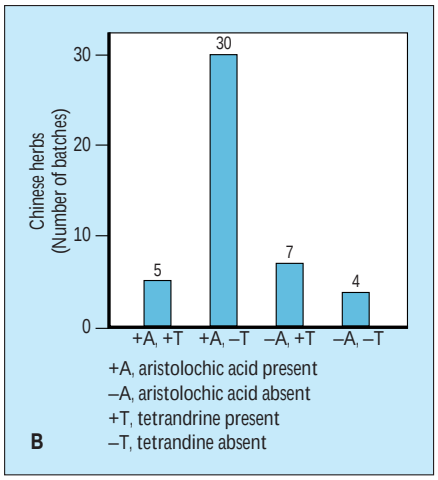

FIGURE 10-37

Role of *Aristolochia* in Chinese herbs nephropathy. *Stephania tetrandra* was the Chinese herb chronologically associated with the development of Chinese herbs nephropathy. However, tetrandrine, the alkaloid characterizing *Stephania tetrandra* was not found in the capsules taken by the patients. In fact, confusion between *Stephania tetrandra* and *Aristolochia* fang chi was done in the delivery of Chinese herbs in Belgium [33]. Chinese characters and the pingin name of *Stephania tetrandra* (Han fang-ji) are identical to that of *Aristolochia* fang chi (Guang fang-ji). Investigations conducted on batches of *Stephania tetrandra* powders distributed in Belgium have shown that most of them contained aristolochic acids (characteristic of *Aristolochia*) and not tetrandrine (*From* Vanhaelen and coworkers [33] and P Daenens, Katholiek Universiteit Leuven, Belgium, report of expertise 1996.)

DNA ADDUCTS FORMED BY ARISTOLOCHIC ACID IN RENAL TISSUE

Chinese Herb Nephropathy (n = 5)	Controls (n = 6)
0.7–5.3 per 10^7 nucleotides	0

FIGURE 10-38
DNA aristolochic acid adducts in kidney tissues of patients with Chinese herbs nephropathy. The role of *Aristolochia* in the pathogenesis of Chinese herbs nephropathy was confirmed by the demonstration of DNA aristolochic acid adducts (a biomarker of aristolochic acids exposure) in renal tissue of patients with Chinese herbs nephropathy, whereas these adducts were absent in the renal tissue of control cases. (*Adapted from* Schmeiser and coworkers [34].)

CLINICAL FEATURES OF CHINESE HERB NEPHROPATHY

Rapidly progressive renal failure
Microproteinuria of tubular type
Unremarkable urinary sediment
Small and shrunken kidneys
Valvular hear diseases (dexfenfluramine-associated therapy), 30%
Associated urothelial cancers

FIGURE 10-39
The clinical features of Chinese herbs nephropathy are characterized by rapidly progressive renal failure without both urinary sediment abnormalities and proteinuria except for a microproteinuria of tubular type. The kidneys are small and shrunken. Vascular heart diseases are associated in 30% of cases (probably owing to dexfenfluramine administered with the Chinese herbs for slimming purposes) [35]. Some cases of associated urothelial cancers also are described [36,37].

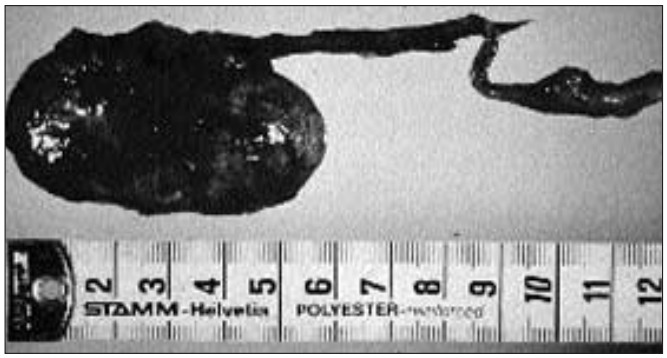

FIGURE 10-40
Photographic image of the pathology of Chinese herbs nephropathy. Chinese herbs nephropathy is characterized by a large reduction in kidney volume. Moreover, an associated tumor of the lower ureter is shown.

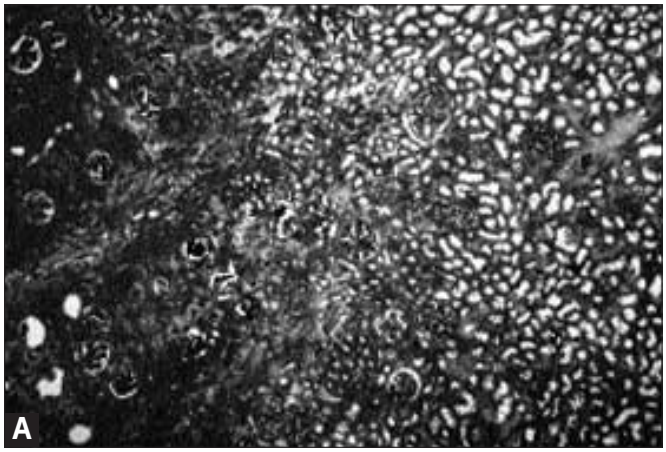

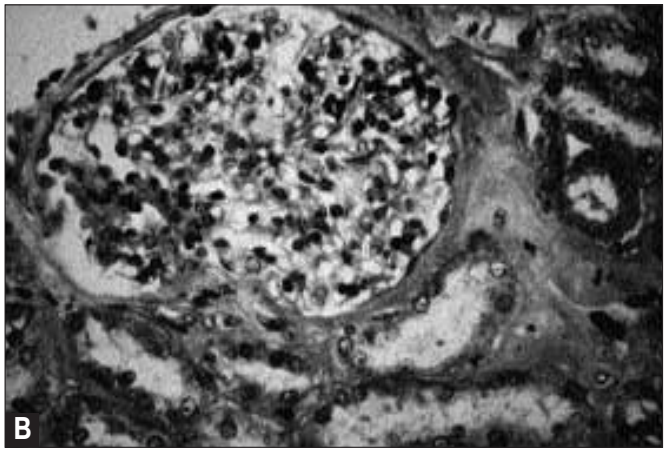

FIGURE 10-41 (*see* Color Plate)
Pathology of Chinese herb nephropathy. The major pathologic lesion consists of extensive interstitial fibrosis with atrophy and loss of the tubules, predominantly located in superficial cortex [38,39]. **A**, A low-power view of transition between superficial cortex (*left*) and deep cortex (*right*) shows an extensive interstitial fibrosis with relative sparing of glomeruli. (Masson trichrome stain, magnification × 50.) **B**, A normal glomerulus surrounded by a paucicellular interstitial fibrosis and atrophic tubules. (Masson's trichrome stain, magnification × 300.)

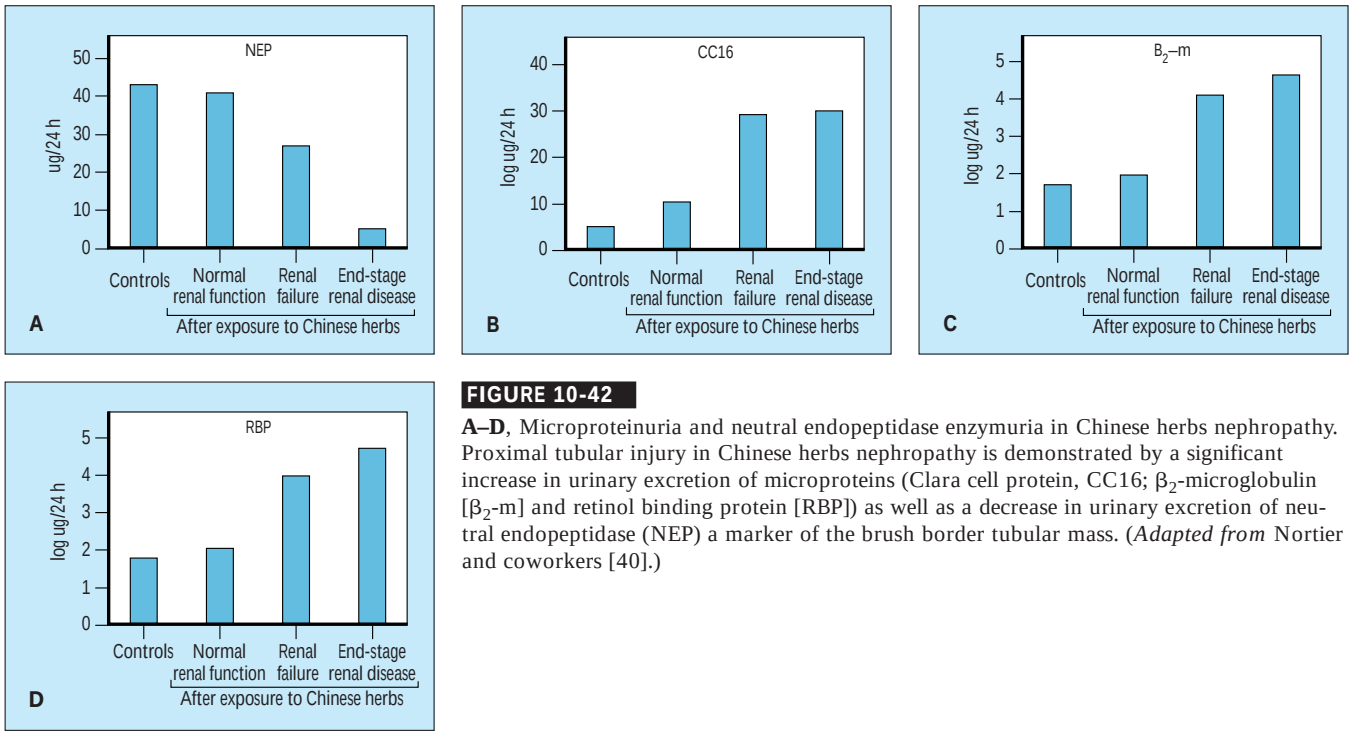

FIGURE 10-42

A–D, Microproteinuria and neutral endopeptidase enzymuria in Chinese herbs nephropathy. Proximal tubular injury in Chinese herbs nephropathy is demonstrated by a significant increase in urinary excretion of microproteins (Clara cell protein, CC16; β_2-microglobulin [β_2-m] and retinol binding protein [RBP]) as well as a decrease in urinary excretion of neutral endopeptidase (NEP) a marker of the brush border tubular mass. (*Adapted from* Nortier and coworkers [40].)

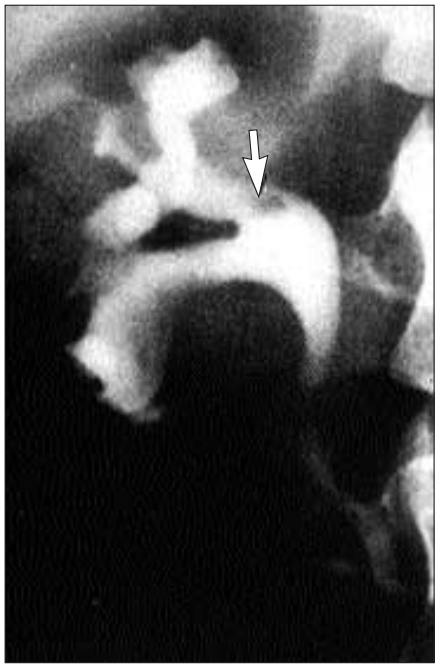

FIGURE 10-43

Chinese herbs nephropathy and renal pelvic carcinoma. Urothelial cancers are associated with Chinese herbs nephropathy [36,37]. Shown is a filling defect (*arrow*) in the renal pelvis in an antegrade pyelogram obtained from a patient with Chinese herbs nephropathy and hematuria. (*From* Vanherweghem and coworkers [37]; with permission).

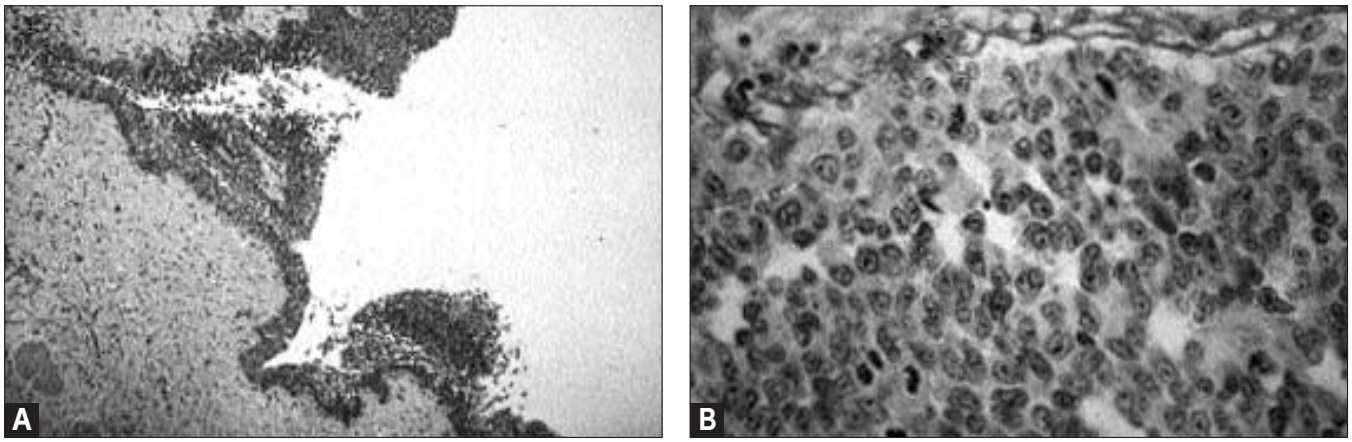

FIGURE 10-44

Pathology of urothelial tumors associated with Chinese herbs nephropathy. Microscopic pattern is shown of a lower urothelial tumor obtained by ureteronephrectomy of a native kidney in a patients with transplantation who has Chinese herbs nephropathy (the macroscopic appearance of the nephrectomy is shown in Fig. 10-40). **A**, Part of the urothelial proliferation. Plurifocal thickening of the urothelium is present. (Hematoxylin and eosin stain x 50.) **B**, *In situ* transitional cell carcinoma with high mitotic rate. (Magnification x 400 periodic acid–Schiff reaction.)

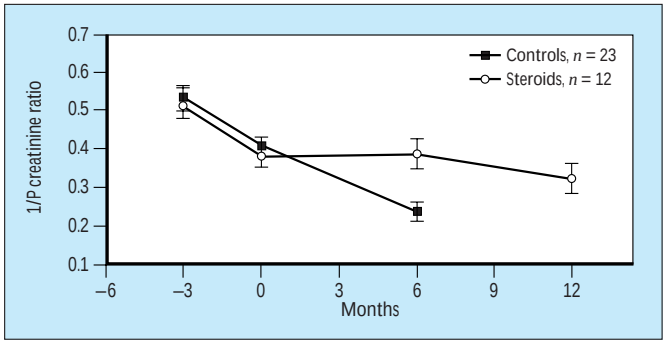

FIGURE 10-45

Effects of steroids on the evolution of renal failure in Chinese herbs nephropathy. Steroid therapy was shown to decrease the evolution of renal failure in a subgroup of patients with Chinese herbs nephropathy [41]. The evolution is shown of the 1/P creatinine ratio of patients with Chinese herbs nephropathy, 12 of whom were treated with steroids as compared with 23 not treated with steroids (control group). In the control group the 1/P creatinine curve was limited to 6 months of follow-up because at 12 months, 17 of the 23 patients were on renal replacement therapy. (*From* Vanherweghem and coworkers [41]; with permission.)

TOXIC CHRONIC INTERSTITIAL NEPHROPATHIES WITH UROTHELIAL CANCERS

Analgesic nephropathy (phenetidin compounds)
Balkan nephropathy (ochratoxins)
Chinese herbs nephropathy (aristolochic acids)

FIGURE 10-46

Of interest is the association between chronic renal interstitial fibrosis and urothelial cancers. This association appears, at least, in three chronic toxic nephropathies: analgesic nephropathy, Balkan nephropathy, and Chinese herbs nephropathy. This association indicates that nephrotoxins promoting interstitial fibrosis (analgesics, ochratoxins, and aristolochic acids) also may be oncogenic substances.

References

1. Nuyts GD, Van Vlem E, Thys J, *et al.*: New occupational risk factors for chronic renal failure. *Lancet* 1995, 346:7–11.
2. Nuyts GD, Daelemans RA, Jorens PG, *et al.*: Does lead play a role in the development of chronic renal disease? *Nephrol Dial Transplant* 1991, 6:307–315.
3. Batuman V, Maesaka JK, Haddad B, *et al.*: The role of lead in gout nephropathy. *N Engl J Med* 1981, 304:520–523.
4. Sanchez-Fructuoso AI, Torralbo A, Arroyo M, *et al.*: Occult lead intoxication as a cause of hypertension and renal failure. *Nephrol Dial Transplant* 1996, 11:1775–1780.
5. Roels HA, Lauwerys RR, Buchet JP, *et al.*: Health significance of cadmium induced renal dysfunction: a five year follow up. *Br J Ind Med* 1989, 46:755–764.
6. Nortier J, Bernard A, Roels H, *et al.*: Urinary neutral endopeptidase in workers exposed to cadmium: interaction with cigarette smoking. *Occup Environ Med* 1997, 54:432–436.
7. Walker RG: Lithium nephrotoxicity. *Kidney Int* 1993, 44(suppl 42):S93–S98.
8. Bendz H, Aurell M, Balldin J, *et al.*: Kidney damage in long-term lithium patients: a cross-sectional study of patients with 15 years or more on lithium. *Nephrol Dial Transplant* 1994, 9:1250–1254.
9. Sanai T, Okuda S, Onoyama K, *et al.*: Germanium dioxide-induced nephropathy: a new type of renal disease. *Nephron* 1990, 54:53–60.
10. Van Der Spoel JI, Stricker BH, Esseveld MR, Schipper MEI: Dangers of dietary germanium supplements. *Lancet* 1990, 336:117.
11. Takeuchi A, Yoshizawa N, Oshima S, *et al.*: Nephrotoxicity of germanium compounds: report of a case and review of the literature. *Nephron* 1992, 60:436–442.
12. Hess B, Raisin J, Zimmermann A, *et al.*: Tubulointerstitial nephropathy persisting 20 months after discontinuation of chronic intake of germanium lactate citrate. *Am J Kidney Dis* 1993, 21:548–552.
13. Elseviers MM, Bosteels V, Cambier P, *et al.*: Diagnostic criteria of analgesic nephropathy in patients with end-stage renal failure: results of the Belgian study. *Nephrol Dial Transplant* 1992, 7:479–486.
14. Drukker W, Schwarz A, Vanherweghem JL: Analgesic nephropathy: an underestimated cause of end-stage renal disease. *Int J Artif Organs* 1986, 9:216–243.
15. Klag MJ, Whelton PK, Perneger TV: Analgesics and chronic renal disease. *Curr Opinion Nephrol Hypertens* 1996, 5:236–241.
16. Vanherweghem JL, Even-Adin D: Epidemiology of analgesic nephropathy in Belgium. *Clin Nephrol* 1982, 17:129–133.
17. Perneger TV, Whelton PK, Klag MJ: Risk of kidney failure associated with the use of acetaminophen, aspirin, and nonsteroidal anti-inflammatory drugs. *N Engl J Med* 1994, 331:1675–1679.
18. Elseviers MM, De Broe ME: Analgesic nephropathy in Belgium is related to the sales of particular analgesic mixtures. *Nephrol Dial Transplant* 1994, 9:41–46.
19. Elseviers MM, De Schepper A, Corthouts R, *et al.*: High diagnostic performance of CT scan for analgesic nephropathy in patients with incipient to severe renal failure. *Kidney Int* 1995, 48:1316–1323.
20. Shihab FS: Cyclosporine nephropathy: pathophysiology and clinical impact. *Sem Nephrol* 1996, 16:536–547.
21. Bennett WM, De Mattos A, Meyer MM, *et al.*: Chronic cyclosporine nephropathy: The Achilles' heel of immunosuppressive therapy. *Kidney Int* 1996, 50:1089–1100.
22. Luke RG: Mechanism of cyclosporine-induced hypertension. *Am J Hypertens* 1991, 4:468-471.
23. Ellis CN, Fradin MS, Messana JM, *et al.*: Cyclosporine for plaque-type psoriasis. *N Engl J Med* 1991, 324:277–284.
24. Feutren G, Mihatsch MJ: Risk factors for cyclosporine-induced nephropathy in patients with autoimmune diseases. *N Engl J Med* 1992, 326: 1654–1660.
25. Myers BD, Newton L: Cyclosporin induced chronic nephropathy: an obliterative renal injury. *J Am Soc Nephrol* 1991, 2:S45–S52.
26. Deray G, Benhmida M, Le Hoang P, *et al.* Renal function and blood pressure in patients receiving long-term, low-dose cyclosporine therapy for idiopathic autoimmune uveitis. *Ann Intern Med* 1992, 117:578–583.
27. World MJ, Stevens PE, Ashton MA, Rainford DJ: Mesalazine-associated interstitial nephritis. *Nephrol Dial Transplant* 1996, 11:614–621.
28. De Broe ME, Stolear JC, Nouwen EJ, Elseviers MM: 5-Aminosalicylic acid (5-ASA) and chronic tubulointerstitial nephritis in patients with chronic inflammatory bowel disease: Is there a link? *Nephrol Dial Transplant* 1997; 12:1839–1841.
29. Godin M, Fillastre JP, Simon P, *et al.*: L'ochratoxine est-elle néphrotoxique chez l'homme ? In *Actualités Néphrologiques*. Edited by Brentano JL, Bach JF, Kreis H, Grunfeld JP. Paris: Flammarion–Medecine Sciences; 1996:225–250.
30. Stefanovic V, Polenakovic MH: Balkan nephropathy: kidney disease beyond the Balkans? *Am J Nephrol* 1991, 11:1–11.
31. Krogh P, Hald B, Plestina R, Ceovic S: Balkan (endemic) nephropathy and foodborn ochratoxin A: preliminary results of a survey of foodstuffs. *Acta Path Microbiol Scand Sect B* 1977, 85:238–240.
32. Vanherweghem JL, Depierreux M, Tielemans C, *et al.*: Rapidly progressive interstitial renal fibrosis in young women: association with slimming regimen including Chinese herbs. *Lancet* 1993, 341:387–391.
33. Vanhaelen M, Vanhaelen-Fastre R, But P, Vanherweghem JL: Identification of aristolochic acid in Chinese herbs. *Lancet* 1994, 343:174.
34. Schmeiser HH, Bieler CA, Wiessler M, *et al.*: Detection of DNA-adducts formed by aristolochic acid in renal tissue from patients with Chinese herbs nephropathy. *Cancer Res* 1996, 56:2025–2028.
35. Vanherweghem JL: Association of valvular heart disease with Chinese herbs nephropathy. *Lancet* 1997, 350:1858.
36. Cosijns JP, Jadoul M, Squifflet JP: Urothelial malignancy in nephropathy due to Chinese herbs. *Lancet* 1994, 344:118.
37. Vanherweghem JL, Tielemans C, Simon J, Depierreux M: Chinese herbs nephropathy and renal pelvic carcinoma. *Nephrol Dial Transplant* 1995, 10:270–273.
38. Depierreux M, Van Damme B, Vanden Houte K, Vanherweghem JL: Pathologic aspects of a newly described nephropathy related to the prolonged use of Chinese herbs. *Am J Kidney Dis* 1994, 24:172–180.
39. Cosijns JP, Jadoul M, Squifflet JP *et al.*: Chinese herbs nephropathy: a clue to Balkan endemic nephropathy? *Kidney Int* 1994, 45:1680–1688.
40. Nortier JL, Deschodt-Lankman MM, Simon S, *et al.* Proximal tubular injury in Chinese herbs nephropathy: monitoring by neutral endopeptidase enzymuria. *Kidney Int* 1997, 51:288–293.
41. Vanherweghem JL, Abramowicz D, Tielemans C, Depierreux M: Effects of steroids on the progression of renal failure in chronic interstitial renal fibrosis: a pilot study in Chinese herbs nephropathy. *Am J Kidney Dis* 1996, 27:209–215.

Metabolic Causes of Tubulointerstitial Disease

Steven J. Scheinman

A variety of metabolic conditions produce disease of the renal interstitium and tubular epithelium. In many cases, disease reflects the unique functional features of the nephron, in which the ionic composition, pH, and concentration of both the tubular and interstitial fluid range widely beyond the narrow confines seen in other tissues. Recent genetic discoveries have offered new insights into the molecular basis of some of these conditions, and have raised new questions. This chapter discusses nephrocalcinosis, the relatively nonspecific result of a variety of hypercalcemic and hypercalciuric states, as well as the renal consequences of hyperoxaluria, hypokalemia, and hyperuricemia.

CHAPTER

11

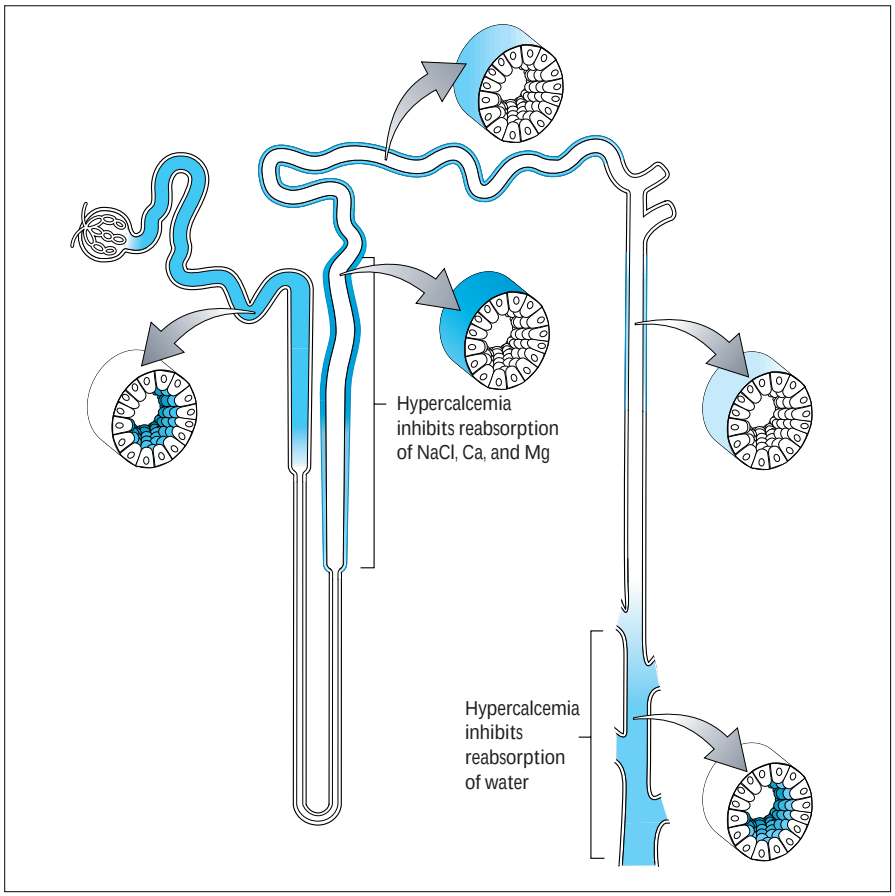

FIGURE 11-1

The recent discovery of the calcium-sensing receptor and increased understanding of its expression along the nephron have provided explanations for many of the known effects of hypercalcemia to cause clinical disturbances in renal tubular function [1]. In the parathyroid gland the calcium-sensing receptor allows the cell to sense extracellular levels of calcium and transduce that signal to regulate parathyroid hormone production and release. In the nephron, expression of the calcium receptor can be detected on the apical surface of cells of the papillary collecting duct, where calcium inhibits antidiuretic hormone action. Thus, hypercalcemia impairs urinary concentration and leads to isotonic polyuria. The most intense expression of the calcium receptor is in the thick ascending limb of the loop of Henle, particularly the cortical portion, where the calcium receptor protein is located on the basolateral side of the cells; this explains the known effects of hypercalcemia in inhibiting reabsorption of calcium, magnesium, and sodium chloride in the thick ascending limb [2]. In addition, hypercalcemia causes hypercalciuria through an increased filtered calcium load and suppression of parathyroid hormone release with a consequent reduction in calcium reabsorption. Ca—calcium; Mg—magnesium; NaCl—sodium chloride.

RENAL EFFECTS OF CALCIUM

- Hypercalcemia
  - Collecting duct
    - Resistance to vasopressin, leading to isotonic polyuria
  - Thick ascending limb of the loop of Henle
    - Impaired sodium chloride reabsorption, leading to modest salt wasting
    - Inhibition of calcium transport, leading to hypercalciuria
    - Inhibition of magnesium transport, leading to hypomagnesemia
  - Renal vasculature
    - Arteriolar vasoconstriction
    - Reduction in ultrafiltration coefficient
- Hypercalciuria
  - Microscopic hematuria
  - Nephrocalcinosis
  - Impaired urinary acidification

FIGURE 11-2

Hypercalcemia leads to renal vasoconstriction and a reduction in the glomerular filtration rate. However, no expression of the calcium-sensing receptor has been reported so far in renal vascular or glomerular tissue. Calcium receptor expression is present in the proximal convoluted tubule, on the basolateral side of cells of the distal convoluted tubule, and on the basolateral side of macula densa cells. Functional correlates of calcium receptor expression at these sites are not yet clear [3].

Hypercalciuria leads to microscopic hematuria and, in fact, is the most common cause of microscopic hematuria in children. The mechanism is presumed to involve microcrystallization of calcium salts in the tubular lumen. Conflicting effects of calcium on urinary acidification have been reported in clinical settings in which other factors, such as parathyroid hormone levels, may explain the observations. whether or not it is the result of renal tubular acidosis, Nephrocalcinosis often is associated with impaired urinary acidification, whether or not it is the result of renal tubular acidosis.

CAUSES OF NEPHROCALCINOSIS

Medullary (total)	**97.6**
Primary hyperparathyroidism	32.4
Distal renal tubular acidosis	19.5
Medullary sponge kidney	11.3
Idiopathic hypercalciuria	5.9
Dent's disease	4.3
Milk-alkali syndrome	3.2
Oxalosis	3.2
Hypomagnesemia-hypercalciuria	1.6
Sarcoidosis	1.6
Renal papillary necrosis	1.6
Hypervitaminosis D	1.6
Other*	4.0
Undiscovered causes	6.7
Cortical (total)	**2.4**

Adapted from Wrong [3]; with permission.

* Other causes include Bartter syndrome, idiopathic Fanconi syndrome, hypothyroidism, and severe acute tubular necrosis.

FIGURE 11-3

Nephrocalcinosis represents calcification of the renal parenchyma. It is primarily medullary in most cases except in dystrophic calcification associated with inflammatory, toxic, or ischemic disease. Nephrocalcinosis can be seen in association with chronic or severe hypercalcemia or in a variety of hypercalciuric states. The spectrum of causes of nephrocalcinosis is described by Wrong [3]. The numbers represent the percentage of the total of 375 patients. It is likely that the case mix is affected to some extent by Wrong's interests in, *eg*, renal tubular acidosis (RTA) and Dent's disease, but this is by far the largest published series. As in other studies, the most important causes of nephrocalcinosis are primary hyperparathyroidism, distal RTA, and medullary sponge kidney. The primary factor predisposing patients to renal calcification in many of these conditions is hypercalciuria, as occurs in idiopathic hypercalciuria, Dent's disease, milk-alkali syndrome, sarcoidosis, hypervitaminosis D, and often in distal RTA. In distal RTA and milk-alkali syndrome, relative or absolute urinary alkalinity promote precipitation of calcium phosphate crystals in the tubular lumena, and hypocitraturia is an important contributing factor in distal RTA. Causes of cortical nephrocalcinosis in this study included acute cortical necrosis, chronic glomerulonephritis, and chronic pyelonephritis.

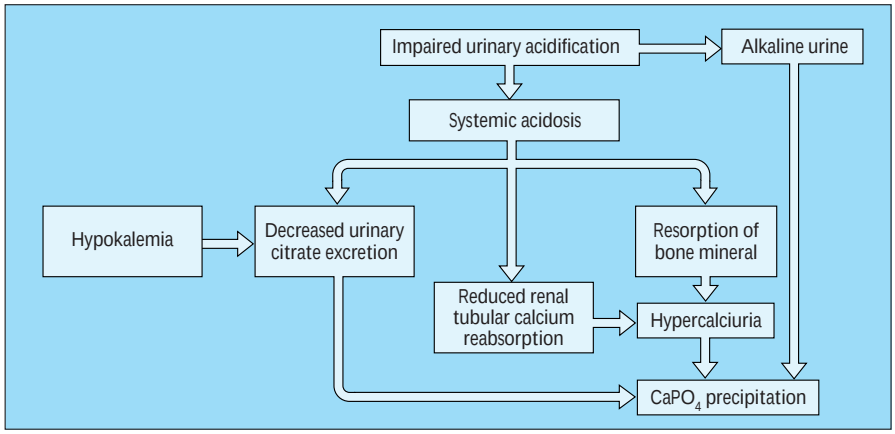

FIGURE 11-4

Nephrocalcinosis in type I (distal) renal tubular acidosis. Nephrocalcinosis and nephrolithiasis are common complications in distal renal tubular acidosis (RTA-1). Several factors contribute to the pathogenesis. The most important of these factors are a reduction in urinary excretion of citrate and a persistently alkaline urine. Citrate inhibits the growth of calcium stones; its excretion is reduced in RTA-1 as a result of both systemic acidosis and hypokalemia. The high urine pH favors precipitation of calcium phosphate ($CaPO_4$). Thus, RTA-1 should be suspected in any patient with pure calcium phosphate stones [4]. Systemic acidosis also promotes hypercalciuria, although not all patients with RTA-1 have excessive urinary calcium excretion [5]. Hypercalciuria results from resorption of bone mineral and the consequent increased filtered load of calcium as acidosis leads to consumption of bone buffers. Acidosis also has a direct effect of inhibiting renal tubular calcium reabsorption. Conversely, nephrocalcinosis from other causes can impair urinary acidification and lead to RTA in some patients. The mainstay of therapy for RTA-1 is potassium citrate, which corrects acidosis, replaces potassium, restores urinary citrate excretion, and reduces urinary loss of calcium [5]. (*From* Buckalew [5]; with permission.)

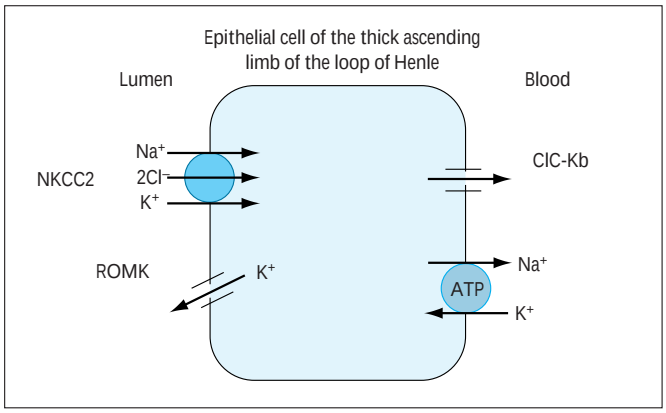

FIGURE 11-5

Bartter syndrome. Bartter syndrome is a hereditary renal functional disorder characterized by hypokalemic metabolic alkalosis, renal salt wasting with normal or low blood pressure, polyuria, and hypercalciuria. Other features include juxtaglomerular hyperplasia, secondary hyperreninemia and hyperaldosteronism, and excessive urinary excretion of prostaglandin E. It often has been noted that patients with Bartter syndrome appear as if they were chronically exposed to loop diuretics; in fact, the major differential diagnosis is with diuretic abuse. Bartter syndrome often presents with growth retardation in children, and nephrocalcinosis is common. Bartter syndrome is inherited as an autosomal recessive trait.

The speculation that this syndrome could be explained by impaired reabsorption in the loop of Henle has now been confirmed by molecular studies. R.P. Lifton's group [6–8] identified loss-of-function mutations in three genes encoding different proteins, each involved in the coordinated transport of salt in the thick ascending limb of the loop of Henle. In this nephron segment, sodium chloride is transported into the cell together with potassium by the bumetamide-inhibitible sodium-potassium-2 chloride cotransporter (NKCC2). Recycling of potassium back to the lumen through an apical potassium channel (ROMK) allows an adequate supply of potassium for optimal activity of the NKCC2. Chloride exits the basolateral side of the cell through a voltage-gated chloride channel (ClC-Kb), and sodium is expelled separately by the sodium-potassium adenosine triphosphatase cotransporter. Inactivating mutations in NKCC2, ROMK, and ClC-Kb have been identified in patients with Bartter syndrome [6–8].

Approximately 20% of filtered calcium is reabsorbed in the thick ascending limb, and inactivation of any of these three transport proteins can lead to hypercalciuria. Nephrocalcinosis occurs in almost all patients with mutations in NKCC2 or ROMK, but it is less common in patients with a mutation in the basolateral chloride channel ClC-Kb, even though patients with chloride-channel mutations currently make up the largest reported group [8]. This interesting observation is unexplained at present. In addition, a significant number of patients with Bartter syndrome have been found to have normal coding sequences for all three of these genes, indicating that mutations in other gene(s) may explain Bartter syndrome in some patients.

In contrast, the Gitelman variant of Bartter syndrome is associated with hypocalciuria. In this respect these patients resemble people treated with thiazide diuretics. In fact, mutations have been found in the thiazide-sensitive sodium chloride cotransporter of the distal tubule [9]. Hypomagnesemia is common and often severe, and patients with Gitelman syndrome do not develop nephrocalcinosis.
ATP—adenosine triphosphate. (*From* Simon and coworkers [8]; with permission.)

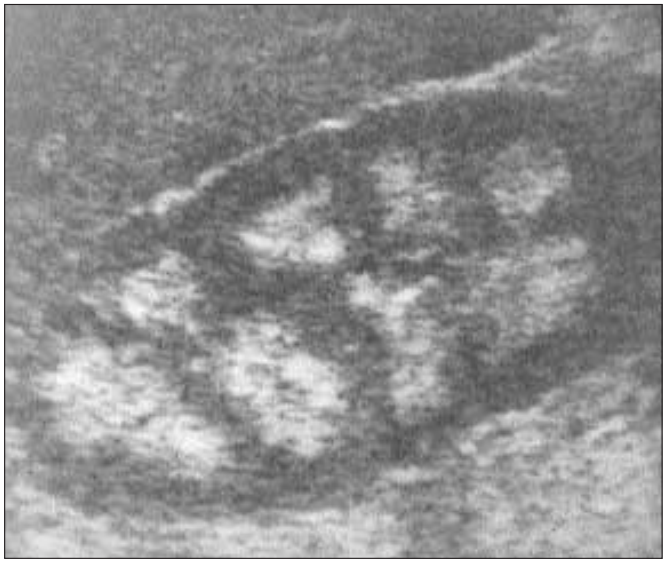

FIGURE 11-6

Nephrocalcinosis. Ultrasound image of right kidney in a patient with primary hyperparathyroidism. Echogenicity of the renal cortex is comparable to that of the adjacent liver. The dense nephrocalcinosis is entirely medullary. (*Courtesy of* Robert Botash, MD.)

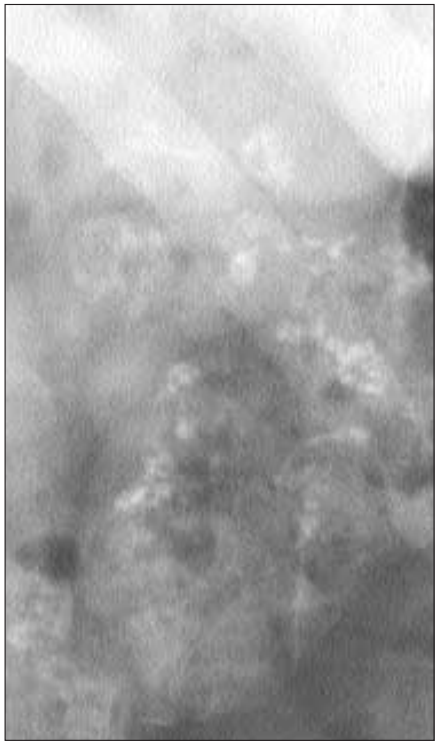

FIGURE 11-7

Noncontrast abdominal radiograph in a 24-year-old man with X-linked nephrolithiasis (Dent's disease). The patient had recurrent calcium nephrolithiasis beginning in childhood and developed end-stage renal disease requiring dialysis at 40 years of age. Extensive medullary calcinosis is evident.

X-LINKED NEPHROLITHIASIS (DENT'S DISEASE)

	Males who are affected	Females who are carriers
Low molecular weight proteinuria	Extreme	Absent, mild, or moderate
Other defects in proximal tubular function	Variable	Uncommon
Hypercalciuria	Occurs early in most	Present in half
Nephrocalcinosis	Nearly all have it	Rare
Calcium stones	Common but not universal	Uncommon
Renal failure	Common but not universal	Rare
Rickets	Present in some	Not reported

FIGURE 11-8

Syndromes of X-linked nephrolithiasis have been reported under various names, including Dent's disease in the United Kingdom, X-linked recessive hypophosphatemic rickets in Italy and France, and a syndrome of low molecular weight (LMW) proteinuria with hypercalciuria and nephrocalcinosis in Japanese schoolchildren. Mutations in a gene encoding a voltage-gated chloride channel (ClC-5) are present in all of these syndromes, establishing that they represent variants of one disease [10]. The disease occurs most often in boys, with microscopic hematuria, proteinuria, and hypercalciuria. Many but not all have recurrent nephrolithiasis from an early age. Affected males excrete extremely large quantities of LMW proteins, particularly β_2-microglobulin and retinol-binding protein. Other defects of proximal tubular function, including hypophosphatemia, aminoaciduria, glycosuria, or hypokalemia, occur variably and often intermittently. Many affected males have mild to moderate polyuria and nocturia, and they often exhibit this symptom on presentation. Urinary acidification is usually normal, and patients do not have acidosis in the absence of advanced renal insufficiency. Nephrocalcinosis is common by the teenage years, and often earlier. Renal failure is common and often progresses to end-stage renal disease by the fourth or fifth decade, although some patients escape it. Renal biopsy documents a nonspecific pattern of interstitial fibrosis and tubular atrophy, with glomerular sclerosis that is probably secondary [11].

Rickets occurs early in childhood in some patients but is absent in most patients with X-linked nephrolithiasis (Dent's disease). In a few families, all affected males have had rickets. In other families, rickets is present in only one of several males sharing the same mutation. At present, the variability of this feature and other features of the disease is unexplained and may reflect dietary or environmental factors or the participation of other genes in the expression of the phenotype.

Females who are carriers often have mild to moderate LMW proteinuria. This abnormality can be used clinically as a screening test, but LMW protein excretion will not be abnormal in all heterozygous females. Approximately half of women who are carriers have hypercalciuria, but other biochemical abnormalities are rare. Although symptomatic nephrolithiasis and even renal insufficiency have been reported in female carriers, they are very uncommon.

The gene for ClC-5 that is mutated in X-linked nephrolithiasis (Dent's disease) is expressed in the endosomal vacuoles of the proximal tubule; it appears to be important in acidification of the endosome. Thus, defective endosomal function would explain the LMW proteinuria. The mechanism of hypercalcinuria remains unexplained at present. This gene belongs to the family of voltage-gated chloride channels that includes ClC-Kb, one of the gene mutations in some patients with Bartter syndrome. To date, 32 mutations have been reported in 40 families, and nearly all are unique [11].

HYPEROXALURIA

Type	Mechanism	Clinical consequences
Primary (genetic):		
PH1	Functional deficiency of AGT	Nephrolithiasis
		Nephrocalcinosis and progressive renal failure
		Systemic oxalosis (kidneys, bones, cartilage, teeth, eyes, peripheral nerves, central nervous system, heart, vessels, bone marrow)
PH2	Functional deficiency of DGDH	Nephrolithiasis
Secondary:		
Dietary	Sources include for example spinach, rhubarb, beets, peanuts, chocolate, and tea	Increased risk of nephrolithiasis
Enteric	Enhanced oxalate absorption because of increased oxalate solubility, bile salt malabsorption, and altered gut flora (*eg*, inflammatory bowel disease and bowel resection)	Nephrolithiasis Nephrocalcinosis Systemic oxalosis (rarely)
Metabolism from excess of precursors	Ascorbate	Nephrolithiasis
	Ethylene glycol, glycine, glycerol, xylitol, methoxyflurane	Tubular obstruction by crystals leading to acute renal failure
Pyridoxine deficiency	Cofactor for AGT	Nephrolithiasis

FIGURE 11-9

Oxalate is a metabolic end-product of limited solubility in physiologic solution. Thus, the organism is highly dependent on urinary excretion, which involves net secretion. Normal urine is supersaturated with respect to calcium oxalate. Crystallization is prevented by a number of endogenous inhibitors, including citrate. A mild excess of oxalate load, as occurs with excessive dietary intake, contributes to nephrolithiasis. A more severe oxalate overload, as in type 1 primary hyperoxaluria, can lead to organ damage through tissue deposition of calcium oxalate and possibly through the toxic effects of glyoxalate [12].

Two types of primary hyperoxaluria (PH) have been identified (Fig. 11-10), of which type 1 (PH1) is much more common. PH1 results from absolute or functional deficiency of the liver-specific enzyme alanine:glyoxalate aminotransferase (AGT). This deficiency leads to calcium oxalate nephrolithiasis in childhood, with nephrocalcinosis and progressive renal failure. Because the kidney is the main excretory route for oxalate, in the face of excessive oxalate production even mild degrees of renal insufficiency can lead to systemic deposition of oxalate in a wide variety of tissues. It is interesting that the liver itself is spared from calcium oxalate deposition. Clinical consequences include heart block and cardiomyopathy, severe peripheral vascular insufficiency and calcinosis cutis, and bone pain and fractures. Many of these conditions are exacerbated by the effects of end-stage renal disease. In contrast, PH2 is much more rare than is PH1. Patients with PH2 have recurrent nephrolithiasis. Nephrocalcinosis, renal failure, and systemic oxalosis have not been reported in PH2. The metabolic defect in PH2 appears to be a functional deficiency of D-glycerate dehydrogenase (DGDH) [12].

Secondary causes of hyperoxaluria include dietary excess, enteric hyperabsorption, and enhanced endogenous production resulting from either exposure to metabolic precursors of oxalate or pyridoxine deficiency. Normally, dietary sources of oxalate account for only approximately 10% of urinary oxalate. Restriction of dietary oxalate can be effective in some patients with kidney stones who are hyperoxaluric, but even conscientious adherence to dietary restriction is disappointing in many patients who may have mild metabolic hyperoxaluria, an entity that probably exists but is poorly understood. Intestinal absorption of oxalate can be enhanced markedly in patients with bowel disease, particularly inflammatory bowel disease or after extensive bowel resection or jejunoileal bypass. In this setting, several mechanisms have been described including a) enhanced oxalate solubility as a consequence of binding of calcium to fatty acids in patients with fat malabsorption; b) a direct effect of malabsorbed bile salts to enhance absorption of oxalate by intestinal mucosa, and c) altered gut flora with reduction in the population of oxalate-metabolizing bacteria [4,12]. Because of the important role of the colon in absorbing oxalate, ileostomy abolishes enteric hyperoxaluria [4].

Excessive endogenous production of oxalate occurs in patients ingesting large quantities of ascorbic acid, which may increase the risk of nephrolithiasis. In the setting of acute exposure to large quantities of metabolic precursors, such as ingestion of ethylene glycol or administration of glycine or methoxyflurane, tubular obstruction by calcium oxalate crystals can lead to acute renal failure. Pyridoxine deficiency is associated with increased oxalate excretion clinically in humans and experimentally in animals; it can contribute to mild hyperoxaluria. In all patients with primary hyperoxaluria, a trial of pyridoxine therapy should be given, because some patients will have a beneficial response.

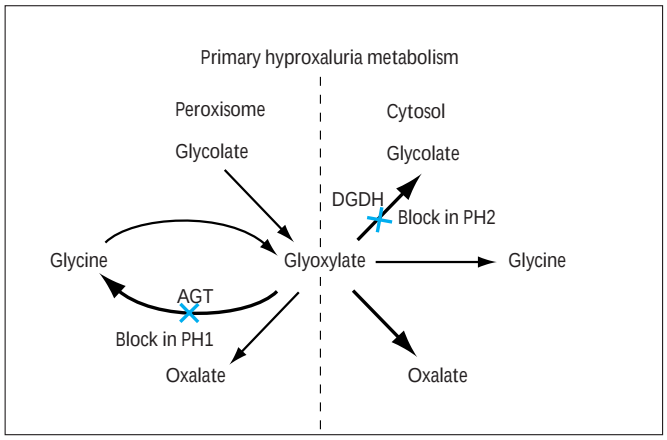

FIGURE 11-10

Metabolic events in the primary hyperoxalurias. Primary hyperoxaluria type 1 (PH1) results from functional deficiency of the peroxisomal enzyme alanine:glyoxalate aminotransferase (AGT). PH2 results from a deficiency of the cytosolic enzyme d-glycerate dehydrogenase (DGDH), which also functions as glyoxalate reductase. This figure presents a simplified illustration of the metabolic consequences of these defects. Both diseases are inherited as autosomal recessive traits.

In PH1, much clinical, biochemical, and molecular heterogeneity exists. Liver AGT catalytic activity is absent in approximately two thirds of patients with PH1. It is detectable in the remaining third, however, in whom the enzyme is targeted to the mitochondria rather than peroxisomes. Absence of peroxisomal AGT activity leads to impaired transamination of glyoxalate to glycine, with excessive production of oxalate and, usually, glycolate. In PH2, deficiency of cytosolic DGDH results in overproduction of oxalate and glycine. Mild cases of PH1, without nephrocalcinosis or systemic oxalosis, resemble PH2 clinically, but the two usually can be distinguished by measurement of urinary glycolate and glycine. Assay of AGT activity in liver biopsy specimens can be diagnostic in PH1 even when renal failure prevents analysis of urinary excretion.

The gene encoding AGT has been localized to chromosome 2q37.3 and has been cloned and sequenced. Mutations in this gene have been identified in patients with absent enzymatic activity, abnormal enzyme targeting to mitochondria, aggregation of AGT within peroxisomes, and absence of both enzymatic activity and immunoreactivity. However, mutations have not been identified in all patients with PH1 who have been studied, and molecular diagnosis is not yet routinely available [12]. (*Adapted from* Danpure and Purdue [12].)

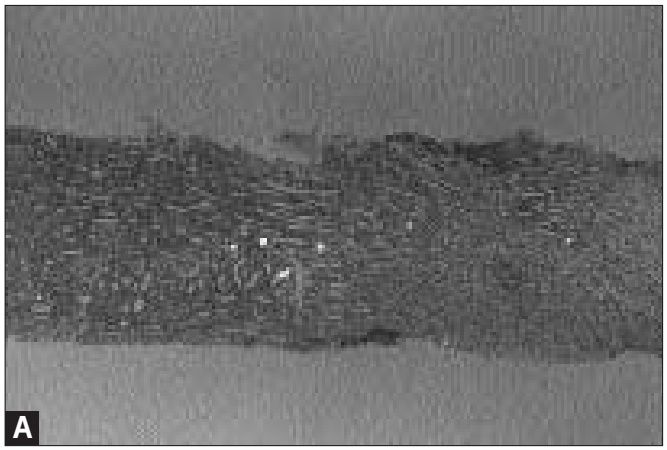

FIGURE 11-11

Sequential biopsies of a transplanted kidney documenting progressive recurrence of renal oxalosis. This patient with primary hyperoxaluria type I received renal transplantation, without liver transplantation, at 24 years of age. Panels *A–D* show tissue stained with hematoxylin and eosin. Panels *A–C* show specimens viewed by polarization microscopy, all at the same low-power magnification, from biopsies taken after transplantation within the first year (*A*), third year (*B*),

(Continued on next page)

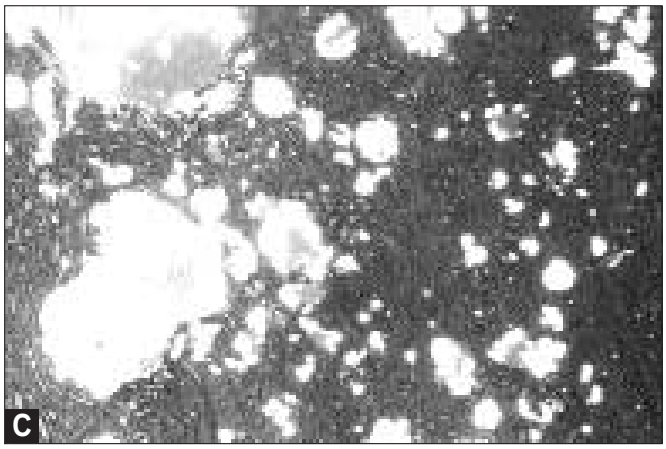

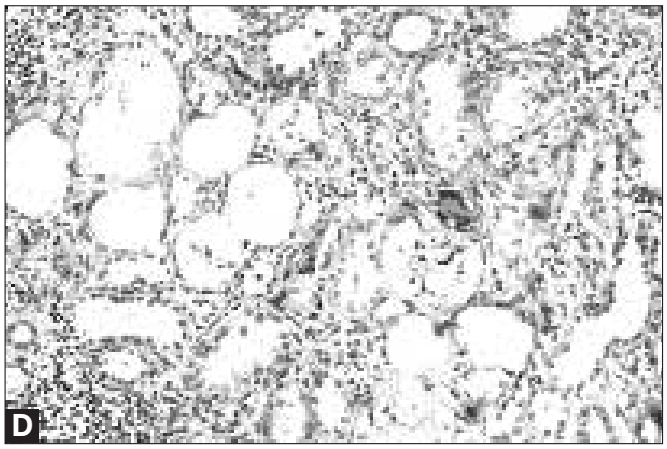

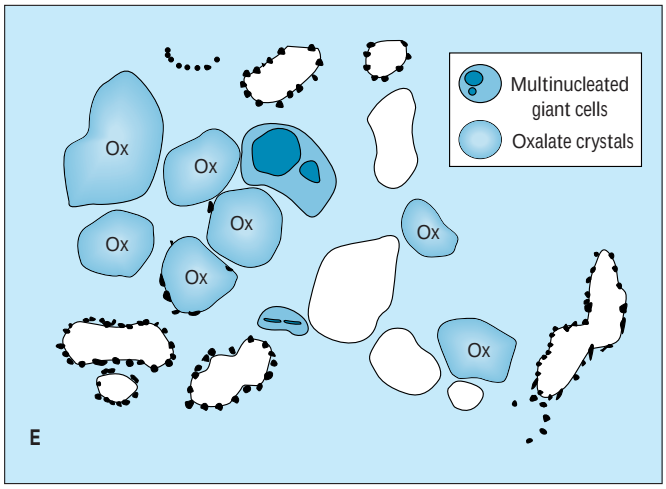

FIGURE 11-11 *(Continued)*

and fifth year (*C*), following renal transplantation. Deposition of oxalate crystals became progressively more severe with time, and the kidney failed after 5 years. Panel *D* illustrates a higher-power magnification, without polarization, of the biopsy at 5 years, showing a radial array of oxalate crystals and phagocytosis of small crystals by multinucleated giant cells (*E*).

Conservative treatment of PH1 is of limited efficacy. Dietary restriction has little effect on the course of the disease. High-dose pyridoxine should be tried in all patients, but many patients do not respond. Strategies to prevent calcium oxalate stone formation include a high fluid intake (recommended in all patients), magnesium oxide (because magnesium increases the solubility of calcium oxalate salts), and inorganic phosphate. Lithotripsy or surgery may be necessary but do not alter the progression of nephrocalcinosis [12,13].

Hemodialysis is superior to peritoneal dialysis in its ability to remove oxalate, but neither one is able to maintain a rate of oxalate removal sufficient to keep up with the production rate in patients with PH1. Once end-stage renal disease develops, hemodialysis does not prevent the progression of systemic oxalosis. In some patients, renal transplantation accompanied by an aggressive program of management has been followed by a good outcome for years [14]. However, oxalosis often recurs in the transplanted kidney, particularly if any degree of renal insufficiency develops for any reason. In recent years, liver transplantation has been used with success, with or without renal transplantation, and offers the prospect of definitive cure. Results of liver transplantation are best in patients who have not yet developed significant renal insufficiency [12]. (*Courtesy of* Paul Shanley, MD.)

URIC ACID AND RENAL DISEASE

Disease	Clinical setting	Features	Therapeutic issues
Uric acid nephrolithiasis	Hyperuricosuria	Uric acid nephrolithiasis Calcium nephrolithiasis	Allopurinol; alkalinize urine Allopurinol
Acute uric acid nephropathy	Cytotoxic chemotherapy for leukemia or lymphoma; occasionally spontaneous	Intratubular obstruction by uric acid crystals in acidic urine	Prevention with allopurinol, fluids, and alkalinization Acute dialysis as indicated
Chronic gouty nephropathy	Gout or hyperuricemia in the setting of hypertension, preexisting renal disease, advanced age, vascular disease, inflammatory reaction, and chronic exposure to lead	Intrarenal tophi; sodium urate crystals in interstitium with accompanying destructive inflammatory reaction	Hemodialysis for renal failure
Familial hyperuricemic nephropathy	Autosomal dominant inheritance	Interstitial fibrosis, chronic inflammation; crystals are rare	No consensus regarding allopurinol

FIGURE 11-12

Uric acid contributes to the risk of kidney stones in several ways. Pure uric acid stones occur in patients with hyperuricosuria, particularly when the urine is acidic. Thus, therapy involves both allopurinol and alkalinization with potassium alkali salts. Hyperuricosuria also promotes calcium oxalate stone formation. In these patients, calcium nephrolithiasis can be prevented by therapy with allopurinol. The mechanism may involve heterogenous nucleation of calcium oxalate by uric acid microcrystals, binding of endogenous inhibitors of calcium crystallization, or "salting out" of calcium oxalate by urate [4].

Acute uric acid nephropathy occurs most often in the setting of brisk cell lysis from cytotoxic therapy or radiation for myeloproliferative or lymphoproliferative disorders or other tumors highly responsive to therapy. Uric acid nephropathy can uncommonly occur spontaneously in malignancies or other states of high uric acid production. Examples are infants with the Lesch-Nyhan syndrome who have excessive uric acid production resulting from deficiency of hypoxanthine-guanine phosphoribosyltransferase deficiency and, rarely, adults with gout who become volume-contracted and whose urine is concentrated and acidic. The mechanism involves intratubular obstruction by crystals of uric acid in the setting of an acute overwhelming load of uric acid, particularly in acidic urine. In recent years, the widespread use of an effective prophylactic regimen for chemotherapy has made acute uric acid nephropathy much less common [15]. This regimen includes preparation of the patient with high-dose allopurinol, volume-expanding the patient to maintain a dilute urine, and alkaline diuresis. In patients whose tumor lysis leads to hyperphosphatemia, however, it is important to discontinue urinary alkalinization or else calcium phosphate precipitation may occur. Occasionally, patients will develop renal failure despite these measures. In such patients, hemodialysis is preferable to peritoneal dialysis because of the higher clearance rates for uric acid. Frequent hemodialysis, even multiple times per day, may be necessary to prevent extreme hyperuricemia and facilitate recovery of renal function. A modification of continuous arteriovenous hemodialysis has recently been reported to be effective in management of these patients [16].

Chronic gouty nephropathy is a term referring to deposition of sodium urate crystals in the renal interstitium, with an accompanying destructive inflammatory reaction. As a specific entity with intrarenal tophi, gouty nephropathy appears to have become uncommon. It appears clear that long-standing hyperuricemia alone is not sufficient to cause this condition in most patients, and that renal failure in patients with hyperuricemia or gout is almost always accompanied by other predisposing conditions, particularly hypertension or exposure to lead [17].

Familial hyperuricemic nephropathy is an entity that now has been reported in over 40 kindreds. It is characterized by recurrent gout, often occurring in youth and even childhood; hyperuricemia; and renal failure. Histopathology reveals interstitial inflammation and fibrosis, almost always without evidence of urate crystal deposition, although this has been found in two patients. In contrast to gouty nephropathy, hypertension usually is absent until renal failure is advanced. The hyperuricemia appears to reflect decreased renal excretion of urate rather than overproduction of urate. Although hyperuricemia precedes and is disproportionate to any degree of renal failure, the role, if any, that uric acid plays in the pathogenesis of the renal failure remains unclear. These is no consensus among authors regarding the potential value of allopurinol in this disease. The inheritance follows an autosomal dominant pattern, but, beyond this, the genetics of the disease are not understood [18,19].

References

1. Hebert SC: Extracellular calcium-sensing receptor: implications for calcium and magnesium handling in the kidney. *Kidney Int* 1996, 50:2129–2139.
2. Riccardi D, Hall A, Xu J, *et al*.: Localization of the extracellular Ca^{2+} (polyvalent) cation-sensing receptor in kidney. *Am J Physiol* (*Renal Fluid Electrolyte Physiol*), 1998, in press.
3. Wrong OM: Nephrocalcinosis. In *The Oxford Textbook of Clinical Nephrology*. Edited by Davison AM, *et al*. London: Oxford University Press; 1997:1378–1396.
4. Coe FL, Parks JH, Asplin JR: The pathogenesis and treatment of kidney stones. *N Engl J Med* 1992, 327:1141–1152.
5. Buckalew VM: Nephrolithiasis in renal tubular acidosis. *J Urol* 1989, 141:731–737.
6. Simon DB, Karet FE, Hamdan JM, *et al*.: Bartter's syndrome, hypokalaemic alkalosis with hypercalciuria, is caused by mutations in the Na-K-2Cl cotransporter NKCC2. *Nature Genet* 1996, 13:183–188.
7. Simon DB, Karet FE, Rodriguez-Soriano J, *et al*.: Genetic heterogeneity of Bartter's syndrome revealed by mutations in the K+ channel, ROMK. *Nature Genet* 1996, 14:152–156.
8. Simon DB, Bindra RS, Mansfield TA, *et al*.: Mutations in the chloride channel gene, CLCNKB, cause Bartter's syndrome type III. *Nature Genet* 1997, 17:171–178.
9. Simon DB, Nelson-Williams C, Bia MJ, *et al*.: Gitelman's variant of Bartter's syndrome, inherited hypokalaemic alkalosis, is caused by mutations in the thiazide-sensitive Na-Cl cotransporter. *Nature Genet* 1996, 12:24–30.
10. Lloyd SE, Pearce SHS, Fisher SE, *et al*.: A common molecular basis for three inherited kidney stone diseases. *Nature* 1996, 379:445–449.
11. Scheinman SJ: X-linked hypercalciuric nephrolithiasis: clinical syndromes and chloride channel mutations. *Kidney Int* 1998, 53:3–17.
12. Danpure CJ, Purdue PE: Primay hyperoxaluria. In *The Metabolic and Molecular Bases of Inherited Disease*, edn 6. Edited by Scriver CR, *et al*. New York: McGraw-Hill; 1995:2385–2424.
13. Scheinman JI: Primary hyperoxaluria. *Miner Electrolyte Metab* 1994, 20:340–351.
14. Katz A, Freese D, Danpure CJ, *et al*.: Success of kidney transplantation in oxalosis is unrelated to residual hepatic enzyme activity. *Kidney Int* 1992, 42:1408–1411.
15. Razis E, Arlin ZA, Ahmed T, *et al*.: Incidence and treatment of tumor lysis syndrome in patients with acute leukemia. *Acta Haematol* 1994, 91:171–174.
16. Pichette V, Leblanc M, Bonnardeaux A, *et al*.: High dialysate flow rate continuous arteriovenous hemodialysis: a new approach for the treatment of acute renal failure and tumor lysis syndrome. *Am J Kidney Dis* 1994, 23:591–596.
17. Beck LH: Requiem for gouty nephropathy. *Kidney Int* 1986, 30:280–287.
18. Puig JG, Miranda ME, Mateos FA, *et al*. Hereditary nephropathy associated with hyperuricemia and gout. *Arch Intern Med* 1993, 153:357–365.
19. Reiter L, Brown MA, Edmonds J: Familial hyperuricemic nephropathy. *Am J Kidney Dis* 1995, 25:235–241.

Renal Tubular Disorders

Lisa M. Guay-Woodford

Inherited renal tubular disorders involve a variety of defects in renal tubular transport processes and their regulation. These disorders generally are transmitted as single gene defects (Mendelian traits), and they provide a unique resource to dissect the complex molecular mechanisms involved in tubular solute transport. An integrated approach using the tools of molecular genetics, molecular biology, and physiology has been applied in the 1990s to identify defects in transporters, channels, receptors, and enzymes involved in epithelial transport. These investigations have added substantial insight into the molecular mechanisms involved in renal solute transport and the molecular pathogenesis of inherited renal tubular disorders. This chapter focuses on the inherited renal tubular disorders, highlights their molecular defects, and discusses models to explain their underlying pathogenesis.

CHAPTER

12

Overview of Renal Tubular Disorders

OVERVIEW OF RENAL TUBULAR DISORDERS INHERITED AS MENDELIAN TRAITS

Inherited disorder	Transmission mode	Defective protein
Renal glucosuria	?AR, AD	Sodium-glucose transporter 2
Glucose-galactose malabsorption syndrome	AR	Sodium-glucose transporter 1
Acidic aminoaciduria	AR	Sodium-potassium–dependent glutamate transporter
Cystinuria	AR	Apical cystine-dibasic amino acid transporter
Lysinuric protein intolerance	AR	Basolateral dibasic amino acid transporter
Hartnup disease	?	?
Blue diaper syndrome	AR	Kidney-specific tryptophan transporter
Neutral aminoacidurias:	AR	?
Methioninuria		
Iminoglycinuria		
Glycinuria		
Hereditary hypophosphatemic rickets with hypercalciuria	AR	? Sodium-phosphate cotransporter
X-linked hypophosphatemic rickets	X-linked dominant	Phosphate-regulating with endopeptidase features on the X chromosome
Inherited Fanconi's syndrome isolated disorder	AR and AD	?
Inherited Fanconi's syndrome associated with inborn errors of metabolism	AR	–
Carbonic anhydrase II deficiency	AR	Carbonic anhydrase type II
Distal renal tubular acidosis	AR	?
	AD	Basolateral anion exchanger (AE1)
Bartter-like syndromes:		
Antenatal Bartter variant	AR	NKCC2, ROMK, ClC-K2
Classic Bartter variant	AR	ClC-K2b
Gitelman's syndrome	AR	NCCT
Pseudohypoparathyroidism:		
Type Ia	AD	Guanine nucleotide–binding protein
Type Ib	?	
Low-renin hypertension:		
Glucocorticoid-remedial aldosteronism	AD	Chimeric gene (11β-hydroxylase and aldosterone synthase)
Liddle's syndrome	AD	β and γ subunits of the sodium channel
Apparent mineralocorticoid excess	AR	11-β-hydroxysteroid dehydrogenase
Pseudohypoaldosteronism:		
Type 1	AR and AD	α and β subunits of the sodium channel
Type 2 (Gordon's syndrome)	AD	?
Nephrogenic diabetes insipidus:		
X-linked	X-linked recessive	Arginine vasopressin 2 receptor
Autosomal	AR and AD	Aquaporin 2 water channel
Urolithiases:		
Cystinuria	AR	Apical cystine–dibasic amino acid transporter
Dent's disease	X-linked	Renal chloride channel (ClC-5)
X-linked recessive nephrolithiasis	X-linked	Renal chloride channel (ClC-5)
X-linked recessive hypophosphatemic rickets	X-linked	Renal chloride channel (ClC-5)
Hereditary renal hypouricemia	AR	? Urate transporter

AD—autosomal dominant; AR—autosomal recessive; ClC-K2—renal chloride channel; NCCT—thiazide-sensitive cotransporter; NKCC2—bumetanide-sensitive cotransporter; ROMK—inwardly rectified.

FIGURE 12-1

Inherited renal tubular disorders generally are transmitted as autosomal dominant, autosomal recessive, X-linked dominant, or X-linked recessive traits. For many of these disorders, the identification of the disease-susceptibility gene and its associated defective protein product has begun to provide insight into the molecular pathogenesis of the disorder.

Renal Glucosuria

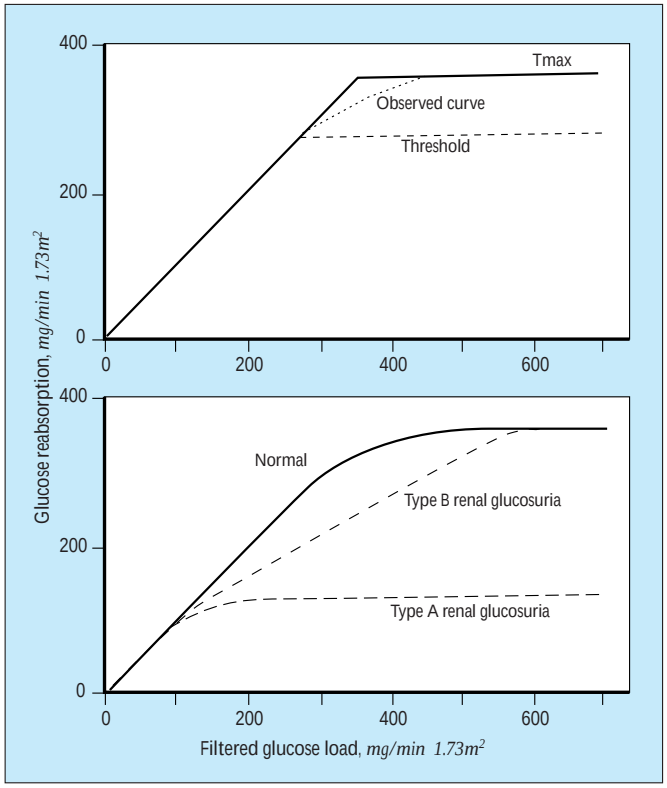

FIGURE 12-2

Physiology and pathophysiology of glucose titration curves. Under normal physiologic conditions, filtered glucose is almost entirely reabsorbed in the proximal tubule by way of two distinct sodium-coupled glucose transport systems. In the S1 and S2 segments, bulk reabsorption of glucose load occurs by way of a kidney-specific high-capacity transporter, the sodium-glucose transporter-2 (SGLT2) [1]. The residual glucose is removed from the filtrate in the S3 segment by way of the high-affinity sodium-glucose transporter-1 (SGLT1) [2]. This transporter also is present in the small intestine.

As are all membrane transport systems, glucose transporters are saturable. The top panel shows that increasing the glucose concentration in the tubular fluid accelerates the transport rate of the glucose transporters until a maximal rate is achieved. The term *threshold* applies to the point that glucose first appears in the urine. The maximal overall rate of glucose transport by the proximal tubule SGLT1 and SGLT2 is termed the *Tmax*. Glucose is detected in urine either when the filtered load is increased (as in diabetes mellitus) or, as shown in the bottom panel, when a defect occurs in tubular reabsorption (as in renal glucosuria). Kinetic studies have demonstrated two types of glucosuria caused by either reduced maximal transport velocity (type A) or reduced affinity of the transporter for glucose (type B) [3]. Mutations in the gene encoding SGLT1 cause glucose-galactose malabsorption syndrome, a severe autosomal recessive intestinal disorder associated with mild renal glucosuria (type B). Defects in SGLT2 result in a comparatively more severe renal glucosuria (type A). However, this disorder is clinically benign. Among members of the basolateral glucose transporter (GLUT) family, only GLUT1 and GLUT2 are relevant to renal physiology [4]. Clinical disorders associated with mutations in the genes encoding these transporters have yet to be described. (*From* Morris and Ives [5]; with permission.)

Aminoacidurias

CLASSIFICATION OF INHERITED AMINOACIDURIAS

Major categories	Forms	OMIM number*	Amino acids involved
Acidic amino acids	Acidic aminoaciduria	222730	Glutamate, aspartate
Basic amino acids and cystine	Cystinuria	220100, 600918, 104614	Cystine, lysine, arginine, ornithine
	Lysinuric protein intolerance	222690, 222700, 601872	Lysine, arginine, ornithine
	Isolated cystinuria	238200	Cystine
	Lysinuria	–	Lysine
Neutral amino acids	Hartnup disease	234500, 260650	Alanine, asparagine, glutamine, histidine, isoleucine, leucine, phenylalanine, serine, threonine, tryptophan, tyrosine, valine
	Blue diaper syndrome	211000	Tryptophan
	Iminoglycinuria	242600	Glycine, proline, hydroxyproline
	Glycinuria	138500	Glycine
	Methioninuria	–	Methionine

*OMIM—Online Mendelian Inheritance in Man (accessible at http://www3.ncbi.nlm.nih.gov/omin/).

FIGURE 12-3

Over 95% of the filtered amino acid load is normally reabsorbed in the proximal tubule. The term *aminoaciduria* is applied when more than 5% of the filtered load is detected in the urine. Aminoaciduria can occur in the context of metabolic defects, which elevate plasma amino acid concentrations and thus increase the glomerular filtered load. Aminoaciduria can be a feature of generalized proximal tubular dysfunction caused by toxic nephropathies or Fanconi's syndrome. In addition, aminoaciduria can arise from genetic defects in one of the several amino acid transport systems in the proximal tubule. Three distinct groups of inherited aminoacidurias are distinguished based on the net charge of the target amino acids at neutral pH: acidic (negative charge), basic (positive charge), and neutral (no charge) [5].

Acidic aminoaciduria involves the transport of glutamate and aspartate and results from a defect in the high-affinity sodium-potassium–dependent glutamate transporter [6]. It is a clinically benign disorder.

Four syndromes caused by defects in the transport of basic amino acids or cystine have been described: cystinuria, lysinuric protein intolerance, isolated cystinuria, and isolated lysinuria. Cystine actually is a neutral amino acid that shares a common carrier with the dibasic amino acids lysine, arginine, and ornithine. The transport of all four amino acids is disrupted in cystinuria. The rarer disorder, lysinuric protein intolerance, results from defects in the basolateral transport of dibasic amino acids but not cystine. Increased intracelluar concentrations of lysine, arginine, and ornithine are associated with disturbances in the urea cycle and consequent hyperammonemia [7].

Disorders involving the transport of neutral amino acids include Hartnup disease, blue diaper syndrome, methioninuria, iminoglycinuria, and glycinuria. Several neutral amino acid transporters have been cloned and characterized. Clinical data suggest that Hartnup disease involves a neutral amino acid transport system in both the kidney and intestine, whereas blue diaper syndrome involves a kidney-specific tryptophan transporter [5]. Methioninuria appears to involve a separate methionine transport system in the proximal tubule. Case reports describe seizures, mental retardation, and episodic hyperventilation in affected patients [8]. The pathophysiologic basis for this phenotype is unclear. Iminoglycinuria and glycinuria are clinically benign disorders.

ROSENBERG CLASSIFICATION OF CYSTINURIAS

Category	Phenotype	Intestinal transport defect
I		
Heterozygote	No abnormality	
Homozygote	Cystinuria, basic aminoaciduria, cystine stones	Cystinine, basic amino acids
II		
Heterozygote	Excess excretion of cystine and basic amino acids	
Homozygote	Cystinuria, basic aminoaciduria, cystine stones	Basic amino acids only
III		
Heterozygote	Excess excretion of cystine and basic amino acids	
Homozygote	Cystinuria, basic aminoaciduria, cystine stones	None

From Morris and Ives [5]; with permission.

FIGURE 12-4

In this autosomal recessive disorder the apical transport of cystine and the dibasic amino acids is defective. Differences in the urinary excretion of cystine in obligate heterozygotes and intestinal amino acid transport studies in homozygotes have provided the basis for defining three distinct phenotypes of cystinuria [9]. Genetic studies have identified mutations in the gene (SCL3A1) encoding a high-affinity transporter for cystine and the dibasic amino acids in patients with type I cystinuria [10,11]. In patients with type III cystinuria, SCL3A1 was excluded as the disease-causing gene [12]. A second cystinuria-susceptibility gene recently has been mapped to chromosome 19 [13].

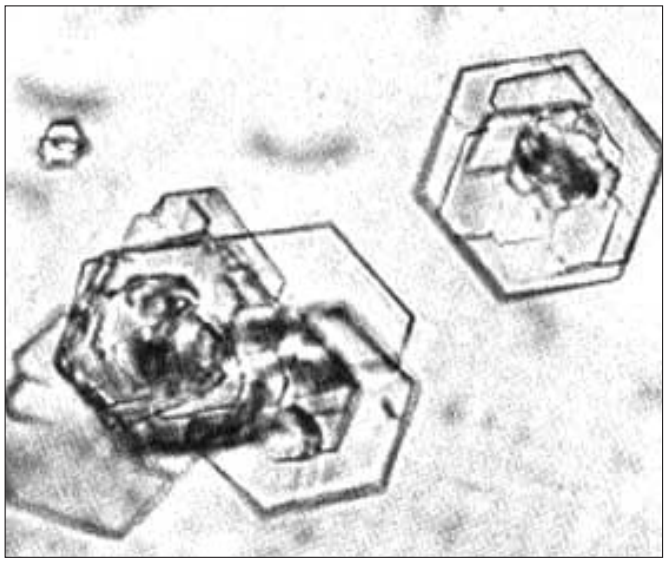

FIGURE 12-5

Urinary cystine crystals. Excessive urinary excretion of cystine (250 to 1000 mg/d of cystine/g of creatinine) coupled with its poor solubility in urine causes cystine precipitation with the formation of characteristic urinary crystals and urinary tract calculi. Stone formation often causes urinary tract obstruction and the associated problems of renal colic, infection, and even renal failure. The treatment objective is to reduce urinary cystine concentration or to increase its solubility. High fluid intake (to keep the urinary cystine concentration below the solubility threshold of 250 mg/L) and urinary alkalization are the mainstays of therapy. For those patients refractory to conservative management, treatment with sulfhydryl-containing drugs, such as D-penicillamine, mercaptopropionylglycine, and even captopril can be efficacious [14,15].

Renal Hypophosphatemic Rickets

INHERITED FORMS OF HYPOPHOSPHATEMIC RICKETS

Disorder	Vitamin D	Parathyroid hormone	Serum calcium	Urinary calcium	Treatment
X-linked hypophosphatemic rickets	Low, low normal	Normal, high normal	Low, normal	Elevated	Calciferol, phosphate supplementation
Hereditary hypophosphatemic rickets with hypercalciuria	Elevated	Low, low normal	Normal	Elevated	Phosphate supplementation

Vitamin D—1,25-dihydroxy-vitamin D_3

FIGURE 12-6

Several inherited disorders have been described that result in isolated renal phosphate wasting. These disorders include X-linked hypophosphatemic rickets (HYP), hereditary hypophosphatemic rickets with hypercalciuria (HHRH), hypophosphatemic bone disease (HBD), autosomal dominant hypophosphatemic rickets (ADHR), autosomal recessive hypophosphatemic rickets (ARHR), and X-linked recessive hypophosphatemic rickets (XLRH). These inherited disorders share two common features: persistent hypophosphatemia caused by decreased renal tubular phosphate (Pi) reabsorption (expressed as decreased ratio of plasma concentration at which maximal phosphate reabsorption occurs [TmP] to glomerular filtration rate [GFR], [TmP/GFR], a normogram derivative of the fractional excretion of Pi); and associated metabolic bone disease, *eg,* rickets in children or osteomalacia in adults [5]. These disorders can be distinguished on the basis of the renal hormonal response to hypophosphatemia, the biochemical profile, and responsiveness to therapy. In addition, the rare disorder XLRH is associated with nephrolithiasis. The clinical features of the two most common disorders HYP and HHRH are contrasted here. Whereas both disorders have defects in renal Pi reabsorption, the renal hormonal response to hypophosphatemia is impaired in HYP but not in HHRH. Indeed, in children with HHRH, phosphate supplementation alone can improve growth rates, resolve the radiologic evidence of rickets, and correct all biochemical abnormalities except the reduced TmP GFR [5].

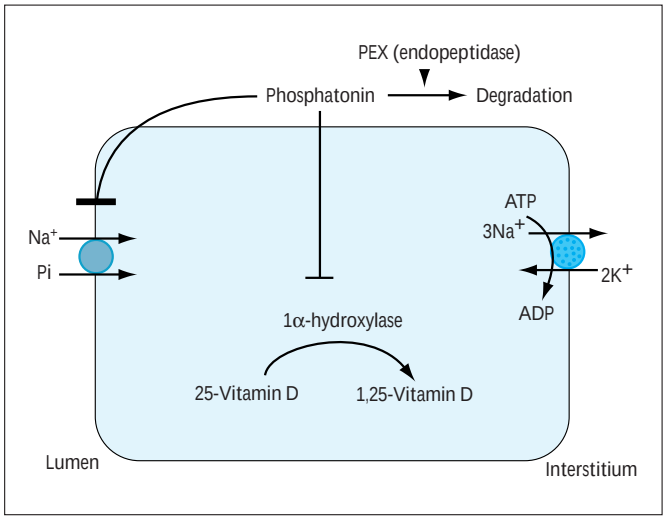

FIGURE 12-7

Proposed pathogenesis of X-linked hypophosphatemic rickets (HYP). HYP, the most common defect in renal phosphate (Pi) transport, is transmitted as an X-linked dominant trait. The disorder is characterized by growth impairment in children, metabolic bone disease, phosphaturia, and abnormal bioactivation of vitamin D [16]. Cell culture, parabiosis, and transplantation experiments have demonstrated that the defect in HYP is not intrinsic to the kidney but involves a circulating humoral factor other than parathyroid hormone [16,17].

Phosphate is transported across the luminal membrane of the proximal tubule by a sodium-phosphate cotransporter (NaPi). This transporter is regulated by multiple hormones. Among these is a putative phosphaturic factor that has been designated phosphatonin [18]. It is postulated that phosphatonin inhibits Pi reabsorption by way of the sodium-coupled phosphate cotransporter, and it depresses serum 1,25-dihydroxy-vitamin D_3 production by inhibiting 1-α-hydroxlase activity and stimulating 24-hydroxylase activity. Positional cloning studies in families with HYP have identified a gene, designated PEX (phosphate-regulating gene with homologies to endopeptidases on the X chromosome), that is mutated in patients with X-linked hypophosphatemia [19]. PEX, a neutral endopeptidase, presumably inactivates phosphatonin. Defective PEX activity would lead to decreased phosphatonin degradation, with excessive phosphaturia and deranged vitamin D metabolism. A similar scenario associated with increased phosphatonin production has been proposed as the basis for oncogenic hypophosphatemic osteomalacia, an acquired disorder manifested in patients with tumors of mesenchymal origin [17].
Na^+—sodium ion; K^+—potassium ion.

Fanconi's Syndrome

INHERITED FANCONI'S SYNDROME

Disorder	OMIM number*
Idiopathic	227700, 227800
Cystinosis	219800, 219900, 219750
Hepatorenal tyrosinemia (tyrosinemia type I)	276700
Hereditary fructose intolerance	229600
Galactosemia	230400
Glycogen storage disease type I	232200
Wilson's disease	277900
Oculocerebrorenal (Lowe's) syndrome	309000
Vitamin-D–dependent rickets	264700

*OMIM—Online Mendelian Inheritance in Man (accessible at http://www3.ncbi.nlm.nih.gov/omin/).

From Morris and Ives [5]; with permission.

FIGURE 12-8

Fanconi's syndrome is characterized by two components: generalized dysfunction of the proximal tubule, leading to impaired net reabsorption of bicarbonate, phosphate, urate, glucose, and amino acids; and vitamin D–resistant metabolic bone disease [20]. The clinical manifestations in patients with either the hereditary or acquired form of Fanconi's syndrome include polyuria, dehydration, hypokalemia, acidosis, and osteomalacia (in adults) or impaired growth and rickets (in children). Inherited Fanconi's syndrome occurs either as an idiopathic disorder or in association with various inborn errors of metabolism.

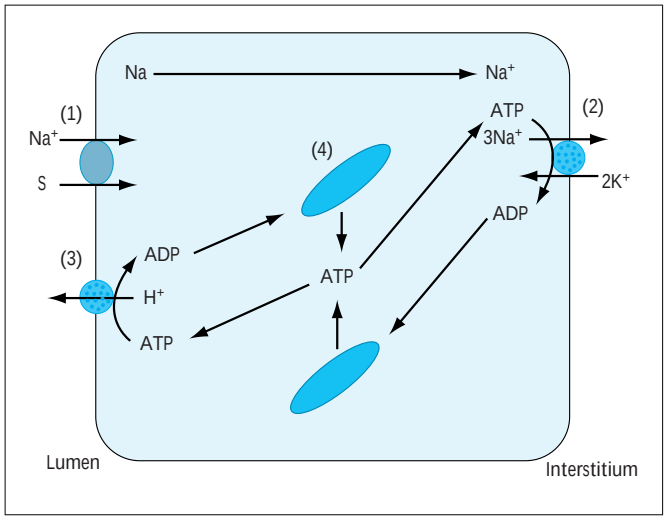

FIGURE 12-9

Proposed pathogenic model for Fanconi's syndrome. The underlying pathogenesis of Fanconi's syndrome has yet to be determined. It is likely, however, that the various Mendelian diseases associated with Fanconi's syndrome cause a global disruption in sodium-coupled transport systems rather than a disturbance in specific transporters. Bergeron and coworkers [20] have proposed a pathophysiologic model that involves the intracellular gradients of sodium, adenosine triphosphate (ATP), and adenosine diphosphate (ADP). A transepithelial sodium gradient is established in the proximal tubule cell by sodium (Na) entry through Na-solute cotransport systems (Na-S) (1) and Na exit through the sodium-potassium adenosine triphosphatase (Na-K ATPase) (2). This Na gradient drives the net uptake of cotransported solutes. A small decrease in the activity of the Na-K ATPase cotransporter may translate into a proportionally larger increment in the Na concentration close to the luminal membrane, thus decreasing the driving force that energizes all Na-solute cotransport systems. Concomitantly, reciprocal ATP and ADP gradients are established in the cell by the activity of membrane bound ATPases (Na-K ATPase (2) and hydrogen-ATPase (3)) and mitochondrial (4) ATP synthesis. A small reduction in mitochondrial rephosphorylation of ADP may result in a juxtamembranous accumulation of ADP and a reciprocal decrease in ATP, altering the ADP-ATP ratio and downregulating pump activities. Therefore, a relatively small mitochondrial defect may be amplified by the effects on the intracellular sodium gradients and ADP-ATP gradients and may lead to a global inhibition of Na-coupled transport. H^+—hydrogen ion.

Renal Tubular Acidoses

INHERITED RENAL TUBULAR ACIDOSES

Disorder	Transmission mode
Isolated proximal RTA	Autosomal recessive
Carbonic anhydrase II deficiency	Autosomal recessive
Isolated distal RTA	Autosomal dominant
Distal RTA with sensorineural deafness	Autosomal recessive

RTA—renal tubular acidosis.

FIGURE 12-10

Renal tubular acidosis (RTA) is characterized by hyperchloremic metabolic acidosis caused by abnormalities in renal acidification, *eg*, decreased tubular reabsorption of bicarbonate or reduced urinary excretion of ammonium (NH_4^+). RTA can result from a number of disease processes involving either inherited or acquired defects. In addition, RTA may develop from an isolated defect in tubular transport; may involve multiple tubular transport abnormalities, *eg*, Fanconi's syndrome; or may be associated with a systemic disease process. Isolated proximal RTA (type II) is rare, and most cases of proximal RTA occur in the context of Fanconi's syndrome. Inherited forms of classic distal RTA (type I) are transmitted as both autosomal dominant and autosomal recessive traits. Inherited disorders in which RTA is the major clinical manifestation are summarized.

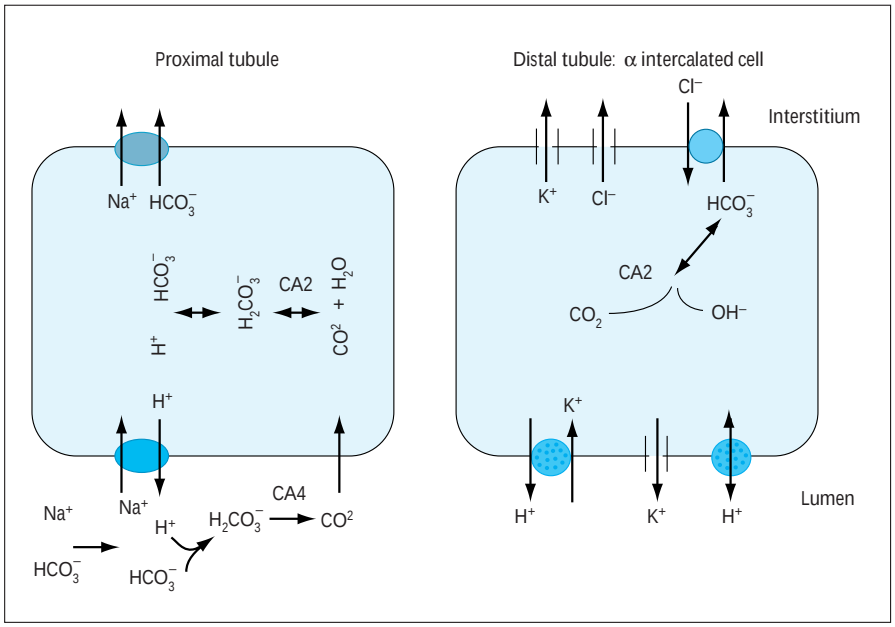

FIGURE 12-11

Carbonic anhydrase II deficiency. Carbonic anhydrase II deficiency is an autosomal recessive disorder characterized by renal tubular acidosis (RTA), with both proximal and distal components, osteopetrosis, and cerebral calcification. Carbonic anhydrase catalyzes the reversible hydration of carbon dioxide (CO_2), and thereby accelerates the conversion of carbon dioxide and water to hydrogen ions (H^+) and bicarbonate (HCO^-_3) [21]. A least two isoenzymes of carbonic anhydrase are expressed in the kidney and play critical roles in urinary acidification. In the proximal tubule, bicarbonate reabsorption is accomplished by the combined action of both luminal carbonic anhydrase type IV (CA4) and cytosolic carbonic anhydrase type II (CA2), the luminal sodium-hydrogen exchanger, and the basolateral sodium-bicarbonate exchanger. Impaired bicarbonate reabsorption in the proximal tubule is the underlying defect in type II or proximal RTA. In the distal nephron, carbonic anhydrase type II is expressed in the intercalated cells of the cortical collecting duct. There carbonic anhydrase type II plays a critical role in catalyzing the condensation of hydroxy ions, generated by the proton-translocating H^+-adenosine triphosphatase (H^+ ATPase), with carbon dioxide to form bicarbonate. In carbonic anhydrase type II deficiency, the increase in intracellular pH impairs the activity of the proton-translocating H-ATPase. Carbonic anhydrase inhibitors (*eg*, acetazolamide) act as weak diuretics by blocking bicarbonate reabsorption. Cl^-—chloride ion; H_2CO_3—carbonic acid; K^+—potassium ion; Na^+—sodium ion.

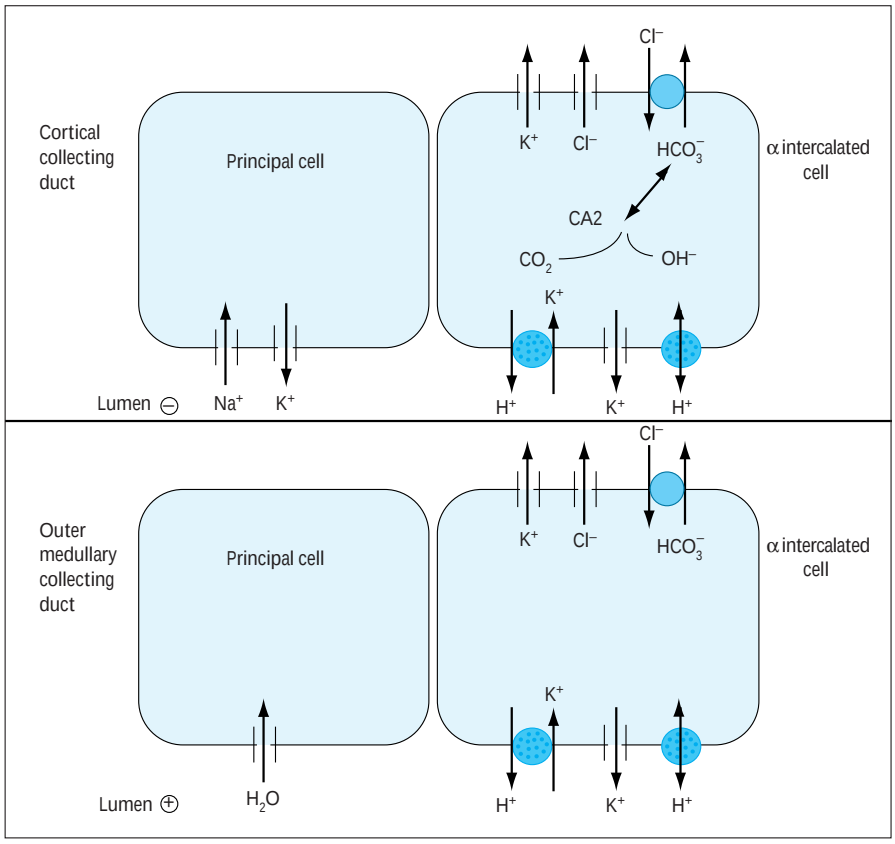

FIGURE 12-12

Distal renal tubular acidosis (RTA). The collecting duct is the principal site of distal tubule acidification, where the final 5% to 10% of the filtered bicarbonate load is reabsorbed and the hydrogen ions (H^+) generated from dietary protein catabolism are secreted. The distal nephron is composed of several distinct segments, *eg*, the connecting tubule, cortical collecting duct, and medullary collecting duct. The tubular epithelia within these segments are composed of two cell types: principal cells that transport sodium, potassium, and water; and intercalated cells that secrete hydrogen ions and bicarbonate (HCO^-_3) [22].

Urinary acidification in the distal nephron depends on several factors: an impermeant luminal membrane capable of sustaining large pH gradients; a lumen-negative potential difference in the cortical collecting duct that supports both hydrogen and potassium ion (K^+) secretion; and secretion of hydrogen ions by the intercalated cells of the cortical and medullary collecting ducts at a rate sufficient to regenerate the bicarbonate consumed by metabolic protons [22]. Abnormalities in any of these processes could result in a distal acidification defect.

Recent studies in families with isolated autosomal dominant distal RTA have identified defects in the basolateral chloride-bicarbonate exchanger, AE1 [23,24]. Defects in various components of the H^+-adenosine triphosphatase (H^+ ATPase) and subunits of the H^+-K^+ ATPase ($H^+\backslash K^+$ ATPase) also have been proposed as the basis for other hereditary forms of distal RTA. CA2—cytosolic carbonic anhydrase type II; Cl^-—chloride ion; CO_2—carbon dioxide; Na^+—sodium ion; OH^-—hydroxy ions.

Bartter-like Syndromes

CLINICAL FEATURES DISTINGUISHING BARTTER-LIKE SYNDROMES

Feature	Classic Bartter's syndrome	Gitelman's syndrome	Antenatal Bartter's syndrome
Age at presentation	Infancy, early childhood	Childhood, adolescence	In utero, infancy
Prematurity, polyhydramnios	+/-	-	++
Delayed growth	++	-	+++
Delayed cognitive development	+/-	-	+
Polyuria, polydipsia	++	+	+++
Tetany	Rare	++	-
Serum magnesium	Low in 20%	Low in about 100%	Low-normal to normal
Urinary calcium excretion	Normal to high	Low	Very high
Nephrocalcinosis	+/-	-	++
Urine prostaglandin excretion	High	Normal	Very high
Clinical response to indomethacin	+/-	-	Often life-saving

From Guay-Woodford [25]; with permission.

FIGURE 12-13

Familial hypokalemic, hypochloremic metabolic alkalosis, or Bartter's syndrome, is not a single disorder but rather a set of closely related disorders. These Bartter-like syndromes share many of the same physiologic derangements but differ with regard to the age of onset, presenting symptoms, magnitude of urinary potassium and prostaglandin excretion, and extent of urinary calcium excretion. At least three clinical phenotypes have been distinguished: classic Bartter's syndrome, the antenatal hypercalciuric variant (also called *hyperprostaglandin E syndrome*), and hypocalciuric-hypomagnesemic Gitelman's syndrome [25].

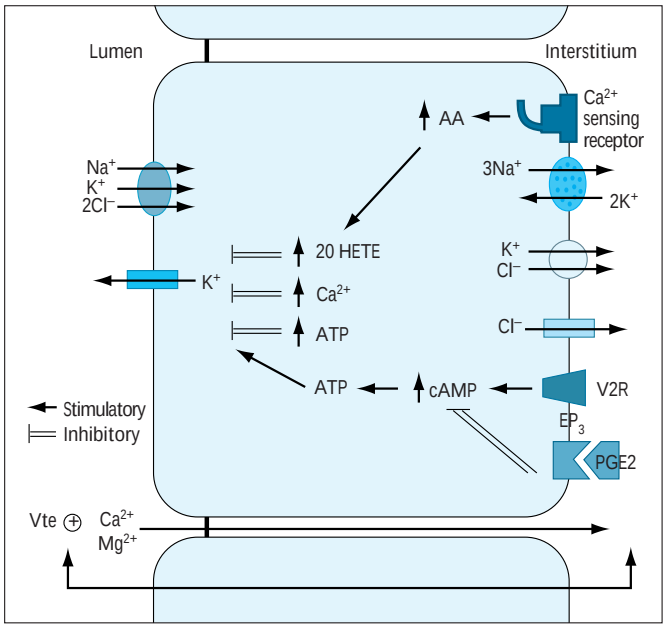

FIGURE 12-14

Transport systems involved in transepithelial sodium-chloride transport in the thick ascending limb (TAL). Clinical data suggest that the primary defect in the antenatal and classic Bartter syndrome variants involves impaired sodium chloride transport in the TAL. Under normal physiologic conditions, sodium chloride is transported across the apical membrane by way of the bumetanide-sensitive sodium-potassium-2chloride (Na-K-2Cl) cotransporter (NKCC2). This electroneutral transporter is driven by the low intracellular sodium and chloride concentrations generated by the sodium-potassium pump and the basolateral chloride channels and potassium-chloride cotransporter. In addition, apical potassium recycling by way of the low-conductance potassium channel (ROMK) ensures the efficient functioning of the Na-K-2Cl cotransporter. The activity of the ROMK channel, in turn, is regulated by a number of cell messengers, *eg*, calcium (Ca^{2+}) and adenosine triphosphate (ATP), as well as by the calcium-sensing receptor (CaR), prostaglandin EP_3 receptor, and vasopressin receptor (V2R) by way of cAMP-dependent pathways and arachidonic acid (AA) metabolites, *eg*, 20-hydroxy-eicosatetraenoic acid (20-HETE). The positive transluminal voltage (Vte) drives the paracellular reabsorption of calcium ions and magnesium ions (Mg^{2+}) [25]. cAMP—cyclic adenosine monophosphate; PGE2—prostaglandin E2; PKA—protein kinase A.

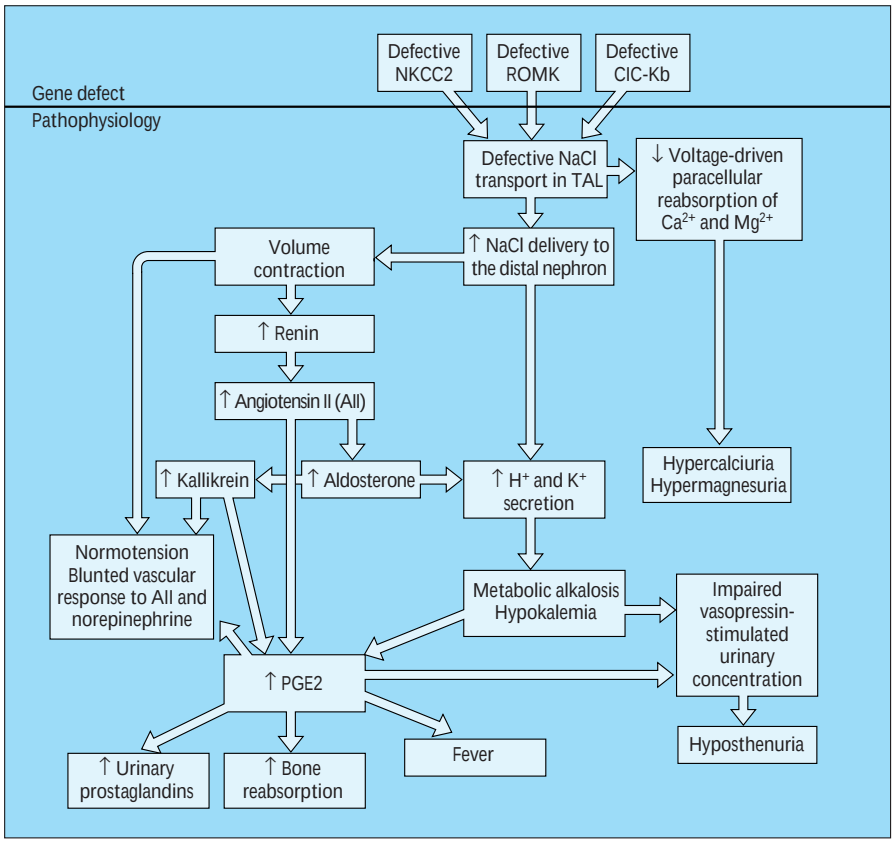

FIGURE 12-15

Proposed pathogenic model for the antenatal and classic variants of Bartter's syndrome. Genetic studies have identified mutations in the genes encoding the bumetanide-sensitive sodium-potassium-2chloride cotransporter (NKCC2), luminal ATP–regulated potassium channel (ROMK), and kidney-specific chloride channel (ClC-K2). These findings support the theory of a primary defect in thick ascending limb (TAL) sodium-chloride (Na-Cl) reabsorption in, at least, subsets of patients with the antenatal or classic variants of Bartter's syndrome. In the proposed model the potential interrelationships of the complex set of pathophysiologic phenomena are illustrated. The resulting clinical manifestations are highlighted in boxes [25]. Ca^{2+}—calcium ion; H^+—hydrogen ion; K^+—potassium ion; Mg^{2+}—magnesium ion; PGE2—prostaglandin E2.

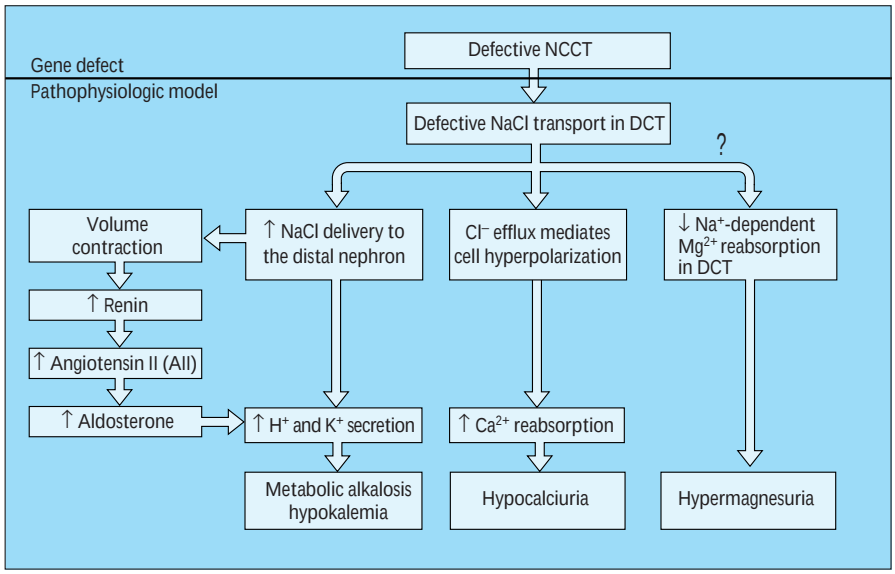

FIGURE 12-16

Proposed pathogenic model for Gitelman's syndrome. The electrolyte disturbances evident in Gitelman's syndrome also are observed with administration of thiazide diuretics, which inhibit the sodium-chloride (Na-Cl) cotransporter in the distal convoluted tubule (DCT). In families with Gitelman's syndrome, genetic studies have identified defects in the gene encoding the thiazide-sensitive cotransporter (NCCT) protein. The proposed pathogenic model is predicated on loss of function of the NCCT protein and, thus, most closely applies to those patients who inherit Gitelman's syndrome as an autosomal recessive trait. Given that the physiologic features of this syndrome are virtually indistinguishable in familial and sporadic cases, it may be reasonable to propose the same pathogenesis for all patients with Gitelman's syndrome. However, it is important to caution that evidence for NCCT mutations in sporadic cases has not yet been established [25]. Ca^{2+}—calcium ion; Cl^-—chloride ion; H^+—hydrogen ion; K^+—potassium ion; Mg^{2+}—magnesium ion; Na^+—sodium ion.

Pseudohypoparathyroidism

CLINICAL SUBTYPES OF PSEUDOHYPOPARATHYROIDISM

Disorder	Pathophysiology	Skeletal anomalies	Associated endocrinopathies
Pseudohypoparathyroidism type Ia	Defect in guanine nucleotide—binding protein	Yes	Yes
Pseudohypoparathyroidism type Ib	Resistance to parathyroid hormone, normal guanine nucleotide—binding protein activity ? Defect in parathyroid hormone receptor	No	No

FIGURE 12-17

Pseudohypoparathyroidism applies to a heterogeneous group of hereditary disorders whose common feature is resistance to parathyroid hormone (PTH). Affected patients are hypocalcemic and hyperphosphatemic, despite elevated plasma PTH levels. Hypocalcemia and hyperphophatemia result from the combined effects of defective PTH-mediated calcium reabsorption in the distal convoluted tubule and reduced formation of 1,25-dihydroxy-vitamin D_3. The latter leads to defects in renal phosphate excretion, calcium mobilization from bone, and gastrointestinal calcium reabsorption. Differences in clinical features and urinary cyclic adenosine monophosphate response to infused PTH provide the basis for distinguishing three distinct subtypes of pseudohypoparathyroidism (type Ia, type Ib, and type II) [26].

Pseudohypoparathyroidism type Ia (Albright's hereditary osteodystrophy) is associated with a myriad of physical abnormalities and resistance to multiple adenylate cyclase–coupled hormones, most notably thyrotropin and gonadotropin [27]. The molecular defect in a guanine nucleotide–binding protein (Gs) blocks the coupling of PTH and other hormone receptors to adenylate cyclase. The molecular defect has not been identified in type Ib, although specific resistance to PTH suggests a defect in the PTH receptor. Oral supplementation with 1,25 dihydroxy-vitamin D_3 and, if necessary, oral calcium, is used to correct the hypocalcemia and minimize PTH-induced bone disease [26]. Pseudohypoparathroidism type II may be an acquired disease.

Disorders of Aldosterone-Regulated Transport

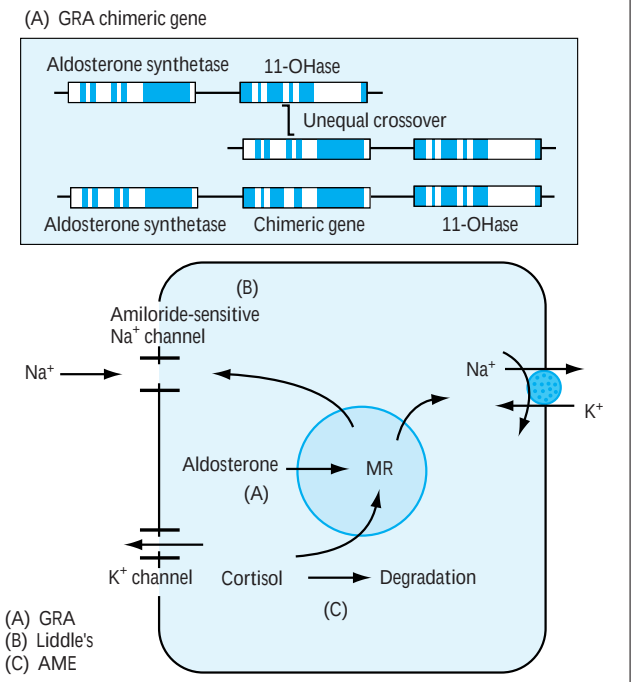

FIGURE 12-18

Aldosterone-regulated transport in the cortical collecting duct and defects causing low-renin hypertension. The mineralocorticoid aldosterone regulates electrolyte excretion and intravascular volume by way of its action in the principal cells of the cortical collecting duct. The binding of aldosterone to its nuclear receptor (MR) leads directly or indirectly to increased activity of the apical sodium (Na) channel and the basolateral sodium-potassium adenosine triphosphatase (Na-K ATPase). Sodium moves from the lumen into the cell and down its electrochemical gradient, thus generating a lumen-negative transepithelial voltage that drives potassium secretion from the principal cells and hydrogen secretion from the intercalated cells. The type I mineralocorticoid receptor (MR) is nonspecific and can bind both aldosterone and cortisol, but not cortisone. The selective receptor specificity for aldosterone is mediated by the kidney isoform of the enzyme, 11-β-hydroxysteroid dehydrogenase, which oxidizes intracellular cortisol to its metabolite cortisone.

Three hypertensive syndromes, glucocorticoid-remedial aldosteronism (GRA), Liddle's syndrome, and apparent mineralocorticoid excess (AME), share a common clinical phenotype that is characterized by normal physical examinations, hypokalemia, and very low plasma renin activity. The molecular defect in GRA derives from an unequal crossover event between two adjacent genes encoding 11-β-hydroxylase and aldosterone synthase (A). The resulting chimeric gene duplication fuses the regulatory elements of 11-β-hydroxylase and the coding sequence of aldosterone synthase. Consequently, aldosterone is ectopically synthesized in the adrenal zona fasciculata and its synthesis regulated by adrenocorticotropic hormone rather than its physiologically normal secretagogue, angiotensin II [28]. Activating mutations in the β and γ regulatory subunits of the epithelial sodium channel (B) are responsible for Liddle's syndrome [29]. Deficiency of the kidney type 2 isozyme of 11-β-hydroxysteroid dehydrogenase (C) can render type I MR responsive to cortisol and produce the syndrome of apparent mineralocorticoid excess [30]. Inhibitors of this enzyme (*eg,* licorice) also can produce an acquired form of apparent mineralocorticoid excess. Medical management of these disorders focuses on dietary sodium restriction, blocking the sodium channel with the potassium-sparing diuretics triamterene and amiloride, downregulating the ectopic aldosterone synthesis with glucocorticoids (GRA), or blocking the MR using the competitive antagonist spironolactone (GRA and AME).

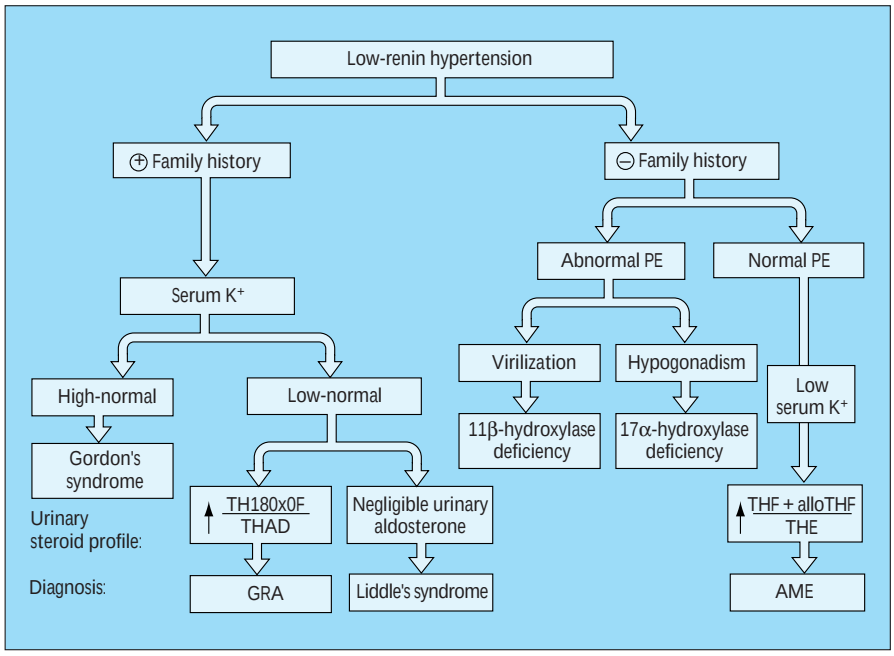

FIGURE 12-19

Algorithm for evaluating patients with low-renin hypertension. Glucocorticoid-remedial aldosteronism (GRA), Liddle's syndrome, and apparent mineralocorticoid excess (AME) can be distinguished from one another by characteristic urinary steroid profiles [31]. K^+—potassium ion; PE—physical examination; TH18oxoF/THAD—ratio of urinary 18-oxotetrahydrocortisol (TH18oxoF) to urinary tetrahydroaldosterone (normal: 0–0.4; GRA patients: >1); THF + allo-THF/THE—ratio of the combined urinary tetrahydrocortisol and allotetrahydrocortisol to urinary tetrahydrocortisone (normal: <1.3; AME patients: 5–10-fold higher).

CLINICAL SUBTYPES OF PSEUDOHYPOALDOSTERONISM

Disorder	Clinical features	Treatment
Pseudohypoaldosteronism type I		
Autosomal recessive	Dehydration, severe neonatal salt wasting, hyperkalemia, metabolic acidosis	Sodium chloride supplementation
	Elevated plasma renin activity	Ion-binding resin; dialysis
	Severity of electrolyte abnormalities may diminish after infancy	
Autosomal dominant	Mild salt wasting	
Pseudohypoaldosteronism type II (Gordon's syndrome)	Hypertension, hyperkalemia, mild hyperchloremic metabolic acidosis	Thiazide diuretics
	Undetectable plasma renin activity	

FIGURE 12-20

Mineralocorticoid resistance with hyperkalemia (pseudohypoaldosteronism) includes at least three clinical subtypes, two of which are hereditary disorders. Pseudohypoaldosteronism type I (PHA1) is characterized by severe neonatal salt wasting, hyperkalemia, and metabolic acidosis. The diagnosis is supported by elevated plasma renin and plasma aldosterone concentrations. Life-saving interventions include aggressive sodium chloride supplementation and treatment with ion-binding resins or dialysis to reduce the hyperkalemia. This autosomal recessive form of PHA1 results from inactivating mutations in the α or β subunits of the epithelial sodium channel [32]. A milder form of PHA1 with autosomal dominant inheritance also has been described; however, the molecular defect remains unexplained [33]. Adolescents or adults with hyperkalemic, hyperchloremic metabolic acidosis, low-normal renin and aldosterone levels, and hypertension have been recently described and classified as having pseudohypoaldosteronism type II (PHA2) or Gordon's syndrome [34]. Phenotypically, this disorder is the mirror image of Gitelman's syndrome; however, the thiazide-sensitive cotransporter (NCCT) has been excluded as a candidate gene [35].

Nephrogenic Diabetes Insipidus

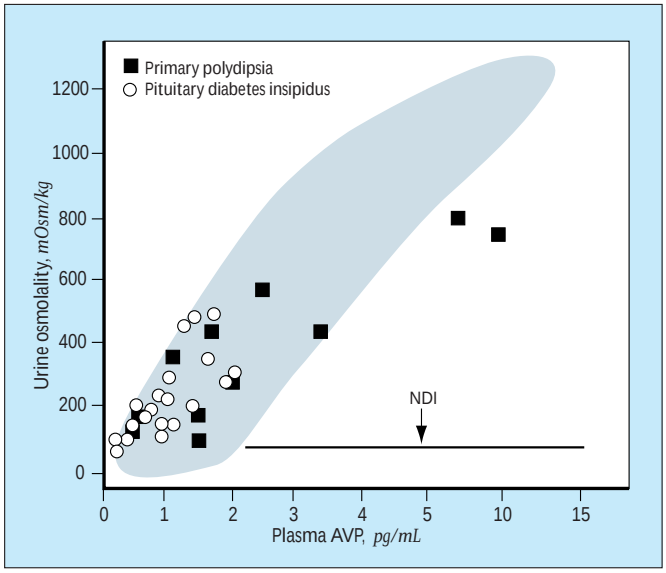

FIGURE 12-21

The relationship between urine osmolality and plasma arginine vasopressin (AVP). Nephrogenic diabetes insipidus (NDI) is characterized by renal tubular unresponsiveness to the antidiuretic hormone AVP or its antidiuretic analogue 1-desamino-8-D-arginine vasopressin (DDAVP). In both the congenital and acquired forms of this disorder the clinical picture is dominated by polyuria, polydipsia, and hyposthenuria despite often elevated AVP levels [17]. (*From* Robertson *et al*. [36]; with permission.)

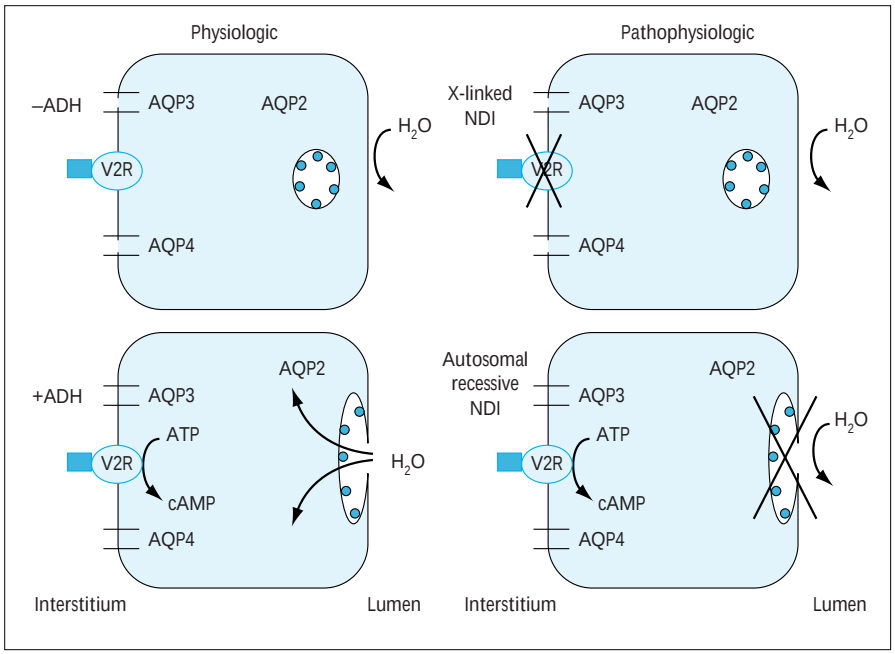

FIGURE 12-22

Pathogenic model for nephrogenic diabetes insipidus (NDI). The principle cell of the inner medullary collecting duct is the site where fine tuning of the final urinary composition and volume occurs. As shown, the binding of arginine vasopressin (AVP) to the vasopressin V2 receptor (V2R) stimulates a series of cyclic adenosine monophosphate–(cAMP) mediated events that results in the fusion of cytoplasmic vesicles carrying water channel proteins (aquaporin-2 [AQP2]), with the apical membrane, thereby increasing the water permeability of this membrane. Water exits the cell through the basolateral water channels AQP3 and AQP4. In the absence of AVP, water channels are retrieved into cytoplasmic vesicles and the water permeability of the apical membrane returns to its baseline low rate [37].

Genetic studies have identified mutations in two proteins involved in this water transport process, the V2 receptor and AQP2 water channels. Most patients (>90%) inherit NDI as an X-linked recessive trait. In these patients, defects in the V2 receptor have been identified. In the remaining patients, the disease is transmitted as either an autosomal recessive or autosomal dominant trait involving mutations in the AQP2 gene [38,39]. ADH— antidiuretic hormone; ATP—adenosine triphosphate.

Urolithiases

INHERITED CAUSES OF UROLITHIASES

Disorder	Stone characteristics	Treatment
Cystinuria	Cystine	High fluid intake, urinary alkalization Sulfhydryl-containing drugs
Dent's disease	Calcium-containing	High fluid intake, urinary alkalization
X-linked recessive nephrolithiasis	Calcium-containing	High fluid intake, urinary alkalization
X-linked recessive hypophosphatemic rickets	Calcium-containing	High fluid intake, urinary alkalization
Hereditary renal hypouricemia	Uric acid, calcium oxalate	High fluid intake, urinary alkalization Allopurinol
Hypoxanthine-guanine phosphoribosyltransferase deficiency	Uric acid	High fluid intake, urinary alkalization Allopurinol
Xanthinuria	Xanthine	High fluid intake, dietary purine restriction
Primary hyperoxaluria	Calcium oxalate	High fluid intake, dietary oxalate restriction Magnesium oxide, inorganic phosphates

FIGURE 12-23

Urolithiases are a common urinary tract abnormality, afflicting 12% of men and 5% of women in North America and Europe [40]. Renal stone formation is most commonly associated with hypercalciuria. Perhaps in as many as 45% of these patients, there seems to be a familial predisposition. In comparison, a group of relatively rare disorders exists, each of which is transmitted as a Mendelian trait and causes a variety of different crystal nephropathies. The most common of these disorders is cystinuria, which involves defective cystine and dibasic amino acid transport in the proximal tubule. Cystinuria is the leading single gene cause of inheritable urolithiasis in both children and adults [41,42]. Three Mendelian disorders, Dent's disease, X-linked recessive nephrolithiasis, and X-linked recessive hypophosphatemic rickets cause hypercalciuric urolithiasis. These disorders involve a functional loss of the renal chloride channel ClC-5 [43]. The common molecular basis for these three inherited kidney stone diseases has led to speculation that ClC-5 also may be involved in other renal tubular disorders associated with kidney stones. Hereditary renal hypouricemia is an inborn error of renal tubular transport that appears to involve urate reabsorption in the proximal tubule [16].

In addition to renal transport deficiencies, defects in metabolic enzymes also can cause urolithiases. Inherited defects in the purine salvage enzymes hypoxanthine-guanine phosphoribosyltransferase (HPRT) and adenine phosphoribosyltransferase (APRT) or in the catabolic enzyme xanthine dehydrogenase (XDH) all can lead to stone formation [44]. Finally, defective enzymes in the oxalate metabolic pathway result in hyperoxaluria, oxalate stone formation, and consequent loss of renal function [45].

Acknowledgment

The author thanks Dr. David G. Warnock for critically reviewing this manuscript.

References

1. Wells R, Kanai Y, Pajor A, *et al.*: The cloning of a human cDNA with similarity to the sodium/glucose cotransporter. *Am J Physiol* 1992, 263:F459–F465.
2. Hediger M, Coady M, Ikeda T, Wright E: Expression cloning and cDNA sequencing of the Na/glucose co-transporter. *Nature* 1987, 330:379–381.
3. Woolf L, Goodwin B, Phelps C: Tm-limited renal tubular reabsorption and the genetics of renal glycosuria. *J Theor Biol* 1966, 11:10–21.
4. Meuckler M: Facilitative glucose transporters. *Euro J Biochem* 1994, 219:713–725.
5. Morris JR, Ives HE: Inherited disorders of the renal tubule. In *The Kidney*. Edited by Brenner B, Rector F. Philadelphia: WB Saunders, 1996:1764–1827.
6. Kanai Y, Hediger M: Primary structure and functional characterization of a high affinity glutamate transporter. *Nature* 1992, 360:467–471.
7. Oynagi K, Sogawa H, Minawi R,*et al.*: The mechanism of hyperammonemia in congenital lysinuria. *J Pediatr* 1979, 94:255.
8. Smith A, Strang L: An inborn error of metabolism with the urinary excretion of α-hydroxybutric acid and phenyl-pyruvic acid. *Arch Dis Child* 1958, 33:109.
9. Rosenberg LE, Downing S, Durant JL, Segal S: Cystinuria: biochemical evidence for three genetically distinct diseases. *J Clin Invest* 1966, 45:365–371.
10. Pras E, Arber N, Aksentijevich I, *et al.*: Localization of a gene causing cystinuria to chromosome 2p. *Nature Genet* 1994, 6:415–419.
11. Calonge MJ, Gasparini P, Chillaron J, *et al.*: Cystinuria caused by mutations in rBAT, a gene involved in the transport of cystine. *Nature Genet* 1994, 6:420–425.
12. Calonge M, Volpini V, Bisceglia L, *et al.*: Genetic heterogeneity in cystinuria: the SLC3A1 gene is linked to type I but not to type III cystinuria. *Proc Am Acad Sci USA* 1995, 92:9667–9671.

13. Wartenfeld R, Golomb E, Katz G, Bale S, *et al*.: Molecular analysis of cystinuria in Libyan Jews: exclusion of the SLC3A1 gene and mapping a new locus on 19q. *Am J Med Genet* 1997, 60:617–624.
14. Stephens AD: Cystinuria and its treatment: 25 years' experience at St. Bartholomew's Hospital. *J Inherited Metab Dis* 1989, 12:197–209.
15. Perazella M, Buller G: Successful treatment of cystinuria with captopril. *Am J Kidney Dis* 1993, 21:504–507.
16. Grieff M: New insights into X-linked hypophosphatemia. *Curr Opin Nephrol Hypertens* 1997, 6:15–19.
17. Robertson GL: Vasopressin in osmotic regulation in man. *Annu Rev Med* 1974, 25:315.
18. Econs M, Drezner M: Tumor-induced osteomalacia: unveiling a new hormone. *N Engl J Med* 1994, 330:1679–1681.
19. The HYP Consortium: A gene (PEX) with homologies to endopeptidases is mutated in patients with X-linked hypophosphatemic rickets. *Nature Genet* 1995, 11:130–136.
20. Bergeron M, Gougoux A, Vinay P: The renal Fanconi syndrome. In *The Metabolic and Molecular Bases of Inherited Diseases*. Edited by Scriver CH, Beaudet AL, Sly WS, Valle D. New York: McGraw-Hill, 1995:3691–3704.
21. Sly W, Hu P: The carbonic anhydrase II deficiency syndrome: osteopetrosis with renal tubular acidosis and cerebral calcification. In *The Metabolic and Molecular Bases of Inherited Diseases*. Edited by Scriver CH, Beaudet AL, Sly WS, Valle D. New York: McGraw-Hill; 1965:3581–3602.
22. Bastani B, Gluck S: New insights into the pathogenesis of distal renal tubular acidosis. *Miner Electrolyte Metab* 1996, 22:396–409.
23. Bruce L, Cope D, Jones G, *et al*.: Familial distal renal tubular acidosis is associated with mutations in the red cell anion exchanger (band 3, AE1) gene. *J Clin Invest* 1997, 100:1693–1707.
24. Jarolim P, Shayakul C, Prabakaran D, *et al*.: Autosomal dominant distal renal tubular acidosis is associated in three families with heterozygosity for the R589H mutation in the AE1 (band 3) Cl^-/HCO^-_3 exchanger. *J Biol Chem*, 1998, 273:6380–6388.
25. Guay-Woodford L: Bartter syndrome: unraveling the pathophysiologic enigma. *Am J Med*, 1998, 105:151–161.
26. Spiegel A, Weinstein L: Pseudohypoparathyroidism. In *The Metabolic and Molecular Bases of Inherited Diseases*. Edited by Scriver CH, Beaudet AL, Sly WS, Valle D. New York: McGraw-Hill; 1995:3073–3085.
27. Van Dop C: Pseudohypoparathyroidism: clinical and molecular aspects. *Semin Nephrol* 1989, 9:168–178.
28. Lifton RP, Dluhy RG, Powers M., *et al*.: A chimaeric 11-β-hydroxylase aldosterone synthase gene causes glucocorticoid-remediable aldosteronism and human hypertension. *Nature* 1992, 355:262–265.
29. Shimkets RA, Warnock DG, Bositis CM, *et al*.: Liddle's syndrome: heritable human hypertension caused by mutations in the β subunit of the epithelial sodium channel. *Cell* 1994, 79:407–414.
30. White P, Mune T, Rogerson F, *et al*.: 11-β-hydroxysteroid dehydrogenase and its role in the syndrome of apparent mineralocorticoid excess. *Pediatr Res* 1997, 41:25–29.
31. Yiu V, Dluhy R, Lifton R, Guay-Woodford L: Low peripheral plasma renin activity as a critical marker in pediatric hypertension. *Pediatr Nephrol* 1997, 11:343–346.
32. Chang S, Grunder S, Hanukoglu A, *et al*.: Mutations in subunits of the epithelial sodium channel cause salt wasting with hyperkalemic acidosis, pseudohypoaldosteronism type 1. *Nature Genet* 1996, 12:248–253.
33. Kuhle U: Pseudohypoaldosteronism: mutation found, problem solved? *Mol Cell Endocrinol* 1997, 133:77–80.
34. Gordon R: Syndrome of hypertension and hyperkalemia with normal glomerular filtration rate. *Hypertension* 1986, 8:93–102.
35. Mansfield T, Simon D, Farfel Z, *et al*.: Multilocus linkage of familial hyperkalaemia and hypertension, pseudohypoaldosteronism type II, to chromosomes 1q31-42 and 17p11-q2. *Nature Genet* 1997, 16:202–205.
36. Robertson GL, *et al*: Development and clinical application of a new method for the radioimmunoassay of arginine vasopressin in human plasma. *J Clin Invest* 1973, 52:2340–2352.
37. Bichet D, Osche A, Rosenthal W: Congenital nephrogenic diabetes insipidus. *JASN* 1997, 12:1951–1958.
38. van Lieburg A, Verdijk M, Knoers N, *et al*.: Patients with autosomal recessive nephrogenic diabetes insipidus homozygous for mutations in the aquaporin 2 water channel gene. *Am J Hum Genet* 1994, 55:648–652.
39. Bichet D, Arthus M-F, Lonergan M, *et al*.: Autosomal dominant and autosomal recessive nephrogenic diabetes insipidus: novel mutations in the AQP2 gene. *J Am Soc Nephrol* 1995, 6:717A.
40. Coe F, Parks J, Asplin J: The pathogenesis and treatment of kidney stones. *N Engl J Med* 1992, 327:1141–1152.
41. Segal S, Thier S: Cystinuria. In *The Metabolic and Molecular Bases of Inherited Diseases*. Edited by Scriver CH, Beaudet AL, Sly WS, Valle D. York: McGraw-Hill; 1995:3581–3602.
42. Polinsky MS, Kaiser BA, Baluarte HJ: Urolithiasis in childhood. *Pediatr Clin North Am* 1987, 34:683–710.
43. Lloyd S, Pearce S, Fisher S, *et al*.: A common molecular basis for three inherited kidney stone diseases. *Nature* 1996, 379:445–449.
44. Cameron J, Moro F, Simmonds H: Gout, uric acid and purine metabolism in paediatric nephrology. *Pediatr Nephrol* 1993, 7:105–118.
45. Danpure C, Purdue P: Primary Hyperoxaluria. In *The Metabolic and Molecular Bases of Inherited Diseases*. Edited by Scriver CH, Beaudet AL, Sly WS, Valle D. New York: McGraw-Hill; 1995:2385–2424.